

**GEOLOGICAL SURVEY OF WESTERN AUSTRALIA**

**REPORT 34**

**PROFESSIONAL PAPERS**



**DEPARTMENT OF MINERALS AND ENERGY**



**GEOLOGICAL SURVEY OF WESTERN AUSTRALIA**

**REPORT 34**

# **PROFESSIONAL PAPERS**

**Perth 1993**

**MINISTER FOR MINES**  
The Hon. George Cash, J.P., M.L.C.

**ACTING DIRECTOR GENERAL**  
L. C. Ranford

**DIRECTOR, GEOLOGICAL SURVEY OF WESTERN AUSTRALIA**  
Pietro Guj

Copy editor: I. R. Nowak

National Library of Australia Card Number and ISBN 0 7309 4451 4

ISSN0508-4741

ISSN0812-8952

Copies available from:  
Director  
Geological Survey of Western Australia  
100 Plain Street  
EAST PERTH Western Australia 6004  
Telephone (09) 222 3222

## Contents

<b>A. Salinity control by groundwater pumping at Lake Toolibin, Western Australia</b>	
by M. W. Martin .....	1
<b>B. The geology and hydrogeology of the superficial formations between Cervantes and Lancelin, Western Australia</b>	
by A. M. Kern .....	11
<b>C. The location and significance of point sources of groundwater contamination in the Perth Basin</b>	
by K-J. B. Hirschberg .....	37
<b>D. Proposed stratigraphic subdivisions of the Marra Mamba Iron Formation and the lower Wittenoom Dolomite, Hamersley Group, Western Australia</b>	
by J. G. Blockley, I. J. Tehnas, A. Mandyczewsky, and R. C. Morris ..	47
<b>E. Lithology and proposed revisions in stratigraphic nomenclature of the Wittenoom Formation (Dolomite) and overlying formations, Hamersley Group, Western Australia</b>	
by Bruce M. Simonson, Scott W. Hassler, and Kathryn A. Schubel ....	65
<b>F. Further isotopic evidence for the existence of two distinct terranes in the southern Pinjarra Orogen, Western Australia</b>	
by I. R. Fletcher and W. G. Libby .....	81
<b>G. Cainozoic stratigraphy in the Roe Palaeodrainage of the Kalgoorlie region, Western Australia</b>	
by A. M. Kern and D. P. Commander .....	85
<b>H. Municipal waste disposal in Perth and its impact on groundwater quality</b>	
by K-J. B. Hirschberg .....	97
<b>I. Palynology and correlation of Permian sediments in the Perth, Collie, and Officer Basins, Western Australia</b>	
by John Backhouse .....	111
<b>J. Hydrogeology of the Collie Basin, Western Australia</b>	
by J. S. Moncrieff .....	129



# Salinity control by groundwater pumping at Lake Toolibin, Western Australia

by

M. W. Martin

## Abstract

Lake Toolibin is a shallow, ephemeral, freshwater lake in the wheatbelt of Western Australia. It is an important breeding area for water birds and is threatened by salinization from a rising, saline watertable.

Groundwater occurs in a heterogeneous unconfined aquifer in weathered granitic rocks. The watertable is less than 2 m below the lake floor and the groundwater salinity ranges from 30 000 to 60 000 mg/L.

Analysis of the drawdown response to the pumping of a production bore on the western side of Lake Toolibin (after 113 days at an average rate of 16 m<sup>3</sup>/d) indicates an aquifer transmissivity of 4.92 m<sup>2</sup>/d, hydraulic conductivity of 0.15 m/d and specific yield of 0.01. After 1 year of pumping (pseudo steady-state condition) a drawdown of 1.5 m would occur 30–40 m from the production bore with no drawdown beyond about 650 m.

These results show that control of salinization at Lake Toolibin can be achieved by locating production bores about 300 m apart to give a drawdown of at least 1.5 m by mutual interference. A total of 25 production bores would be required to lower the watertable at the sites that are threatened by salinization.

Discharge of saline water from the pumping to nearby Lake Taarblin is unlikely to result in a significant increase in the salinity of flow in the Blackwood River. However, the environmental impact of the discharge, and the feasibility of recovering both salt and freshwater from the discharge by solar distillation should be considered.

**KEYWORDS:** Groundwater, salinity, watertable, pumping, lake

## Introduction

Lake Toolibin is a small, shallow, ephemeral lake in the Northern Arthur River drainage system about 200 km southeast of Perth (Fig. 1). It is one of a small number of relatively freshwater lakes in the region, and provides an important breeding area for a wide variety of waterbirds.

A report by the Northern Arthur River Wetlands Committee (NARWC, 1987) on the status and future of Lake Toolibin highlights both the importance of the lake to the wildlife ecosystem and the degradation, due to salinization, of lakebed vegetation. The recommendations of that report prompted the Geological Survey of Western Australia to undertake a drilling and pumping program during 1988/89 to assess the extent to which dewatering would lower groundwater levels in areas where the lakebed is salinized.

This paper describes the drilling and pumping program and the effectiveness of pumping to lower groundwater levels. The predicted distance–drawdown response is used to determine the spacing between pumping bores and to establish the measures required to lower groundwater levels in the salinized areas.

## Physiography

Lake Toolibin is one of several shallow, ephemeral lakes in a palaeodrainage now occupied by the headwaters of the Arthur River, a tributary of the Blackwood River. The catchment area for Lake Toolibin covers 476 km<sup>2</sup> of which some 90% has been cleared of native vegetation for dryland agriculture (Stokes and Martin, 1986). Clearing has resulted in the appearance and subsequent spreading of salinized land, and about 6% of the catchment is now moderately to severely affected by high salt levels.

The climate of the area is Mediterranean with mild, wet winters and hot, dry summers. The mean annual rainfall is 420 mm and pan evaporation averages 1800 mm/year.

From historical rainfall records, it has been shown that inflow to Lake Toolibin occurs, on average, 7 years out of 10 (Stokes and Sheridan, 1985). However, because of recent below-average rainfall, significant inflow to the lake has occurred in only 3 years (1981, 1983, and 1990) since lake-level gauging began in 1977. When full, the lake covers an area of about 3 km<sup>2</sup> with a maximum water depth approaching three metres.

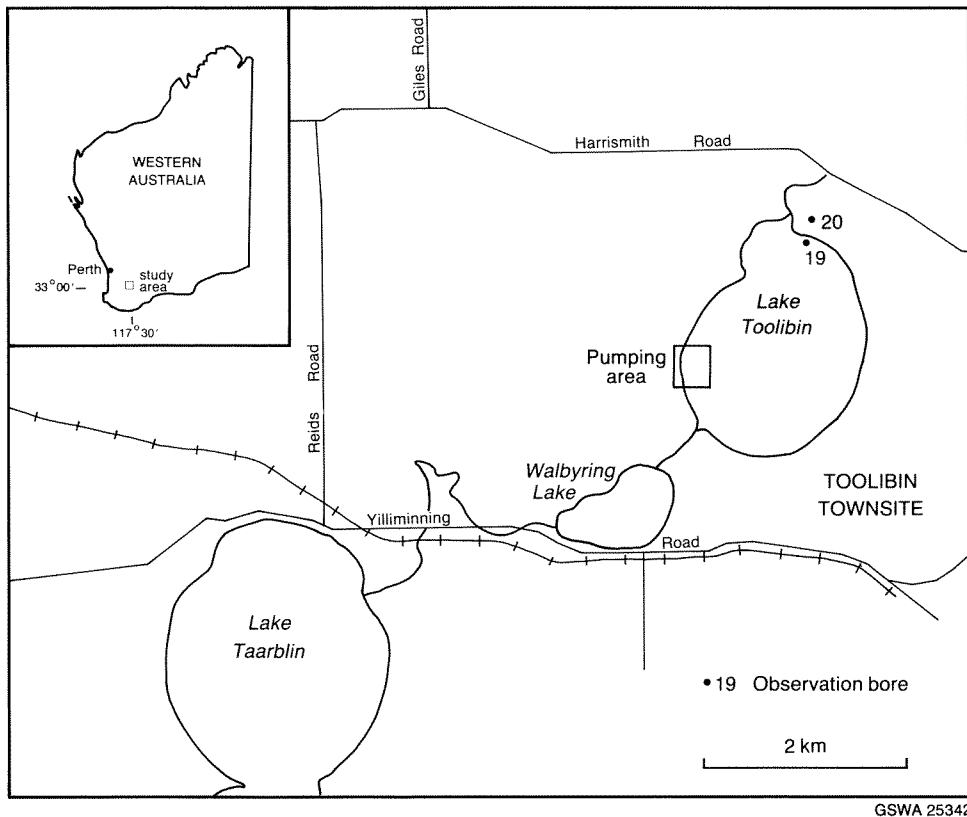


Figure 1. Lake Toolibin — location map

## Previous investigations

Investigations into salinization at Lake Toolibin began in 1977, and the Northern Arthur River Wetlands Committee was established. In 1987, the committee reported on the status and future of Lake Toolibin in its final report (NARWC, 1987). The hydrogeology of Lake Toolibin has been described by Martin (1986), and the lake hydrology discussed by Stokes and Sheridan (1985). A vegetation study was carried out by Mattiske (1986), and Halse (1987) discussed the effect of increased salinity on the waterbirds of Lake Toolibin.

## Methods

A production bore was drilled through the lakebed on the western side of Lake Toolibin (Fig. 1) in an area where the shallow depth to saline groundwater has resulted in severe salinization of the lakebed. The production bore and observation bores were drilled by the Mines Department Drilling Branch during 1988. Completion details for the bores are given in Table 1 and their locations are shown on Figure 2. The production bore (1/88), and the deep and intermediate observation bores (denoted by the suffix A and B respectively) were drilled using a mud-flush rotary method; the other (shallow) bores were drilled using solid augers. The annulus adjacent to the slotted intervals of the bores was packed with graded sand and the remaining annulus was sealed with cement slurry. All bores were developed by airlifting.

The casing of the production bore extends about 2.5 m above the lake floor and preformed-concrete well-liners with base and lid were placed around the casing. The concrete lid stands about 2.7 m above the lake floor and provides a platform, above the maximum lake waterlevel, for the automatic pump control. The control switches the pump off when the waterlevel in the bore is drawn down to about 28 m below ground level, and restarts the pump when the waterlevel recovers to about 25 m below ground level. The discharge from the bore is measured with an in-line flow meter, and the water is piped through about 8 km of 40 mm diameter poly-pipe to Lake Taarblin, a salinized lake downstream of Lake Toolibin.

## Geology

Much of the Lake Toolibin area is mantled by thin Cainozoic deposits consisting of laterite, colluvium, and reworked alluvium. The region, which lies within the Yilgarn Craton, is underlain by Precambrian granitic rocks and occasional dolerite dykes. The rocks have been weathered and lateritized and the thickness of the weathered profile ranges from a few to about 40 metres. Thin lacustrine sediments have been deposited in the lakes.

At the pumping area, the weathered profile is about 33 m thick and consists of variably coloured brown to white sandy clay and clayey sand. The profile intersected by bores O3A and O4A is weathered dolerite, whilst at all other sites weathered granite or migmatite is

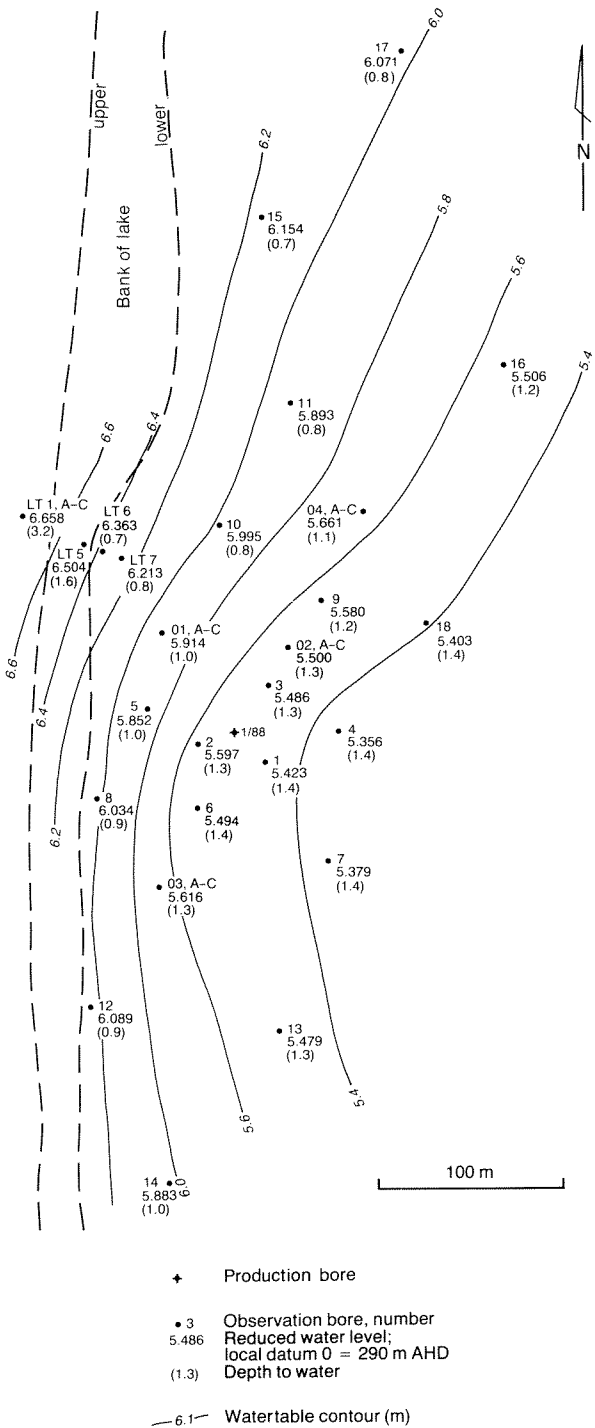


**Figure 2. Watertable contours at the pumping area, March 1989**

encountered. The upper 0.5–2 m of the weathered profile has been lateritized, and this is overlain by thin (<0.5 m) lacustrine deposits.

## Hydrogeology

The groundwater system at Lake Toolibin is unconfined and is recharged by direct rainfall infiltration

and by downward leakage from the lake when it contains water. When the lake is dry, the depth to groundwater beneath the lakebed is less than 2 m (Fig. 2) with groundwater being lost partly by evaporation and to some extent by transpiration from vegetation on the lake floor. During winter, when evaporation is low, the groundwater level rises and seepage faces develop in the salinized areas.

The direction of groundwater flow is normally towards Lake Toolibin but, when the lake contains water, there is some flow away from the lake near the southern end (Fig. 3). The March 1989 watertable contours for the pumping area (Fig. 2) imply an easterly groundwater flow towards the lake. The flattening of the watertable gradient in the direction of groundwater flow is probably due to loss of groundwater by evaporation.

The groundwater hydrographs of two bores, 19 and 20, near the northern end of Lake Toolibin are shown on Figure 4. The waterlevel in these bores is unaffected by the pumping, and the hydrographs show that the seasonal fluctuation in the watertable approached 1.7 m with minimum levels at the end of April and maximum levels between July and October. At the pumping area, the watertable rises to the floor of the lake during winter in response to reduced evaporation.

The groundwater in the region is saline and at the pumping area, the general range of salinity was 30 000–50 000 mg/L (total dissolved solids, Table 1). The salinity of the groundwater increased to about 60 000 mg/L near the centre of Lake Toolibin.

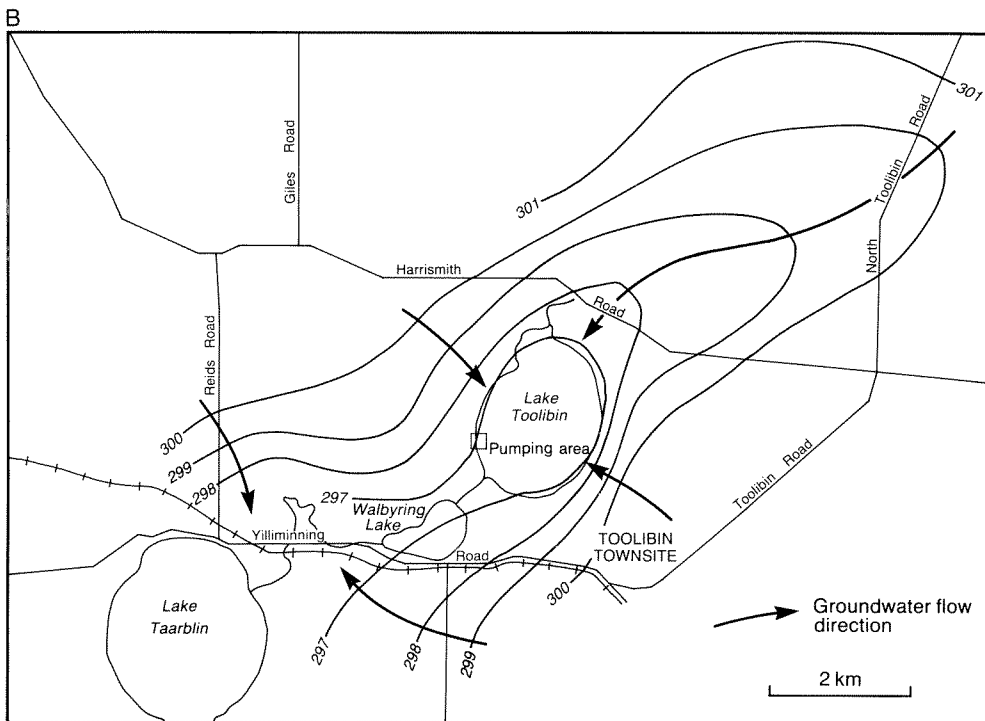
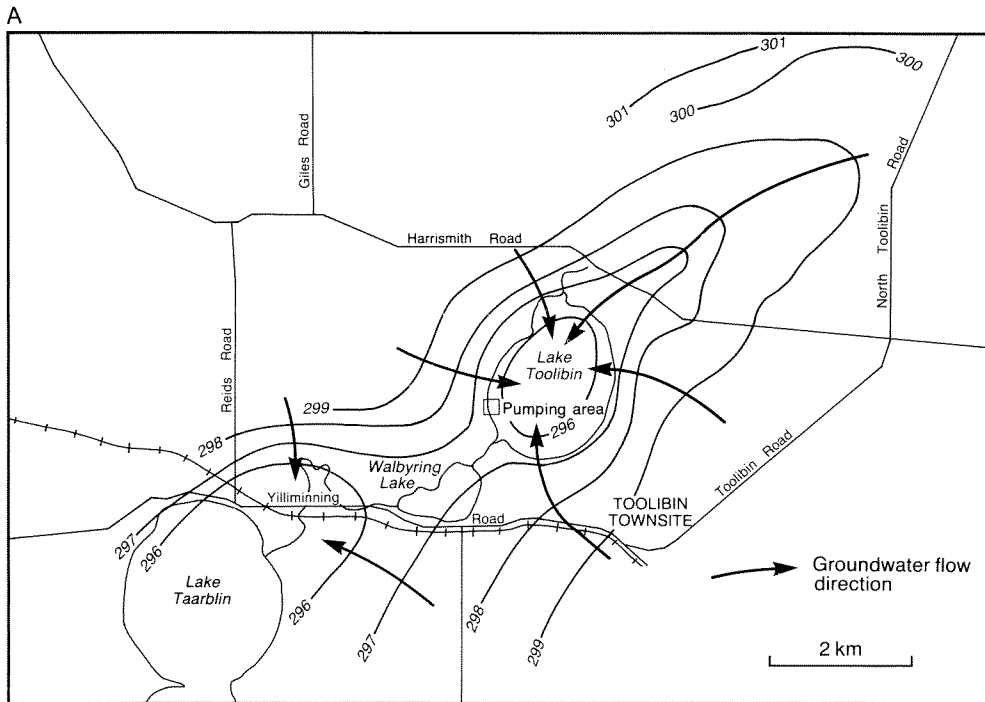
## Response to pumping

Pumping from production bore 1/88 commenced on 28 June 1989 and continued until the pump failed on about 9 November 1989. Pumping recommenced on 28 November, but heavy rainfall from the remnants of tropical cyclone Tina filled the lake in January 1990.

The waterlevels in the observation bores and the cumulative discharge from the production bore were monitored fortnightly for the first month of pumping, and monthly thereafter. The discharge rate between 28 June and 19 October ranged from 14.4 to 18.6 m<sup>3</sup>/day with an average of about 16 m<sup>3</sup>/day.

The watertable contours for 19 October (before the pump failed) are shown on Figure 5. With the exception of the area within about 30 m of the production bore, the watertable was higher than that recorded in March 1989; a reflection of the seasonal rise in the watertable. However, the watertable contours indicate radial groundwater flow toward the production bore. The regional inflow of groundwater toward the east is largely responsible for the observed steeper hydraulic gradient west of the production bore.

The changes in waterlevels in the observation bores result from a combination of pumping, variation in evapotranspiration, and seasonal recharge. Before the response to pumping can be evaluated, the recorded waterlevel changes at the pumping site need to



GSWA 25344

**Figure 3. Watertable contours and direction of groundwater flow at Lake Toolibin**  
**A. Lake dry**  
**B. Lake full**

**Table 1. Bore completion details**

Bore no.	Distance from 1/88 (m)	Depth (m)	Reduced level		Slotted interval (m BGL)	Salinity	
			TOC	GL (m AHD)		TDS (mg/L)	Date sampled
1/88	0	35.5	299.584	296.84	1 – 32.3	47 000	7/4/88
O1A	65.0	37.0	297.488	296.88	33.3 – 36.3	23 500	“
O1B	65.5	17.0	297.533	296.85	14 – 17	36 500	“
O1C	64.8	2.7	297.094	296.86	0.2 – 2.7	41 000	“
O2A	49.8	35.0	297.374	296.80	31 – 34	29 000	“
O2B	48.6	17.0	297.363	296.78	14 – 17	35 500	“
O2C	51.6	3.1	297.178	296.82	0.1 – 3.1	50 000	“
O3A	85.1	29.5	297.342	296.88	26 – 28	44 000	“
O3B	83.7	16.0	297.340	296.89	13 – 16	28 000	“
O3C	90.6	3.4	297.150	296.88	0.2 – 3.4	40 000	“
O4A	130.5	33.0	297.173	296.74	30 – 33	47 000	“
O4B	129.0	17.0	297.209	296.73	14 – 17	32 000	“
O4C	133.4	3.3	296.906	296.71	0.3 – 3.3	46 000	“
1	21.8	4.3	297.153	296.80	0.2 – 4.3	46 000	“
2	20.3	3.0	297.185	296.87	0.2 – 3.0	41 500	“
3	30.2	3.5	297.139	296.83	0.2 – 3.4	47 000	“
4	53.1	3.3	297.118	296.79	0.3 – 3.3	46 000	“
5	47.9	2.8	297.112	296.87	0.3 – 2.8	35 500	“
6	43.7	3.4	297.106	296.88	0.2 – 3.4	43 500	“
7	82.1	3.2	297.002	296.79	0.3 – 3.2	47 500	“
8	80.4	3.5	297.229	296.94	0.3 – 3.5	31 000	“
9	83.2	3.0	297.004	296.74	0.3 – 3.0	49 000	“
10	108.8	3.3	297.010	296.81	0.3 – 3.3	43 000	“
11	173.3	3.3	297.013	296.75	0.3 – 3.3	45 000	“
12	163.2	3.3	297.134	296.98	0.3 – 3.3	31 500	“
13	158.1	3.3	297.074	296.82	0.3 – 3.3	49 000	“
14	237.7	3.3	297.133	296.87	0.3 – 3.3	45 000	“
15	266.4	2.1	297.229	296.86	0.2 – 2.1	34 000	“
16	239.5	2.9	296.986	296.75	0.3 – 2.9	44 000	“
17	362.5	3.3	297.119	296.83	0.3 – 3.3	38 500	“
18	117.9	2.8	296.993	296.76	0.3 – 2.8	50 000	“
19	-	4.7	297.438	297.21	0.4 – 4.7	44 000	“
20	-	6.5	298.879	298.44	0.2 – 6.5	34 500	“
TO1A	160.0	38.0	300.734	299.92	33 – 36	42 000	22/3/83
TO1B	160.0	17.5	300.718	299.86	14.5 – 17.5	32 800	“
TO1C	160.0	6.3	300.726	299.88	3.3 – 6.3	8 500	11/9/84
TO5	126.2	2.2	298.891	298.10	0.2 – 2.2	ns	
TO6	116.7	1.1	297.963	297.10	0.2 – 1.1	ns	
TO7	108.8	1.1	297.813	296.96	0.2 – 1.1	35 500	11/9/84

Note: AHD Australian height datum  
 BGL below ground level  
 TDS total dissolved solids  
 TOC top of casing  
 GL ground level  
 ns not sampled

be corrected for the influence of evapotranspiration and recharge. This has been done by noting the changes in waterlevel, since pumping commenced, in observation bores 19 and 20 (Fig. 3). Because of the difference in the response of the two bores, the average change has been used to correct the drawdown.

**Analysis**

The corrected drawdown versus distance from the production bore for 19 October (113 days pumping) is shown on Figure 6. Two factors contribute to the observed scatter in the data points; the heterogeneity of the aquifer, and the use of an average correction for the regional trend.

The response to pumping has been analysed applying the Jacob distance–drawdown method (Kruseman and de Ridder, 1976) to the data obtained after 113 days pumping, with:

$$T = \frac{2.30 Q}{2\pi\delta s} \tag{1}$$

$$S = \frac{2.25Tt}{r_0^2} \tag{2}$$

$$k = T/b \tag{3}$$

- where T = transmissivity (m<sup>2</sup>/d)
- Q = pumping rate (16 m<sup>3</sup>/d)
- δs = slope of straight line per log cycle (1.19)
- S = specific yield
- t = time elapsed since pumping commenced (113 days)
- r<sub>0</sub> = distance from pumping bore zero drawdown (360 m)
- k = hydraulic conductivity (m/d)
- b = aquifer thickness (33 m)

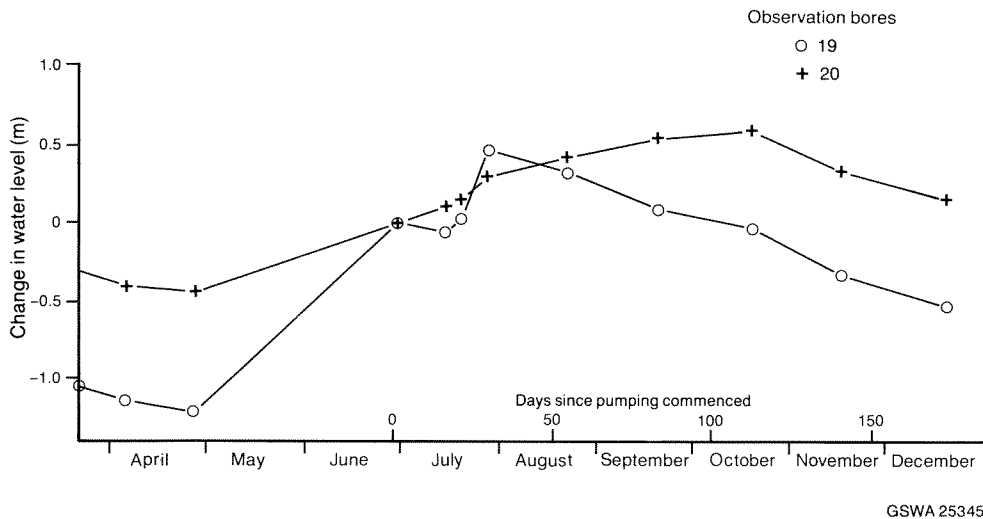


Figure 4. Groundwater hydrographs for bores 19 and 20

By substitution, the following values are obtained:

Transmissivity	=	4.92 m <sup>2</sup> /d
Specific yield	=	0.01
Hydraulic conductivity	=	0.15 m/d

### Long-term drawdown

The drawdown due to pumping for 300 and for 400 days has been evaluated by rearranging equation 2 to solve for  $r_0$ , and the resulting distance–drawdown lines are shown on Figure 6. Beyond this time, drawdown approaches steady-state conditions in response to regional groundwater inflow, local recharge, and reduced evaporation because of the greater depth to groundwater.

The results indicate that a drawdown of 1.5 m would occur 35–40 m from the production bore and that no drawdown would occur beyond about 650 metres. Additional production bores would be required to achieve the recommended Northern Arthur River Wetlands Committee (1987) minimum drawdown of 1.5 m over a larger area. The principle of superposition can be used to evaluate the drawdown resulting from the mutual interference of a number of pumping bores located some distance apart. A minimum drawdown of 1.5 m by mutual interference between two pumping bores would require a drawdown of 0.75 m midway between each bore. From the distance–drawdown data (Fig. 6), this would occur at 150 m from each bore, and a 1.5 m drawdown would require a spacing of about 300 m between the bores. The effect of mutual interference is shown schematically in Figure 7 for three pumping bores, firstly 300 m apart and in-line and, secondly, at the apices of a 300 m equilateral triangle.

### Borefield dewatering design

The salinized areas at Lake Toolibin, shown on Figure 8, are predominantly on the western and southern parts of the lake. In order to lower the watertable to a level which would effectively control salinization, at least 9 pumping bores (8, in addition to 1/88) would be required along the western side of the lake and a further 16 bores would be required for the remaining areas. The suitability of a site for a production bore will depend largely on avoiding weathered dolerite dykes and other locations with high proportions of clay in the weathered profile. Geophysical techniques involving the use of magnetic, electromagnetic, and possibly resistivity methods may be suitable for locating dykes and also for defining areas where drilling is most likely to be successful. Proposed drillhole sites are indicated on Figure 8.

### Discharge of groundwater

The groundwater pumped from production bore 1/88 has a salinity of 47 000 mg/L and is discharged to Lake Taarblin at a rate of 16 m<sup>3</sup>/day. This is equivalent to a discharge of about 270 tonnes of salt per year. With 25 production bores, each discharging 20 m<sup>3</sup>/day of 50 000 mg/L salinity water, about 9000 tonnes per year of salt would be discharged to Lake Taarblin. The accumulated salt would be flushed to the Blackwood River drainage system when the lake overflows. At present, the Blackwood system discharges about 2 x 10<sup>6</sup> tonnes per year of salt, and the additional salt from pumping Lake Toolibin would represent an increase of about 0.5%. Because Lake Taarblin discharges during large flow events, the effect of the additional salt on the salinity of the Blackwood river is likely to be small. If Lake

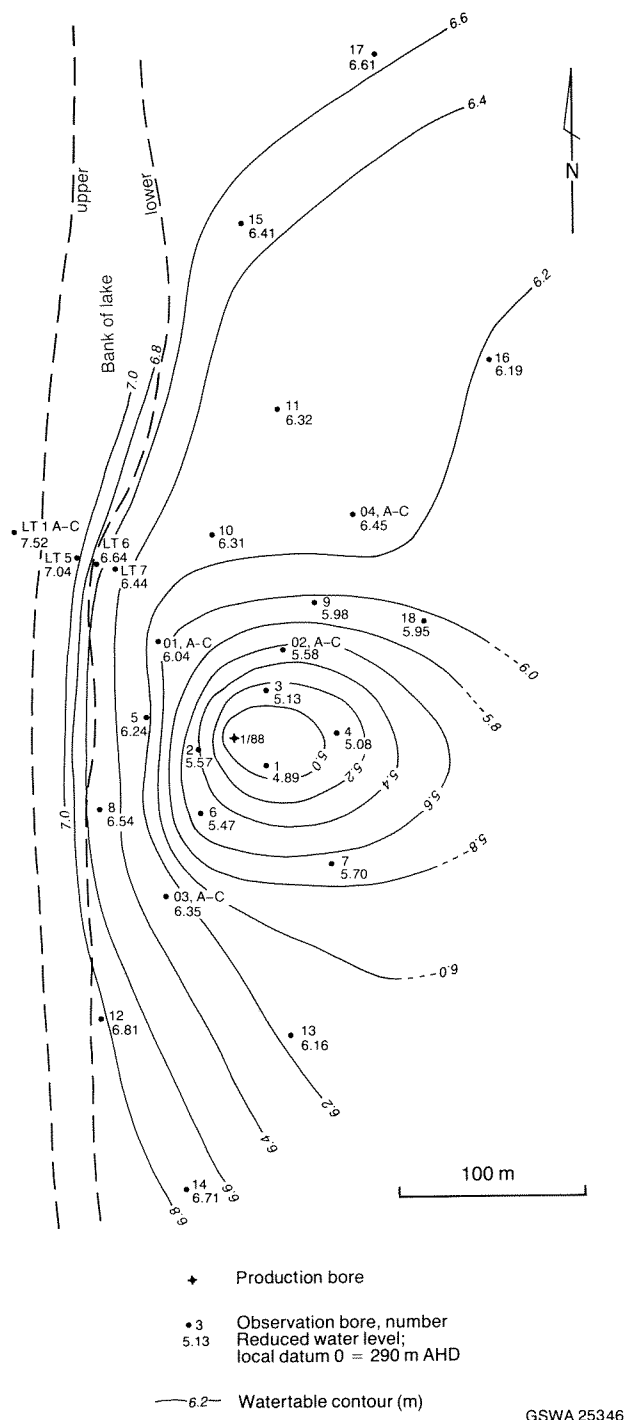
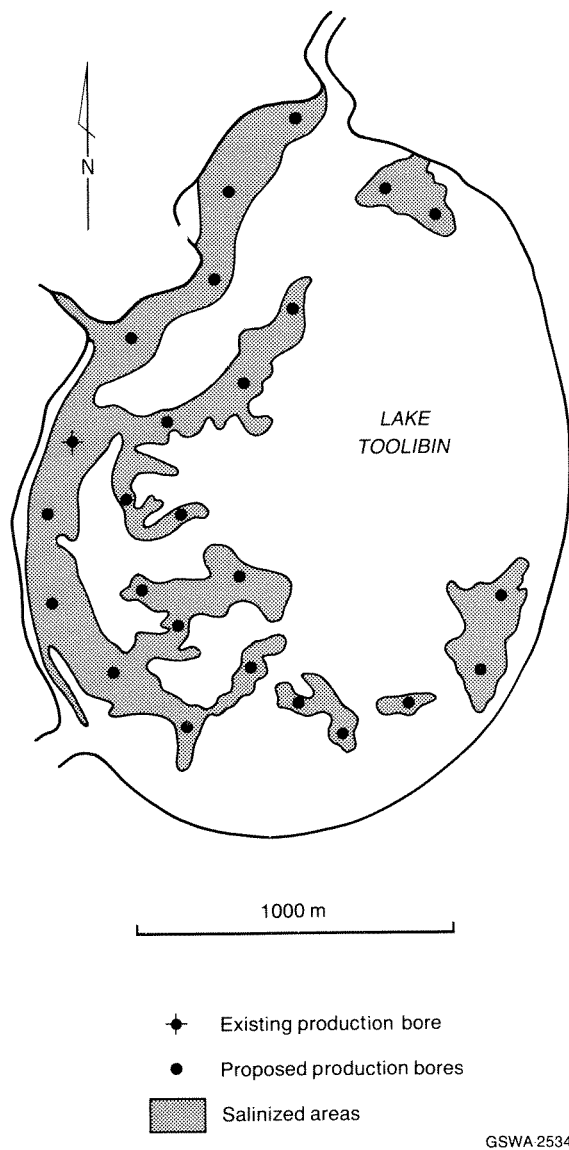


Figure 5. Watertable contours at the pumping area, October 1989





**Figure 8. Proposed locations for production bores**

Toolibin became completely salinized, and periodically flushed, the effect on the salinity of the Blackwood River may be greater than that resulting from pumping the groundwater to Lake Taarblin and subsequent flushing to the Blackwood River. However, the environmental impact of discharging saline groundwater into the Blackwood River system should be considered.

The potential use of solar distillation technology to recover freshwater and salt products from the groundwater pumped from Lake Toolibin should also be examined.

## Conclusions

The aquifer beneath Lake Toolibin is about 33 m thick and is heterogeneous and unconfined with a watertable less than 2 m below the lake floor, and salinity at that level of 30 000–60 000 mg/L. The hydraulic parameters of

the aquifer are: transmissivity 4.92 m<sup>2</sup>/d, hydraulic conductivity 0.15 m/d, and specific yield 0.01.

Control of salinization at Lake Toolibin can be achieved by lowering the watertable by mutual interference from pumping production bores located 300 m apart. Pumping from nine production bores on the western side of the lake and sixteen at other sites would lower the watertable by at least 1.5 m in areas which are threatened by salinization. About 20 shallow (<4 m) observation bores, midway between production bores, would be required to monitor the effect of pumping.

The discharging of saline water to Lake Taarblin is unlikely to significantly affect salinity in the Blackwood River, but both the environmental impact of this discharge, and the feasibility of salt and of freshwater reclamation by solar distillation should be considered.

The results from this investigation show that pumping groundwater can lower the watertable and thereby assist in the control of land salinization resulting from the clearing of native vegetation in agricultural areas of Western Australia.

## Acknowledgements

The Department of Conservation and Land Management (CALM) provided the electrical power and pipeline for the investigation. Particular thanks are due to Mr D. Graham of CALM, Narrogin, who monitored waterlevels and the discharge.

## References

- HALSE, S. A., 1987, Probable effect of increased salinity on the water birds of Lake Toolibin: Dept of Conservation and Land Management, Technical Report No. 15.
- KRUSEMAN, G. P., and de RIDDER, N. A., 1976, Analysis and evaluation of pumping test data: International Institute for Land Reclamation and Improvement, Bulletin 11.
- MARTIN, M. W., 1986, Hydrogeology of Lake Toolibin: Western Australia Geological Survey, Record 1986/13.
- MATTISKE, E. M., 1986, Progress report — Lake Toolibin vegetation study, December 1986: E.M. Mattiske and Associates (unpublished).
- NORTHERN ARTHUR RIVER WETLANDS COMMITTEE, 1987, The status and future of Lake Toolibin as a wildlife reserve: Western Australia Water Authority, Report No. WS2.
- STOKES, R. A., and MARTIN, M. W., 1986, The hydrology of an ephemeral lake in the Wheatbelt of South Western Australia: Hydrology and Water Resources Symposium 1986. The Institution of Engineers, Australia.
- STOKES, R. A., and SHERIDAN, R. J., 1985, Hydrology of Lake Toolibin: Western Australia Water Authority, Report No. WH2.



# The geology and hydrogeology of the superficial formations between Cervantes and Lancelin, Western Australia

by  
A. M. Kern

## Abstract

From 1985 to 1987, drilling at 35 sites on the Swan Coastal Plain between Cervantes and Lancelin was undertaken to investigate the hydrogeology, assess the groundwater resources, and provide a network of bores for long-term monitoring. A total of 65 bores was drilled, with up to four monitoring bores at each site. The aggregate depth drilled was 2825 m and the deepest bore was 111 m.

The superficial formations in this area consist mainly of shallow-water marine and eolian sands and limestone, unconformably overlying Mesozoic formations. In the eastern part of the coastal plain, they range in thickness from about 50 m in the south to less than 10 m in the north. The thickness of these deposits is more variable in the Coastal Belt due to the rugged topography.

The superficial formations contain a predominantly unconfined regional groundwater flow system which receives recharge from rainfall over the whole area. Groundwater flows westwards from the Gingin Scarp to discharge along the coast. The aquifer is recharged mainly by direct infiltration of rainfall supplemented by both seepage from runoff and upward leakage from Mesozoic aquifers in the northeast and the coastal area. Groundwater discharge occurs along the shoreline above a saltwater wedge. There is also significant downward leakage to the Leederville Formation in the southeast.

Groundwater storage in the superficial formations and the annual outflow at the coast are estimated to be  $10 \times 10^9 \text{ m}^3$  and  $100 \times 10^6 \text{ m}^3/\text{year}$  respectively. The major groundwater resources of the area lie west of Regans Ford where the salinity is less than 1000 mg/L (total dissolved solids) and where the saturated thickness of the unconfined superficial formations exceeds 40 m. There is also groundwater of low salinity (less than 500 mg/L) within the Tamala Limestone between Lancelin and Wedge Island. The groundwater in the northern part of the area and along the Gingin Scarp is generally brackish.

**KEYWORDS:** Groundwater, salinity, hydrogeology, Swan Coastal Plain, geology, stratigraphy, Perth Basin

## Introduction

The area investigated extends over 1900 km<sup>2</sup> on the Swan Coastal Plain between Cervantes and Lancelin. The project was named the Cataby Project after a small settlement on the Brand Highway located approximately 170 km north of Perth (Fig. 1).

The project, carried out by the Geological Survey of Western Australia (GSWA), is a northward extension of the Salvado Project drilled in 1980 (Moncrieff and Tuckson, 1989). The objectives of the project were to investigate the geology of the superficial formations\* and to identify the underlying Mesozoic formations, to investigate the hydrogeology and assess the groundwater resources of the area, and to provide a network of groundwater observation bores for long-term monitoring.

The project is part of a long-term program to evaluate the groundwater resources of the Perth Basin. Funding was initially jointly provided by the Commonwealth and State Governments under the National Water Resources Assessment Programme. From mid-1986, however, the State Government alone has financed the project.

\* Superficial formations are Pliocene to Holocene sedimentary rocks which underlie the Swan Coastal Plain in the Perth Basin; despite the variability in lithologies, these formations form a single aquifer system (Allen, 1976).

About two-thirds of the project area (including the Nambung National Park and numerous nature reserves) is covered by native vegetation. Most of the clearing for agriculture has taken place in the sandy central area and along the Gingin Scarp. The largest towns in the area are Lancelin and Cervantes, and there are smaller coastal settlements at Wedge Island and Grey.

## Previous work

The superficial formations of the coastal plain were mapped by Low (1972) and Lowry (1974). Exploration for oil and gas by West Australian Petroleum Pty (Wapet) provided the first information on the underlying Mesozoic formations (Moyes, 1970; Bird and Moyes, 1971) and led to the discovery of gas at Walyering, approximately 7 km northwest of Cataby. Prospecting for heavy minerals in the early 1970s along the foot of the Gingin Scarp in the project area resulted in the discovery of the Gingin and Munbinea Shorelines (Baxter, 1977). Commercial development of the mineral-sand deposit at Cooljarloo is under way.

Numerous exploratory drilling programs for coal were carried out in the late 1970s and early 1980s in the northern part of the project area where the Cattamarra Member of the Cockleshell Gully Formation underlies a veneer of Cainozoic sediments.

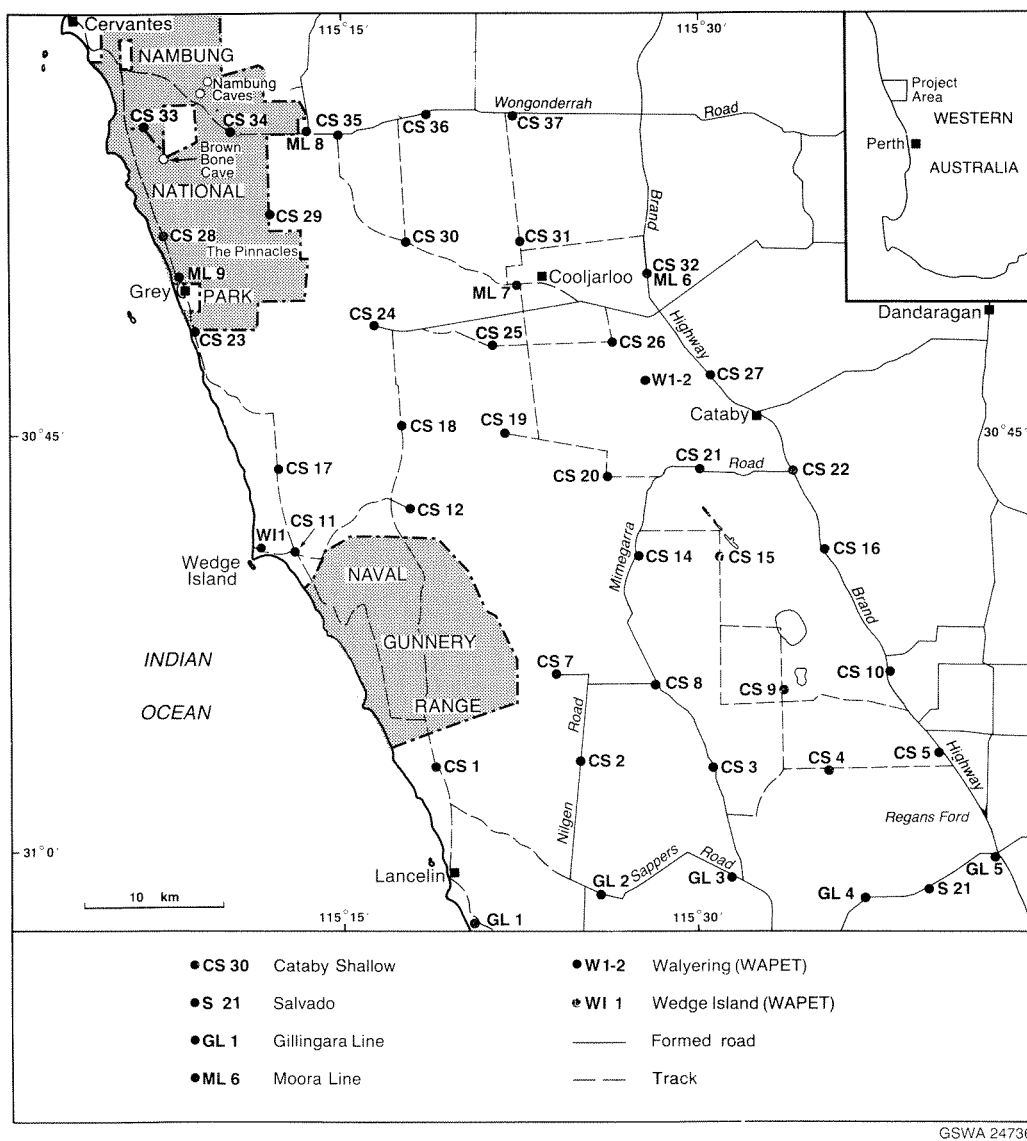


Figure 1. Bore location and access

In 1974, deep exploratory drilling for water along the Moora Line (ML) was carried out in the area by the GSWA (Briese, 1979). The Gillingarra Line (GL) was drilled along the southern boundary of the project area between 1982 and 1986 (Moncrieff, 1989).

The hydrogeology of the superficial formations south of Lancelin has been described by Moncrieff and Tuckson (1989). Details of the present project are given by Kern (1988a,b).

## Climate

The region has a mediterranean climate characterized by hot, dry summers and mild, wet winters. The average annual rainfall decreases northward from about 630 mm at Lancelin to about 570 mm at Cervantes. Most of the rain falls during the winter months between April and October. The average annual evaporation is about

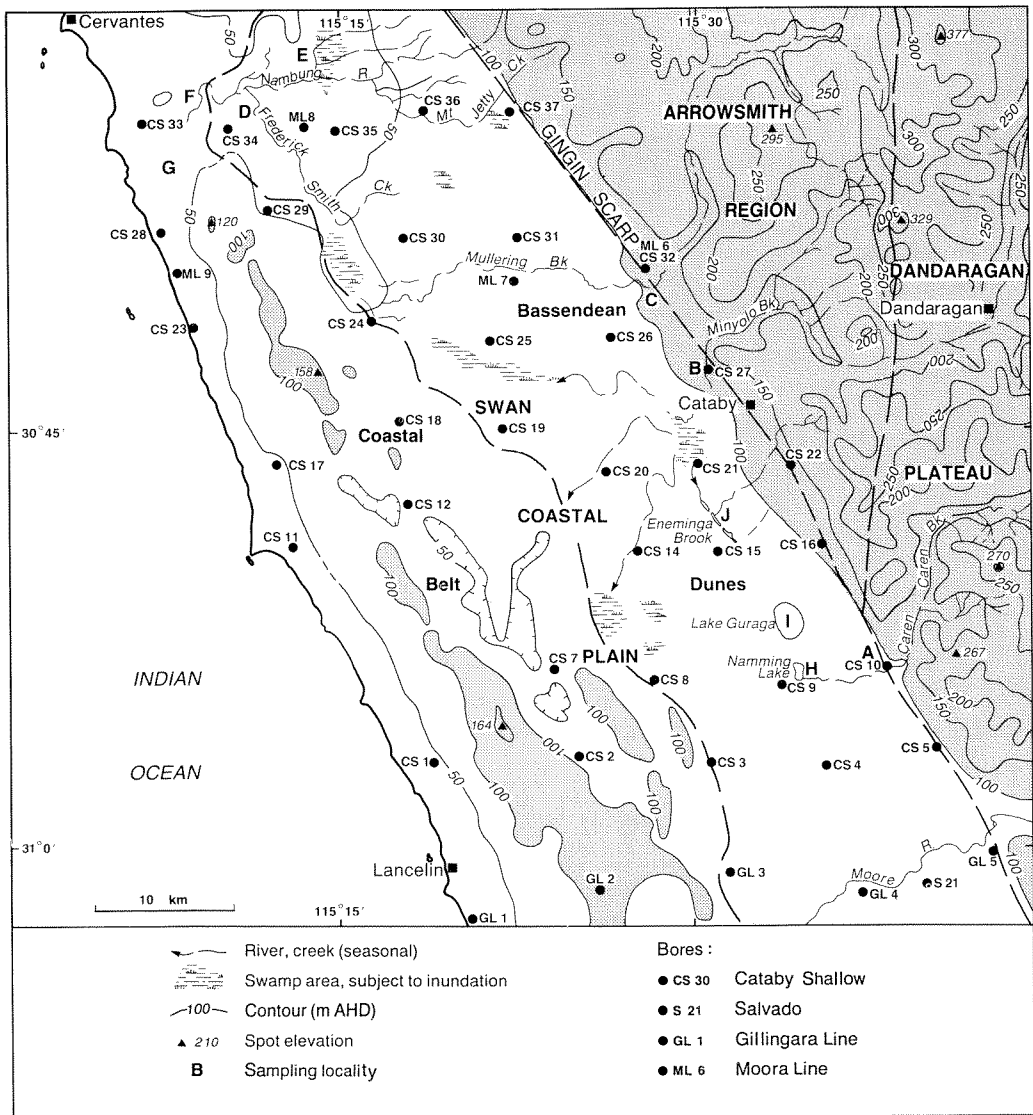
2000 mm and rainfall exceeds evaporation only during the winter months.

## Physiography

### Landform

The investigation area lies on the Swan Coastal Plain which is bounded to the east by the Gingin Scarp. The scarp was formed by marine erosion and separates the coastal plain from the Dandaragan Plateau in the southeast and the Arrowsmith Region in the northeast (Fig. 2).

The coastal plain is a low-lying, gently undulating area covered by Holocene and Pleistocene coastal dunes and shoreline deposits, with belts of alluvium and colluvium along the foot of the Gingin Scarp. The coastal plain may be subdivided into two main



GSWA 24737

Figure 2. Physiography and drainage

geomorphic units; the Coastal Belt and the Bassendeau Dunes.

The Coastal Belt consists of Quaternary shoreline deposits and the Quindalup and Spearwood Dunes. The Quindalup Dunes are composed of the Safety Bay Sand, which forms both stabilized and mobile dunes up to 150 m high. These overlap the Spearwood Dunes, which consist largely of lithified Pleistocene eolianite with leached quartz sand (Tamala Limestone), and form linear ridges rising to 164 m AHD and a low limestone plateau.

Well-developed cave systems occur in the limestone in a number of localities in the Nambung National Park. Limestone pinnacles are particularly well developed in the Tamala Limestone near Cervantes. The cylindrical columns of limestone represent strongly lithified fillings of solution pipes which formed in eolianite during an earlier erosion cycle.

The Bassendeau Dunes occur in a zone about 15 km wide between the Coastal Belt and the Gingin Scarp. They consist of a belt of low dunes of leached quartz sand (Bassendeau Sand) with numerous interdunal lakes and seasonal swamps.

### Surface water

The area is drained by watercourses originating on the Dandaragan Plateau and Arrowsmith Region. All except the Moore River are seasonal streams terminating in large swamps or lakes in the Bassendeau Dunes (Fig. 2). Surface drainage is absent in the Coastal Belt, but there are well-developed cave systems which allow extensive subsurface flow of water. When the Nambung River is active it flows through limestone caves towards the sea.

Stream salinity ranges from fresh to brackish with the highest salinities occurring in early winter when salinized

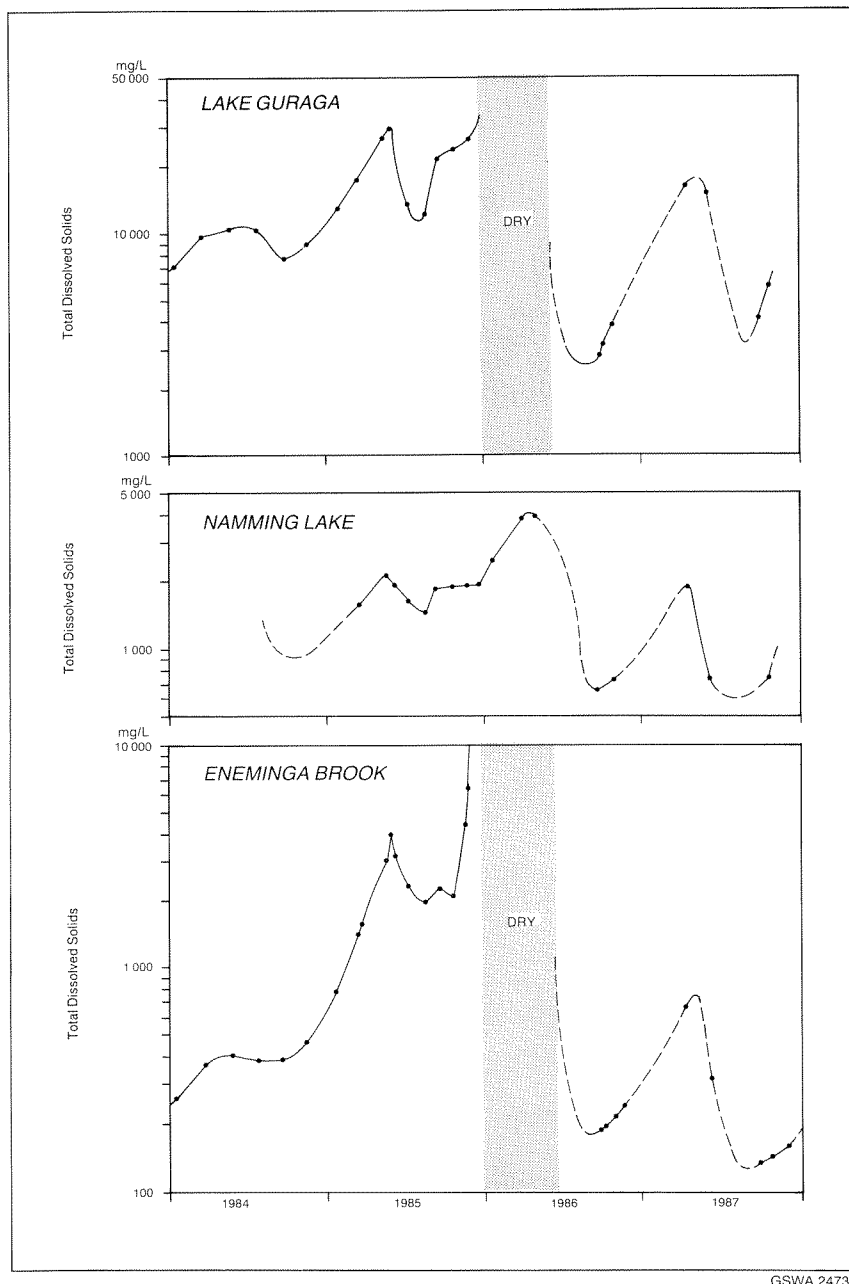


**Figure 3. Wetland salinity**

areas are flushed by heavy rainfall (Kern, 1988a). The salinity of the Nambung River decreases downstream owing to dilution by tributaries with lower salinities. It is lowest where it enters the caves in the Tamala Limestone.

A number of permanent and seasonal lakes and swamps occur in interdunal depressions in the Bassendean Dunes. They occupy about 100 km<sup>2</sup> and usually fill with water at the end of winter when chains of swamps and lakes connect to form broad streams which flow northwest toward the Nambung River.

Major lakes are generally permanent and in hydraulic connection with the unconfined aquifer. The lake levels are highest at the end of winter (September) and lowest at the end of summer (May). They were extremely low during the 1985/86 summer following below-average winter rainfall, and some lakes were completely dry (Fig. 3).

Three wetlands in the project area were closely monitored during the period 1985–1987 (Figs 2 and 3). Two of these, Namming Lake and Eneminga Brook, contain fresh to brackish water, whereas the third

wetland, Lake Guraga, contains brackish to saline water. Monitoring shows that the salinities are highest when waterlevels are lowest.

## Investigation techniques

### Drilling and bore construction

The project commenced in February 1985 and was completed in July 1987. Drilling was carried out at thirty-five sites located in seven easterly trending lines across the coastal plain. Sixty-five bores (prefixed CS) were drilled to a maximum depth of 111 m; 60 bores were cased and completed (Table 1). The remaining bores were abandoned due to drilling or construction difficulties. The aggregate depth drilled by the Mines Department Drilling Branch was 2825 m.

At each site, a deep bore was first drilled to about 10 m into the Mesozoic strata underlying the superficial formations. Where the superficial formations were thin, drilling was continued to a total depth of about 50 m. Following lithological and geophysical logging, the bore was cased to the appropriate depth and a second, shallower bore drilled alongside. Where required, a third bore was drilled and, very rarely, a fourth. The shallowest bores were generally completed at about 10 m below the watertable.

The observation bores were cased with PVC or polyethylene pipes (slotted over the selected interval) with a protective steel casing at the surface. Steel casing was used throughout where PVC was impractical. The casing diameter in cored holes is either 35 mm or 50 mm internal diameter and generally 100 mm in rotary-drilled holes. The annulus between the casing and the borehole was packed with graded sand.

### Sampling, logging, and testing

In the bores drilled using the Jacro rotary rig, samples were taken at 3 m intervals and at any change in lithology. Continuous cores were obtained with the wireline-drilling technique used by the Edson rig, and sludge samples were collected only when core recovery was uncertain. The wireline-drilling technique provided good core recovery commonly varying between 30% and 80%.

On completion of drilling, a suite of geophysical logs was generally run. Natural gamma, normals resistivity, point resistance, and caliper logs were run in rotary-drilled holes. Neutron logs were run through drillpipe in a few of the cored holes. Sidewall cores for palynological and lithological determinations were collected at five sites after completion of the geophysical logging.

All the bores were developed by air-lifting and water samples were submitted to the Chemistry Centre (W.A.) for chemical analysis.

All observation bores were levelled to the Australian Height Datum (AHD) by the Surveys and Mapping Division of the Department of Mines. Monitoring of waterlevels in the observation bores was carried out at the end of winter and of summer when waterlevels are respectively at their highest and lowest. Some sites were monitored over two years until October 1987.

## Geology

### Setting

The Cataby area is located in the central part of the Perth Basin where two structural subdivisions are recognized: the Dandaragan Trough and the Beagle Ridge (Playford et al., 1976). The Dandaragan Trough contains as much as 15 000 m of Phanerozoic sediments, mostly of Permian and Mesozoic age. The Beagle Ridge is a narrow mid-basin ridge of relatively shallow basement between the Dandaragan Trough and the Abrolhos Sub-basin.

Sediments of Triassic to Quaternary age were intersected during drilling (Table 2). The Tertiary and Quaternary units together are referred to as the superficial formations (Fig. 4).

### Structure

The Perth Basin is characterized by normal faulting, with minor folding (Fig. 5). Three major faults with a north-northwesterly to northerly trend occur in the project area. These are the Beagle, Lesueur and Warradarge Faults. A strongly faulted anticline is developed between the Lesueur and Warradarge Faults. A syncline occurs in the southern part of the project area and is referred to as the Yancheep Syncline.

The erosion surface on which the Cainozoic sediments were deposited slopes towards the coast from about 120 m AHD at Cataby to about 25 m below sea level between Wedge Island and Lancelin (Fig. 5). The gradient is steep along the Gingin Scarp and near the coast between Cervantes and Wedge Island.

The Cainozoic sediments are generally flat lying and range in thickness from a maximum of about 170 m in the Coastal Belt to less than 10 m along the northern boundary of the project area (Fig. 6).

### Stratigraphy

Only those formations encountered in the drilling program are described and these are listed, in order, from oldest to youngest.

#### *Kockatea Shale*

The Kockatea Shale was intersected at shallow depth at three sites on the Beagle Ridge where it is overlain

**Table 1. Bore data**

Bore	Grid ref. AMG Zone 50	Drilling		Elevation (m AHD)		Total depth (m)	Top of Mesozoic (m AHD)	Casing size (mm)	Slotted/screened interval (m bns)	Aquifer	Head (m AHD) (26.5.87)	Salinity TDS (mg/L)	Status
		Comm.	Compl.	Surface	Top casing								
CS1D	392E/747N	14.04.86	21.04.86	25.126	26.124	59.0	-22	35	44.0 – 46.0	Tamala	0.6	650	obs
CS2A	489E/753N	04.12.85	12.12.85			90.5	-1	103					abd
CS2B	489E/753N	05.02.86	13.02.86			91.5	-1	152					abd
CS2C	489E/753N	11.03.86	20.03.86			66.0	-1	155					abd
CS2D	489E/757N	21.03.86	14.04.86	79.725	80.128	111.0	-1	103	1.0 – 77.0	Tamala	20.9	580	obs
CS3S	577E/752N	12.05.86	12.05.86	65.925	66.698	19.0	11	35	12.0 – 18.0	Guildford	48.7		obs
CS3D	577E/752N	07.05.86	12.05.86	5.905	66.730	68.3	11	35	48.0 – 54.0	Guildford/Ascot	48.6	220	obs
CS4D	654E/751N	23.05.86	23.05.86	77.990	78.857	19.0	10	35	11.0 – 17.0	Guildford	73.1	700	obs
CS4S	654E/751N	13.05.86	23.05.86	77.961	78.731	77.5	10	35	33.5 – 39.5	Guildford	68.0	1 040	obs
CS5I	727E/754N	28.02.85	06.03.85	89.816	90.826	60.5	60	100	21.0 – 26.0	Guildford	80.3	1 220	obs
CS7D	471E/754N	22.04.85	29.04.86	80.462	81.576	87.3	1	35	73.5 – 79.5	Tamala	19.7	950	obs
CS8S	538E/805N	06.05.86	06.05.86	57.585	58.542	12.0	10	35	6.0 – 12.0	Guildford	49.4		obs
CS8I	538E/805N	01.05.86	06.05.86	57.594	58.563	32.4	10	35	26.5 – 32.5	Guildford	49.4	4 420	obs
CS8D	538E/804N	30.04.86	01.05.86	57.622	58.456	50.8	10	35	41.5 – 46.5	Ascot	49.4	2 820	obs
CS9S	623E/804N	03.04.85	03.04.85	80.135	81.112	15.5	19	100	8.0 – 14.0	Guildford	73.9	700	obs
CS9M	623E/804N	02.04.85	04.04.85	80.172	81.139	50.0	19	100	42.0 – 48.0	Ascot	68.5	1 860	obs
CS9D	623E/804N	01.04.85	02.04.85	80.172	81.187	71.0	19	100	56.0 – 62.0	Ascot	68.5	2 030	obs
CS10S	691E/814N	25.02.85	26.02.85	97.622	98.564	20.0	76	100	13.0 – 19.0	Guildford	81.5		obs
CS10D	691E/814N	21.02.85	25.02.85	97.524	98.529	45.0	76	100	31.5 – 35.5	Leederville	78.6	1 570	obs
CS11S	296E/889N	18.06.87	19.06.87	28.735	29.090	45.2	-14	50	33.0 – 45.0	Tamala	0.2	910	obs
CS11D	296E/889N	10.06.87	18.06.87	28.750	29.110	107.3	-14	50	86.0 – 102.0	Yarragadee	0.1	22 300	obs
CS12D	371E/918N	22.06.87	26.06.87	45.229	45.656	66.0	1	50	30.0 – 42.0	Tamala	16.8	530	obs
CS14S	524E/891N	18.03.85	19.03.85	63.242	64.215	9.0	15	100	2.0 – 8.0	Guildford	61.7	390	obs
CS14M1	524E/891N	15.03.85	18.03.85	63.398	64.329	28.0	15	100	21.0 – 27.0	Ascot	59.6	810	obs
CS14M2	524E/891N	14.03.85	15.03.85	63.423	64.397	43.0	15	100	36.0 – 42.0	Ascot	59.4	920	obs
CS14D	524E/891N	11.03.85	13.03.85	63.345	64.394	63.0	15	100	51.0 – 57.0	Leederville	59.4	940	obs
CS15S	579E/891N	27.03.85	28.03.85	77.124	78.040	16.0	19	100	9.0 – 15.0	Guildford	71.6	860	obs
CS15M	579E/891N	26.03.85	28.03.85	77.046	78.030	37.0	19	100	30.0 – 36.0	Ascot	64.8	820	obs
CS15D1	579E/891N	20.03.85	23.05.85			65.0	19						abd
CS15D2	579E/891N	25.03.85	28.03.85	77.124	78.040	61.0	19	100	51.0 – 57.0	Ascot	64.8	680	obs
CS16D	647E/897N	19.02.85	20.02.85	117.527	118.559	39.0	72	100	28.0 – 36.0	Guildford			abd
CS16DA	647E/897N	19.11.86	24.11.86	117.618	118.784	50.7	72	35	34.0 – 40.0	Guildford	86.5		obs
CS17D	283E/943N	22.05.87	09.06.87	35.982	36.525	54.2	2	50	36.2 – 54.2	Lesueur	8.5	460	obs
CS18D	364E/973N	04.12.86	05.12.86	44.739	45.595	59.9	8	35	28.0 – 36.0	Tamala	32.2	600	obs
CS19D	452E/968N	10.12.86	11.12.86	59.823	60.908	48.0	13	35	35.0 – 45.0	Ascot	45.1	770	obs
CS20S	403E/942N	02.12.86	02.12.86	70.312	71.291	19.0	19	35	9.0 – 18.0	Guildford	59.2	810	obs
CS20D	503E/942N	26.11.86	01.12.86	70.282	71.277	80.8	19	35	37.0 – 46.0	Ascot	58.9	940	obs
CS21D	564E/949N	06.03.85	08.03.85	85.361	86.379	31.0	25	100	25.5 – 30.0	Guildford	72.2	620	obs
CS22D	627E/948N	14.02.85	18.02.85	136.959	137.837	26.0	116	100	15.5 – 19.5	Guildford			abd
CS22DA	627E/948N	24.11.86	25.11.86	136.949	137.828	53.8	116	35	29.0 – 35.0	Yarragadee	100.1		obs
CS23D	225E/035N	01.09.86	09.09.86	7.424	8.526	17.5	-4	35	3.0 – 11.0	Guildford	0.1	430	obs
CS24D	345E/040N	03.12.86	04.12.86	44.875	45.755	30.8	28	35	8.0 – 16.0	Guildford	44.0		obs
CS25S	426E/027N	18.08.86	19.08.86	64.520	65.194	25.0	20	35	17.0 – 23.0	Yarragadee	50.3	930	obs

Table 1. (continued)

Bore	Grid ref. AMG Zone 50	Drilling		Elevation (m AHD)		Total depth (m)	Top of Mesozoic (m AHD)	Casing size (mm)	Slotted/screened interval (m bns)	Aquifer	Head (m AHD) (26.5.87)	Salinity TDS (mg/L)	Status
		Comm.	Compl.	Surface	Top casing								
CS25D	426E/027N	13.08.86	14.08.86	64.522	65.178	80.5	20	35	68.0 – 74.5	Guildford	50.6	1 220	obs
CS26S	505E/031N	13.08.86	13.08.86	87.151	88.007	14.0	32	35	6.0 – 12.0	Guildford	81.4	240	obs
CS26D	505E/031N	08.08.86	12.08.86	87.183	87.853	56.6	32	35	47.0 – 53.0	Ascot	81.4	560	obs
CS27D	571E/011N	12.02.85	14.02.85	106.171	107.181	30.6	81	100	19.0 – 24.0	Guildford	97.2	1 180	obs
CS28D	203E/095N	28.08.86	28.08.86	2.301	3.132	14.4	-7	35	4.5 – 8.0	Tamala	0.1	2 170	obs
CS29S	275E/112N	23.06.86	24.06.86	41.669	42.797	12.0	33	35	5.0 – 11.0	Tamala/Lesueur	37.2	350	obs
CS29D	275E/112N	19.06.86	23.06.86	41.667	42.526	50.5	33	35	41.0 – 47.0	Lesueur	37.2	690	obs
CS30S	356E/096N	16.07.86	16.07.86	51.999	52.746	10.0	28	35	4.0 – 9.0	Guildford	47.9	2 740	obs
CS30D	560E/096N	14.07.86	16.07.86	51.974	52.746	50.0	28	35	42.9 – 48.5	Yarragadee	47.8	7 510	obs
CS31S	441E/097N	21.08.86	22.08.86	67.348	68.127	15.0	33	35	8.0 – 14.0	Guildford	65.6	1 170	obs
CS31D	441E/097N	19.08.86	20.08.86	67.369	68.075	38.6	33	35	28.0 – 34.0	Guildford	64.8	880	obs
CS32D	528E/077N	07.02.85	11.02.85	112.135	113.054	25.8	109	100	7.5 – 12.5	Yarragadee	106.4	2 370	obs
CS33D	188E/167N	27.08.86	28.08.86	2.787	3.884	17.5	-10	35	4.0 – 11.0	Tamala	0.1	760	obs
CS34S	248E/166N	17.06.86	18.06.86	36.424	37.153	24.0	23	35	17.0 – 23.0	Guildford	22.7	780	obs
CS34D	248E/166N	12.06.86	17.06.86	36.356	37.071	50.5	23	35	43.0 – 48.0	Lesueur	22.7	1 020	obs
CS35S	320E/166N	01.07.86	01.07.86	45.415	46.113	15.0	38	35	10.0 – 14.0	Cockleshell Gully	40.8	530	obs
CS35D	320E/166N	25.06.86	30.06.86	45.365	46.098	47.5	38	35	36.8 – 42.8	Cockleshell Gully	40.6	1 450	obs
CS36S	378E/182N	09.07.86	09.07.86	55.541	56.301	9.5	47	35	2.0 – 8.5	Guildford	53.4	3 820	obs
CS36D	378E/182N	01.07.86	09.07.86			50.5	47	35					abd
CS37S	434E/182N	24.07.86	25.07.86	88.450	89.172	11.0	86	35	4.0 – 10.0	Yarragadee	84.3	360	obs
CS37D	434E/182N	17.07.86	24.07.86	88.435	89.168	50.5	86	35	41.6 – 47.6	Yarragadee	84.6	260	obs

NOTES: AHD: Australian height datum TDS: total dissolved solids obs: observation bore abd: abandoned

**Table 2. Stratigraphic succession**

<i>System</i>	<i>Age</i>	<i>Series</i>	<i>Formation</i>	<i>Maximum thickness penetrated (m)</i>	<i>Lithology</i>		
QUATERNARY	Holocene		Alluvial, colluvial and swamp deposits	23	sand, clay		
			Safety Bay Sand	3	sand		
	Late Pleistocene		Bassendean Sand	2	sand		
			Tamala Limestone	81	sand, limestone, clay		
	Pleistocene		Guildford Formation	53	sand, clay		
TERTIARY	Pliocene		Yoganup Formation	20	sand, clay		
			Ascot Formation	29	limestone, sand		
			-----UNCONFORMITY-----				
CRETACEOUS	Early-Late		Coolyena Group				
			Lancelin Formation	-	marl		
			Osborne Formation	-	shale, siltstone, sandstone		
	-----UNCONFORMITY-----						
	Early		Leederville Formation	20	sandstone, siltstone, shale		
South Perth Shale			-	shale			
-----UNCONFORMITY-----							
	Middle-Late		Yarragadee Formation	46	sandstone, siltstone		
	Middle		Cadda Formation	-	shale, siltstone, sandstone		
	JURASSIC	Early		Cockleshell Gully Formation			
Cattamarra Member				42	sandstone, siltstone, shale		
Eneabba Member				40	sandstone, siltstone, shale		
TRIASSIC	Middle-Late		Lesueur Sandstone	42	sandstone		
			Early		Woodada Formation	-	sandstone, siltstone, shale
					Kockatea Shale	7	siltstone

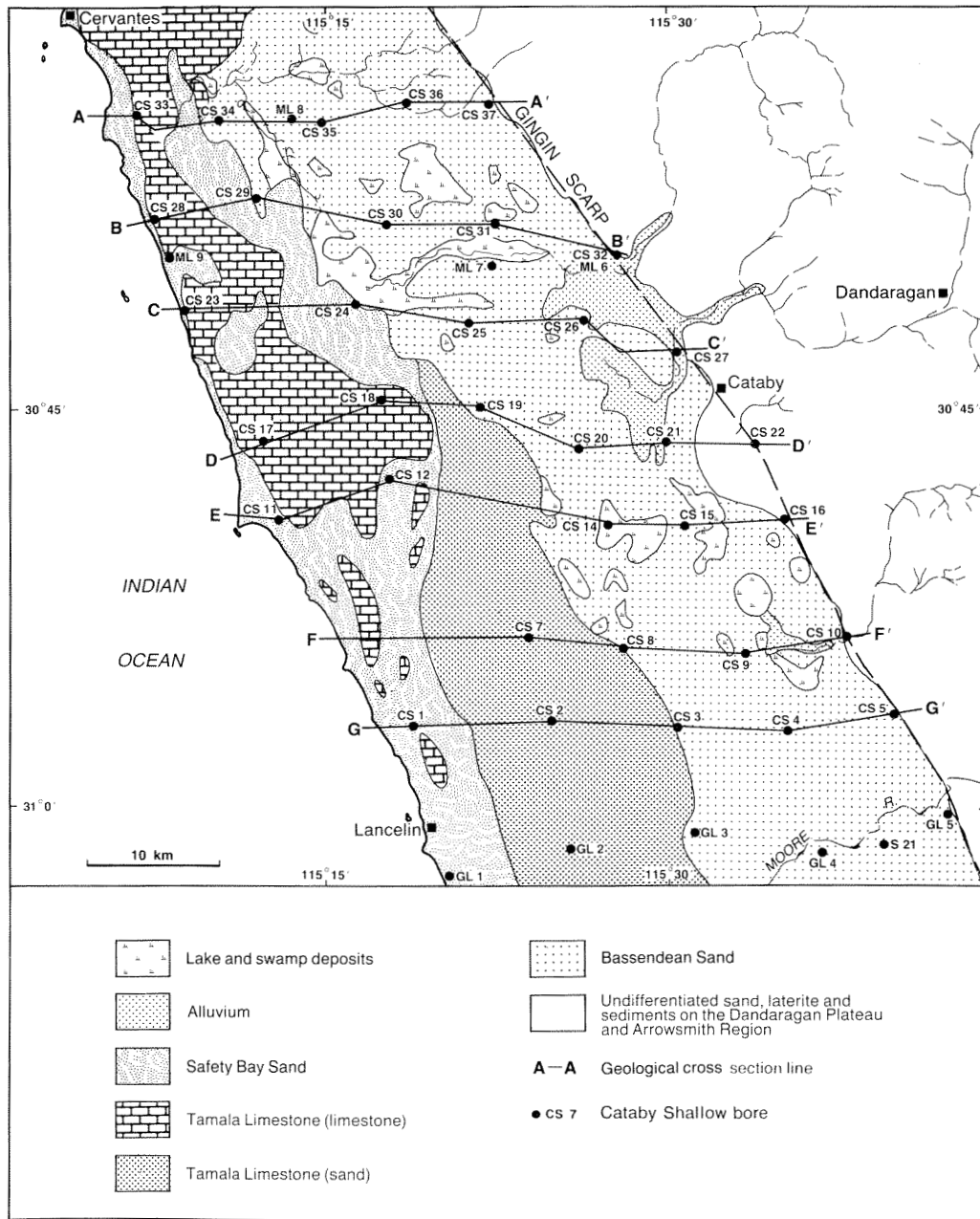


Figure 4. Surface geology

by Quaternary sediments. The formation is characterized by micaceous siltstone and shale. Spores and pollen indicate a marine depositional environment of Griesbachian to Dienerian age (all dating in this paper is based on the work of J. Backhouse, quoted in Kern (1988a)).

#### Lesueur Sandstone

The Lesueur Sandstone is present in the westernmost part of the Dandaragan Trough. It was intersected under a thin cover of Quaternary sediments at three sites, and is characterized by ferruginous sandstone. The sandstone

is mottled yellow and red, and composed of coarse to medium, angular to subangular, well-sorted quartz grains with a variable amount of feldspar and mica. A massive ferruginous 'coffee rock' is developed at the watertable. The microflora of the Lesueur Sandstone indicate a late Middle to Late Triassic age for the unit.

#### Cockleshell Gully Formation

The Cockleshell Gully Formation consists of two members: the Eneabba and Cattamarra Members. The basal Eneabba Member was intersected at site CS35 and consists of fine- to coarse-grained sandstone with

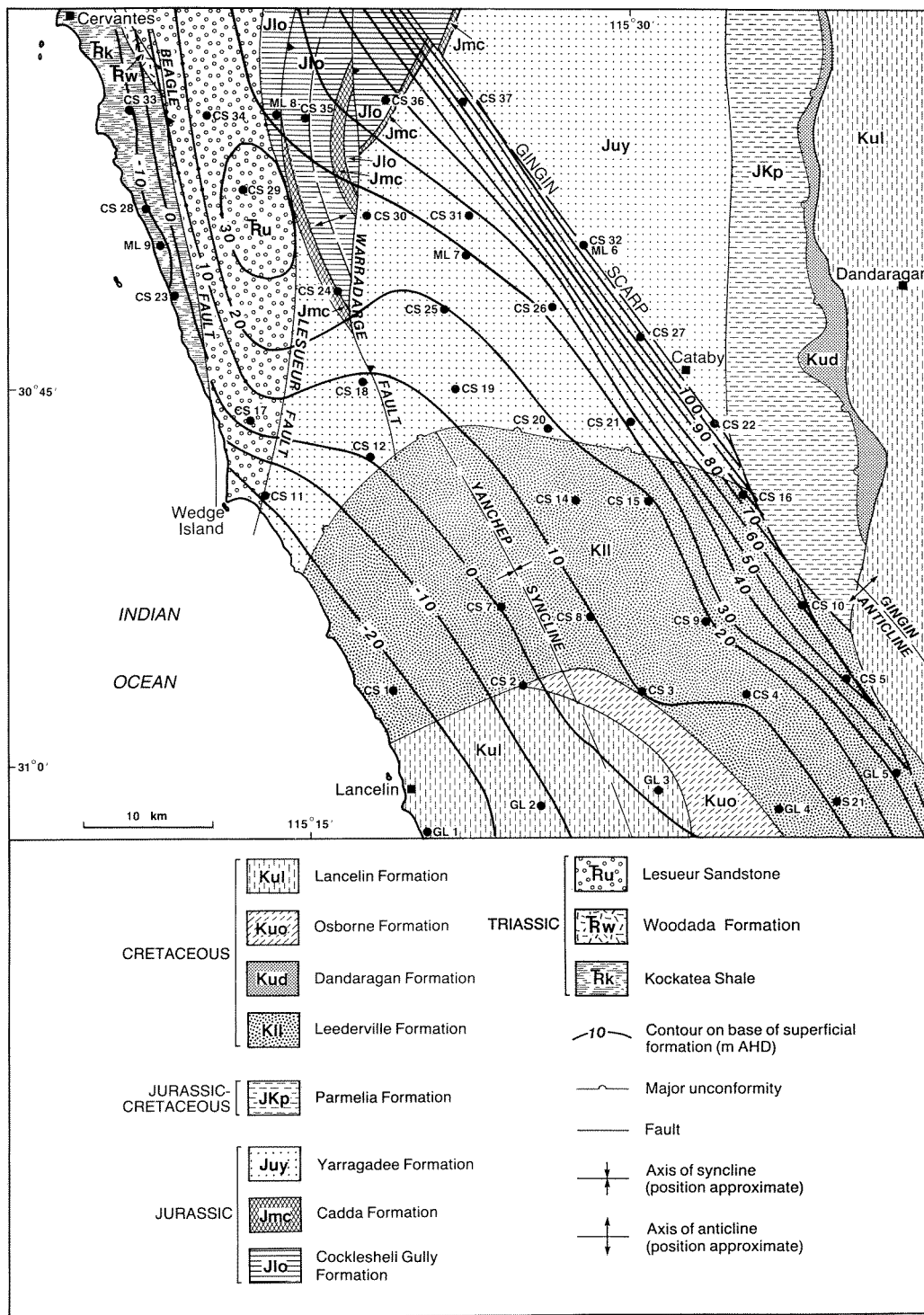
Table 3. Chemical analyses

Bore	Sample no.	Date sampled	pH	Conduct. mS/m (at 25 °C)	TDS mg/L (Calc at 180° C)	Total hardness (as CaCO <sub>3</sub> )	Total alkalinity (as CaCO <sub>3</sub> )	Ca	Mg	Na	K	CO <sub>3</sub>	HCO <sub>3</sub>	Cl	SO <sub>4</sub>	NO <sub>3</sub>	SiO <sub>2</sub>	B	F
								mg/L											
CS2D	82564	29.05.86	8.3	108	580	234	210	69	15	122	4	3	250	213	8	1	22	0.60	0.2
CS3D	82636	14.05.86	7.1	42	220	53	32	8	8	56	4	2	39	98	11	1	16	0.05	0.1
CS4S	82562	27.05.86	7.5	121	700	141	110	17	24	204	5	2	134	234	117	2	33	0.05	0.2
CS4D	82563	26.05.86	8.3	189	1 040	354	280	89	32	244	8	3	335	440	12	1	45	0.05	0.3
CS5D	82604	06.03.85	7.5	231	1 220	205	33	8	45	375	6	2	40	636	65	1	62	0.07	0.3
CS7D	82639	15.05.86	8.6	178	950	281	260	73	24	247	10	9	299	389	26	1	20	0.06	0.3
CS81	82638	08.05.86	8.4	703	4 420	1 550	218	346	166	958	21	6	254	1 760	1 000	1	34	0.05	0.2
CS8D	82637	08.05.86	8.5	463	2 820	948	235	184	119	628	21	6	275	938	742	2	42	0.05	0.3
CS9S	82622	04.04.86	7.2	135	700	170	60	22	28	198	8	2	73	369	14	1	27	0.15	0.1
CS91	82621	04.04.86	7.5	335	1 860	476	250	105	52	154	14	2	305	900	74	1	48	0.34	0.3
CS9D	82620	03.04.86	7.5	370	2 030	527	248	114	59	556	16	2	302	1 000	77	1	53	0.25	0.2
CS10D	82603	25.02.86	7.4	295	1 570	281	45	12	61	486	8	2	55	850	83	1	41	0.22	0.2
CS11S	82594	29.06.87	7.4	169	910	327	214	80	31	223	4	2	261	385	41	1	11	0.04	0.4
CS11D	82593	30.06.87	7.2	3 330	22 300	5 170	168	717	822	6 480	154	2	205	12 300	1 670	1	12	0.40	0.1
CS12D	82592	10.04.85	7.3	91	530	186	235	58	10	136	3	2	287	146	18	1	16	0.02	0.3
CS14S	82616	10.04.85	7.7	63	390	69	162	16	7	119	5	2	198	84	35	1	24	0.18	0.1
CS14M1	82615	10.04.85	8.4	150	810	257	198	62	25	201	8	6	229	324	37	1	30	0.37	0.1
CS14M2	82614	10.04.85	8.4	172	920	296	205	71	29	229	9	9	232	380	43	1	35	0.38	0.2
CS14D	82613	28.03.85	8.1	171	940	289	207	68	29	232	10	21	253	402	39	1	35	0.28	0.2
CS15S	82619	28.03.85	11.0	166	860	65	55	26	1	275	32	12	2	420	65	1	31	(a)1.00	0.1
CS15M	82618	28.03.85	9.6	157	820	56	30	16	4	271	27	6	24	420	57	1	10	(a)1.40	0.1
CS15D	82617	28.03.85	8.0	121	680	203	198	40	25	158	33	2	241	239	36	1	24	0.11	0.2
CS17D	82591	29.05.85	7.8	84	460	235	202	53	25	84	3	2	247	133	25	3	11	0.05	0.5
CS18D	82589	10.12.86	7.9	100	600	187	265	52	14	178	3	2	323	143	29	1	19	0.03	<0.1
CS19D	82590	11.12.86	8.0	139	770	280	216	81	19	173	5	2	64	303	29	1	28	0.01	0.2
CS20S	82584	02.12.86	7.0	143	810	173	128	20	30	278	7	2	256	346	31	1	23	0.01	0.3
CS20D	82583	02.12.86	8.5	168	940	246	213	51	29	257	16	2	250	388	48	1	30	0.04	0.2
CS21D	82601	08.03.85	8.2	106	620	160	155	33	19	155	11	2	189	222	35	1	45	0.05	0.2
CS23D	82580	11.09.86	7.8	81	430	252	209	63	23	64	2	2	255	118	18	5	9	0.08	0.4
CS25S	82579	08.03.85	7.8	181	930	217	169	44	26	264	6	2	206	426	38	1	20	0.05	0.3
CS25D	82578	11.09.86	7.3	229	1 200	320	254	79	30	50	6	2	310	542	36	1	23	0.11	0.1
CS26S	82568	11.09.86	6.8	42	240	26	38	2	5	75	2	2	46	99	8	1	22	0.05	0.1
CS26D	82567	11.09.86	6.9	99	560	26	91	4	4	200	2	2	111	238	27	1	26	0.12	0.1
CS27D	82502	11.09.86	7.2	207	1 080	203	28	9	44	324	9	2	34	582	48	1	50	0.08	0.2
CS28D	82575	14.02.86	7.6	399	2 170	519	295	105	77	590	16	2	360	1 040	140	6	12	0.28	0.4
CS29S	82586	29.08.86	7.9	62	350	214	154	61	15	36	4	2	188	83	20	12	22	0.04	0.4
CS29D	82585	27.09.86	8.0	128	690	248	220	60	24	162	7	2	269	249	25	6	20	0.11	0.4
CS30S	82574	27.09.86	8.0	500	2 740	801	285	115	125	735	20	2	348	1 410	127	1	30	0.17	0.3
CS30D	82573	23.07.86	7.7	1 300	7 510	1 340	361	148	236	2 380	84	2	441	4 020	402	5	14	0.31	0.3
CS31S	82582	23.07.86	6.5	213	1 170	274	22	24	52	312	13	2	27	476	246	1	36	0.04	0.1
CS31D	82581	25.11.86	6.6	164	880	153	52	15	28	266	10	2	64	431	68	1	27	0.03	0.1
CS32D	82605	25.11.86	6.5	467	2 370	218	502	43	27	1 310	11	2	613	170	500	1	3	0.52	0.5

Table 3. (continued)

Bore	Sample no.	Date sampled	pH	Conduct. mS/m (at 25 °C)	TDS mg/L (Calc at 180° C)	Total hardness (as CaCO <sub>3</sub> )	Total alkalinity (as CaCO <sub>3</sub> )	mg/L											
								Ca	Mg	Na	K	CO <sub>3</sub>	HCO <sub>3</sub>	Cl	SO <sub>4</sub>	NO <sub>3</sub>	SiO <sub>2</sub>	B	F
CS33D	82572	21.02.85	8.0	148	760	272	185	68	25	181	5	2	226	325	33	3	9	0.08	0.1
CS34S	82588	05.09.86	7.8	152	780	333	195	89	27	160	4	2	238	317	37	3	24	0.03	0.1
CS34D	82587	27.11.86	7.9	199	1 020	275	281	96	33	244	7	2	343	412	39	1	20	0.10	0.2
CS35S	82571	27.11.86	6.6	99	530	161	30	30	21	125	7	2	36	234	62	6	25	0.06	0.1
CS35D	82570	28.07.86	7.0	278	1 450	302	164	27	57	440	13	2	200	762	28	3	20	0.15	0.2
CS36S	82569	28.07.86	7.1	688	3 820	544	159	60	96	1 260	27	2	194	2 070	182	1	25	0.34	0.2
CS37D	82568	24.07.86	6.6	69	360	55	15	4	11	108	4	2	18	176	24	7	21	0.05	0.1
CS37D	82567	24.07.86	6.6	49	260	36	20	3	7	70	9	2	24	123	14	1	25	0.05	0.1

(a) High values of pH and boron are attributed to contamination from cement slurry.



GSWA 24740

Figure 5. Mesozoic geology, and structure contours on base of superficial formations

interbedded siltstone and shale. The sediments are characteristically multicolored red, yellow, brown, pink, purple, grey and white.

The upper Cattamarra Member was intersected at two sites, and is composed of shale at site CS24 and siltstone

at site CS36. The siltstone is in part carbonaceous and contains seams of coal up to 0.6 m thick.

The Cockleshell Gully Formation is believed to be a continental fluvial deposit. The formation is dated palynologically as being of Early Jurassic age.

### ***Yarragadee Formation***

The Yarragadee Formation was intersected at fourteen sites. It consists mainly of poorly sorted sandstone with very coarse to very fine subangular to subrounded quartz grains. The sediments are light to dark grey and along the Gingin Scarp are weathered to yellow and pink. At site CS11, the uppermost 59 m of the formation consists of cross-bedded sandstone.

The Yarragadee Formation is interpreted to be a continental fluvial deposit laid down during the main period of Mesozoic movement along the Darling Fault. Spores and pollen indicate a Middle to Late Jurassic age.

### ***Leederville Formation***

The Leederville Formation was intersected at 12 sites and consists of sandstone, siltstone, and shale. The sandstone is medium grey with coarse to very fine, angular to subangular, poorly to well-sorted quartz grains. The siltstone varies from light grey to dark grey and is commonly micaceous and slightly carbonaceous. The shale is medium grey to black and also contains mica and carbonaceous material.

The Leederville Formation is interpreted as a non-marine to near-shore depositional unit. Spores and pollen indicate a Valanginian to Early Aptian age.

### ***Laterite and associated sands***

Laterite and associated sands were intersected at site CS32 where they are developed on top of the weathered Yarragadee Formation. They are considered to be of Late Oligocene to Early Miocene age (Schmidt and Embleton, 1976).

### ***Ascot Formation***

The Ascot Formation rests unconformably on the Yarragadee Formation in the northern half of the project area, and on the Leederville Formation in the south. The unit appears to interfinger with the Yoganup Formation along the Gingin Scarp; elsewhere it is overlain unconformably by the Guildford Formation.

Baxter and Hamilton (1981) suggested that the Ascot Formation is a facies equivalent of the Yoganup Formation and they show that there are complex interrelationships between the two units at Cooljarloo, about 20 km northwest of Cataby. The sequence is a barrier sand with carbonate and siliceous facies, which are referred to as Ascot Formation and Yoganup Formation respectively.

The Ascot Formation was intersected at ten sites along a subsurface northwest-trending ridge parallel to the Gingin Scarp (Fig. 7). The thickness is variable as a result of post-Pliocene erosion. The sediments reach a maximum thickness of 29 m at site CS15, but are usually 10–20 m thick. The unit is characterized by buff to light-grey, coarse- to medium-grained calcarenite interbedded with sand. The calcarenite is friable to hard and contains

a variable amount of quartz sand. The sand is characterized by a rich molluscan fauna and abundant spicules and foraminifera. A basal bed containing phosphate nodules and phosphatized fossils was intersected at three sites (CS4, CS19 and CS25).

The Ascot Formation is a marine calcarenite deposited in a sub-littoral inner shelf environment at a time of low supply of terrigenous sediments. The molluscan fauna and the microflora indicate a Pliocene age for the unit (Kendrick, 1981, 1986 pers. comm.; Kern, 1988a).

### ***Yoganup Formation***

The Yoganup Formation, which occurs at the foot of the Gingin Scarp, unconformably overlies sediments of the Yarragadee and Leederville Formations, and may interfinger with the Ascot Formation. It is overlain by the Guildford Formation.

The Yoganup Formation was identified at six boresites. It is 20 m thick at site CS10 but elsewhere is generally less than 10 m thick. The unit consists of buff to light-grey, coarse to fine, subangular to subrounded quartz sand which is clayey in places. Heavy minerals constitute generally less than 2% of the unit, although greater concentrations have been found along the Gingin and Munbinea Shorelines (Baxter, 1977, 1982). The formation is up to 9 km wide, and the base of the unit ranges in elevation from about 30 m AHD to 90 m AHD.

The Yoganup Formation is interpreted as a paralic sequence, the sandy unit being barrier sheets whereas the clay beds may represent interdunal or estuarine deposits (Baxter, 1981). Based on its correlation with the Ascot Formation, the Yoganup Formation is of Pliocene age.

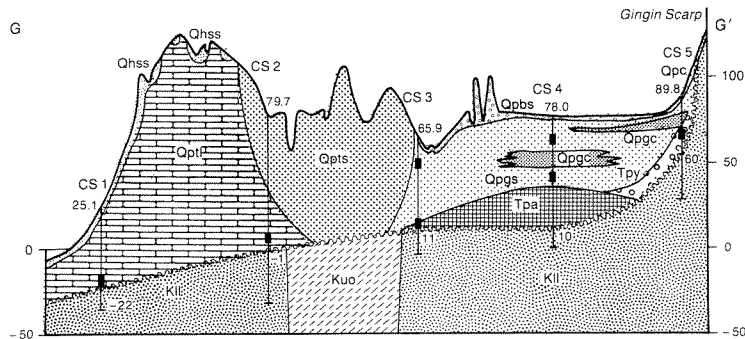
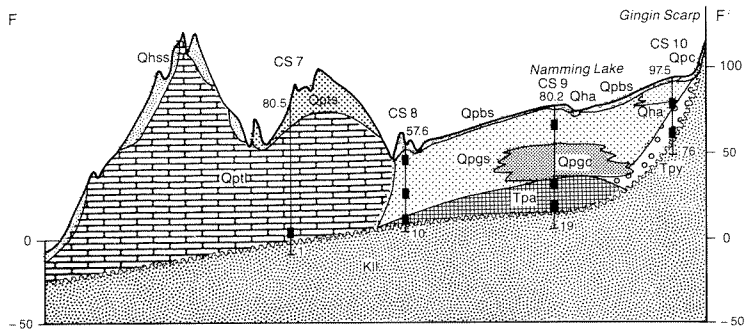
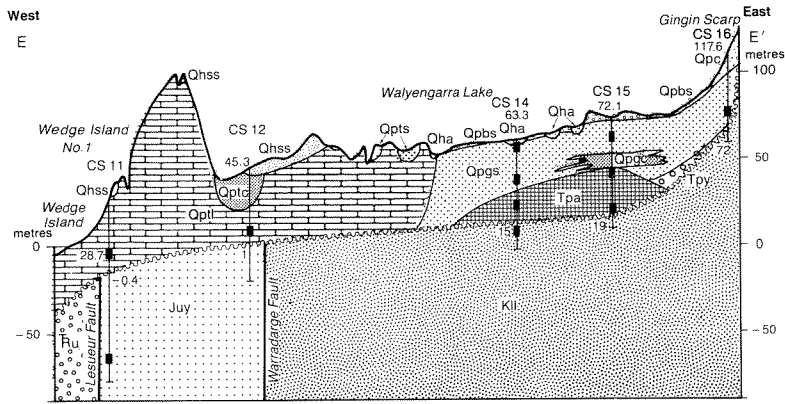
### ***Guildford Formation***

The Guildford Formation occurs in the subsurface between the Coastal Belt and the Gingin Scarp. It unconformably overlies the Ascot or Yoganup Formations where these are present; otherwise it overlies Mesozoic strata. The formation is unconformably overlain by the Bassendean Sand and possibly by the Tamala Limestone along the Coastal Belt.

The Guildford Formation was intersected at 23 sites and is typically between 30 and 40 metres thick. A maximum thickness of 53 m was encountered at site CS26. The formation is characterized by both a sandy and a clayey facies, the latter occurring mainly along the Gingin Scarp where it interfingers with the sand facies to the west. The sand is light grey with coarse to fine, subangular to subrounded quartz. Accessory minerals are generally not abundant, although minor heavy minerals and feldspar may occur. The clay is commonly brown to grey and sandy. In some places limonite-cemented sandstone ('coffee rock') is developed at or near the watertable. Its development may be controlled by the presence of permeable zones within the formation.

Most of the unit is of fluvial origin, with estuarine and shallow marine intercalations, especially at the base





- |      |                           |                               |                       |
|------|---------------------------|-------------------------------|-----------------------|
| Qha  | Alluvium                  | Kuo                           | Osborne Formation     |
| Qhss | Safety Bay Sand           | KII                           | Leederville Formation |
| Qpc  | Colluvium, sand, laterite | Juy                           | Yarragadee Formation  |
| Qpbs | Bassendean Sand           | Cadda                         | Cadda Formation       |
| Qppl | Tamala Limestone          | Jioc                          | Cattamarra Member     |
| Qpts | - limestone               | Jloa                          | Eneabba Member        |
| Qpts | - sand                    | } Cockleshell Gully Formation |                       |
| Qptc | - sand, clay, limestone   |                               |                       |
| Qpcc | Guildford Formation       | Rus                           | Lesueur Sandstone     |
| Qpcc | - sand                    | Rk                            | Kockatea Shale        |
| Qpcc | - clay                    |                               |                       |
| Qpy  | Yoganup Formation         |                               |                       |
| Tpa  | Ascot Formation           |                               |                       |
- 
- |      |                                   |
|------|-----------------------------------|
| 63.2 | Elevation natural surface (m AHD) |
|      | Bore open interval                |
|      | Unconformity (m AHD)              |
|      | Fault                             |

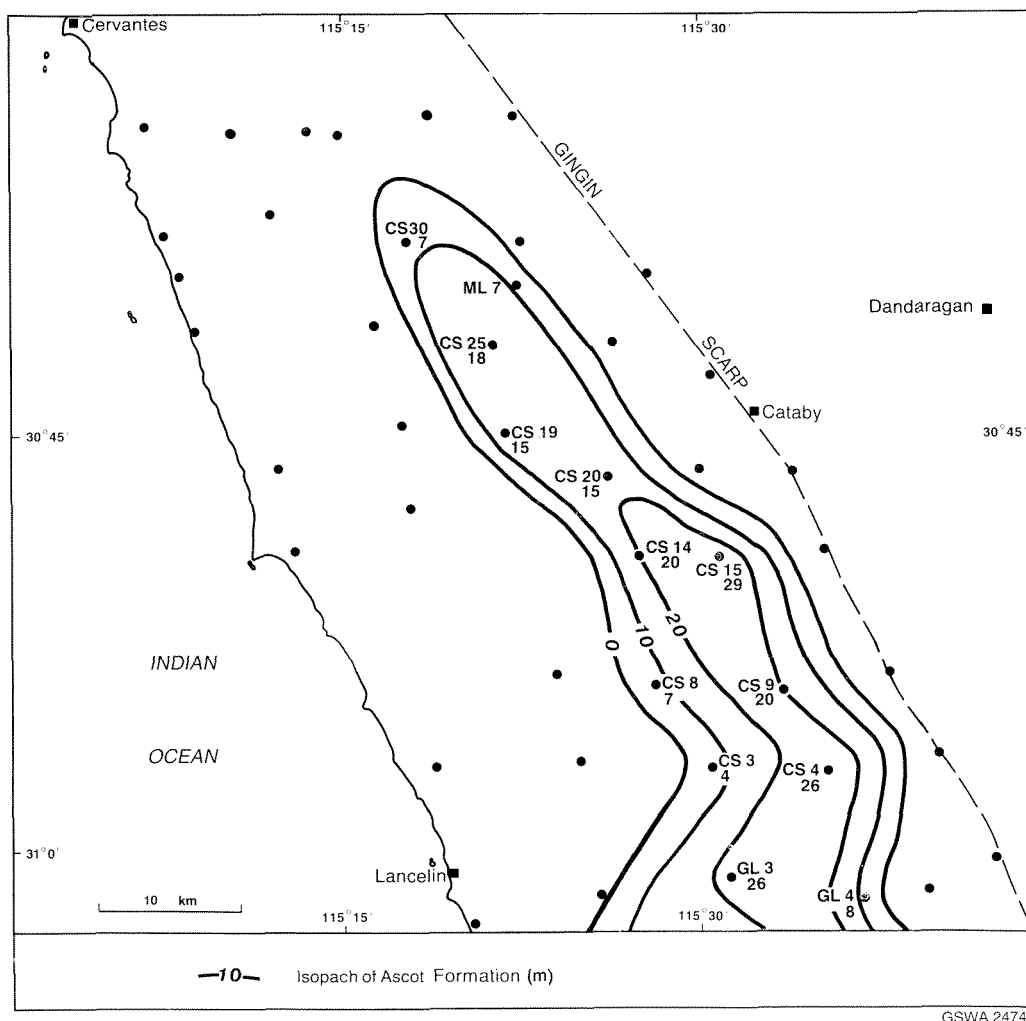


Figure 7. Extent and thickness of the Ascot Formation

(Playford et al., 1976). The fauna and the stratigraphic position suggest a Pleistocene age (Darragh and Kendrick, 1971).

### Tamala Limestone

The Tamala Limestone was deposited as coastal sand dunes (lime-sand eolianite) along the Coastal Belt. It unconformably overlies Mesozoic strata and possibly the Guildford Formation along its eastern margin, and is disconformably overlain by the Safety Bay Sand.

The Tamala Limestone outcrops extensively along the coast and adjacent islands. It was intersected at eleven sites. The thickness of the formation varies greatly, depending on the topography. It is probably up to 150 m thick south of the Nambung National Park. Three lithological facies, limestone, sand, and clay were recognized (Figs 5 and 6).

The limestone facies is buff to pale yellow, weathering to grey, and consists of quartzo-calcareous sand commonly cemented into limestone. The carbonate fragments are mainly foraminifers and mollusc shells.

Accessory heavy minerals (up to 5%), glauconite, and feldspar occur. The limestone varies from strongly lithified to friable. Hard calcrete horizons (capstone) occur in places and may be overlain by grey to brown fossil soils and underlain by softer limestone with abundant fossil root structures. The formation also shows large-scale eolian cross-bedding.

Well-developed cave systems occur in the limestone at a number of localities in the Nambung National Park, e.g. Brown Bone and Nambung Caves (Figs 1 and 5).

The sandy facies is restricted to the southwest where the Tamala Limestone is commonly leached at the surface, leaving a residue of yellow to white quartz sand (Figs 4 and 6). This can be up to 100 m thick where the limestone facies is absent. The contact between sand and unleached limestone is irregular, and rounded pinnacles of limestone sometimes extend upwards into the sand. At The Pinnacles, near Cervantes, the loose sand has been blown away to expose the limestone pinnacles.

A clayey lacustrine facies consisting of lenticular interbeds of sand, clay and limestone was intersected at sites CS12 and CS18 (Fig. 6).

The Tamala Limestone is of Late Pleistocene age (Playford et al., 1976).

### ***Bassendean Sand***

The Bassendean Sand forms the Bassendean Dunes, a series of low sandhills resulting from the reworking of underlying sand units. The formation disconformably overlies the Yoganup and Guildford Formations, and possibly overlaps the eastern edge of the Tamala Limestone.

The Bassendean Sand was intersected at 21 sites where it has an average thickness of 1–2 m. Elsewhere, depending on the topography, it may reach a maximum thickness of about 30 m. The formation consists of light-grey, coarse to fine, subangular to subrounded and moderately sorted quartz with traces of heavy minerals. Thin clay beds may also occur. 'Coffee rock' is commonly developed at or near the watertable.

The Bassendean Sand was deposited as sand dunes at various periods during the Late Pleistocene to Holocene.

### ***Safety Bay Sand***

The Safety Bay Sand forms the coastal dune and beach sediments of the Quindalup Dunes. The formation extends discontinuously along the coast and up to 14 km inland, and disconformably overlies the Tamala Limestone. Large mobile dunes occur at Lancelin and in the Nambung National Park.

The Safety Bay Sand was intersected at eight sites where a maximum thickness of 3 m was encountered, although it is thicker elsewhere. Coastal mobile dunes are as much as 100 m above AHD and the base is about 5 m below sea level at the coast.

The formation consists of buff, calcareous, weakly lithified sand. The quartz is medium to fine, angular to rounded and moderately sorted. The calcium carbonate content is generally greater than 50% and includes carbonate grains, foraminifers and mollusc fragments. Traces of heavy minerals also occur.

The Safety Bay Sand is of Holocene age and its deposition is continuing.

### ***Alluvial, colluvial, and swamp deposits***

Alluvial deposits occur along the Moore River and, to a lesser extent, along Caren Caren, Minyolo, and Mullering Brooks. Sandy alluvial deposits about 12 m thick were intersected at site CS10. They consist of buff to grey, coarse- to fine-grained, subangular to subrounded quartz.

Colluvial deposits occur along the Gingin Scarp and consist of gravel, sand, silt, clay, and laterite derived from the laterite-capped Arrowsmith Region and Dandaragan Plateau. These deposits were intersected at site CS16.

Holocene lake and swamp deposits are common in the Bassendean Dunes, where numerous fresh to saline lakes occur, and to a lesser extent in the Spearwood Dunes. They include various clay, sand, peat, marl and diatomaceous deposits and rarely exceed 3 m in thickness.

## **Hydrogeology**

### **Flow system**

The superficial formations are considered to constitute a single aquifer containing a mainly unconfined groundwater flow system. Significant variations occur within the system owing to the differences in hydraulic conductivities of the Guildford Formation and Tamala Limestone. The groundwater flow system is bounded to the west by the Indian Ocean and to the east by the limit of superficial formations along the Gingin Scarp. The area covered in this paper extends from the Moore River in the south to the Nambung River in the north. Along the Gingin Scarp, there are hydraulic connections between the superficial formations and the adjacent Mesozoic formations to the east.

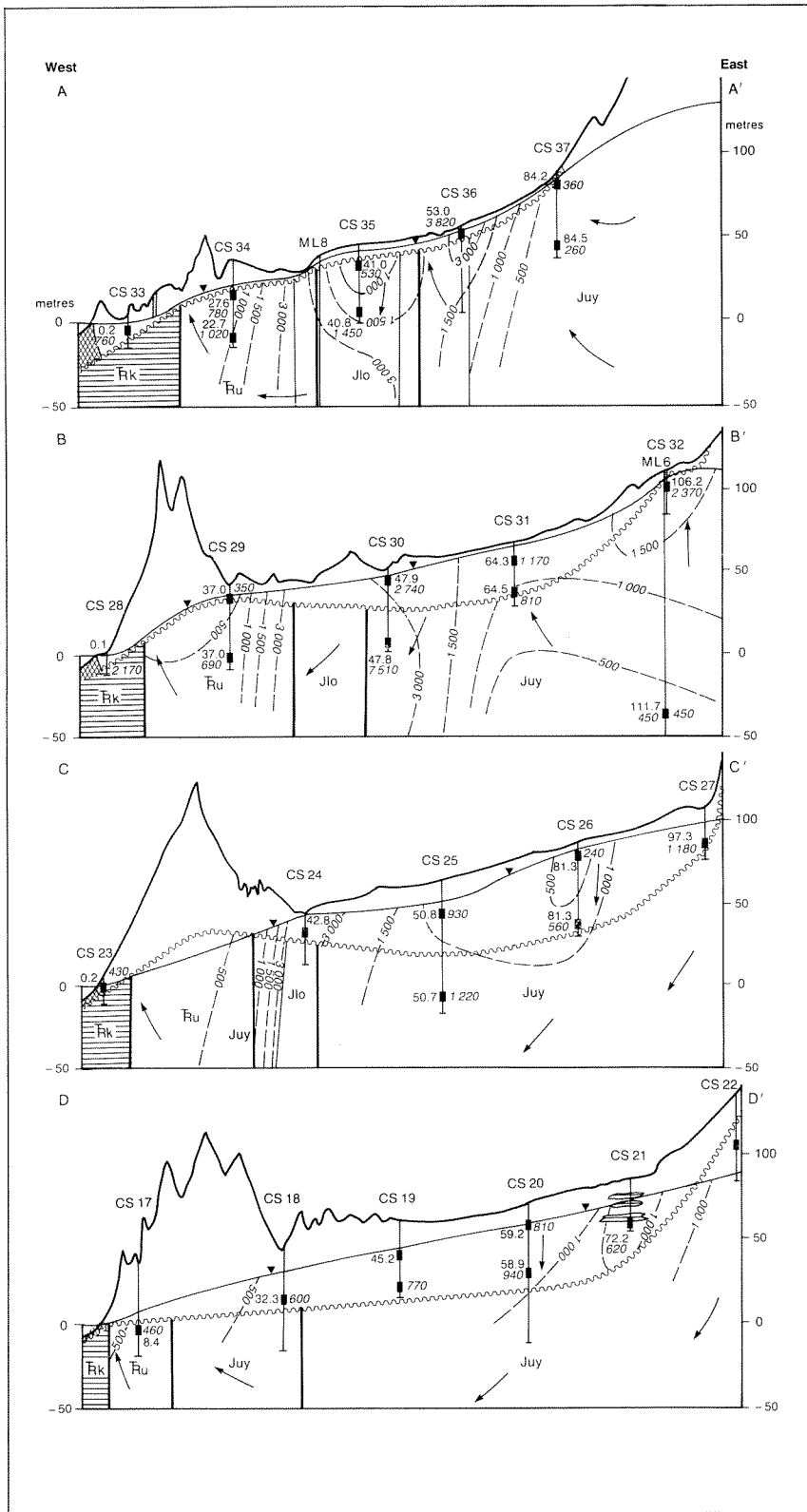
Groundwater flow in the superficial formations is generally in a westerly direction. Downward leakage from the flow system is thought to be significant in the eastern part of the coastal plain from the Guildford and Ascot Formations into the underlying Mesozoic aquifers. Upward leakage, by discharge from the Mesozoic aquifers into the flow system, takes place in the coastal area and in the northeast (Figs 8 and 9). Upward leakage also occurs from the Yarragadee Formation in the northeast where the Warradarge Fault acts as a hydraulic barrier to westward groundwater movement below the superficial formations. In the southwest and northwest, where the superficial formations overlie the impermeable Coolyena Group and Kockatea Shale respectively, there is no leakage from or into the flow system.

The saturated thickness of the superficial formations varies substantially in the area. It exceeds 50 m in the southeast, and decreases northward to less than 10 m in the Nambung River area and toward the coast (Figs 8 and 10). The superficial formations are unsaturated east of Grey where the watertable is in the Lesueur Sandstone (Figs 10 and 11).

### **Watertable configuration**

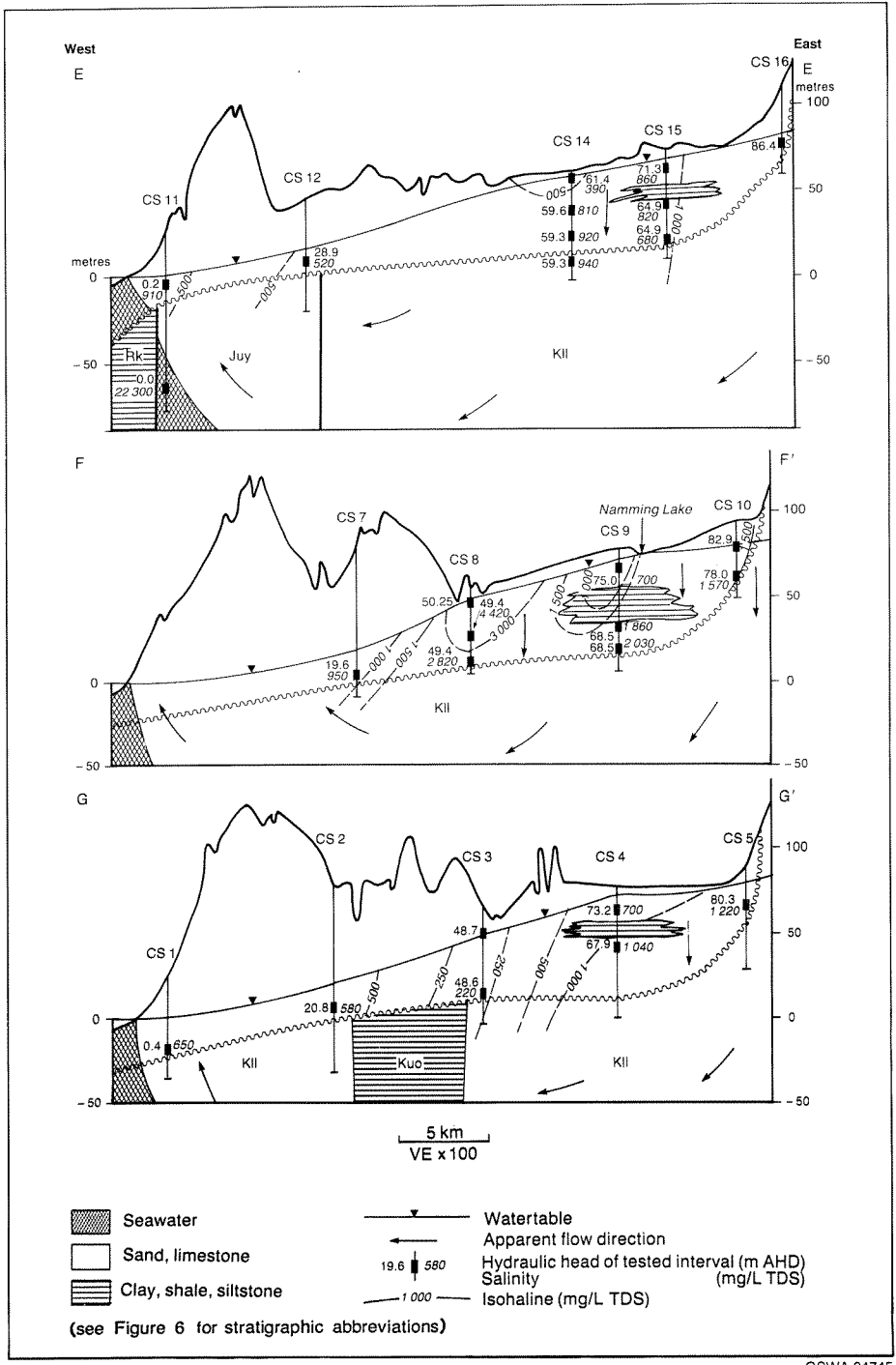
The watertable slopes westwards from the Gingin Scarp toward the sea where groundwater discharge occurs. The watertable contours are sub-parallel to the coast and the predominant flow directions are to the west and southwest (Fig. 11).

In the Bassendean Dunes, the watertable is generally close to the surface and numerous lakes and swamps occur in interdunal depressions (Fig. 8). The watertable in the Tamala Limestone is generally deep and unrelated to the topography of the Coastal Belt.

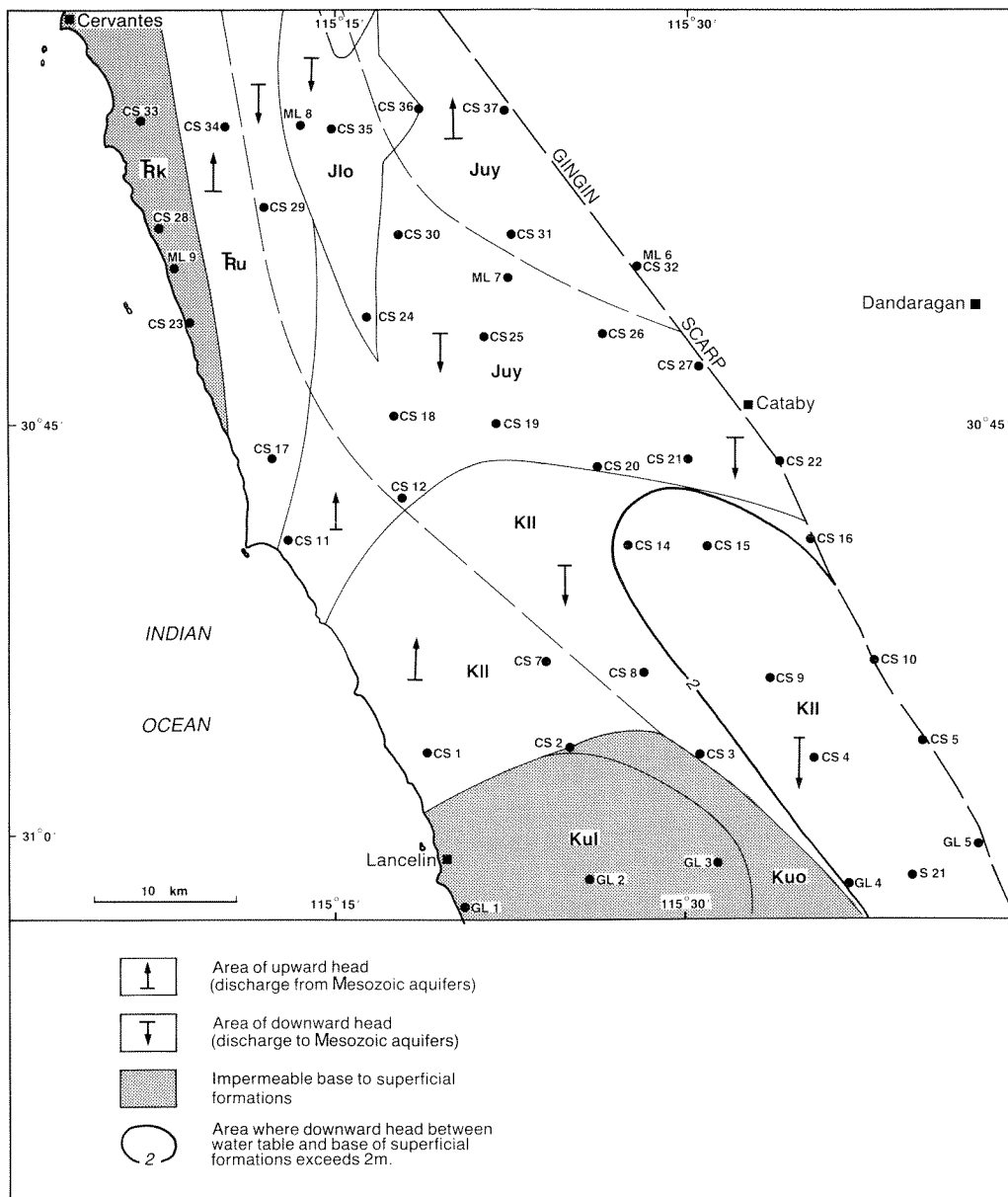


GSWA 24744

Figure 8. Hydrogeological cross sections (see Fig. 4 for locations)



GSWA 24745



GSWA 24746

Figure 9. Hydraulic-head difference between superficial formations and underlying Mesozoic aquifers

The level of the watertable in the Guildford Formation is controlled mainly by the land surface and the aquifer is maintained in a virtually full condition. Any excess recharge is accounted for by increased transpiration and evaporation from swamps. The hydraulic gradient in the Guildford Formation is controlled mainly by the slope of the land surface. At the contact of the Guildford Formation with the Tamala Limestone there is a sharp increase in the hydraulic gradient which is due largely to contrasting hydraulic conductivities, but possibly also to a zone of subsurface seepage caused by the karstic nature of the Tamala Limestone. The hydraulic gradient is very low along the coast between Wedge Island and Lancelin, reflecting the high transmissivity of the Tamala Limestone.

## Recharge

Recharge to the superficial formations is mainly by direct infiltration of rainfall and associated runoff. There is only episodic recharge from streams originating on the Dandaragan Plateau and Arrowsmith Region as these do not flow during the whole year. When the Nambung River is active it recharges the groundwater system via caves near the coast.

There is recharge by upward leakage from the Mesozoic aquifers in the northeast and the coastal area. At site CS32 (ML6) there is an upward hydraulic head gradient of 5.5 m over 140 m in the top of the Yarragadee Formation (Figs 8 and 9). Along the coast where

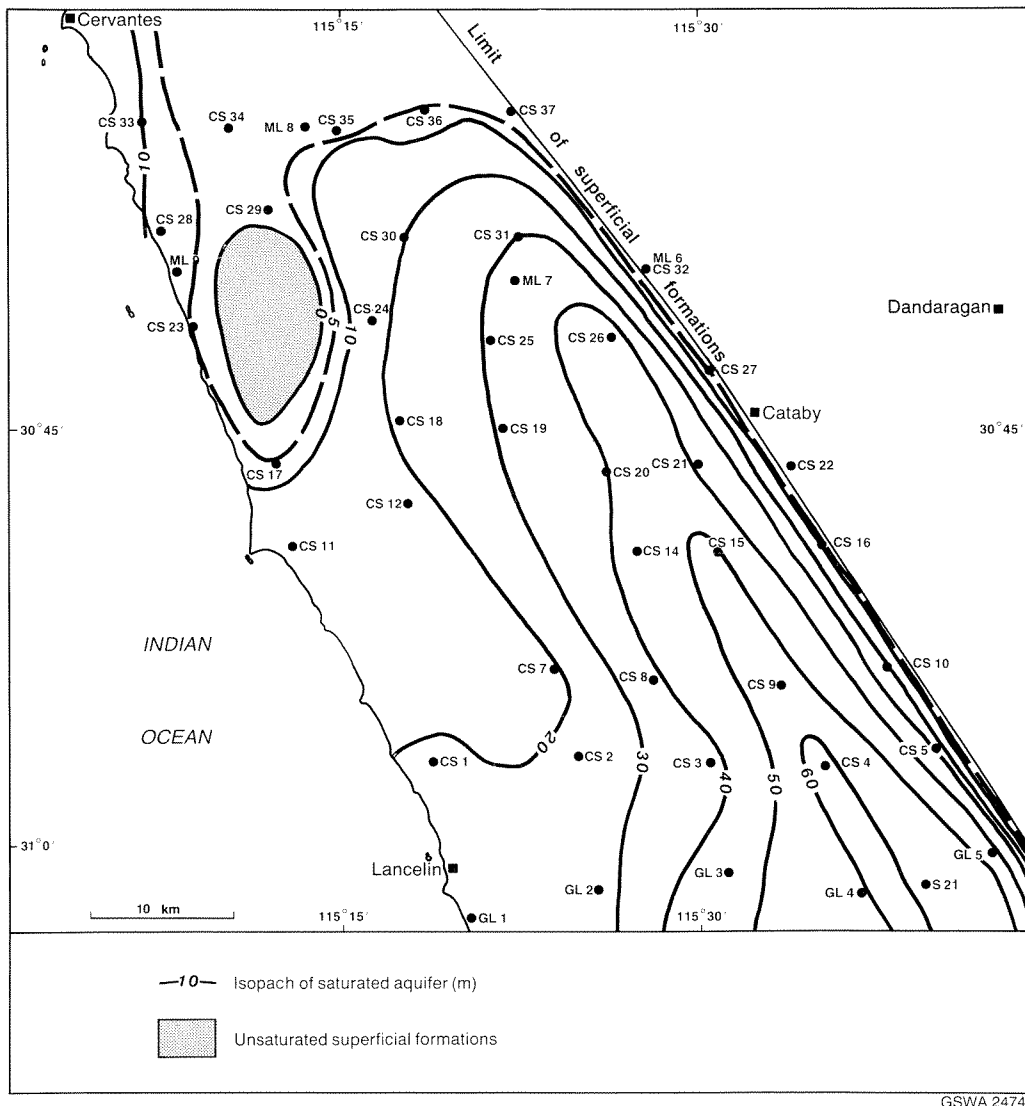


Figure 10. Superficial formations: saturated aquifer thickness

the Lesueur Sandstone, Yarragadee and Leederville Formations subcrop beneath the superficial formations there is also potential for upward leakage. This is due to regional groundwater discharge along the coast and a hydraulic barrier formed by the impermeable Kockatea Shale.

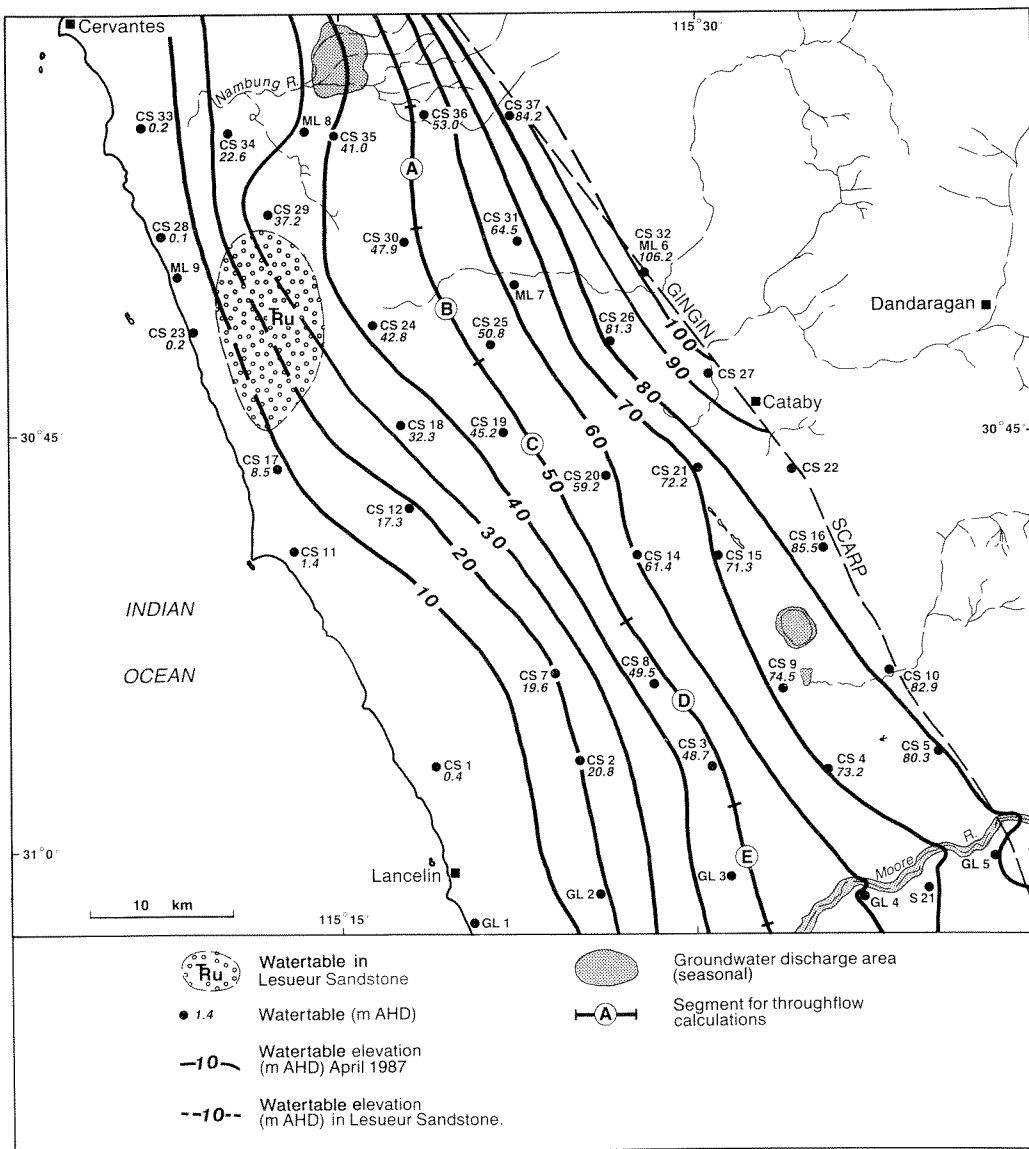
Recharge to the aquifer varies according to seasonal rainfall. In 1985 rainfall was well below average, whereas in the following two years there was near-average rainfall (Kern, 1988a). Lower watertable levels reflected the low rainfall in 1985 but recovery followed the increased precipitation of the succeeding years (Fig. 12). Recharge also varies spatially, depending upon landuse, vegetation cover, and depth to the watertable.

There is considerable variation in the response of waterlevels to winter rainfall. The waterlevels in the Guildford Formation respond quickly to rainfall and are highest in September–October and lowest in March–April with a typical seasonal range of

0.3–1.7 m. The largest seasonal changes of over 1 m occur in the wetlands southwest of Cataby (Figs 2 and 12). Smaller waterlevel variations occur where the flow system is confined by beds of clay and where the aquifer is in downward hydraulic connection with the Leederville Formation (CS15I and CS15D on Fig. 12). The smallest seasonal fluctuation of less than 0.2 m occurs in the Tamala Limestone.

Recharge can also occur from summer rainfall, and a waterlevel rise was recorded in bore CS14S in March 1986 following heavy rainfall in February of that year (Fig. 12).

Net recharge contributing to groundwater flow, expressed as a percentage of rainfall, can be estimated from the ratio of the concentration of chloride ions in rainfall (input) with the minimum concentration in groundwater. The lowest chlorinities averaged 94 mg/L and were recorded at bores CS3D, CS14S and CS26S where recharge is solely by rainfall. The chloride



GSWA 24748

Figure 11. Watertable contours in the superficial formations

concentration in rainfall recorded at Boothendarra, about 30 km north of Cataby, was approximately 7.8 mg/L (Hingston and Gailitis, 1977), which matches the long-term mean annual chloride concentration in rainfall (7.5 mg/L) on the Gnangara groundwater mound to the south (Farrington and Bartle, 1988). From the chloride ion ratio the rainfall recharge is estimated to be 8% of average annual rainfall. Using the same method, a recharge rate of about 7% was determined for the area to the south (Moncrieff and Tuckson, 1989).

The extent of recharge from streams draining the Gingin Scarp seems to be minor since there is no marked effect on the watertable contours (Fig. 11).

### Throughflow

The westward groundwater flow through the superficial formations in the Bassendeans Dunes area (about 800 km<sup>2</sup>) has been calculated, using the Darcy equation, as 44 x 10<sup>6</sup> m<sup>3</sup>/year (Kern, 1988a).

The hydraulic conductivity and hydraulic gradient are difficult to establish for the Tamala Limestone owing to its karstic nature. However, the throughflow at the coast resulting from recharge over the Coastal Belt (about 1200 km<sup>2</sup>) can be calculated from chloride data using a recharge rate of about 7.5% of average rainfall. This

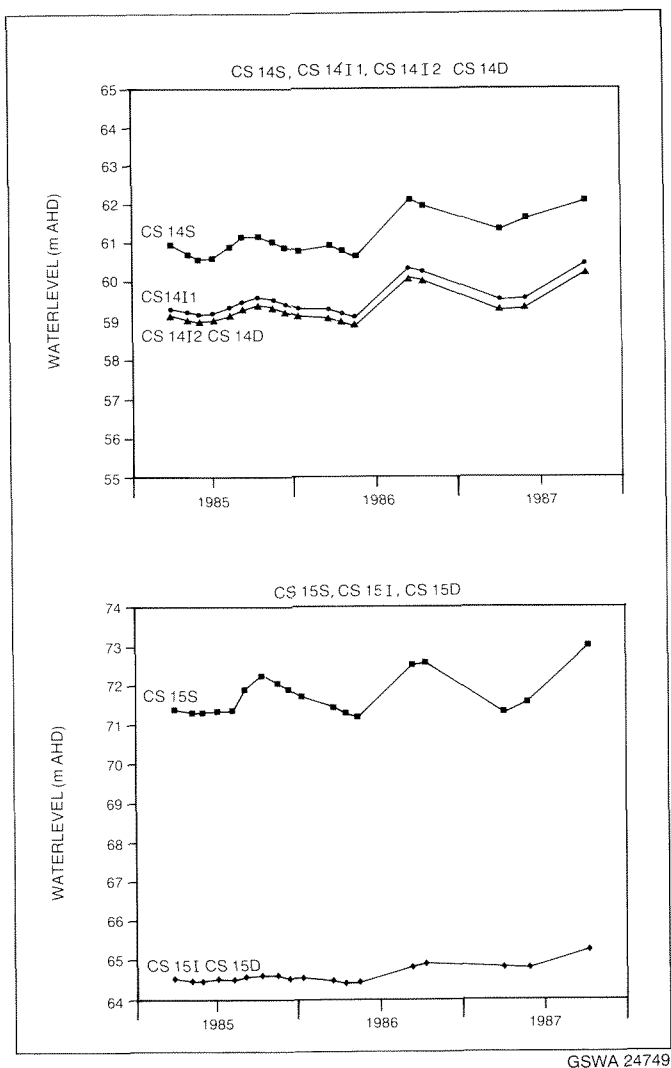


Figure 12. Selected bore hydrographs

gives a throughflow of about  $55.6 \times 10^6 \text{ m}^3/\text{year}$  for the Coastal Belt.

Therefore, the total outflow at the coast between Cervantes and Lancelin is estimated to be  $100 \times 10^6 \text{ m}^3/\text{year}$ . These figures are probably conservative because no account is taken of upward leakage from the Mesozoic aquifers.

## Discharge

Groundwater discharge occurs mainly along the shoreline above a saltwater wedge. The interface between fresh groundwater and the seawater wedge was intersected at sites CS11 and CS28. The watertable contours on Figure 11 imply seasonal groundwater discharge to the Moore River in the Regans Ford area and also to the Nambung River north of CS35. Discharge by evapotranspiration also occurs in the Bassendean Dunes where the watertable is shallow. The numerous lakes and swamps, as well as phreatophytic vegetation, also give rise to significant groundwater losses.

The maximum head difference between the watertable and the underlying Mesozoic formations occurs in the southeast where the saturated aquifer thickness exceeds 50 m in conjunction with the thickest section of clay in the Guildford Formation (Fig. 8). This difference reaches 6.5 m at site CS15. The substantial downward hydraulic gradient in the southeast implies that significant discharge may occur by leakage into the underlying Leederville Formation.

## Storage

The volume of the saturated sediments in the project area is estimated to be  $50 \times 10^9 \text{ m}^3$ . Most of the sediments are sand and limestone with the clay of the Guildford Formation constituting less than 3%. The specific yield is assumed to be 0.2, as for similar sediments in the Perth area (Cargeeg et al., 1987). Consequently the volume of groundwater in storage in the project area is about  $10 \times 10^9 \text{ m}^3$ . Assuming a recharge rate of 8% of average annual rainfall (620 mm), this figure represents about 100 years of recharge over the whole project area ( $2000 \text{ km}^2$ ).

## Groundwater quality

### Salinity

#### Superficial formations

The variation in groundwater salinity at the watertable is shown in Figure 13. The pattern of vertical groundwater salinity variation is shown in the hydrogeological cross sections (Fig. 8).

The groundwater salinity is less than 1000 mg/L total dissolved solids (TDS) in two-thirds of the area. The salinity is lowest in the Coastal Belt, and this probably results from additional recharge from rainfall with the deep watertable in the area preventing evapotranspirative losses.

Local areas with groundwater salinity greater than 1000 mg/L occur along the Gingin Scarp where the Guildford Formation is clayey, and in areas with numerous lakes and swamps where the watertable is shallow. Brackish groundwater is also found along drainage lines. The salinity exceeds 3000 mg/L in both the vicinity of Frederick Smith Creek and the upper section of the Nambung River where there is seasonal groundwater discharge.

The configuration of the isohalines generally demonstrates the effects of evapotranspiration from lakes and swamps. Monitoring of major lakes has shown that the water ranges from fresh to saline. Lake Guraga has an exceptionally high salinity, as much as 30 000 mg/L toward the end of summer (Fig. 3). Plumes of higher salinity groundwater are believed to extend down-gradient from the lakes, with a plume at the base of the aquifer observed at boresite CS9 (Fig. 8). In the

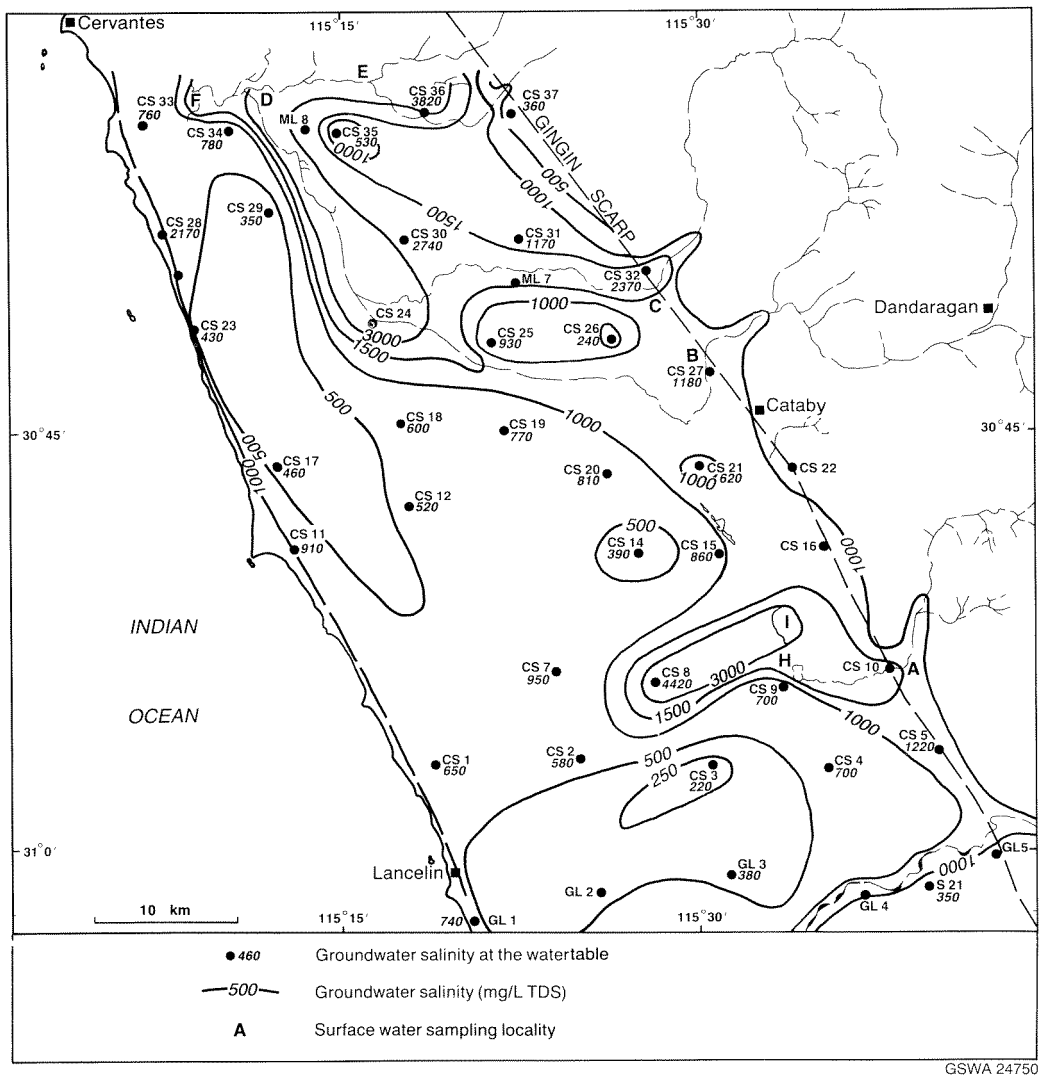


Figure 13. Groundwater salinity at the watertable

southeast, where there is a substantial downward hydraulic gradient, this higher salinity groundwater is likely to recharge the Leederville Formation. The highest groundwater salinities (in excess of 3000 mg/L) were recorded at boresites CS8, CS24, and CS36 which are situated in extensive swamplands.

The regional salinity pattern is also controlled by drainages which contribute brackish water from the flushing of salinized areas east of the Gingin Scarp.

### Mesozoic formations

The quality of the groundwater in the Yarragadee Formation also ranges from fresh to saline. The salinity increases upward at site CS32 where there is also upward groundwater discharge (Fig. 8). There is a significant increase in salinity in the Yarragadee Formation westward toward the Warradarge Fault where there is downward leakage of saline groundwater from the superficial formations. The groundwater salinity reaches 7510 mg/L in bore CS30D.

Most of the Cockleshell Gully Formation contains brackish groundwater. This is due to the low permeability of the interbedded siltstone and shale, and also to recharge by brackish water from the overlying superficial formations.

The groundwater salinity in the Lesueur Sandstone is generally low except along the Lesueur Fault where there is leakage of saline groundwater from the Cockleshell Gully Formation, and seasonal recharge from Frederick Smith Creek. The coastal seawater wedge was penetrated in the Lesueur Sandstone in bore CS11D, but fresh groundwater was encountered in the superficial formations in bore CS23D, only 200 m from the coast.

### Hydrochemistry

Chemical analyses of the groundwater are given in Table 3 and are plotted in Figure 14.

The trilinear diagram (Fig. 14) indicates that the groundwater chemistry is mainly of the sodium

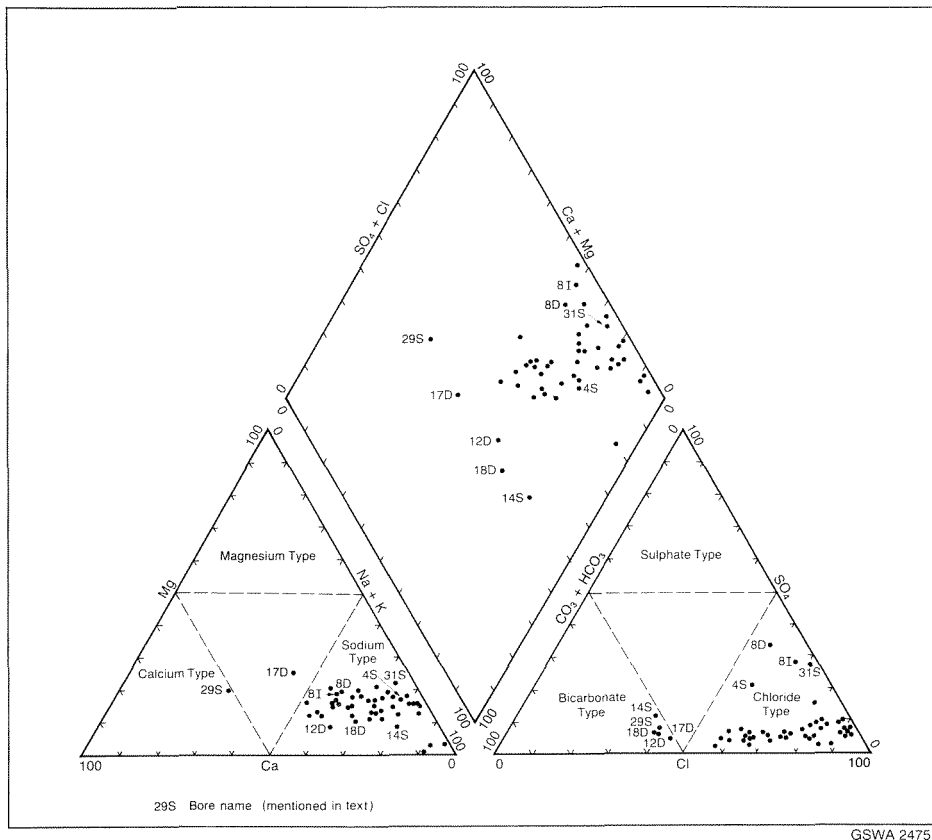


Figure 14. Piper trilinear diagram

bicarbonate to sodium chloride type. High chloride proportions coincide with higher salinity, whereas the proportions of bicarbonate are more significant in lower salinity water (CS14S and CS17D) and also in the Tamala Limestone (CS12D, CS18S and CS29S).

Sulfate concentration exceeds 20% of the total anions in bores CS4S, CS8I, CS8D and CS31S. This is likely to have resulted from oxidation of the abundant organic matter in the wetland soils.

Nitrate content is generally low but several high values, with a maximum of 12 mg/L (CS29S), may indicate groundwater contamination. Silica attains fairly high values (up to 62 mg/L) compared with values from the area to the south (Moncrieff and Tuckson, 1989). Boron and fluorine values are generally lower than 1.0 and 0.5 mg/L respectively and lie within normal background concentrations.

The groundwater pH is neutral with values ranging from 6.5 to 8.5. It is very slightly alkaline in the Ascot Formation and Tamala Limestone.

The similarity between the chemical compositions of the groundwater in the superficial formations and in the underlying Mesozoic aquifers confirms that these are in close hydraulic connection.

## Conclusions

The drilling has shown that the superficial formations thin to the north from a thickness of some 50 m near the Moore River to less than 10 m near the Nambung River. The drilling has also defined the northern extent of both the Ascot and the Leederville Formations beneath the Swan Coastal Plain, and the subcrop of Triassic and Jurassic formations.

Groundwater in the unconfined superficial formations in the Coastal Belt area has a salinity of less than 1000 mg/L. However, the salinity ranges from 250 to 3850 mg/L in the Bassendean Dunes area where the watertable is shallow. The highest salinities were recorded in bores located in extensive swamplands and in the vicinity of drainage lines.

The groundwater storage of the superficial formations is estimated to be about  $10 \times 10^9 \text{ m}^3$ , two-thirds of which is fresh with a salinity less than 1000 mg/L. The total outflow of fresh groundwater at the coast is estimated to be  $100 \times 10^6 \text{ m}^3/\text{year}$ . The major groundwater resources occur in the southeast, between Caren Caren Brook and the Moore River, where the saturated thickness in the superficial formations is about 50 m and the salinity lies between 500 and 1000 mg/L.

## References

- ALLEN, A. D., 1976, Outline of the hydrogeology of the superficial formations of the Swan Coastal Plain: Western Australia Geological Survey, Annual Report 1975, p. 31–42.
- BAXTER, J. L., 1977, Heavy mineral sand deposits of Western Australia: Western Australia Geological Survey, Mineral Resources Bulletin 10, 148p.
- BAXTER, J. L., 1981, Geology of mineral sand deposits in Western Australia, in Selective reference papers for mineral-sand mining: Western Australia School of Mines, WAIT-AID Ltd, Perth.
- BAXTER, J. L., 1982, History of mineral sand mining in Western Australia, in Reference papers; Exploitation of mineral sands: Western Australia School of Mines, WAIT-AID Ltd, Perth.
- BAXTER, J. L., and HAMILTON, R., 1981, The Yoganup Formation and the Ascot Beds as possible facies equivalents: Western Australia Geological Survey, Annual Report 1980, p. 42–43.
- BIRD, K. J., and MOYES, C. P., 1971, Walyering No. 1 well completion report: West Australian Petroleum Pty Ltd; Petroleum Search Subsidy Acts (P.S.S.A.) Report (unpublished); Western Australia Geological Survey, S-series Open File, microfilm roll 6.
- BRIESE, E. H., 1979, The geology and hydrogeology of the Moora borehole line: Western Australia Geological Survey, Annual Report 1978, p. 16–22.
- CARGEEG, G. C., BOUGHTON, G. N., TOWNLEY, L. R., SMITH, G. R., APPELYARD, S. J., and SMITH, R. A., 1987, Perth water balance study: Western Australia Water Authority, v. 1–2.
- DARRAGH, T. A., and KENDRICK, G. W., 1971, *Zenatiopsis ultima* sp. nov., terminal species of the *Zenatiopsis* lineage (Bivalvia: Mactridae) with notes on its stratigraphic significance on Flinders Island and in the Perth Basin, southern Australia: Royal Society of Victoria. Proceedings, v. 84, p. 87–91.
- FARRINGTON, P., and BARTLE, G. A., 1988, Accession of chloride from rainfall on the Gnangara groundwater mound, Western Australia: Australia CSIRO Division of Land Resources Management, Perth Technical Memorandum 88/1.
- HINGSTON, F. J., and GAILITIS, V., 1977, Salts in rainfall in Western Australia (1973–1974): Australia CSIRO Division of Land Resources Management, Perth Technical Memorandum 77/1.
- KENDRICK, G. W., 1981, Molluscs from the Ascot Beds from Cooljarloo heavy minerals deposits, Western Australia: Western Australia Geological Survey, Annual Report 1980, p. 44.
- KERN, A. M., 1988a, The geology and hydrogeology of the superficial formations between Cervantes and Lancelin, Perth Basin: Western Australia Geological Survey, Hydrogeology Report 1988/32 (unpublished).
- KERN, A. M., 1988b, Cataby project bore completion reports: Western Australia Geological Survey, Hydrogeology Report 1988/43 (unpublished).
- LOW, G. H., 1972, Explanatory notes on the Moora 1:250 000 geological sheet, Western Australia: Western Australia Geological Survey, Record 1972/21.
- LOWRY, D. C., 1974, Dongara–Hill River, W.A.: Western Australia Geological Survey, 1:250 000 Geological Series Explanatory Notes.
- MOYES, C. P., 1970, Wedge Island stratigraphic well, Perth Basin: Western Australian Petroleum Pty Ltd, Petroleum Search Subsidy Acts (P.S.S.A.) Report (unpublished), Western Australia Geological Survey, S-series Open File, microfilm roll 55.
- MONCRIEFF, J. S., and TUCKSON, M., 1989, Hydrogeology of the superficial formations between Lancelin and Guilderton, Perth Basin: Western Australia Geological Survey, Report 25, Professional Papers, p. 39–57.
- MONCRIEFF, J. S., 1989, Hydrogeology of the Gillingarra borehole line, Perth Basin: Western Australia Geological Survey, Report 26, Professional Papers, p. 105–126.
- PLAYFORD, P. E., COCKBAIN, A. E., and LOW, G. H., 1976, Geology of the Perth Basin, Western Australia: Western Australia Geological Survey, Bulletin 124, 311p.
- SCHMIDT, P. W., and EMBLETON, B. J. J., 1976, Palaeomagnetic results from sediments of the Perth Basin, Western Australia and their bearing on the timing of regional lateritization: Palaeogeography, Palaeoclimatology, Palaeoecology, v. 19, p. 257–273.

# The location and significance of point sources of groundwater contamination in the Perth Basin

by

K-J. B. Hirschberg

## Abstract

Over 1100 point sources of groundwater contamination have been identified in the Perth Basin. Of these, some 700 are in the Perth metropolitan area, while about 400 are located in the remainder of the basin. A risk ranking has been assigned to major waste-creating activities. Most of the point sources of a high-, or moderate to high-risk ranking are within the Perth region and concentrated mainly in zoned industrial areas. The predominantly sandy sediments of the Swan Coastal Plain, which has a generally shallow watertable, are most at risk from groundwater contamination. The groundwater resources in the Perth Basin beyond the metropolitan area are presently at little risk from point sources in the high-risk categories, due to the concentration of both population and secondary industry in the Perth area. The major impact on groundwater quality in the rural parts of the Perth Basin is likely to be from non-point sources, e.g. fertilizer, herbicide and pesticide application in agriculture and horticulture. Non-point sources are also suspected to be major contributors to groundwater contamination in the Perth metropolitan area.

**KEYWORDS:** Groundwater, contamination, point sources, Perth Basin.

## Introduction

### Background

The Perth Basin contains large amounts of usable groundwater, often at shallow depth and therefore susceptible to contamination. More than 80% of Western Australia's population reside on the basin and, in many areas, groundwater is the only water supply. Total abstraction of groundwater from the Perth Basin is estimated to be about  $300 \times 10^6$  m<sup>3</sup>/year, most of it from the shallow, unconfined aquifers (Australian Water Resources Council, 1987). For the Perth area, annual abstraction from the unconfined aquifers is about  $220 \times 10^6$  m<sup>3</sup>, or about 75% of the total groundwater usage for the basin. Contamination of groundwater is almost unavoidably connected with many human activities, be it industrial development, agriculture, residential development, or outdoor sporting and recreational facilities. An increase in awareness of the hazards and consequences of such contamination has raised public concern over the last few years about the threat to valuable groundwater resources.

The Geological Survey of Western Australia (GSWA) has been involved in groundwater contamination studies since the early 1970s, principally in the role of advisers in hydrogeological matters to various other government agencies, including the former Effluent Licensing Advisory Panel responsible for the licensing of industrial waste discharges until the mid-1980s. Data from past

investigations into numerous groundwater contamination problems have been collected and held by a variety of government and local government bodies, and individual industries and consultants. It was also found that, in many cases, the mode of data collection and storage differed from agency to agency, often making the interpretation and comparison of different data sets difficult and, in some cases, almost impossible.

### Purpose and scope

In the mid-1980s, the GSWA began the task of incorporating the existing data on point sources of groundwater contamination in Western Australia into one readily accessible file with a uniform classification system. Non-point sources of contamination, e.g. fertilizer, herbicide and pesticide application in agriculture, roadside spraying, and areas serviced by septic tanks were omitted from this compilation. Also excluded were accidental spills, and leaking underground storage tanks.

It was recognized that the compilation of such an inventory would constitute a major task and would best be approached in several stages. The first stage was centred on Perth, where the majority of Western Australia's population (about 70%) resides, and where most secondary industry is situated. This study extended from Two Rocks in the north to Mandurah in the south, and eastward to just beyond Wundowie. Two maps and a computer listing presenting the results of this investigation were published by the GSWA (Hirschberg, 1988), and the results of the investigation were reviewed by Hirschberg (1989).

The second phase of the investigation extended the coverage to the remainder of the Perth Basin (Hirschberg, 1991). The onshore Perth Basin extends from Northampton in the north, to Augusta in the south, and from the coast in the west to the Darling Scarp in the east (Fig. 1). It forms a long and narrow coastal strip of approximately 1000 km in length, and an average width of about 45 km, covering an area of about 45 000 km<sup>2</sup>.

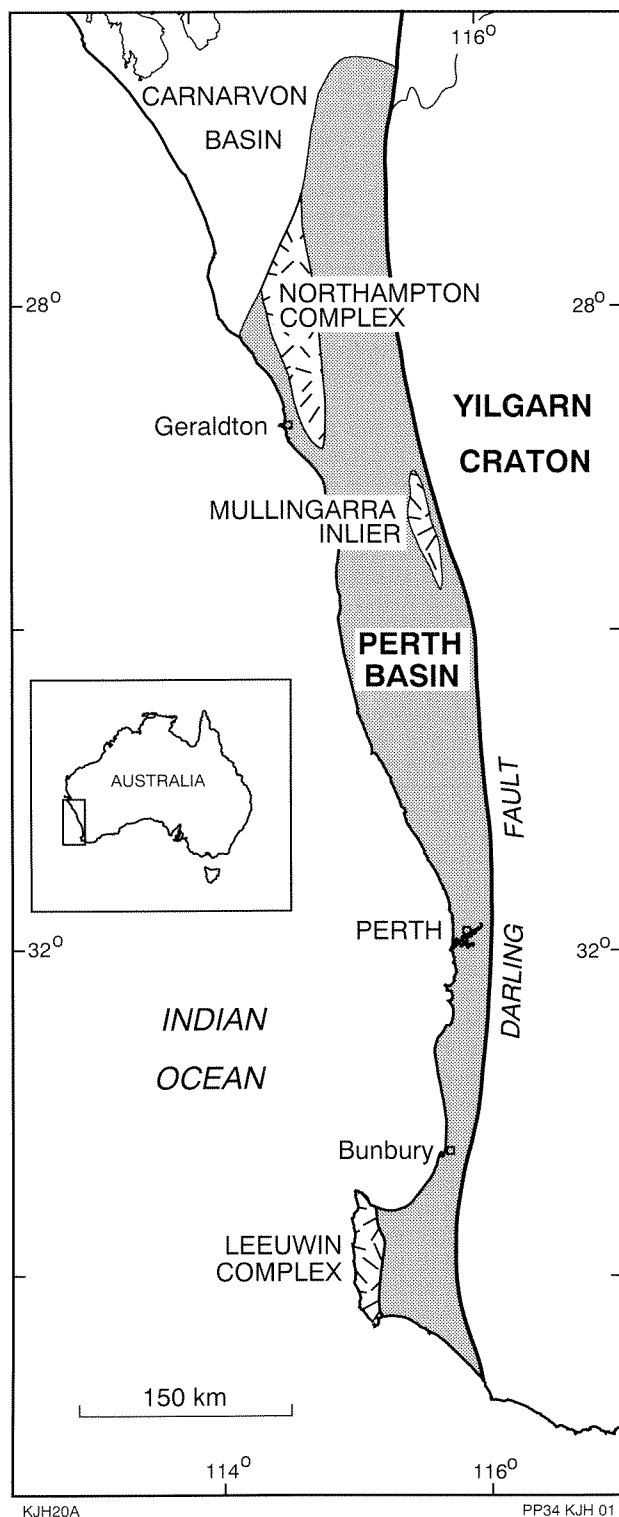


Figure 1. Location plan, Perth Basin

This paper reviews the results of the two investigations, and complements the groundwater contamination vulnerability maps of the Perth Basin, currently being prepared by the GSWA.

### Previous work

Previous studies of point sources of groundwater contamination in the Perth region have been detailed by Hirschberg (1986, 1989). Outside the Perth metropolitan area there have been few such investigations apart from a few local assessments of waste-disposal licence applications. Regionally, several maps at various scales have been published showing at least some aspects of groundwater contamination. The GSWA has produced several 1:50 000 environmental geology maps of selected areas of the basin, and these include comments on waste-disposal aspects. Land-suitability maps, at the scale of 1:1 000 000, were prepared by D. P. Commander of the GSWA and published by the Department of Agriculture (Ryan and Payne, 1989). These maps assessed the potential impact of piggeries, and assist in their improved siting in the future.

### Climate

The Perth Basin has a mediterranean-type climate, with warm, dry summers and cool, wet winters. The annual rainfall decreases from about 1200 mm in the far south to less than 400 mm in the north. The average annual pan evaporation increases from about 1000 mm in the south to about 2600 mm in the north and, for most of the basin, greatly exceeds the annual rainfall.

### Population

The population distribution for the Perth Basin is shown in Figure 2 (Commonwealth Bureau of Statistics figures for 1990). Approximately 1.33 million people, or about 81% of the population of Western Australia, live on the basin. About 70% of the total population (1.19 million) live in the Perth metropolitan area. Apart from Perth and its surroundings, there are only four population centres with more than 10 000 inhabitants—Geraldton, Mandurah, Bunbury and Busselton. South of Perth there are a number of small to medium-sized settlements, but to the north of Perth the population is sparse with only Dongara and Moora of any notable size. This pattern is also reflected in the density of the rural population, with 100–500 people per 100 km<sup>2</sup> in the southern part of the basin, and 5–20 people per 100 km<sup>2</sup> in the northern part. The population distribution can be expected to influence the locations and density of point sources of groundwater contamination.

### Physiography

The physiography of the onshore Perth Basin has been described by Playford et al. (1976) who divided the basin into a number of physiographic regions (Fig. 3) which can

Plain, which stretches from near Geraldton in the north to Busselton in the south.

## Hydrogeology

The Perth Basin is an elongate sedimentary trough, bounded in the east by the Darling Fault, which separates the sedimentary sequence of the basin from the mainly crystalline rocks of the Archaean Yilgarn Craton. Several inliers of Proterozoic rocks (Northampton Complex, Mullingar Inlier, and Leeuwin Complex) are located within its boundaries (Fig. 1). The basin contains up to 15 000 m of sedimentary rocks which range in age from Silurian to Quaternary. The pre-Quaternary sediments consist predominantly of formations of interbedded sandstone and shale of varying thickness and proportions, and occur in a number of structurally controlled subdivisions. The pre-Quaternary sediments outcrop on the upland plateaus where they are generally heavily lateritized whereas, on the coastal plains, they are blanketed by the Quaternary sediments collectively referred to as 'superficial formations' which consist mainly of sand, silt, clay, and limestone.

The Perth Basin contains a number of major confined and unconfined aquifers (Allen, 1990; Commander et al., 1990). Groundwater in the pre-Quaternary aquifers is mostly confined, although beneath the upland plateaus which form the main intake areas, the shallow groundwater is unconfined. The depth to watertable in these areas is usually more than 20 m. The Quaternary superficial formations constitute a major aquifer and contain unconfined groundwater, with the watertable usually at shallow depth. This shallow groundwater is particularly vulnerable to contamination.

## Point sources of groundwater contamination

### Definitions

'Contamination' and 'pollution' are used in most dictionaries as synonyms. The Western Australian Environmental Protection Act of 1986 defines both terms as 'any direct or indirect alteration of the environment to its detriment or degradation or to the detriment of any beneficial use'. This definition is adopted here; however, only the term 'contamination' is used.

Point sources of contamination are known or inferred localized sites of waste production or disposal. Non-point sources, however, generally cover larger areas over which diffuse groundwater contamination occurs.

### Data sources

The data for the Perth metropolitan region were obtained in 1987 from a number of Western Australian government agencies, the major ones being the Water

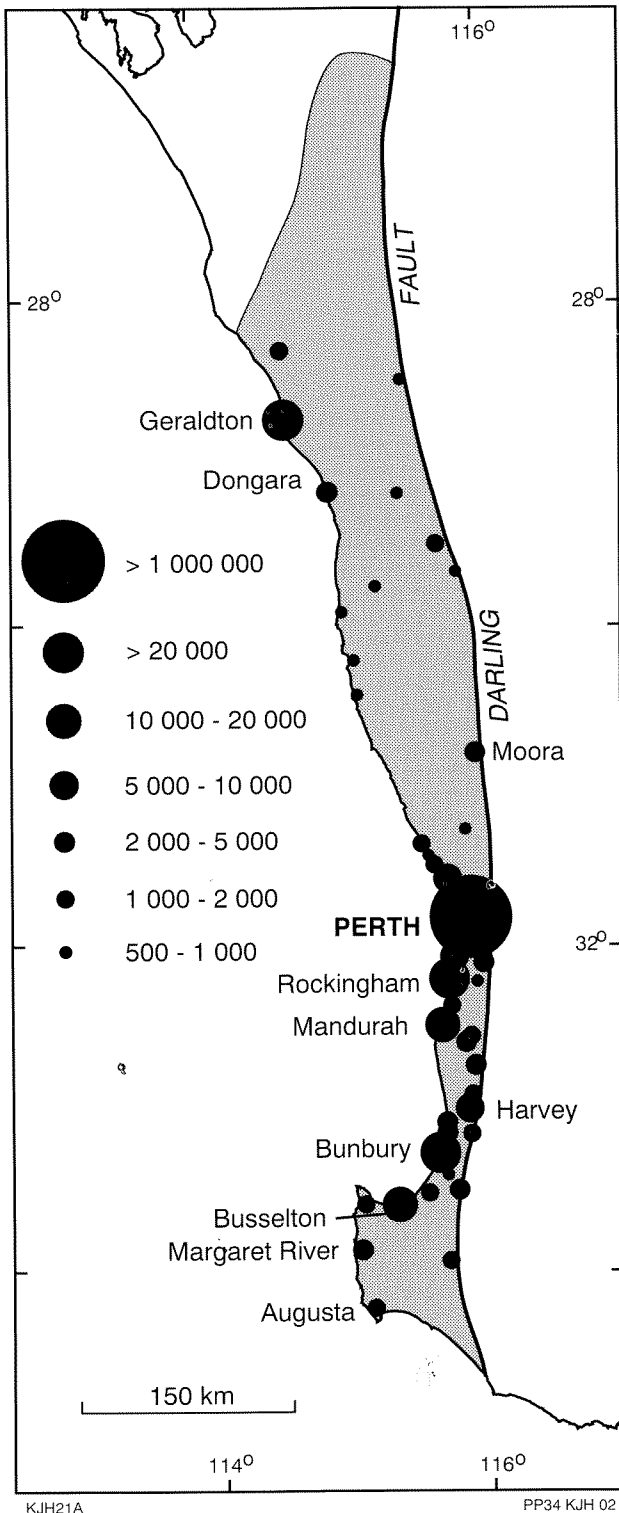
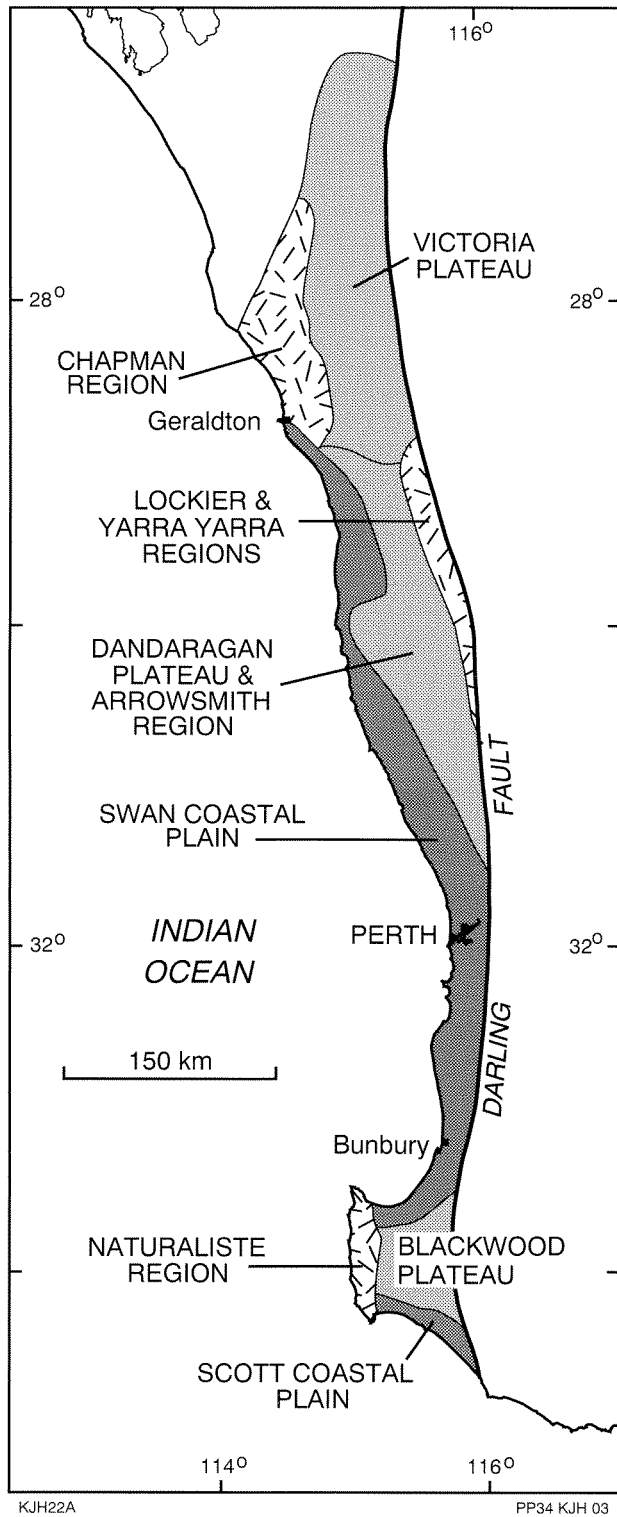


Figure 2. Perth Basin — population distribution 1990

be broadly grouped into coastal plains (Swan and Scott Coastal Plains), upland plateaus (Victoria, Dandaragan and Blackwood Plateaus), and miscellaneous regions (Chapman, Lockier, Yarra-Yarra, Arrowsmith and Naturaliste Regions). The most important region in the context of groundwater contamination is the Swan Coastal



**Figure 3. Perth Basin — physiographic subdivisions**

Authority, the Health Department, the Chemistry Centre (W.A.), the Department of Agriculture, and the GSWA. Data were also collected by interviewing all local government authorities and a number of other organizations, and this information was supplemented by numerous site visits and data supplied by individual companies. The data for the remainder of the Perth Basin

were obtained in 1990/91 through interviews with all local government authorities, and inspections of a limited number of sites. It is estimated that about 95% of all point sources in the Perth area were recorded during the 1987 survey. However, there has been intensive industrial development since then, especially in Kwinana and Canning Vale, and the data file does not include most of these new sites. These industrial areas probably require update surveys every few years. It is considered that almost 100% of all sources outside the metropolitan area have been recorded.

The information collected usually consisted of the names and addresses of companies and industries, the local government authority, the location and type of activity, the type of waste produced, and sometimes the major contaminants. A computer data base has been established which also includes grid coordinates, and data on existing monitoring and remedial measures where applicable.

### Grouping of contamination sources

There is a very wide range of industrial and other human activities, and they can be assigned to broad groupings according to the major contaminants they are expected to produce. Following discussions with officers of the Chemistry Centre, seven main groups were defined by Hirschberg (1989) for the Perth area investigation. These main groups, and their predominant activities, are given in Table 1.

### Risk ranking

Some contaminants pose a greater threat to the environment, including human health, than others. Once the main contaminants from each activity are known, the anticipated severity of groundwater contamination can be assessed. In a report of the Kwinana Industries Co-ordinating Committee in 1987, three categories of contamination risk were defined. In the present paper, the number of categories has been expanded to five, as follows.

- Category 1 - high risk to the environment or population due to toxicity, volume of material, or location. Requires careful management, regulation, and rehabilitation.
- Category 2 - moderate to high risk due to toxicity, volume of material, or location. Requires careful management and regulation.
- Category 3 - moderate risk due to type, volume, or location of material. Requires regular monitoring and assessment.
- Category 4 - moderate to low risk due to type, volume, or location of material. Requires regular assessment, and often also monitoring.
- Category 5 - low risk due to type, volume, or location of material. Should be recognized and recorded; no monitoring or control required.

**Table 1. Grouping and risk ranking of contamination sources**

Contamination Group	Major Activities	Risk category	Number of Sources		Total
			Perth metropolitan area	Outside metropolitan area	
Industrial-waste sources	metal-finishing shops	1	44	4	48
	metal prod., foundries, casting sand disposal, power stations	2	48	34	82
	mech. workshops, battery recycling	2	65	5	70
	prod. of cement, bitumen, fibreglass, paper etc	3	57	5	62
	laboratories, photo proc.	3	28	0	28
	laundries, drycleaners	3	8	2	10
Chemical-based waste sources	production of all chemicals and pesticides	1	42	-3	39
	prod. of paints, glues, solvents	1	11	1	12
	prod. of fertilizers	2	7	2	9
	Sub-total		310	50	360
Landfill sites	domestic-waste disposal	3	96	96	192
Liquid-disposal sites	domestic-liquid disposal, sewage-treatment plants, large septic systems	3	57	126	183
		Sub-total	153	222	375
Animal-based waste sources	woolscourers	1	7	0	7
	tanneries	1	16	1	17
	piggeries	3	106	42	148
	meat rendering, packing, processing	3	27	10	37
	abattoirs, feedlots	3	20	28	48
Food-production waste sources	prod. of starch/gluten, bakeries	4	16	1	17
	dairies, cheese factories	4	10	5	15
	fruit/veg. producers, wineries, breweries, soft-drink production	4	21	4	25
Sites for disposal of bodies	cemeteries	5	16	43	59
	burial sites for animals	5	4	0	4
	Sub-total		243	134	377
		<b>Total</b>	<b>706</b>	<b>406</b>	<b>1 112</b>

In general, heavy metals, cyanide, arsenic, and all herbicides, pesticides, hydrocarbons, and phenolic compounds would fall into categories 1 and 2; high levels of nutrients and surfactants into categories 3 and 4; and moderate nutrient levels, and increased salinity, into category 5.

The risk categories for the various activities in the seven contamination groups used in this paper are given in Table 1. Most industrial activities, including chemicals production, woolscouring and skin tanning have a high-risk ranking and are in category 1; battery recycling and fertilizer production are in category 2 of high to moderate risk; most animal-based activities (other than woolscouring and tanning), waste from food production, and also domestic waste disposal, are of moderate risk and are in category 3; waste from food production is in the moderate-to low-risk category 4; and cemeteries and disposal sites for animal carcasses constitute the low-risk

category 5. Owing to the great variety of activities, most contamination groups contain more than one risk category.

## Distribution of contamination sources

A total of 1112 point sources of groundwater contamination have been identified in the Perth Basin. Of these, 706 (63%) are located in the Perth metropolitan area (Hirschberg, 1989).

For convenience, the seven contamination groups have been combined into three more general classifications: the first (Fig. 4) comprises all sources of industrial and chemical waste production; the second (Fig. 5) contains all landfill sites and domestic liquid-waste disposal sites; and the third (Fig. 6) is made up of all sources of animal-based waste, waste from food production, and also cemeteries and sites for the burial of animal carcasses.

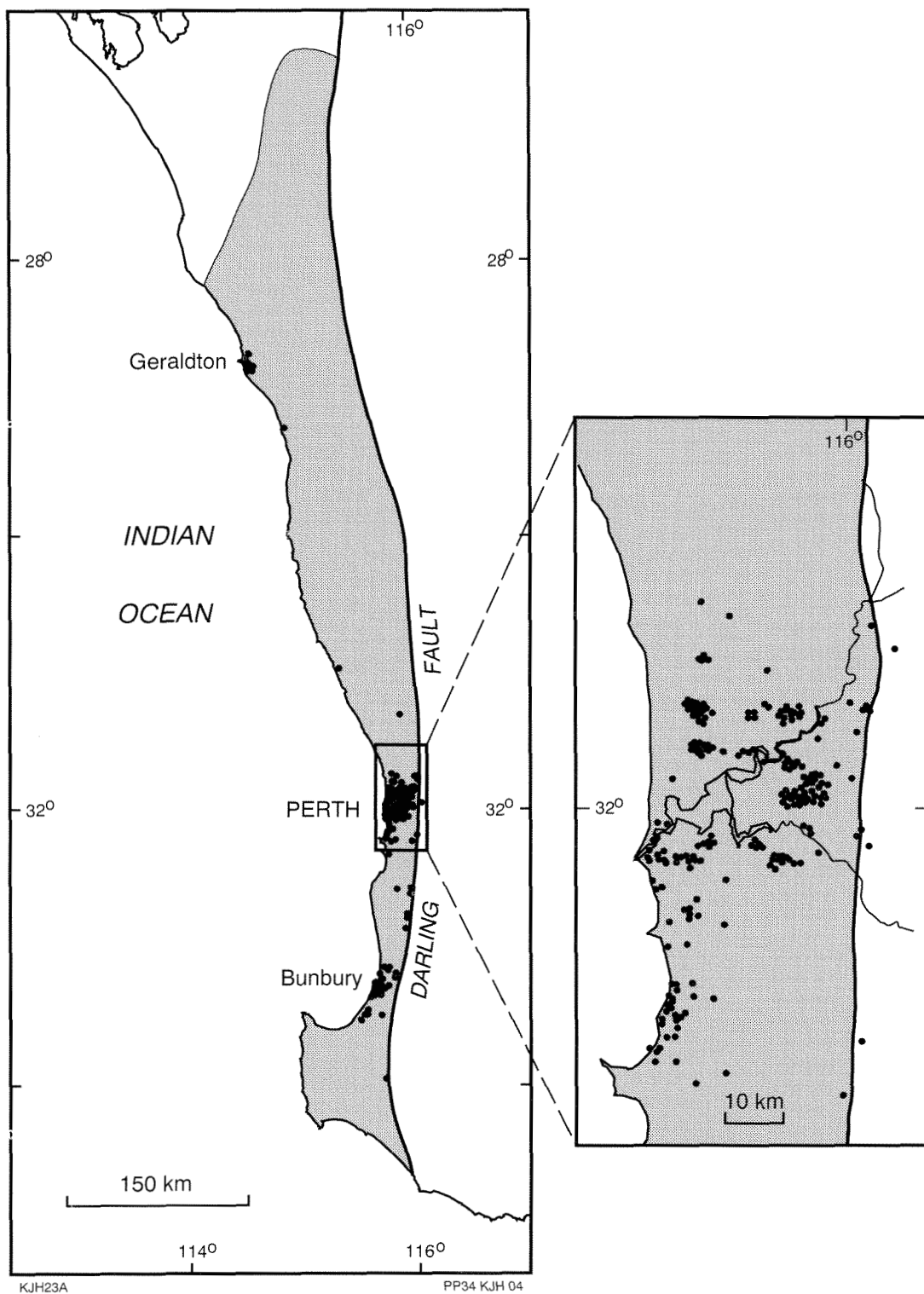


Figure 4. Sources of industrial and chemical waste

### Industrial and chemical-based waste sources

Figure 4 shows the locations of the point sources of industrial and chemical waste production, with those for the Perth metropolitan area shown in the inset. In Perth, 310 industrial and chemical point sources were identified. These sources are concentrated mostly in zoned

industrial areas, particularly in Kwinana. It is here, and also in Canning Vale, O'Connor, Osborne Park, and Welshpool-Kewdale that most of the cases of severe groundwater contamination in Perth are located. Only 50 additional sites of this kind occur in the remainder of the Perth Basin, and there are only two other locations where sources of industrial and chemical waste are

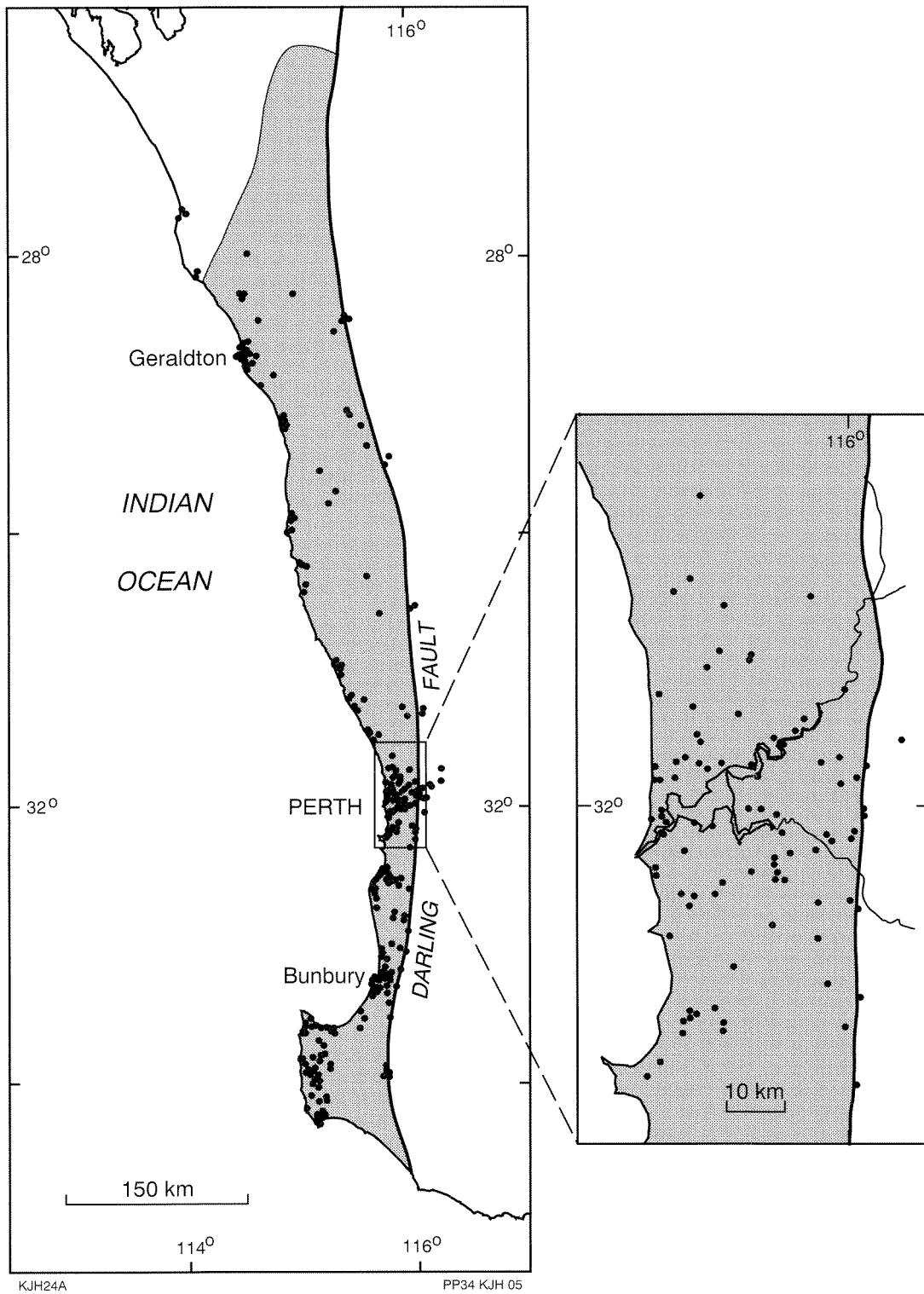


Figure 5. Landfill sites and liquid-disposal sites

concentrated, namely the Bunbury–Kemerton area, and the Geraldton–Narngulu area. The few remaining sites of this type are scattered along the Darling Scarp between Pinjarra and Harvey. Of the total of 360 such sources, 260 have the high- or moderately high-risk ranking of 1 or 2, while the remaining 100 sources are in the moderate-risk category 3.

### Landfill sites and liquid-disposal sites

Figure 5 shows the distribution of landfill sites and liquid-disposal sites which are in the moderate-risk category 3. In the Perth metropolitan area, 153 such sites were identified, but a further 222 sites occur in the remainder of the Perth Basin. Compared with the

distribution of industrial and chemical waste sources (Fig. 4), these sites are more evenly distributed over the basin, with noticeable concentrations at the major population centres of Geraldton, Dongara, Mandurah, Bunbury, and Busselton. Leachate production can be expected to be much less in the northern parts of the basin, owing to the decrease in the annual rainfall and the increase in evaporation reducing the impact of contamination from landfill sites in these areas.

Approximately one-third of all sites in this group outside the Perth metropolitan region are septic systems for caravan parks and tourist developments. They occur in smaller clusters, predominantly along the coast, where most holiday resort centres are located. A surprising feature in the southern part of the basin is the relatively dense distribution of landfill sites on the western part of the Blackwood Plateau, and on the Leeuwin Complex. Most of these sites have never been gazetted, and they are comparatively small. The Shire of Augusta–Margaret River is at present undertaking to close most of these uncontrolled waste-disposal sites and to replace them with a small number of properly approved and managed landfill sites.

### Animal-based and food production waste sources, and cemeteries

The contamination sources related to animal-based waste, waste from the food industry, and cemeteries and sites for the disposal of animal carcasses, are shown in Figure 6. The animal-based waste sources have a moderate-risk ranking of 3, with the exception of tanning and woolscouring which have a high-risk ranking of 1. All sources of food production waste have a moderate- to low-risk ranking of 4, and cemeteries and sites for animal carcass burial are of the low-risk category 5.

In the Perth inventory, 176 animal-based sources, 47 sources related to food industry, and 20 cemeteries and four sites for the burial of animal carcasses were identified. An additional 81 animal-based sources, 10 food-industry sources, and 43 cemeteries are located in the remainder of the Perth Basin. Within the Perth area the sites are evenly distributed, with the only major concentration of tanneries, fellmongers, and related industries, in the Coogee area. Outside the Perth area the sources consist mostly of piggeries and dairies and are concentrated mainly in the Geraldton, Moora–Gingin, and Harvey–Bunbury areas. Cemeteries are found at or near all settlements of any size. Outside Perth, animal carcasses are generally buried at the municipal waste-disposal sites.

### Threat to groundwater resources

The seriousness of existing or potential groundwater contamination from point sources can be assessed from both quantitative and qualitative aspects: by determining firstly the number and locations of such sources; and secondly, where the majority of sources in the higher risk categories are situated (Table 2).

**Table 2. Contamination risk ranking**

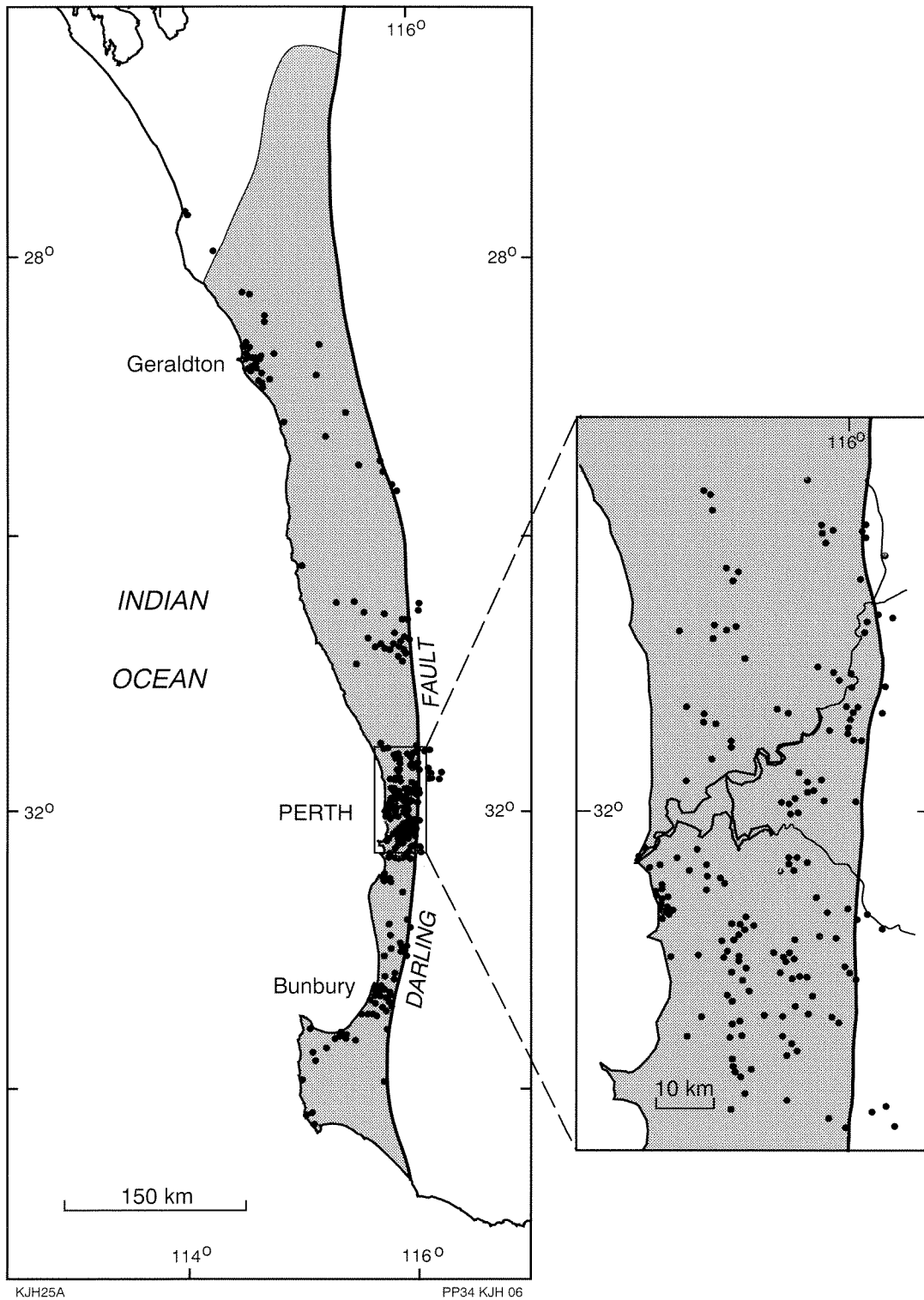
<i>Risk category</i>	<i>Perth Basin total</i>	<i>Perth metropolitan area</i> <i>(percentage of total)</i>	<i>Perth Basin outside metropolitan area</i>
1	123	120 (98)	3 (2)
2	161	120 (75)	41 (25)
3	708	399 (56)	309 (44)
4	57	47 (82)	10 (18)
5	63	20 (32)	43 (68)
Total	1 112	706 (63)	406 (37)

Of the total of 1112 point sources of groundwater contamination identified in the Perth Basin, 706 (about 63%) are located in the Perth metropolitan region, as was expected from the distribution of the population. The remaining 406 sources (37%) are spread over the wider area of the Perth Basin, with noticeable concentrations in the Geraldton and Bunbury regions.

The sources in the high- and moderate to high-risk categories 1 and 2 originate mainly from secondary industry and the production of chemicals, but also include tanneries and woolscourers (Table 1). Table 2 shows that 98% of all sources with a risk ranking of 1, and 75% of those with a ranking of 2, are located in the Perth metropolitan area. The remainder are located mostly in the industrial areas of Narngulu and Kemerton, with a few scattered over the remaining area of the basin. Point sources in these categories pose the greatest threat to groundwater quality should contamination occur.

The moderate-risk category 3 comprises landfill and domestic liquid-disposal sites, and waste from piggeries and other animal-based industry. The Perth area contains 56% of these sources. The remaining 44% are scattered over the basin and include about 60% of all landfill and liquid-disposal sites.

Compared with a typical metropolitan landfill site, the country waste-disposal sites are generally quite small although, due to the general lack of supervision and control, the risk of some local groundwater contamination cannot be discounted. The liquid-disposal sites include septic/leach drain systems of larger than domestic size. These service country hospitals, schools, and caravan parks: the latter are mostly located along the ocean foreshore, at the outflow end of the groundwater flow systems. This category can therefore generally be considered to pose only a minor threat to groundwater resources.



KJH25A

PP34 KJH 06

**Figure 6. Sources of animal-based waste, food industry waste, and cemeteries**

Category 4 sources, with a moderate to low-risk ranking, consist of waste from food production: 82% are within the Perth area. Category 5, with a low-risk ranking, comprises cemeteries and sites for animal carcass disposal. The Perth area contains 32% of these. The threat of

groundwater contamination from these sources is considered to be minimal.

Analysis of these data indicates that the unconfined aquifers of the Swan Coastal Plain, particularly in the

metropolitan region, are most at risk of contamination from point sources. Contributing factors include the predominantly sandy sediments, a generally shallow watertable, population concentration, and the location of secondary industry. Careful planning in particularly sensitive areas is essential to avoid problems in the future.

The Perth Basin outside the metropolitan area is to date relatively unaffected by groundwater contamination from point sources. The normally shallow unconfined groundwater in the Quaternary sediments of the coastal plains is so far largely unaffected because contamination sources with a high- or moderate to high-risk ranking are scarce. Moreover, many of the sources in the moderate- and low-risk categories are located along the ocean foreshore at the outflow end of the groundwater systems. The unconfined groundwater beneath the upland plateaus is to a large extent protected from groundwater contamination by a depth to the watertable commonly in excess of 20 m. The groundwater in the pre-Quaternary confined aquifers is least at risk, because overlying extensive clay formations largely retard downward movement of groundwater and contaminants. As the clays also usually have good adsorptive capacity, the risk of contamination of the confined aquifers is considered minimal.

The major impact on groundwater quality in the Perth Basin outside the metropolitan area is considered more likely to come from non-point sources such as fertilizer, herbicide and pesticide application in agriculture, and urban areas with septic systems. The non-point sources are also suspected of being major contributors to groundwater contamination within the Perth metropolitan area. Large parts of urban Perth are still unsewered; many local government authorities apply large amounts of weedicides during roadside spraying; fertilizer application in horticulture and viticulture is extensive; and fertilizers and pesticides are also applied regularly and extensively on the numerous parks, playgrounds, sportsgrounds, and golf courses. The impact of these non-point sources warrants special study.

## Conclusions

Over 1100 point sources of groundwater contamination have been identified in the Perth Basin. Of these, some 700 are in the Perth metropolitan area, and about 400 have been identified in the remainder of the Perth Basin.

Of the major aquifers in the Perth Basin, the groundwater resources in the predominantly sandy Quaternary sediments of the Swan Coastal Plain, with a generally shallow watertable, are most at risk from groundwater contamination. The risk to the groundwater in the unconfined aquifers in areas where the watertable is deep, and to the confined aquifers in the pre-Quaternary sediments, is considered to be small.

Ninety-eight percent of all point sources of groundwater contamination of a high-risk ranking, and the majority of the sources with a moderate to high-risk ranking, are in the Perth metropolitan region and

predominantly in areas which are zoned industrial. Of these, the Kwinana area is the worst affected and contains the majority of serious cases of groundwater contamination known in Perth. Elsewhere on the Perth Basin, the groundwater resources can generally be considered under only minor threat from point sources in the high-risk categories, with the exception of local concentrations of such sources in the Narngulu and Bunbury areas. Owing to rapid industrial development in some areas, update surveys may be required every few years.

Sources in the categories with a moderate to low-risk ranking are more widely scattered over the whole of the Perth Basin. However, the risk of groundwater contamination from these sources is considered small for most of the basin.

The major impact on groundwater quality in the rural parts of the Perth Basin is likely to be from non-point sources, e.g. fertilizer, herbicide and pesticide application in agriculture and horticulture. Non-point sources are also suspected of being major contributors to groundwater contamination within Perth. These sources should be studied in detail.

## References

- ALLEN, A. D., 1976, Outline of the hydrogeology of the superficial formations of the Swan Coastal Plain.: Western Australia Geological Survey, Annual Report 1975, p. 31-42.
- ALLEN, A. D., 1990, Groundwater resources of the Phanerozoic sedimentary basins of Western Australia, *in* Proceedings of the International Conference on Groundwater in Large Sedimentary Basins, Perth: Australian Government Publishing Service, Canberra.
- AUSTRALIAN WATER RESOURCES COUNCIL, 1987, 1985 review of Australia's water resources and water use; Volume 1: Water resource data set: Australian Government Publishing Service, Canberra.
- COMMANDER, D. P., ALLEN, A. D., and DAVIDSON, W. A., 1990, The groundwater resources of the Perth Basin, Western Australia, *in* Proceedings of the International Conference on Groundwater in Large Sedimentary Basins, Perth: Australian Government Publishing Service, Canberra.
- HIRSCHBERG, K-J. B., 1986, Liquid waste disposal in Perth — a hydrogeological assessment: Western Australia Geological Survey, Report 19, Professional Papers, p.55-61.
- HIRSCHBERG, K-J. B., 1988, Perth North and Perth South sheets, groundwater contamination sites: Western Australia Geological Survey, Record 1988/4.
- HIRSCHBERG, K-J. B., 1989, Groundwater contamination in the Perth metropolitan region, *in* Proceedings of the Swan Coastal Plain Groundwater Management Conference *edited by* G LOWE: Western Australia Water Resources Council, Perth, 1988.
- HIRSCHBERG, K-J. B., 1991, Inventory of known and inferred point sources of groundwater contamination in the Perth Basin, W.A.: Western Australia Geological Survey, Record 1991/7.
- KWINANA INDUSTRIES CO-ORDINATING COMMITTEE, 1987, Report of the Groundwater Management Working Group.
- PLAYFORD, P. E., COCKBAIN, A. E., and LOW, G. H., 1976, Geology of the Perth Basin, Western Australia: Western Australia Geological Survey, Bulletin 124.
- RYAN, P. N., and PAYNE, R. W., 1989, Environmental management for animal based industries — Piggeries: Western Australian Department of Agriculture, Miscellaneous Publication 23/89.

# Proposed stratigraphic subdivisions of the Marra Mamba Iron Formation and the lower Wittenoom Dolomite, Hamersley Group, Western Australia

by

J.G. Blockley, I.J. Tehnas<sup>1</sup>, A. Mandyczewsky,<sup>2</sup> and R.C. Morris<sup>3</sup>

## Abstract

A total of four new members is erected within the Wittenoom Dolomite and Marra Mamba Iron Formation in the lower part of the Hamersley Group, in the northwest of Western Australia. Where possible, fresh diamond drillcore has been used to define the type sections of the members. The new definitions formalize, and slightly vary, previous schemes in use by companies mining iron ore in the Hamersley Basin.

The West Angela Member contains a sequence of interbedded dolomite and shaly dolomite. It is now regarded as being in the lower part of the Wittenoom Dolomite, although some earlier stratigraphic schemes place its leached, weathered equivalent at the top of the underlying Marra Mamba Iron Formation.

The Mount Newman Member forms the uppermost subdivision of the Marra Mamba Iron Formation and consists of thick macrobands of banded iron-formation (BIF) separated by thinner macrobands of mixed shale, chert and carbonate. The central part of the Marra Mamba Iron Formation, made up of interbedded shale, chert, carbonate and iron-formation, is named the MacLeod Member. A sequence of poddy, minnesotaite-rich BIF, chert and shale constituting the lower part of the Marra Mamba Iron Formation is defined as the Nammuldi Member.

Individual macrobands within the Mount Newman Member and the upper part of the MacLeod Member can be correlated over a wide area of the Hamersley Basin. However, stratigraphic continuity becomes less pronounced in the lower part of the MacLeod Member and has not been established for the Nammuldi Member.

**KEYWORDS:** Banded iron-formation, Hamersley Basin, Hamersley Group, iron ore, MacLeod Member, Marra Mamba Iron Formation, Mount Newman Member, Nammuldi Member, stratigraphy, West Angela Member, Wittenoom Dolomite.

## Introduction

The Marra Mamba Iron Formation is the lowest unit of the 2500 Ma old Hamersley Group within the Hamersley Basin<sup>4</sup> in the northwest of Western Australia (MacLeod et al., 1963; Trendall and Blockley, 1970). It conformably overlies the Jeerinah Formation in the upper Fortescue Group, and is in turn conformably overlain by the Wittenoom Dolomite<sup>5</sup>. The geological setting of the formation and its main outcrop areas are indicated on Figure 1.

The unit attained economic importance around 1971 when it was found to contain large deposits of high-grade, secondary iron ore which were low in deleterious

impurities such as phosphorus and alumina. Subsequent evaluation by a number of companies of this essentially stratabound mineralization led to the setting up of several different informal stratigraphic subdivisions of the formation, some of which included units more properly forming part of the overlying Wittenoom Dolomite. These various schemes are reported to have led to some confusion amongst potential buyers of Marra Mamba iron ore, and geologists working in this area saw a need to standardize their nomenclature. This need was accentuated when the industry began to computerize drill logs and saw advantages in adopting uniform designations for the stratigraphic units that they were exploring.

The stratigraphic subdivisions proposed in this paper have been agreed to by the Geological Survey of Western Australia (GSWA), the Commonwealth Scientific and Industrial Research Organization (CSIRO), and the principal iron ore mining and exploration companies sponsoring an Australian Mining Industry Research Association iron ore project on the iron ores and BIFs of the Hamersley Group. The elements of the scheme have already been adopted by industry and some names have already appeared in print (e.g. Kneeshaw, 1984).

<sup>1</sup> BHP Iron Ore Ltd, Perth, WA

<sup>2</sup> Climax Management Pty Ltd, Sydney, NSW

<sup>3</sup> CSIRO, Floreat Park, WA

<sup>4</sup> Although the term Hamersley Basin is used here as the name for the repository of the Hamersley Group and related sedimentary and volcanic rocks in accordance with current GSWA practice, it should be noted that Morris and Horwitz (1983) interpret the site of deposition as a platform.

<sup>5</sup> The term Wittenoom Dolomite has been replaced by Wittenoom Formation in the paper by Simonson et al. in this volume.

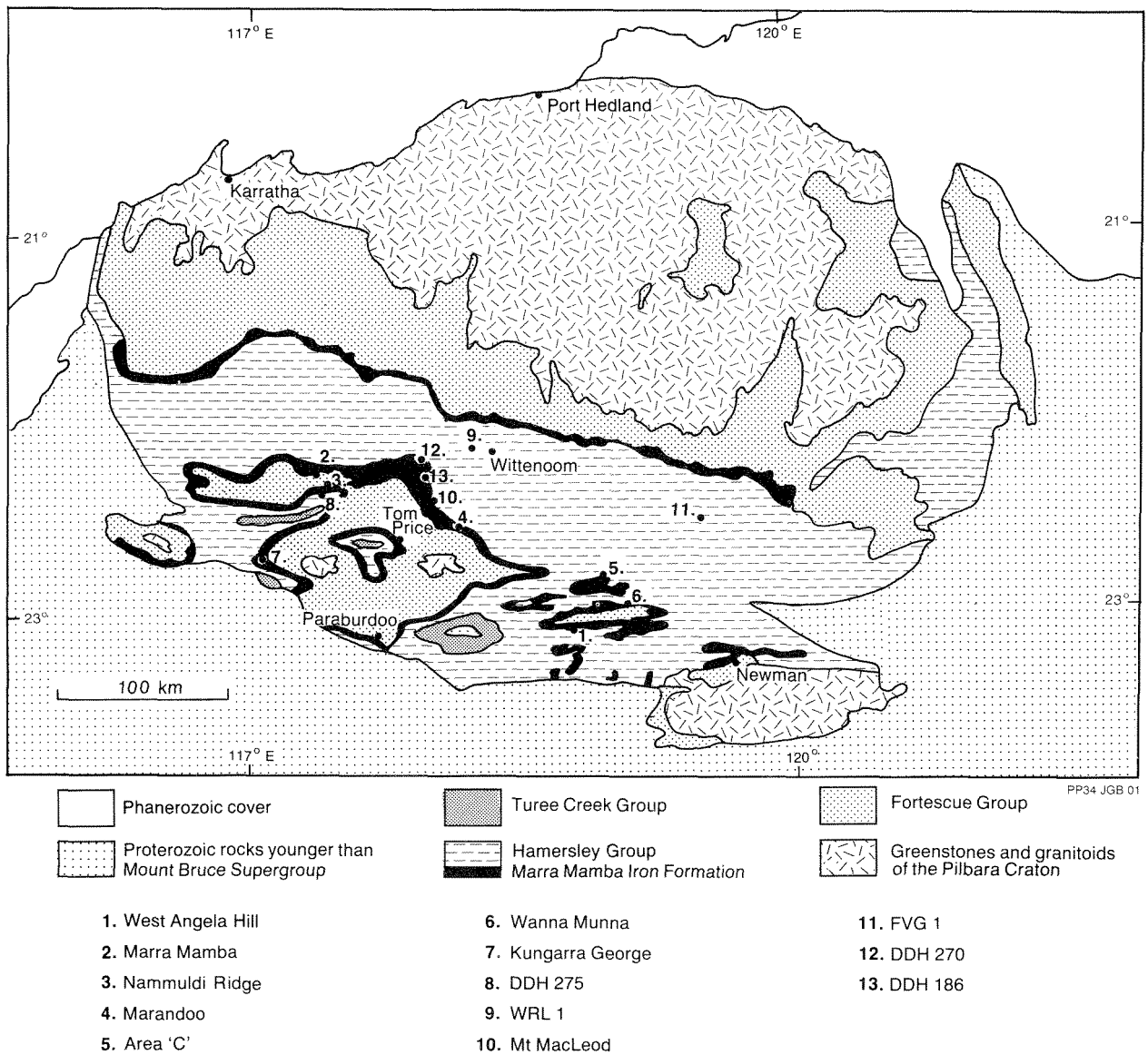


**Figure 1.** Simplified geological map of the Hamersley Basin showing main outcrop areas of the Marra Mamba Iron Formation and localities mentioned in the text

## Previous stratigraphic subdivisions

The earliest attempt to create internal stratigraphic subdivisions within the Marra Mamba Iron Formation was made during an investigation by Ryan and Blockley (1965) of crocidolite deposits within the formation. This study resulted in the naming of two informal members and several crocidolite horizons. While some of the crocidolite horizons were able to be matched over distances of tens of kilometres, the presence of fibre was almost always a prerequisite for successful correlation. Away from the fibre seams no useful correlations were achieved and a composite section published by Blockley (1967), based on measurements of weathered exposures, has been superseded by later drillhole data.

At a later stage of the crocidolite investigations, Trendall and Blockley (1970) recognized a central shaly unit within the formation. This led to an informal

threefold subdivision of the Marra Mamba Iron Formation as follows:

Unit	Thickness (m)
upper BIF member	60
middle shaly member	35
lower BIF member	135

A narrow transition zone of interbedded dolomitic, manganese-bearing shale and chert between the upper BIF member and the first massive dolomite unit within the overlying Wittenoom Dolomite was also recognized but not assigned specifically to either unit. The two informal members named by Ryan and Blockley (1965) were abandoned and it was stated that any scheme of formal nomenclature within this poorly exposed unit should await the availability of drillcore.

Similarly, although the two BIF members of the formation were recognized as being composed largely of

alternating iron-formation and shale units, no attempt was made to subdivide these into numbered macrobands as had been done for the Dales Gorge Member of the Brockman Iron Formation (Trendall and Blockley, 1970).

Throughout most of its outcrop area the Marra Mamba Iron Formation ranges in thickness from about 180 m to 230 m, but marked thinning of the unit to the north and northeast is recorded by Trendall and Blockley (1970, p. 84).

During the early to mid-1970s, drillcore and downhole natural gamma-ray logs became available from a number of iron ore exploration projects within the Marra Mamba Iron Formation. By 1975, most operators had established their own stratigraphic divisions of the formation and had achieved correlations of individual macrobands over considerable distances, particularly in the upper BIF member.

The different schemes used by individual operators between about 1971 and the early 1980s are compared in Table 1. Essentially, all schemes recognized the three informal members proposed by Trendall and Blockley (1970). However, four also included a fourth, uppermost shaly member corresponding to, but generally thicker than, Trendall and Blockley's transition zone.

Apart from the small differences in terminology used in the various schemes, detailed correlations of measured sections and gamma-ray logs indicated that some boundaries between members had been placed at different positions (Blockley, 1979). For example, the 'upper banded iron member' of the Mount Newman Mining scheme (Slepecki, 1981) embraced a sequence of shale and chert which other operators included in their uppermost shaly member.

Goldsworthy Mining differed from the other companies in using the contact between ore and un-enriched BIF as the stratigraphic boundary between its upper and middle members (Neale, 1975). While this contact does show stratigraphic persistence in some areas, it is certainly transgressive on a regional scale, and the general concept contravenes accepted stratigraphic principles.

Another discrepancy between the schemes is the status accorded to the upper shaly member. This unit is a feature of the subdivisions set up in the central and eastern parts of the basin by Robe River Mining Associates, Texasgulf/Hanwright (now CRA/Hanwright) and Mount Newman Mining (now BHP Iron Ore Ltd), but was omitted from the scheme used by Hamersley Exploration Pty Ltd (Hamex) working in the better exposed westerly part of the basin. In this area, the shale was interpreted by Hamex Senior Geologist, John Evans (1977, pers. comm.) as being derived by leaching of laterally equivalent Wittenoom Dolomite.

## Proposed stratigraphic scheme

### General principles

The stratigraphic scheme proposed in this paper recognizes and formalizes all four members which have

gained currency in the industry, but assigns the uppermost shaly member to the Wittenoom Dolomite rather than to the Marra Mamba Iron Formation as drillcore and fresh natural exposures show it to consist mainly of dolomite and dolomitic shale. It should be noted that Simonson et al. (1993) uses the names Bee Gorge and Paraburdoo Members for the upper and middle parts respectively of the Wittenoom Dolomite, and also suggests that the name of the unit be changed to Wittenoom Formation because of its high content of non-carbonate lithologies. His new nomenclature has not been used in this paper.

The four new members proposed here, from youngest to oldest, are:

#### **Wittenoom Dolomite**

West Angela Member

#### **Marra Mamba Iron Formation**

Mount Newman Member

MacLeod Member

Nammuldi Member

Definitions of the three members proposed here for the Marra Mamba Iron Formation are based largely on detailed study of the core of DDH 275 drilled by Hamex at 117° 21.5'E and 22° 25.6'S, about 6.7 km northeast of the Mount Brockman trigonometric station. Additional information on the lowest member has been obtained from the core of DDH 186 drilled by Hamex at 117° 55'E and 22° 24'S

### Repository of cores

The core of DDH 275 is stored at the CSIRO Exploration Geoscience Laboratory, Floreat Park, Western Australia. A set of streak prints prepared by the method of Morris and Ewers (1978) is also held at the CSIRO laboratory to provide a convenient means of examining the lithology of the core.

Core from WRL 1 is stored at the CRA Exploration Pty Ltd depot in Anderson Road, Karratha.

The partial intersection of the Nammuldi Member obtained in DDH 186 is held by the Geological Survey of Western Australia in its core library.

## Wittenoom Dolomite

### West Angela Member

#### *Derivation of name*

The West Angela Member is named after West Angela Hill near the West Angelas iron ore deposits held under a State Agreement by Robe River Mining Associates.

#### *Type section*

The type section of the West Angela Member is herein defined as that part of the core from hole WRL 1 between

**Table 1. Comparison of stratigraphic schemes formerly in use by exploration companies**

<i>'Natural' Lithological Subdivisions</i>	<i>Newman (a)</i>	<i>CRA/Hanwright (b)</i>	<i>Cliffs</i>	<i>HAMEX</i>	<i>Hammersley Iron</i>	<i>Goldsworthy</i>
Interbedded shale, chert, BIF ± dolomite. Thickest where overlying ore in eastern part of basin. Contains iron and manganese concentrations. (Trendall & Blockley's (1970) transition zone)	<b>Upper shale member</b> Typically 30 m thick. 16 shale bands recognized (A1 to A16)	<b>Upper shale member</b> Typically 40 m thick. Some informally named marker beds used.	<b>Upper shale member</b> 30 to 40 m thick. 3 shale bands recognized (480, 490 and 500).	<b>Not recognized</b> (considered to be leached Wittenoom Dolomite)	<b>Upper shale member</b> 10 m thick where unmineralized. Not subdivided but some marker horizons used.	<b>Not recognized</b>
BIF interbedded with shale–chert carbonate units weathering to thin shaly partings. Commonly mineralized to powdery hematite–goethite ore, particularly in upper part.	<b>Upper BIF member</b> Typically 50 m thick (unmineralized). 11 shale bands recognized (B1 to B8 plus U1 to U3)	<b>Upper banded iron member</b> About 46 m thick where unmineralized. 8 shale bands recognized. (F1, F2, G, H, H1, I, J, K).	<b>Upper banded iron</b> Typically 80 m thick where unmineralized. 7 shale bands recognized (numbered 510 to 570 by tens).	<b>Upper BIF member</b> About 30 m thick where mineralized. 4 shale bands recognized (upper, twin shales and lower).	<b>Upper BIF member</b> 80 m thick where unmineralized 8 shale bands recognized (M1 to M8)	<b>Upper member</b> Hematite-goethite ore with up to 10 numbered shale bands.
Interbanded shale, chert, BIF and carbonate. Commonly weathers to form a strike valley. Rarely mineralized.	<b>Middle BIF and shale member</b> Typically 24 m thick. 15 shale recognized (C1 to C15).	<b>Intermediate shale member</b> About 32 m thick. 14 shale bands recognized (L to W plus V1 and and W1)	<b>Intermediate shale member</b> Typically 45 m thick where unmineralized. 16 shale bands recognized (580 to 730 by tens).	<b>Median shale member</b> Not subdivided	<b>Median shale member</b> Thickness ranges from 25 m (mineralized) to 37 m. Not subdivided.	<b>Middle member</b> Cherty BIF over interbedded shale and chert. No subdivisions recorded.
Cherty BIF and chert with numerous shaly bands. Podded yellow chert bands (after minnesotaite) are a feature of most outcrops.	<b>Lower BIF member</b> Typically 70 m thick, but thins to 40 m. 18 shale bands recognized (D1–D18).	<b>Lower banded iron member</b> Thickness not established. No shale band nomenclature.	<b>Lower banded iron member</b> Full thickness not established. 10 shales recognized in upper 50 m. (740 to 830 by tens).	<b>Lower BIF member</b> Not subdivided, but distinctive podded chert beds ('Potato beds') near top are used as a marker.	<b>Lower BIF member</b> 90 to 115 m thick. Subdivisions noted but not named, except for 'potato beds'.	<b>Lower member</b> 125 m thick. No subdivisions recorded

(a) Now BHP Iron Ore  
(b) Formerly Texasgulf/Hanwright

420.4 m and 524.6 m. The upper part of the member is marked by a transition from predominantly massive dolomite to interbedded dolomite and shaly dolomite. This change is reflected in the gamma-ray and caliper logs of the hole (Fig. 2).

The core is stored at the premises of CRA Exploration Pty Ltd at Karratha and the core log, extracted from Meakins (1987), is tabulated in Appendix 1.

As noted above, the near-surface expression of the member may vary quite markedly from that seen in drillcore.

### *Type areas*

Relatively fresh exposures of the West Angela Member are seen at Radio Hill near Paraburdoo and in tributaries of Duck Creek. Cored intersections of the member were also obtained in holes DDH 275 and FVG 1 (Fig. 1).

Typical lithologies of the weathered member can be seen at Newman, particularly in the openpit on Mount Newman Mining's Orebody 29. Other accessible exposures are present at the portal of an exploratory adit on the West Angelas deposits and at the entrance to the test pit at Marandoo.

### *Description*

The dominant lithologies of the fresh West Angela Member are dolomite and shaly dolomite. Chert is a minor component of the upper part of the member, but becomes more common lower down. Near the base of the member there is a 10 to 20 m thick sequence of interbedded chert, BIF and shale that gives rise to three characteristic gamma-ray peaks (Fig. 2). These peaks have been identified wherever the member has been examined in detail and are designated AS1 to AS3 in company logs (Fig. 2).

The dolomite units logged in WRL 1 (Meakins, 1987) are massive and crystalline, laminated with shaly partings, or brecciated with shale fragments. They may exhibit soft-sediment deformation structures and stylolites. The shaly dolomite comprises thinly bedded, grey crystalline dolomite interbedded with carbonaceous shale and siltstone. Sedimentary features noted include inverted graded bedding and flame structures. Pyrite occurs in shale beds as blebs, stringers parallel to bedding, and fracture fillings.

The lower boundary of the member is marked by a sharp contact between shale or shaly dolomite, and a thick unit of podded, magnetite-bearing BIF at the top of the Marra Mamba Iron Formation. It is clearly defined in outcrop and drill logs, and can be traced throughout the greater part of the Hamersley Basin. However, the upper boundary of the member is transitional and, although it can be clearly identified in the geophysical logs of the various core holes that penetrate it, we recognize that there are difficulties in establishing its position in most areas. For this reason it is difficult to estimate the normal thickness of the member.

The West Angela Member is best known where it is found in proximity to iron ore deposits developed in the underlying Mount Newman Member of the Marra Mamba Iron Formation. In these situations the carbonate content of the member is almost always leached, leaving a rock composed mainly of poorly bedded shale with chert bands or breccias. The shales are striped due to alternating bands of manganese and iron oxide enrichment. Locally, manganese oxide concentrations can be high (up to 25% MnO), particularly along a cherty horizon (near the base of the member) which commonly forms a stratigraphic marker known as the 'Manganese Band'. In the Newman pit on Orebody 29, the shale is typically light and porous, and contains secondary gypsum.

### *Stratigraphic continuity*

Lateral persistence within the West Angela Member is best demonstrated by the sequence of interbedded chert, BIF and shale near its base. Above this sequence it is difficult to establish lateral correlations within the member. Comparison of the logs of holes WRL 1 (Meakins, 1987) and FVG 1 (Andrew, 1985) suggests that the member becomes more shaly in the eastern part of the basin. Such a facies change could account for the more prominent development of residual shale at Newman and West Angelas compared with that at Nammuldi and Paraburdoo.

## **Marra Mamba Iron Formation**

### **General features**

Detailed descriptions including mineralogy, petrography, and geochemistry of cores from the Marra Mamba Iron Formation were presented by Davy (1975) for the upper 4 m of the Mount Newman Member at Millstream; Ewers and Morris (1980) for DDH 270, upper Mount Newman Member at Marlathanna bore; Davy (1985) for the lower 88 m of the Nammuldi Member in DDH 186 (about 13 km south of DDH 270); and Morris (1991) for the two upper members and the top 12 m of the Nammuldi Member in DDH 275, at Nammuldi. Klein and Gole (1981) gave a detailed mineralogical and chemical breakdown of four representative 12.5 cm lengths of core from DDH 270 and 182.

The three members of the Marra Mamba Iron Formation differ in their basic features though they have many points in common.

The Mount Newman Member shows a marked subdivision into two major rock types, forming an alternating macroband pattern somewhat similar to that in the Dales Gorge Member. The dominant macrobands consist of magnetite-rich, oxide-type banded iron-formation (BIF) with a significant silicate-carbonate content. The intervening narrower macrobands consist of varying proportions of ferroan dolomite and limestone, with shaly intercalations and occasional chert beds. These horizons are defined as SCC macrobands (silicate-carbonate-chert) following a convention established by CSIRO workers. SCC macrobands show

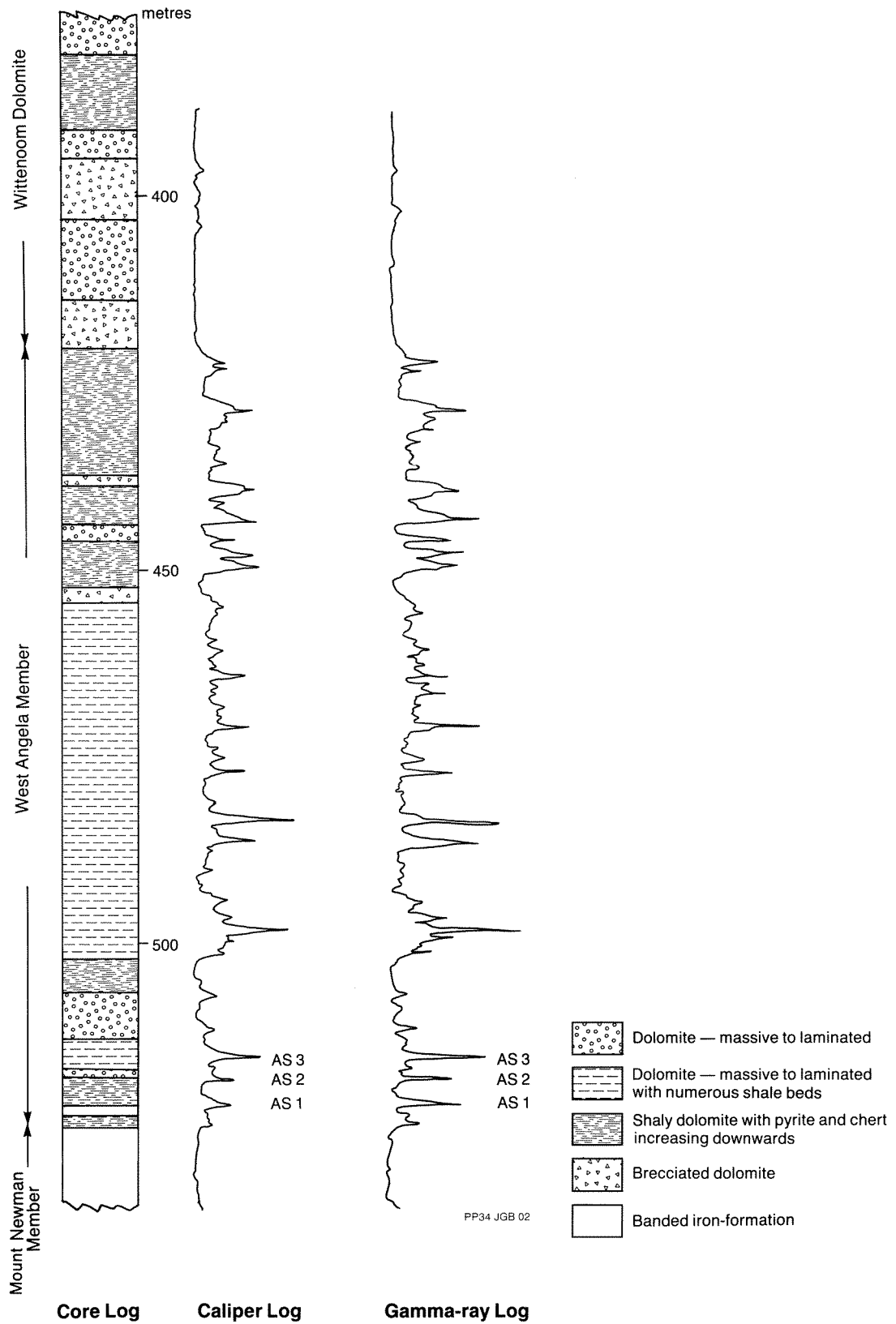


Figure 2. Lithological, gamma-ray and caliper logs of the type section of the West Angela Member in hole WRL 1

little similarity to the S macrobands of the Dales Gorge Member (except for the purely shale horizons) and most closely resemble the lithology of the overlying Wittenoom Dolomite (Ewers and Morris, 1980; Morris, 1991) but with significant iron in the carbonate. The geochemistry of the shales and the occasional shard bands suggest derivation from mainly volcanoclastic components, modified by reaction with iron-bearing marine waters. The SCC macrobands are generally referred to as 'shales' because of their appearance in weathered and enriched exposures.

The upper part of the middle shaly unit, the MacLeod Member, also shows this type of macroband subdivision but with a significantly higher silicate content in the BIF. The limestone–dolomite sequence decreases down the member and, towards the base, it becomes difficult to clearly distinguish shaly BIF from cherty shale.

Macrobanding is poorly defined in the Nammuldi Member which is predominantly silicate–carbonate BIF sequence, with some resemblance to the BIF of the S macrobands, but with a varying magnetite content (Davy, 1985).

The mesobanding of the Marra Mamba Iron Formation is more varied than in the Dales Gorge Member and reflects the significantly higher content of silicates and carbonates of the unit. The mineralogy, though relatively simple, is not easily determined with the microscope, owing to the complex fine-grained mineral intergrowths. The major components are quartz (chert), magnetite, and minnesotaite, with ferroan talc, calcium–magnesium carbonates varying from dolomite to ankerite, abundant ferroan and normal calcite in the SCC macrobands, siderite (particularly in the MacLeod Member), stilpnomelane, riebeckite, chlorite, ?greenalite, phlogopite and undetermined 'mica'. Among the less prominent minerals are widespread pyrite, and very erratic pyrrhotite which, when concentrated, is usually associated with chalcopyrite, sphalerite, and rarely galena and arsenopyrite. Authigenic alkali feldspars, albite, orthoclase, and untwinned microcline, are common in some alumina-rich bands, but are most readily recognized in carbonate zones. Ilmenite, tourmaline and pyrite are commonly associated in narrow bands in the shale zones. Carbon, and rarely graphite, are most easily seen in carbonate areas, commonly associated with stylolites, and as the colouring matter (commonly with pyrite) in black shale.

A significant feature is the absence of well-defined BIF-varves or aftbands (originally called microbands) from the Marra Mamba Iron Formation, despite their prominence in the Dales Gorge Member cores. Nevertheless, some mesobands do show a type of thick, regular banding but lack the well-defined iron-rich and silica–carbonate-rich alternations of the Dales Gorge Member. Instead, variations in the minnesotaite and ankerite distribution in chert, or of stilpnomelane with carbonate, are the most common (Morris, 1991). A much finer, though rarely regular banding results from 'rafts' of magnetite forming fine laminae which alternate with intergrown chert–silicate–carbonate.

### ***Alteration and mineralization***

Oxidized and weathered BIF generally retains the original mesobanding, and the outcrop is typically stained yellow as a result of the breakdown of the abundant carbonate and silicate components. The oxidized shale bands include significant kaolinite, goethite and gibbsite. They usually occur as either well-bedded, white, pink and red-banded horizons or massive khaki units with goethite pods.

The bulk of the potentially commercial iron ores within the Marra Mamba Iron Formation occurs within the Mount Newman Member, although in places mineralization extends upwards into the lowermost part of the West Angela Member of the Wittenoom Dolomite and downwards, normally only for a short distance, into the MacLeod Member. Typically the mineralized zone extends stratigraphically downwards from the top of the member so that there is usually a downward transition from ore to weathered BIF at some variable horizon within the sequence. For example, in Orebody 29 at Newman, the whole of the member is mineralized whereas at Nammuldi, mineralization typically stops at the level of shale NS2.

The enrichment processes are described in detail by Morris (1980, 1985, 1987) and Slepecki (1981). The ore, which consists of goethite, ochreous goethite, and hematite is considered to have been formed by supergene enrichment of BIF followed by variable leaching of the replacement goethite. Original banding within the BIF and many other structures are well preserved, as is the characteristic gamma-ray profile of the member. The transition from iron-formation to ore involves a reduction in thickness by about 35%; subsequent processes, which include metamorphism (rare in the Marra Mamba Iron Formation) and further leaching, can increase this to about 50%.

As a result of the pseudomorphing by goethite of the high silicate and carbonate content of the BIF, and the post-enrichment differential leaching of this goethite, iron ore formed within the Mount Newman Member is typically softer and more friable than that developed within the Brockman Iron Formation. The ore in Orebody 29 at Newman, for example, ranges from weakly cemented biscuit ore to iron ore dust being scaled from 0063 to 0073 in the Pilbara Iron Ore Classification (PIOC) (Kneeshaw, 1984). At Marandoo the ore in the upper 'hardcap' zone is competent (0033) with a biscuit ore (0063) appearing at depth.

## **Mount Newman Member**

### ***Derivation of name***

The Mount Newman Member is the uppermost of the three members of the Marra Mamba Iron Formation. It is named after Mount Newman (latitude 23°16'S, longitude 119°34'E), a prominent peak in the Ophthalmia Range situated about 20 km northwest of the town of Newman. The Mount Newman Mining Company was one of the first to recognize the stratigraphic controls of iron

ore within the Marra Mamba Iron Formation, and was the first to mine this ore type commercially.

### *Type section*

The type section of the Mount Newman Member is defined as the interval of core in hole DDH 275 between the top of the member at 342.5 m and its base at 419.65 m. This section is presented in Figure 3, which includes a gamma-ray log showing the peaks typical of the member. A log of the core making up the type section is given in Appendix 2.

### *Type areas*

The Mount Newman Member has been studied extensively by mining companies because of its concentrations of iron ore, and a number of typical exposures have been recorded. Probably the least weathered and most complete natural exposure is in Kungarra Gorge (Fig. 3) where the member is seen on both limbs of an anticline in a deeply dissected drainage. Other useful exposures are present in the Turner Syncline (latitude 22° 40.5'S, longitude 117° 26.6'E), in two gorges at Wanna Munna (latitude 23° 04.9'S, longitude 119° 9.2'E and latitude 23° 04.9'S, longitude 119° 08.2'E), and in 'Manganese Gorge' at Marandoo. The member is also well documented in exploration holes across the province, having been explored in detail at Paraburdoo, Tom Price, Nammuldi, Marandoo, Area 'C', Wanna Munna and Newman.

In addition to the core of DDH 275, a complete intersection of the member was also achieved in hole WRL 1 drilled near Wittenoorn (Fig. 3) while DDH 270, drilled 38 km west of Wittenoorn, cored the upper 34 m of the member (Ewers and Morris, 1980).

Enriched sections of the Mount Newman Member are well exposed in the opencut on Orebody 29 at Newman, and in various openings at West Angelas, Area 'C', Marandoo and Nammuldi.

The Mount Newman Member is made up of nine macrobands of BIF alternating with 8 SCC macrobands. These 'shale' bands are important stratigraphic markers and are referred to as shales NS1 to NS8, the numbering proceeding from the base of the unit. Other thinner, or less continuous 'shales' have been recorded but are less important as stratigraphic markers and have not been numbered. Similar subdivisions of the member have previously been published by Blockley (1979) and Slepecki (1981), although the presently defined boundaries of the member differ from those used by the earlier authors. Following the same principle, the BIF macrobands separating the shales are designated NB1 to NB9.

Cherts within the BIF macrobands of the Mount Newman Member are strongly podded and give the unit a characteristic wavy bedding locally referred to as 'pinch-and-swell' structure. The pods may be either flat and parallel to the main bedding planes, or inclined to the bedding in a manner reminiscent of the cross pods within the Dales Gorge Member (Trendall and Blockley, 1970,

p. 155). Such cross pods commonly occur in stacks of three or four within stratigraphic intervals of 30 or 40 cm, each pod being slightly offset from the one below.

### *Stratigraphic continuity*

The eight shale bands (NS1 to NS8) referred to above can be traced over the entire extent of the area in which exploration for iron ore has taken place (Blockley, 1979). Throughout this extent they are characterized by distinctive patterns in gamma-ray logs which, in mineralized sections, often provide more-reliable correlations than do the strongly altered lithologies.

Stratigraphic continuity on even finer scales can also be demonstrated. For example, within shale NS3 there is a thin band containing pyrite nodules up to 5 mm in diameter which become goethitic or hematitic in oxidized sections. This band, usually no more than 5 cm thick, has been identified in exposures as far apart as Newman and Nammuldi.

Another stratigraphic indicator of somewhat lesser importance is provided by a group of crocidolite bands commonly appearing within BIF macroband NB2. These bands have been noted in localities ranging from Kungarra Gorge in the west to Wanna Munna in the east. The stratigraphic interval containing these bands and associated massive riebeckite was referred to by Trendall and Blockley (1970) as the Vivash Riebeckite Zone. In most natural exposures the original crocidolite has been replaced by goethite or silica to form griqualandite or tiger eye.

## **MacLeod Member**

### *Derivation of name*

The MacLeod Member is named after Mount MacLeod, one of the higher peaks on the Hamersley Range and situated at latitude 22° 23.8'S, longitude 118° 01'E, about 28 km north-northwest of Marandoo camp.

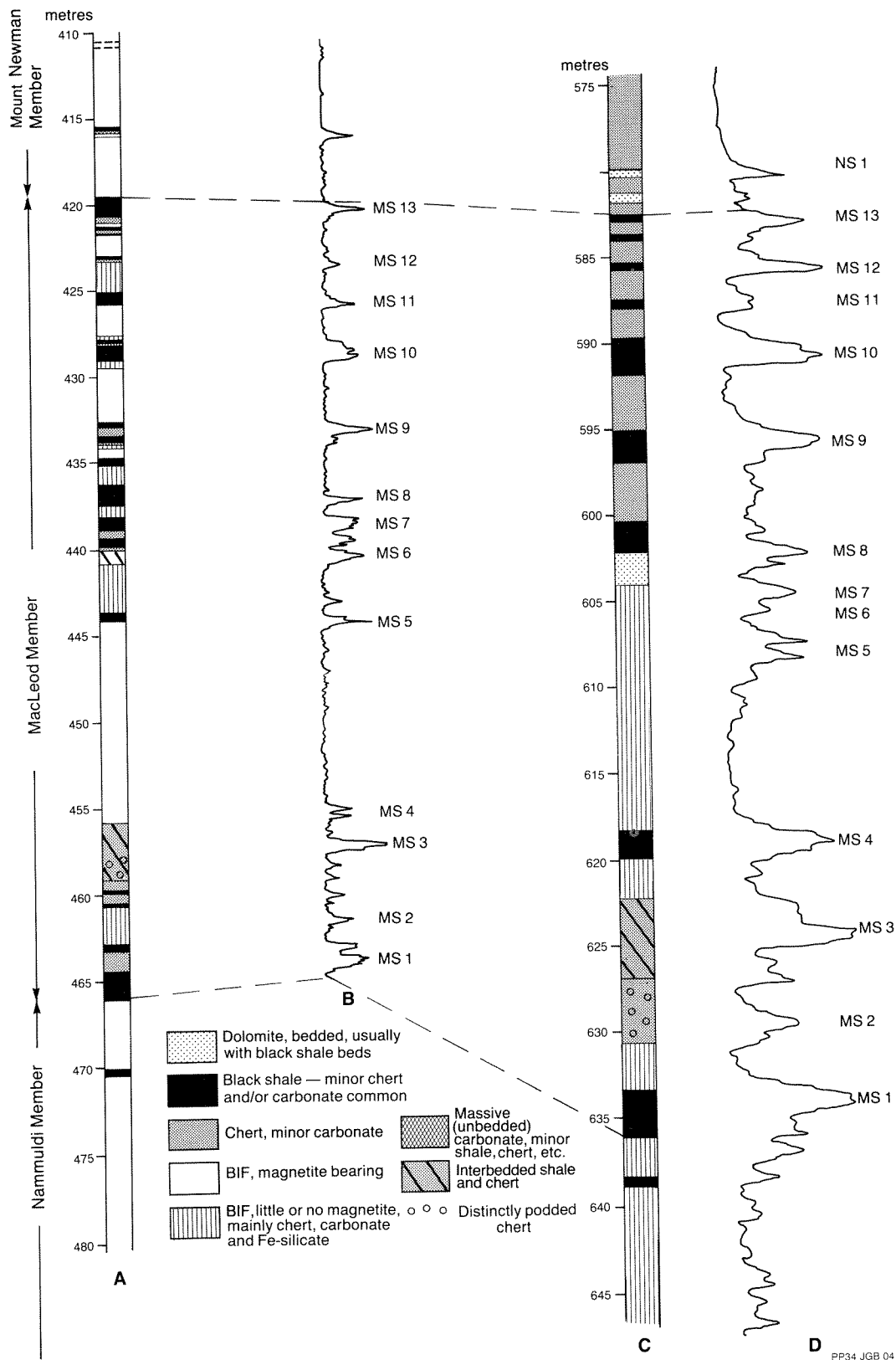
### *Type section*

The type section of the MacLeod Member is defined here as the drillcore from Hamex DDH 275 between the depths of 419.65 m and 465.8 m. A core log of the type section is given in Appendix 3.

### *Type areas*

The MacLeod Member is very susceptible to erosion because of its high content of shaly beds; consequently, complete natural exposures are rare. Sections showing most of the member occur at Kungarra Gorge, in the Turner Syncline (latitude 22° 40.5'S, longitude 117° 26.6'E), and in two gorges at Wanna Munna.

The member has been extensively drilled during the search for iron ore and is generally better known from its gamma-ray logs than from outcrop. In addition to those illustrated from DDH 275 and WRL 1, complete gamma-



PP34 JGB 04

Figure 3. Sections of the Mount Newman Member. A — Core log of the type section in DDH 275. B — Gamma-ray log of the type section in DDH 275. C — Core log of member in WRL 1. D — Section of member measured in Kungarra Gorge

ray profiles are available from Tom Price, Newman, West Angelas and Marandoo. Another complete core of the unweathered member was obtained from hole WRL 1 near Wittenoom.

### **Description**

In fresh drillcore the MacLeod Member consists of interbedded iron-formation, black shale and carbonate. The iron-formation contains chert, iron carbonates and a high proportion of iron silicates, with a variable content of magnetite. Much of this material, particularly toward the base of the member, is best classified as shaly iron-formation.

Weathered exposures of the member consist of shale, chert, and altered iron silicates with minor bands of hematite or goethite. Outcrop is generally poor, with the member typically forming small, strike-controlled gullies.

Gamma-ray logs of the member usually show 13 distinct peaks corresponding to shale bands, although these may be difficult to identify in outcrop. These peaks have been used as the basis for subdividing the unit into numbered shale and BIF bands for use in detailed borehole gamma-ray log interpretation (Fig. 4).

During field mapping the base of the member has commonly been placed at a prominent horizon of chert nodules referred to as the 'potato bed'. The chert pods within this marker vary in size from place to place. They are generally of an oblate spheroid shape, but in places have been deformed into ellipsoids. Internally they contain stellate cracks, usually filled with quartz or carbonate. However, as several chert horizons within the member are known to contain similar nodules, the use of the 'potato bed' to define the base of the member should be discontinued. Nevertheless, this distinctive unit remains a useful marker horizon in many localities. Until further information becomes available, the 'potato bed' is tentatively correlated with the band of chert nodules logged between 457 and 459 m in DDH 275 (Fig. 4). This band is 17 m above the base of the member as defined above.

The Dun Crocidolite Horizon of Trendall and Blockley (1970) is now considered to lie within the MacLeod Member, probably in BIF macroband MB9.

Iron mineralization within the member is minor and of lower grade compared with that in the Mount Newman Member. Near the top of the unit, the ore consists of interbedded goethite, martite (hematite after magnetite) and ferruginous shale, but lower in the section, hematite is absent. The ore is typically of PIOC type 0073 (Kneeshaw, 1984).

## **Nammuldi Member**

### **Derivation of name**

The Nammuldi Member is named after Nammuldi Ridge which is centred at 22° 25'S, 117° 24'E, and forms a low topographic rise to the north of Mount Brockman.

The ridge contains a major deposit of Marra Mamba iron ore under tenure to Hamersley Iron Pty Ltd.

### **Type section**

The type section of the Nammuldi Member is defined as the exposure on the east side of the gorge formed where the Hardey River cuts the Marra Mamba Iron Formation on the south limb of the Turner Syncline (latitude 22° 46.6'S, longitude 117° 30.9'E). A detailed description of the type section is set out in Appendix 4.

The base of the member is clearly defined by its contact with the underlying Roy Hill Shale Member of the Jeerinah Formation, which here is intruded by a dolerite sill at a short distance below the contact. At its top, the member is in contact with poorly exposed shale and chert of the MacLeod Member. The measured thickness of the type section is 125.5 m.

### **Type areas**

No satisfactory section of the entire Nammuldi Member is preserved as drillcore. Hamex hole DDH 275 intersected the upper boundary of the unit at 465.8 m and stopped some way into the member at 480 m. The core from DDH 186 commenced within the member at 54 m and intersected the lower boundary at 141.95 m before passing into the conformably underlying Roy Hill Shale Member of the Jeerinah Formation. It is unlikely that these drill intersections overlap stratigraphically. Hole WRL 1 drilled by CRA Exploration at about 22° 12'S, 118° 13'E, intersected the complete Nammuldi Member from 638.9 to 678.9 m. However, the 40 m thickness indicated is appreciably less than that recorded in other parts of the basin, and there are also lithological differences which suggest that this intersection is not typical of the member as a whole.

Most of the prominent outcrops of the Marra Mamba Iron Formation consist largely of the Nammuldi Member. Reasonably accessible exposures can be seen at the old Marra Mamba crocidolite workings, Mount Lionel near Tom Price, and in the Chichester Range north of Wittenoom.

### **Thickness**

The Nammuldi Member is typically about 130 m thick, but substantial variations have been recorded. The 40 m thickness recorded near Wittenoom is noted above, while the standard gamma-ray log reference section used by Mount Newman Mining indicates a thickness of about 60 m near Newman (Slepecki, 1981).

### **Description**

In oxidized outcrop the member consists predominantly of yellow and brown chert with thin hematite bands. Chert is more predominant than in the Mount Newman Member. A distinctive feature of the Nammuldi Member is the extensive development of chert pods, particularly in the upper part of the unit. The pods are better developed and more numerous than those in the

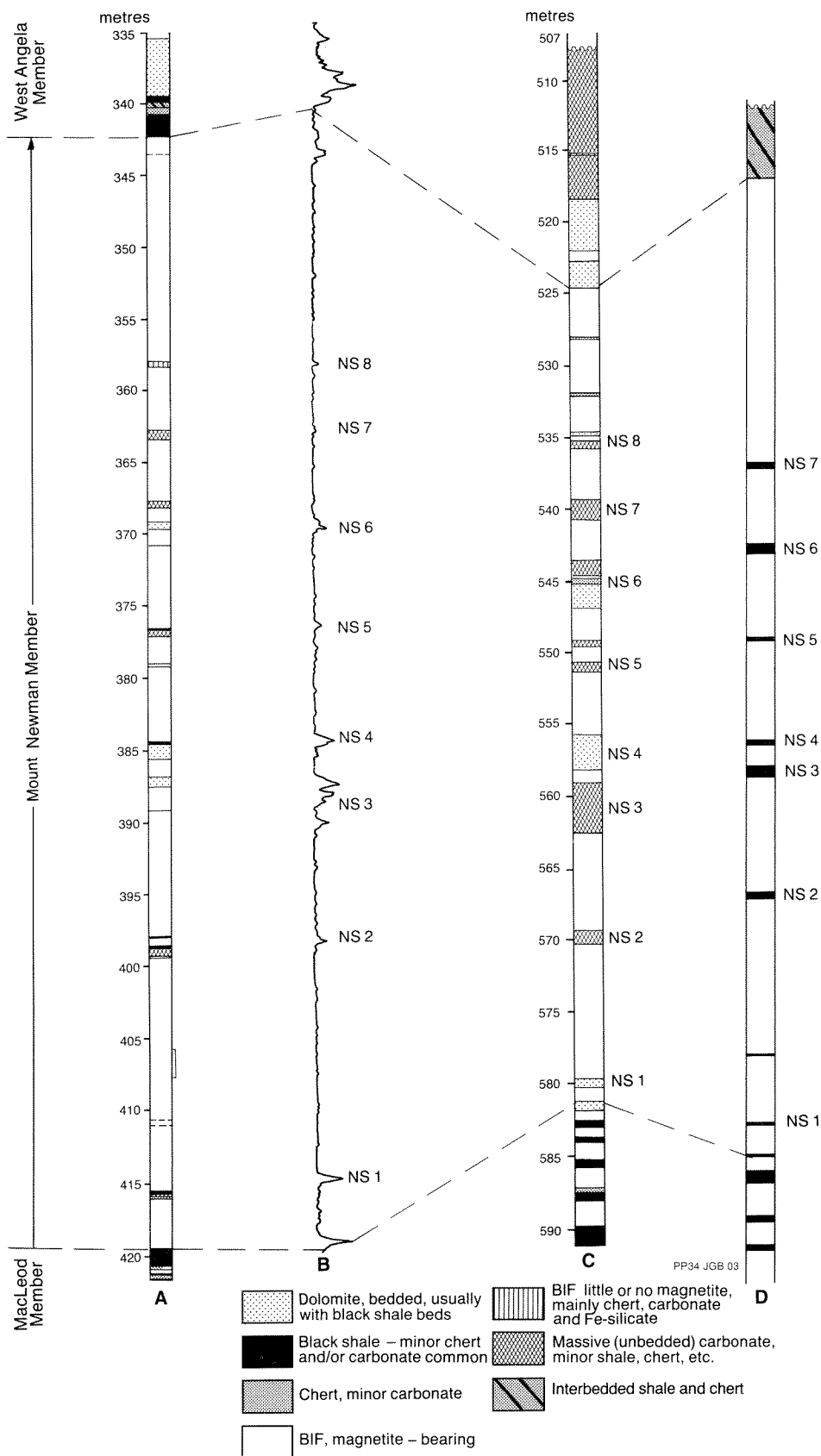


Figure 4. Sections of the MacLeod Member. A — Core log of the type section in DDH 275. B — Gamma-ray log of the type section in DDH 275. C — Core log of member in WRL 1. D — Gamma-ray log of member in WRL1

Mount Newman Member or in any other BIF unit in the Hamersley Group. In many localities, pods are elongated parallel to the axes of regional folds, suggesting an overlap between diagenesis and tectonic deformation. Gamma-ray logs and drillcores of the Nammuldi Member indicate that a significant proportion of it consists of shaly material; however, shale is rarely seen in outcrop, its position being indicated by breaks in exposure.

The upper part of the member in DDH 275 consists of unoxidized magnetite-bearing BIF with minor stilpnomelane, riebeckite and pyrite. Davy (1985) described the lithology of the lower part of the member in DDH 186 as predominantly dark-coloured BIF and interbedded green minnesotaite and stilpnomelane with minor carbonates and quartz. Magnetite decreases with depth and is totally absent from the bottom 9 m which is shaly and transitional into the underlying Roy Hill Shale Member. The pyrrhotite content of the core increases towards the base of the member.

Davy and Hickman (1988) note that while the BIF is banded, the banding is not entirely regular, and the rock varies from laminated to massive. Subdivision of the member depends more on the differences in the proportions of the minerals present (represented visually by colour differences) than on totally different lithologies. There are no macrobands of radically different composition.

The core of the Nammuldi Member in WRL 1 contains very little magnetite, iron being expressed in minerals such as minnesotaite, stilpnomelane, ferroan carbonate and pyrrhotite. Macrobanding and mesobanding are poorly developed. Some sedimentary features, such as tuff beds, scouring and possible cross-bedding have been recognized in the core (Meakins, 1987). Stylolites are common in chert-carbonate horizons.

Although the Nammuldi Member contains numerous shale bands, it has not been possible to establish regional correlations of these beds, although some local correlation has been obtained in the Newman area. As a result, no numbering scheme for the shales is proposed in this paper.

## References

ANDREW, R.L., 1985, Final report on exploration completed within ELs, Roy Hill, Western Australia: Unpublished report for CRA Exploration Pty Ltd on Western Australia Geological Survey open file, Item 3341.

BLOCKLEY, J.G., 1967, The crocidolite deposits of Marra Mamba, West Pilbara Goldfield: Western Australia Geological Survey, Annual Report 1966, p. 71–73.

BLOCKLEY, J.G., 1979, A contribution to the stratigraphy of the Marra Mamba Iron Formation: Western Australia Geological Survey, Annual Report 1978, p. 71–73.

DAVY, R., 1975, A geochemical study of a dolomite–BIF transition in the lower part of the Hamersley Group: Western Australia Geological Survey, Annual Report 1974, p. 88–100.

DAVY, R., 1985, The mineralogy and composition of a core which intersects the Marra Mamba Iron Formation and the Roy Hill Shale Member: Western Australia Geological Survey, Record 1985/6.

DAVY, R., and HICKMAN, A.H., 1988, The transition between the Hamersley and Fortescue Groups as evidenced in a drill core: Western Australia Geological Survey, Report 23, p. 51–85.

EWERS, W.E., and MORRIS, R.C., 1980, Chemical and mineralogical data from the uppermost section of the upper BIF member of the Marra Mamba Iron Formation: Commonwealth Scientific and Industrial Research Organization, Division of Mineralogy, Report FP 23.

KLEIN, C., and GOLE, M.J., 1981, Mineralogy and petrology of parts of the Marra Mamba Iron Formation, Hamersley Basin, Western Australia: *American Mineralogist*, v. 66, p. 507–525.

KNEESHAW, M., 1984, Pilbara iron ore classification—a proposal for a common classification for BIF-derived iron ore: Australasian Institute Mining Metallurgy, Proceedings 289, p. 157–162.

MacLEOD, W.N., de la HUNTY, L.E., JONES, W.R., and HALLIGAN, R., 1963, A preliminary report on the Hamersley Iron Province, North-West Division: Western Australia Geological Survey, Annual Report 1962, p. 44–54.

MEAKINS, A.L., 1987, Final report on exploration completed within the Mulga Project area, Mt. Bruce 1:250 000 sheet, Pilbara region, Western Australia: CRA Exploration Pty Ltd unpublished report on Western Australia Geological Survey open file, Item 3458.

MORRIS, R.C., 1980, A textural and mineralogical study of the relationships of iron ore to banded iron-formation in the Hamersley Iron Province of Western Australia: *Economic Geology*, v. 75, p. 184–209.

MORRIS, R.C., 1985, Genesis of iron ore in banded iron-formation by supergene and supergene–metamorphic processes — a conceptual model, in *Handbook of strata-bound and stratiform ore deposits*, volume 13 edited by K.H. WOLF: Amsterdam, Elsevier, p. 73–235.

MORRIS, R.C., 1987, Iron ores derived by enrichment of banded iron-formation, in *Siliceous sedimentary rock-hosted ores and petroleum* edited by J. R. HEIN: New York, Van Nostrand Reinhold, p. 231–267.

MORRIS, R.C., 1991, The Marra Mamba Iron Formation of the Hamersley Group of Western Australia: Commonwealth Scientific and Industrial Research Organisation Exploration Geoscience Restricted Report 158R (unpublished).

MORRIS, R.C., and EWERS, W.E., 1978, A simple streak-print technique for mapping mineral distributions in ores and other rocks: *Economic Geology* v. 73(4), p. 562–566.

MORRIS, R.C., and HORWITZ, R.C., 1983, The origin of the iron-formation-rich Hamersley Group of Western Australia—deposition on a platform: *Precambrian Research* v. 21, p. 273–297.

NEALE, J., 1975, Iron ore deposits in the Marra Mamba Iron Formation at Mining Area 'C', Hamersley Iron Province, in *Economic Geology of Australia and Papua New Guinea* edited by C.L. KNIGHT: Australasian Institute of Mining and Metallurgy, Monograph 5.

RYAN, G.R., and BLOCKLEY J.G., 1965, Progress report on the Hamersley blue asbestos survey: Western Australia Geological Survey, Record 1965/32.

SIMONSON, B.M., 1990, Locality 9.3, Wittenoorn Dolomite, in *Third International Archaeological Symposium, Perth, 1990, Excursion Guide Book* edited by S.E. HO, J.S. GLOVER, J.S. MYERS, and J.R. MUHLING: The Geology Department and University Extension Service, Western Australia University, Publication no. 21, p. 50.

SIMONSON, B.M., HASSLER, S.W., and SCHUBEL, K.A., 1993, Lithology and proposed revisions in stratigraphic nomenclature of the Wittenoorn Formation (Dolomite) and overlying formations, Hamersley Group, Western Australia: Western Australia Geological Survey, Report 34, Professional Papers, p.65–79.

SLEPECKI, S., 1981, Marra Mamba Iron Ore — a case history in exploration and development of a new ore type, *in* Australasian Institute of Mining and Metallurgy, Sydney Conference, Proceedings, p. 195–207.

TRENDALL, A.F., and BLOCKLEY, J.G., 1970, The iron formations of the Precambrian Hamersley Group with special reference to crocidolite: Western Australia Geological Survey, Bulletin 119.

## Appendix 1

### Core log of type section of the West Angela Member: Hole WRL 1 (after Meakins, 1987)

#### 420.40–428.62 (m) Shaly dolomite

A medium-to pale-grey, medium-crystalline dolomite, intercalated with numerous thin carbonaceous shale and siltstone beds and laminations. Carbonaceous shale beds towards the top of the sequence show inverse graded bedding, otherwise shale horizons occur as thin discrete bands. Occasional flame structures associated with the shale horizons, as are rare pyrite stringers. Notable divisions as follows:

422.15–422.80: grey, medium- to coarse-grained massive dolomite which is distinctive as it is coarser textured and contains a significant amount of non-carbonate (?carbonaceous) matter.

423.37–423.61: brecciated sequence hosting dolomitic fragments containing calcite veins. The matrix consists of dark carbonaceous matter, and the breccia is mainly clast supported, with well-developed stylolite contacts.

#### 428.62–437.40 Shaly dolomite

Thin carbonaceous shale interbeds and laminations are located within significantly coarser grained dolomite containing large amounts of dark, fine, non-carbonate fragments. Carbonaceous shale beds become thinner but more closely spaced up sequence. Rare pyrite stringers occur within the shale horizons. Basal contact is well defined.

#### 437.40–438.73 Brecciated dolomite

A thin, brecciated unit consisting of grey, coarsely crystalline massive dolomite containing common, fine, carbonaceous shale fragments and clasts. Shale fragments are particularly abundant near the base of the unit. Extensive, irregular calcite veining present throughout the unit. The basal and upper contacts are well defined.

#### 438.73–443.99 Shaly dolomite

Numerous wavy to planar carbonaceous shale beds (to 5 cm thickness) and laminations are intercalated in a sequence of medium to coarsely crystalline 'dirty' dolomites. The dolomite is laminated to massive and contains abundant

fine carbonaceous matter. Only minor calcite veining present in the unit. Blebs and stringers of pyrite are more common in shales than in previous units.

#### 443.99–445.87 Massive dolomite

A pale-grey, medium-crystalline massive to poorly laminated dolomite characterized by extensive soft-sediment deformation and common well-developed stylolite contacts. The unit contains only rare shale partings. The dolomite is considerably cleaner than overlying units.

#### 445.87–451.80 Shaly dolomite

A medium-grey, medium- to occasionally fine-crystalline, laminated dolomite with abundant interbedded carbonaceous shale and siltstone beds (up to 13 cm thickness) and laminations. The unit contains minor calcite, vein-associated brecciation and a few cavities near the base. Notable divisions include:

451.56–451.80: a very pale-grey, finely crystalline, massive dolomite, which is distinctly clean carbonate containing only minor carbonaceous material.

#### 451.80–454.01 Dolomite breccia

A pale- to medium-grey, medium crystalline massive dolomite containing occasional laminated dolomite and shaly dolomite fragments with common, fine carbonaceous shale fragments and infillings. Bedding crudely defined in a few locations by scattered carbonaceous shale fragments. Occasional stylolite contacts and rare calcite veining and vugs near the top of sequence. Unit is formed on a mainly carbonaceous shale base (453.41–453.88). Very rare pyrite blebs.

#### 454.01–465.41 Laminated dolomite

A grey, medium- to fine-crystalline, well to poorly laminated dolomite intercalated with numerous black carbonaceous shale and siltstone laminations. Intervals between shale laminations are relatively consistent, whilst shale bedding thickness does not exceed 612 cm. The bedding pattern is generally wavy. The dolomites appear to contain more carbonaceous material down sequence. Stylolite contacts are common whilst calcite veining is rare.

#### 465.41–475.71 Laminated dolomite

A variable sequence consisting of grey to dark-grey, medium- to coarse- crystalline, well-laminated carbonaceous dolomite with occasional planar to wavy subhorizontal carbonaceous shale beds (to 5 cm maximum thickness). Most of the shale beds occur as discrete structureless units. fine, dark ?carbonaceous fragments are present in varying concentrations throughout and often serve to accentuate dolomite laminations which are distinctly wavy in outline. Rare, smeared pyrite occurs along slickenside shale partings. Well-formed stylolite contacts are common. Notable divisions include:

470.60–470.65: a very thin, dull-grey, extremely fine-grained horizon containing pale, scattered and altered

crystals to 1–2 mm. Possibly represents distal ashfall tuff horizon.

475.31–475.61: a well-defined, dark-grey carbonaceous sequence containing a thick interbedded shale horizon located near base. Stained positive for K-feldspar.

#### **475.71–502.25 Laminated to massive dolomite**

A thick, pale- to dark-grey, medium- to coarse-crystalline, laminated to massive dolomite with irregular, wavy carbonaceous shale laminations. The shale units contain rare blebs and laminations of pyrite. The unit is characterized by common well-developed stylolitic contacts. The sequence can be subdivided on the amount of carbonaceous, and possibly clastic material present as follows:

475.71–483.04: mostly pale-grey, poorly laminated to massive dolomite with wavy carbonaceous shale laminations. Although the dolomite is occasionally carbonaceous most of the material is cleaner than overlying units. Vague laminations are wavy in outline possibly reflecting soft-sediment deformation.

483.04–502.25: This unit is very similar in style and content to 475–483.04 m. The basal contact is well defined. Bedding trends at 70° to core axis.

#### **502.25–506.60 Shaly dolomite with thin chert bands**

Grey, fine- to medium- crystalline dolomite interbedded with thin carbonaceous shale and thicker, green and black chloritic chert bands. Chert beds are numerous from 504.00–504.46, 504.76–505.27 and 505.64–506.44 m and are very finely laminated and contain very fine, disseminated pyrite. Bedding trends at 60–70° to core axis whilst bedding contacts are irregular with load cast features present. Dolomites contain variable carbonaceous material. A few thin, nonmagnetic, pink-coloured beds of undetermined mineralogy are present from 503.68–503.72 m. No magnetite was detected in the unit. Shale stained positive for K-feldspar.

#### **506.60–512.87 Massive dolomite**

A mainly pale-grey, medium-crystalline massive dolomite containing numerous well-formed stylolitic contacts and occasional carbonaceous shale beds and laminations. Shale bedding contacts are highly irregular, probably reflecting soft-sediment deformation. Contacts are reasonably well defined. Notable divisions include:

508.90–509.13: dark green to black, chloritic, finely laminated chert with some carbonaceous shale. The chert contains very finely disseminated pyrite.

#### **512.87–516.92 Laminated dolomite**

Mostly medium- to occasionally dark-grey, medium-crystalline, well-laminated dolomite containing numerous carbonaceous shale beds and laminations. Typically laminations are sinuous and wavy in outline. Also present are occasional beds and irregular clots and aggregates of carbonaceous dolomite. Bedding trends at 90° to core axis.

#### **516.92–518.03 A mainly massive dolomite**

A pale-grey to medium-grey medium- crystalline, massive to occasionally laminated dolomite sequence also containing minor chert bands. Chert dolomite contacts have been deformed following compaction. Pods and stringers of pyrite occur within chert bands. The unit contains very well-developed stylolite contacts but only rare carbonaceous shaly horizons.

#### **518.03–521.84 Laminated dolomite, shale and BIF**

An extremely variable unit consisting of medium-crystalline, pale-grey, mostly laminated dolomite with thin carbonaceous shale beds interbedded with chert and magnetite rich bands. Bedding orientations range from horizontal to 60° to the core axis, whilst bedding contacts may be planar, wavy or deformed with load casting and sedimentary dykes (at 520.13 m). Calcite and quartz veins are restricted to chert bands. Notable divisions include:

520.22–521.38: laminated dolomites

521.38–521.53: deformed cherts

521.53–521.84: laminated dolomites

#### **521.84–522.73 BIF**

A well-defined sequence of interbedded dark-green to black, mostly massive cherts with black, medium-crystalline magnetite bands and minor red-brown jasper horizons. The magnetite bands in particular are sinuous and wavy in outline and pinch and swell. Contacts with adjacent dolomite units are well defined.

#### **522.73–524.60 Laminated to shaly dolomite**

A grey, medium-crystalline laminated to massive dolomite containing common wavy carbonaceous shale laminations. Soft-sediment deformation present between 523.58–523.73 m and a few stylolites occur throughout unit. Blebs and stringers of pyrite associated with thicker shale beds. Basal contact well defined.

#### **Marra Mamba Iron Formation**

(524.60–678.90)

---

## **Appendix 2**

### **Core log of type section of the Mount Newman Member: Hole DDH 275**

339.38–339.82 (m)	Weathered shale, some iron oxide near the top
339.82–340.22	Interbedded chert and shale with some BIF in the lower few centimetres
340.22–340.70	Chert with minor BIF and shale

340.70–342.29	Dark shale, somewhat weathered near top; thin chert bands	398.05–398.17	Massive stilpnomelane with a thin white carbonate band at top
342.29–343.50	BIF, silicate-rich in part, and chert. Core broken biscuit fashion	398.17–398.65	Thick-banded BIF with pyrite near base
	<b>Top of Mount Newman Member</b>	398.65–399.38	'Shale' band comprising 7 cm chert 18 cm dark shale with carbonate 37 cm massive carbonate 8 cm silicate iron-formation
343.50–350.20	More continuous core of podded BIF. Appreciable magnetite in chert matrix but not commonly as distinct mesobands at first, although these appear later	399.38–410.65	Mainly even-banded to flat-podded BIF. Some riebeckite bands, one replacing rare bunched pods. A little crocidolite at 405.20 m and some diagenetic pyrite associated with riebeckite at 405.25 m. Podding becomes more pronounced downwards; bunches and ovoid styles between 406 and 408 m
350.20–357.90	Podded BIF with disseminated sulfides (?pyrite) at 350.2 m and 352 m	410.65–411.00	Interbedded BIF, chert and stilpnomelane
357.90–358.30	Chert, carbonate and minor shale; non-magnetic	411.00–415.57	BIF, cherty near top. Some riebeckite bands
358.30–362.80	BIF with carbonate mesobands and some scattered pyrite cubes; less podded than previously	415.57–415.80	Shale, bedded near top
362.80–363.40	Massive carbonate band with 5 cm of shale at top	415.80–416.10	13 cm carbonate, then chert
363.40–367.75	Cherty BIF with two sets of bunched pods but generally fairly evenly banded	416.10–419.65	Thick-banded BIF; cherts greenish, probably due to minnesotaite
367.75–368.15	Massive carbonate with thin silicate bands		<b>Bottom of Mount Newman Member</b>
368.15–369.15	Cherty BIF, thickly banded	419.65–420.80	Shale and chert
369.15–369.70	Well-bedded dolomite and shale		
369.70–370.84	Massive carbonate with some stylolites; last 10 cm fairly well bedded		
370.84–376.60	Generally flat-podded BIF; some chert mesobands 10 to 15 cm thick		
376.60–377.10	15 cm black shale then massive carbonate		
377.10–379.05	Evenly banded BIF with minor podding		
379.05–379.25	Carbonate band		
379.25–384.45	Well-mesobanded BIF with some small ovoid pods and occasional piled pods	416.10–419.65 (m)	Thickly mesobanded BIF with greenish chert bands, ?minnesotaite
384.45–385.65	5 cm white chert, 15 cm black shale, then interbedded carbonate and shale	419.65–421.05	<b>Top of MacLeod Member</b> Dark shale with white, bitter efflorescence and three white chert mesobands. Last 15 cm streaky, laminated chert.
385.65–386.90	BIF comprising mainly chert matrix and carbonate bands	421.05–421.30	Finely microbanded BIF
386.90–387.65	Interbedded carbonate and shale	421.30–421.80	Interbedded stilpnomelane shale and white chert
387.65–389.20	Massive carbonate containing thin shale beds with pyrite nodules (Shale NS 3)	421.80–423.05	BIF with above-normal content of silicate mesobands
389.20–398.05	BIF with carbonate mesobands and two thin beds of black shale near top. Mainly evenly banded to flat podded; some traces of riebeckite	423.05–423.65	Stilpnomelane shale with central 10 cm chert band
		423.65–425.10	Silicate-rich BIF with few chert mesobands

### Appendix 3

#### Core log of type section of the MacLeod Member: Hole DDH 275

425.10–425.85	Interbedded chert and black shale; shale beds have white efflorescence		
425.85–427.65	BIF; flat-podded with greenish cherts	15.0	<b>Top of Nammuldi Member</b>
427.65–427.90	Magnetite-poor BIF (chert and iron silicates)		BIF with flattened chert pods and stilpnomelane partings at approximately 2 m spacings
427.90–429.10	Interbedded black shale and chert. Pyrite nodules and pods at about 428.3 m	2.7	Poddy BIF, transitional to more distinctly podded BIF below
429.10–432.70	BIF; some poor in magnetite	0.5	Shaly band weathering out to a natural stope
432.70–433.80	Interbedded chert and shale	16.5	Distinctively podded BIF comprising rhythmic alternations of very podded cherty BIF and thinner shaly BIF. Most pods are almost circular in cross section. Unit is informally referred to as the ‘ball-stack beds’.
433.80–434.65	BIF; first 20 cm poor in magnetite		
434.65–440.10	Interbedded black shale, chert and carbonate, some silicate-rich BIF; white efflorescence on shales	12.0	Alternations of black and yellow, thickly mesobanded BIF with thinner bands of shaly BIF. Podding becomes more pronounced upwards.
440.10–440.92	Massive chert–carbonate	0.25	Shaly bed
440.92–443.70	Interbedded black shale and chert; some brecciation	1.8	Podded, black and yellow BIF, thickly mesobanded
443.70–444.20	Thickly mesobanded, magnetite-poor BIF	0.8	Goethite and chert; weathers out as a notch
444.20–444.30	Black shale with white efflorescence	2.0	BIF with pinch-and-swell cherts
444.30–455.92	Greyish BIF with numerous carbonate mesobands. Thickly mesobanded at first, but becomes more thinly banded downwards	0.5	Yellow shale
455.92–459.17	Interbedded black shale and chert with distinctive ovoid chert pods at about 456.7 and 457.7 m (‘potato beds’).	16.5	Prominent unit of black, brown and white BIF with poor definition into macrobands. Contains alternations of podded and pinch-and-swell cherts
459.17–459.80	Very poddy chert	4.0	Relatively even-banded BIF with white cherts and rare pods
459.80–460.00	Black shale	13.5	Shaly BIF with thick (15 to 25 cm) chert bands. Weathers out upslope to form a cave
460.00–460.55	Very poddy chert	0.3	Shaly BIF
460.55–460.70	Black shale	4.0	Poddy BIF. Pods occur as overlapping bunches and, in some instances, as discrete eyes
460.70–462.90	Magnetite-poor BIF with minor shale	1.0	More weathered zone with shaly BIF and yellow chert
462.90–463.30	Black shale with white efflorescence	8.5	Poddy, thickly mesobanded BIF. Most pods are connected but some horizons have disconnected pods
463.30–464.40	Thickly mesobanded chert	0.8	Poddy BIF and shale. Pods are elliptical in cross section but elongated down dip
464.40–466.00	Black shale with minor chert pods	2.0	Thickly mesobanded BIF with flattened chert pods
	<b>Base of MacLeod Member</b>	0.25	Exposure gap; probable shale
466.00–480.75	Thickly mesobanded and podded BIF with minor shale macrobands and stilpnomelane mesobands. Riebeckite replaces chert in part.	2.5	Thickly mesobanded, wavy-bedded BIF with few discrete chert pods
N.B.	Misplaced core blocks from 444 m onwards may have introduced minor discrepancies into the subsequent measurements.	0.25	Yellow shale

#### Appendix 4

#### Measured section of the Nammuldi Member in the Hardey River Gorge

7.0 (m)	Chert and shaly BIF	
9.0	Poorly exposed chert and shale	

5.0	Interbedded poddy, cherty BIF and shaly BIF weathers out
0.6	Shale and cherty BIF; weathers out
1.3	Thickly mesobanded BIF
0.25	Shale and chert
2.2	Thickly mesobanded BIF; green chert at 1.2
0.5	Thinly mesobanded, shaly iron formation
4.2	Thickly mesobanded, Mn-stained BIF with shaly (?stilpnomelane) partings
0.2	Massive yellow shale (?weathered stilpnomelane)
4.0	Thickly mesobanded chert with shaly partings up to 10 cm thick
0.15	White-to-pink, well-bedded shale
1.5	Thickly mesobanded BIF with small cavities, possibly after carbonate
	<b>Base of Nammuldi Member</b>
1.0	White-weathering shale of Jeerinah Formation
20+	Dolerite sill

---



# Lithology and proposed revisions in stratigraphic nomenclature of the Wittenoom Formation (Dolomite) and overlying formations, Hamersley Group, Western Australia

by

Bruce M. Simonson<sup>1</sup>, Scott W. Hassler<sup>2</sup>, and Kathryn A. Schubel<sup>3</sup>

## Abstract

The Wittenoom Dolomite is one of the most heterolithic formations in the early Precambrian Hamersley Group and contains an abundance of well-preserved primary sedimentary features. During five field trips between 1985 and 1990, we examined the Wittenoom Dolomite at 37 field sites and in 7 diamond drillcores, and measured sections at most of them. Throughout the Hamersley Basin, we found the Wittenoom Dolomite to consist of 1) a lower unit composed of dolomite with minor chert and argillite and 2) a more heterolithic upper unit composed of argillite with subordinate thicknesses of other lithologies (mainly carbonate, chert, and BIF). We propose these two units be given formal stratigraphic status as 1) the Paraburdoo Member and 2) the Bee Gorge Member of the Wittenoom Dolomite respectively. In addition, the West Angela Member occurs sporadically at the base of the Wittenoom Dolomite, particularly in the southeastern part of the Hamersley Basin (Blockley et al., 1993). The uppermost Bee Gorge Member also contains three informal stratigraphic marker units (the Crystal-rich Tuff, Main Tuff Interval, and Spherule Marker Bed) that persist throughout most of the Hamersley Basin. Analysis of the sedimentary textures and structures of the strata of the Wittenoom Dolomite and the overlying Mount Sylvia Formation and Mount McRae Shale indicates that these three formations consist mainly of lutites with thin layers of arenite, or more rarely intraformational conglomerates, that were deposited in basinal (i.e. deeper-water) palaeoenvironments. The arenites consist mainly of carbonate and volcanoclastic detritus and were deposited mainly by low-density turbidity currents. One exception is the Main Tuff Interval, which records an exceptionally large-volume event of rapid pyroclastic turbidite sedimentation. As dolomite is dominant in only one of the three proposed members, we further propose that the name Wittenoom Formation be substituted for Wittenoom Dolomite.

**KEYWORDS:** Stratigraphy, nomenclature, Hamersley Basin, lithology, Wittenoom Formation, dolomite.

## Introduction

The authors undertook a sedimentological study of the Wittenoom Dolomite and the overlying Mount Sylvia Formation and Mount McRae Shale of the Hamersley Group to help shed new light on depositional processes and palaeoenvironments in the Hamersley Basin.<sup>4</sup> We concentrated on sedimentary rocks such as dolomite, limestone, tuff, and argillite instead of the well-known banded iron-formations or BIFs (Trendall and Blockley, 1970; Ewers and Morris, 1981). Iron-poor sedimentary rocks can be interpreted with greater certainty because

they have numerous potential Phanerozoic analogues. We chose the Wittenoom Dolomite as the focus of our study because it is the most heterogeneous formation in the Hamersley Group and contains many well-preserved sedimentary textures and structures.

We measured detailed stratigraphic sections during five field trips between 1985 and 1990. The Wittenoom Dolomite, which is restricted to the main body of the Hamersley Basin, was examined in surface exposures at 37 different sites and in core from 7 sites (Fig. 1 and Table 1). Sections were also measured in the Mount Sylvia Formation and Mount McRae Shale. These higher units are generally more poorly exposed and more highly weathered.

Field data were augmented by the study of over 1200 samples from the Hamersley Group. All samples were sawn and examined in the form of slabs. In addition, about 450 were studied in thin section, and the

<sup>1</sup> Department of Geology, Oberlin College, Oberlin, Ohio, USA 44074

<sup>2</sup> Department of Geological Sciences, University of California at Santa Barbara, Santa Barbara, USA 93106

<sup>3</sup> Department of Earth and Planetary Sciences, Johns Hopkins University, Baltimore, USA 21218

<sup>4</sup> We use the phrase 'Hamersley Basin' in Trendall's (1983) sense to refer to the suite of palaeoenvironments in which the Mount Bruce Supergroup was deposited with no prior assumptions as to what types of environments they were.

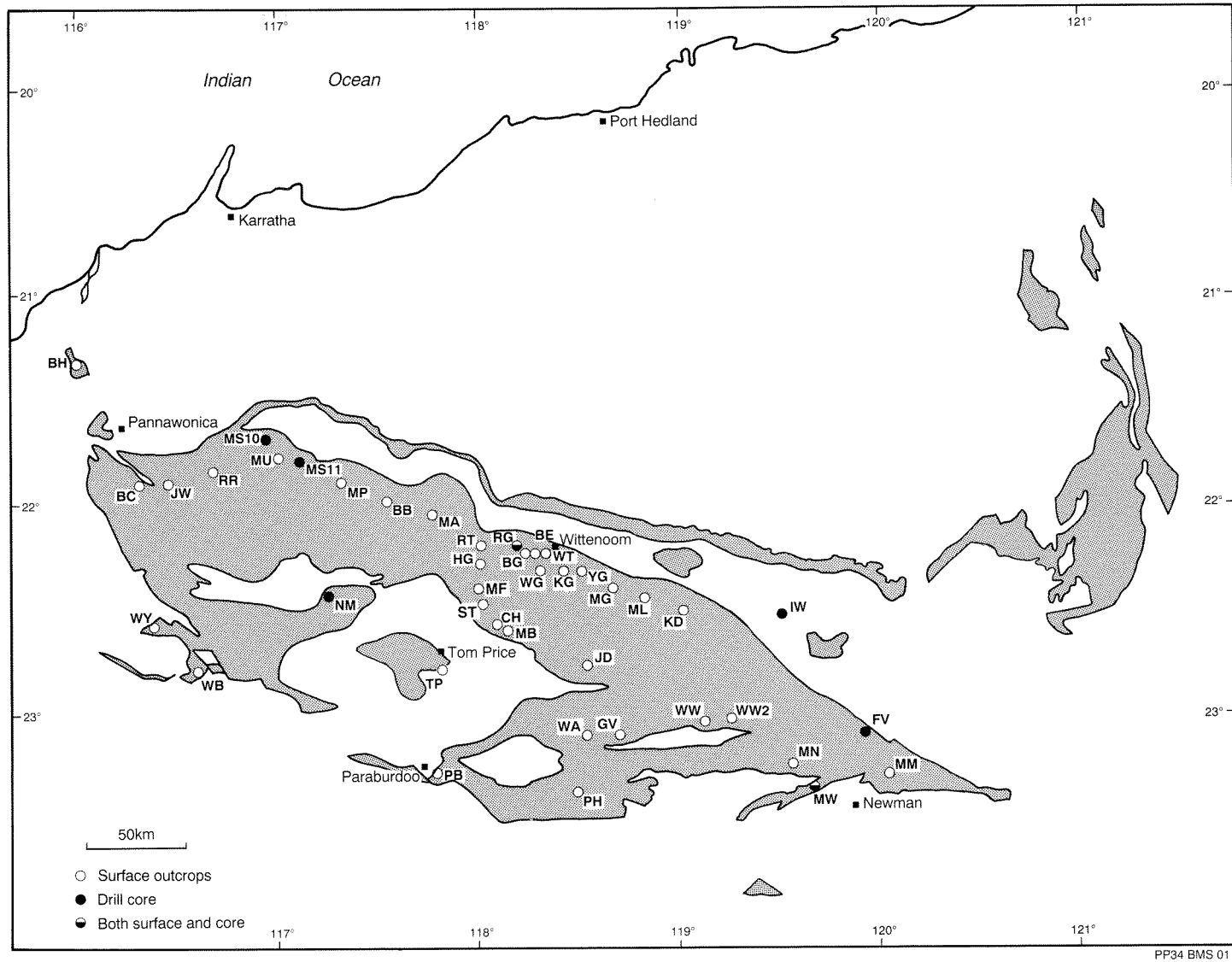


Figure 1. Geological sketch map of the Hamersley Group (after Myers and Hocking, 1988) showing the approximate locations of all study sites; their informal names and exact locations are given in Table 1.

**Table 1. Names, abbreviations, and locations of study sites indicating stratigraphic units examined.**

Site name	Abbreviation	1	2	Lat. (S)	Long. (E)	W	P	B	S	M	Map sheet no. and grid location
Bacon Bore	BB	X		21° 58'	117° 36'			X			2454-619702
Bee Gorge	BG	X		22° 14'	118° 15'			X	X		2553-293414
Bee Gorge east	BE	X		22° 13'	118° 17'		X	X			2553-317422
Bilano Hill	BH	X		21° 16'	116° 9'			X			2155-127477
Bungaroo Creek	BC	X		21° 53'	116° 24'			X	X		2154-382805
Conical Hill	CH	X		22° 35'	118° 5'		X	X	X		2552-120029
The Governor	GV	X		23° 3'	118° 49'			V			2651-867483
Hammersley Gorge	HG	X		22° 15'	117° 59'			X	X		2453-017384
Ibianna Well (FVG-1)	IW		X	22° 33'	119° 30'	X	X	?			2752-570031
Jimmawurrada Creek	JW	X		21° 54'	116° 32'		X	X			2254-523785
Juna Downs	JD	X		22° 52'	118° 33'			V			2652-657165
Kalamina Gorge	KG	X		22° 18'	118° 27'			V			2553-515324
Koodaideri	KD	X		22° 30'	119° 1'			X			2652-057104
McCameys Monster	MM	X		23° 23'	120° 5'			X	X	X	2951-019113
Millstream 10	MS10		X	21° 42'	117° 1'		X	X			2354-017003
Millstream 11 and 11A	MS11		X	21° 49'	117° 10'			X			2354-172874
Mount Bruce	MB	X		22° 36'	118° 9'				X	X	2552-174000
Mount Frederick	MF	X		22° 23'	117° 58'			V			2453-007264
Mount Lockyer	ML	X		22° 26'	118° 50'			X	X		2653-880182
Mount Margaret	MA	X		21° 56'	117° 45'			V			2454-774739
Mount Newman	MN	X		23° 17'	119° 34'		X				2851-630236
Mount Pynton	MP	X		21° 52'	117° 23'			X	X	X	2354-397818
Mount Stevenson	ST	X		22° 29'	118° 1'			V			2553-036116
Mount Ulric	MU	X		21° 50'	117° 12'			V			2354-203852
Mount Whaleback (MD-1, D233, D234-1, and D261)	MW	X	X	23° 22'	119° 42'			X	X	X	2851-760133
Munjina Gorge	MG	X		22° 25'	118° 42'			V			2653-745212
Nammuldi (DDH-275)	NM		X	22° 27'	117° 16'		X	X			2353-369199
Paraburdoo	PB	X		23° 15'	117° 42'	X	X	X	X	X	2451-716286
Pathetic Hill	PH	X		23° 21'	118° 45'			V			2651-805177
Range Gorge (WRL-1)	RG	X	X	22° 12'	118° 13'	X	X				2553-247453
Rio Tinto Gorge	RT	X		22° 12'	118° 1'			X	X		2553-048457
Robe River	RR	X		21° 53'	116° 43'			V			2254-699819
Tom Price	TP	X		22° 45'	117° 45'		X	X	X	X	2452-782852
Weeli Wolli Creek	WW	X		23° 3'	119° 10'		X	X	X		2751-220484
Weeli Wolli Creek 2	WW2	X		22° 59'	119° 11'			V			2752-225557
West Angelas	WA	X		23° 6'	118° 43'			V			2651-743432
Western Mining (FVD-1A)	FV		X	23° 7'	119° 58'		X	?			2851-038404
Wittenoom rubbish tip	WT	X		22° 15'	118° 19'			X			2553-354394
Wittenoom Gorge	WG	X		22° 19'	118° 20'			X		X	2553-365336
Wyloo Dome rockhole	WY	X		22° 34'	116° 25'	?	X	X	X		2152-395041
Wyloo/3 corner bore	WB	X		22° 48'	116° 35'		X	X	X		2252-566795
Yampire Gorge	YG	X		22° 19'	118° 31'			X			2653-565307

Key: 1 = surface exposures, 2 = core, W = West Angela Member, P = Paraburdoo Member, B = Bee Gorge Member, S = Mount Sylvia Formation, and M = Mount McRae Shale.

Note: a V entered in Bee Gorge Member column indicates only Main Tuff Interval was examined at that site.

compositions of selected minerals and samples were determined through staining and X-ray diffraction.

Many of the sedimentological data produced in the course of these investigations are being disseminated elsewhere as both abstracts (Simonson, 1987a, 1988a, b, 1989, 1991, 1992b; Simonson and Goode, 1988; Hassler, 1990a, b, 1991b, 1992; Hassler and Simonson, 1991; Simonson et al., 1991) and papers (Simonson and Goode, 1989; Simonson, 1990, 1992a; Hassler 1991a, in press; Simonson et al., in press). The aim of this paper is to propose several revisions in the stratigraphic nomenclature of the Wittenoom Dolomite. To document the need for the proposed revisions, measured stratigraphic sections of the Wittenoom Dolomite and the overlying Mount Sylvia Formation and Mount McRae Shale are presented,

accompanied by brief lithological descriptions. Because these three stratigraphic units have so much in common lithologically, all three are described in this paper, even though revisions are proposed only for the stratigraphic nomenclature of the Wittenoom Dolomite.

## New stratigraphic nomenclature for the Wittenoom Dolomite

Trendall and Blockley (1970, p. 85) noted that the Wittenoom Dolomite consists of two distinct stratigraphic parts: a lower part composed of dolomite with minor chert and argillite, and a more heterolithic upper part composed of argillite with subordinate thicknesses of other

lithologies (mainly carbonate, chert, and BIF). In addition, Blockley et al. (1993) recently proposed the establishment of a basal West Angela Member within the Wittenoom Dolomite. Based on the data summarized in Figure 2, we propose that the remainder of the Wittenoom Dolomite be divided into two parts: a medial Paraburdoo Member and an uppermost Bee Gorge Member. As dolomite is dominant in only one of these three members, we further propose that the name *Wittenoom Formation* be substituted for *Wittenoom Dolomite*.

The contact between the Paraburdoo and Bee Gorge Members was placed at the transition from continuous dolomite beds with argillite partings (below), to predominantly argillite with or without thin intercalations of other rock types (Fig. 2). While there is no basinwide marker bed right at this contact, it is normally sharp and readily recognized in the field. The precise stratigraphic level of this transition may vary slightly as the dolomites of the Wittenoom Formation have been dissolved in the subsurface in some areas, e.g. the TP site (Simonsen and Hassler, 1991). Nevertheless, we believe this lithologic transition approximates a time-stratigraphic boundary because the upward transition from carbonate to argillite dominance occurs 10 to 20 m beneath a very persistent marker bed in the Bee Gorge Member (the Crystal-rich Tuff described below) in sections measured in various parts of the Hamersley Basin (Fig. 2).

## Proposed stratigraphic subdivisions

### Paraburdoo Member

#### *Type section*

The type section for the Paraburdoo Member is defined as a series of exposures a few kilometres southwest of the town of Paraburdoo along the southern edge of the Hamersley Basin (latitude 23° 15' S, longitude 117° 42' E). These exposures consist of north-facing slopes and cliffs just to the east of the gravel road which reaches the top of a site known locally as Radio Hill. No single cliff contains a full section of the Paraburdoo Member, but a composite section through nearly all of the strata in the Paraburdoo Member (Fig. 2) was constructed using local marker beds to correlate from one cliff to the next.

#### *Type areas*

Exposures of the Paraburdoo Member as extensive as those near the town of Paraburdoo are rare. Exposures of the overlying Bee Gorge Member, which contains a much higher percentage of argillite, are more widespread. The break in slope at the base of many hills in the Hamersley Range nearly coincides with the contact between the Paraburdoo and Bee Gorge Members, e.g. along the Hamersley front. Good exposures of the Paraburdoo Member nevertheless occur in various parts of the Hamersley Basin, including 1) the upper reaches of Weeli Wollie Creek in the east, 2) along Jimmawurrada

Creek and its tributaries in the northwest, and 3) in and around an unnamed creek along the northern edge of the Wyloo Dome in the southwest (see Fig. 1 and Table 1 for precise locations). In addition, several cores through the Paraburdoo Member are in permanent repositories. Two that contain almost the entire thickness of the Paraburdoo Member are WRL-1 (equivalent to section RG), and DDH-275 (equivalent to section NM). These cores are stored at the CRA Exploration Pty Ltd depot in Karratha except for the Marra Mamba section and a few metres of the Wittenoom Dolomite from DDH-275 which remain at the CSIRO Exploration Geoscience Laboratory, Floreat Park, Western Australia.

#### *General description*

The Paraburdoo Member consists of dolomite with minor amounts of chert and argillite and almost always displays even, tabular bedding. Most layers of dolomite are a few centimetres to decimetres thick, and none are thicker than about 1 metre. Argillite layers are thinner on average, occurring mostly in the form of sub-millimetre partings to thin beds up to a few centimetres thick separating the dolomite layers. While argillite is present in minor amounts throughout the Paraburdoo Member, chert is restricted to specific horizons up to 2 m thick that generally contain scattered nodules of grey to black chert. All layers tend to be laterally persistent, but while excellent local marker beds abound, we were unable to correlate any from one section area of the Paraburdoo Member to another.

The exact thickness of the Paraburdoo Member is unknown, but it is at least 260 m at the type section near Paraburdoo. A thickness of over 420 m was transected in the WRL-1 core, but this could be an overestimate given the presence of breccias (Fig. 2) and the lack of marker beds to detect structural duplications.

### Bee Gorge Member

#### *Type section*

The type section for the proposed Bee Gorge Member is defined as the exposures along the eastern slope of Bee Gorge near its mouth (latitude 22° 14' S, longitude 118° 15' E). This site was chosen because it is close to the type area (Wittenoom townsite) of the formation as a whole (MacLeod, 1966), it is readily accessible, and it has the thickest of any of the measured sections of the uppermost member of the Wittenoom Formation. Exposures of the strata in the Bee Gorge Member are discontinuous, but complete sections can be readily measured owing to the abundance of resistant marker beds (see below).

#### *Type areas*

After the type section, the best exposures of the Bee Gorge Member examined in this study are the Mount Pyrton, Hamersley Gorge, Wittenoom Gorge, Mount Lockyer, and Conical Hill sites (Figs 1 and 2). The only drillcore from the Bee Gorge Member in a permanent

repository are incomplete Millstream cores 10 and 11 from the northwestern part of the study area. They are stored in the Geological Survey of Western Australia's core library in Dianella and transect part of the lower Bee Gorge Member (Barnett, 1981, fig. 3).

### *General description*

Thinly laminated, fissile, graphitic (in core) argillite is the main lithology in the Bee Gorge Member. Subordinate thicknesses of carbonate, chert, volcanoclastics, and iron formation are also present, generally occurring as resistant marker beds of lutite, i.e. sediments that originally consisted of muds of various compositions. However, a large minority of these non-argillite layers display clastic textures and current structures (and are described below). The single thickest section of coarser clastic sediment in the Bee Gorge Member is the Main Tuff Interval (defined below), which reaches 16.4 m. The thickness of individual layers of pure carbonate does not exceed 4.2 m, and the thickest layers of pure chert and iron formation are even thinner. The measured thickness of the Bee Gorge Member ranges from a maximum of 227 m at the type locality to a minimum of 111 m in the Tom Price section.

### *Informal stratigraphic units*

In addition to the formal stratigraphic subdivisions proposed above, three marker horizons within the Bee Gorge Member were found to be distinctive and persistent enough to be given informal stratigraphic names. These informal markers, which are indicated on the measured sections (Fig. 2), are listed in ascending stratigraphic order:

#### 1. Crystal-rich Tuff

The Crystal-rich Tuff is one of a variable number of thin, graded beds of medium sand-size and finer volcanoclastic sediment. This particular bed is distinguished by its high content of crystal debris. It rarely exceeds 10 cm in thickness, yet it was recognized at almost every site where the appropriate part of the Bee Gorge Member is exposed. Zircons separated from the Crystal-rich Tuff have been dated at  $2603 \pm 7$  Ma (Hassler, 1991a).

#### 2. Main Tuff Interval

The Main Tuff Interval is a highly distinctive 4.2 to 16.4 m thick sequence of pyroclastic turbidites that has been studied in detail by Hassler (1991a, in press). It contains some of the thickest beds and coarsest sediments in the Wittenoom Formation (and possibly in the entire Hamersley Group) and persists throughout the main body of the Hamersley Basin, with the possible exception of the southwestern region.

#### 3. Spherule Marker Bed

The Spherule Marker Bed is an individual turbidite that consists of a mixture of carbonate and silicate detritus. At about 1 m, it is one of the thickest non-volcanoclastic turbidites in the Wittenoom Formation, and is the only one that contains sand-sized spherules of earlier silicate melt

that Simonson (1992a) ascribes to a major bolide impact (see below). The Spherule Marker Bed was recognized throughout most, but not all, of the main body of the Hamersley Basin.

## **Lithological constituents of the Wittenoom Formation, the Mount Sylvia Formation, and the Mount McRae Shale**

Even though they differ radically in their relative proportions, the major lithological constituents of all three members of the Wittenoom Formation are very similar. Likewise, the Mount Sylvia Formation and the Mount McRae Shale have the same lithological constituents as the Bee Gorge Member, albeit in somewhat different proportions. Summary descriptions of these constituents condensed from the more comprehensive accounts in Simonson and Hassler (1991) form the remainder of this paper. They are presented with the aim of facilitating stratigraphic correlations both in the field and in core. The sedimentological and palaeogeographical significance of these data are discussed elsewhere (Simonson and Goode, 1989; Hassler, 1991a, in press; Simonson, 1992, and Simonson et al., in press).

### **Carbonates**

Carbonate rocks are dominant in the Paraburdoo Member, virtually all of which consists of dolomite. In contrast, carbonates are greatly subordinate to argillite in the overlying Bee Gorge Member, Mount Sylvia Formation, and Mount McRae Shale. The carbonates in these higher, argillite-dominated units also show a wider spread of composition; they range from dolomite to calcite to ferroan carbonate. Because of this stratigraphic variability, the descriptions of the carbonates which follow are grouped according to stratigraphic units, even though they show many similarities.

The Paraburdoo Member of the Wittenoom Formation has one of the highest carbonate contents of any unit in the Hamersley Group, rivalled only by the Carawine Dolomite (Trendall and Blockley, 1970; Goode, 1981). The Paraburdoo Member consists almost entirely of dolomite layers a few centimetres to decimetres thick separated by thin intercalations of argillite. Chert is the only other rock type present. Depositional structures are preserved inside many of the dolomite layers, but their degree of preservation varies greatly. Some dolomites are uniformly coarsely crystalline and sugary and show only faint layering, whereas others show a range of crystal sizes which, together with disseminated impurities, give definition to a number of primary features.

Most of the dolomites in the Paraburdoo Member with well-preserved primary features display thin continuous laminations that are generally one to several millimetres thick. The laminations consist of alternating light and dark rock that consist respectively of nearly pure carbonate contrasting with carbonate rich in carbonaceous and/or

LITHOLOGICAL SYMBOLS IN STRATIGRAPHIC COLUMNS

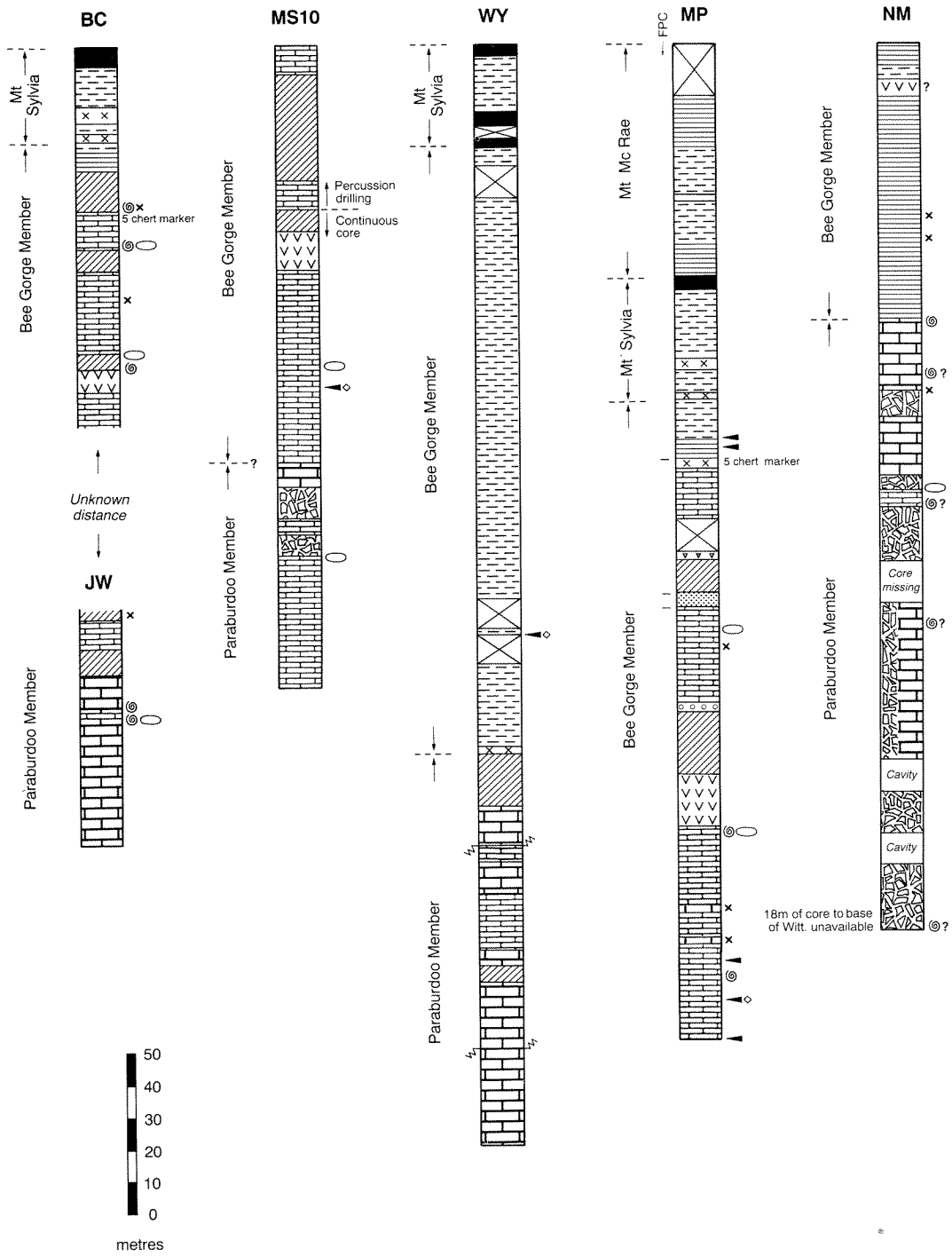
	Pure carbonate (usually dolomite) with argillaceous partings and negligible chert
	Cherty or silicified carbonate (usually dolomite)
	Brecciated carbonate of sedimentary clasts in a coarsely sparry matrix (N.B. such zones exist but were avoided in surface exposures, so symbol only appears in core sections)
	Thinly interbedded argillite and dolomite, limestone and/or ferroan carbonate lutite with negligible chert; argillite usually dominant
	Argillite with thin interbeds of chert lutite and negligible carbonate
	Argillite with thin interbeds of both chert and carbonate lutite
	Argillite with thin interbeds of ferruginous chert arenite and negligible carbonate
	Argillite with thin interbeds of clastic dolomite, limestone and/or ferroan carbonate with or without thin chert interbeds
	Pure argillite
	Volcanics of the Main Tuff Interval ( N.B. see Hassler, 1991, and in press for information on internal features; none are depicted on these sections)
	'Volcanic siltstone' of the Mount McRae Shale
	Bedded chert with minor argillite
	Highly ferruginous chert and banded iron-formation
	Covered interval
	Spherule-bearing turbidite (Spherule Marker Bed)

LITHOGRAPHIC SYMBOLS NEXT TO STRATIGRAPHIC COLUMNS

	Argillite-hosted concretions of limestone, dolomite, and/or ferroan carbonates
	Argillite-hosted chert concretions
	Roll-up or related soft-sediment deformation structure in carbonate
	Ripple cross-lamination, mostly of the climbing current variety
	Thin layer of tuff
	Crystal-rich Tuff marker layer
	Isolated carbonate layer with coarse clastic features
	Carbonate arenite containing oolites
	Prominent cherty marker bed in either carbonate or argillite
	Section line interrupted; unknown amount of section missing

PP34 BMS 02

**Figure 2. Measured sections of the Wittenoom Formation, the Mount Sylvia Formation, and/or the Mount McRae Shale. The sections are keyed to Figure 1 and Table 1 by the abbreviation(s) above the columns. Columns BG/BE and CH/MB are both composites of sections from two closely spaced sites, whereas the rest of the columns represent sections measured at single sites. The symbols to the right of each column indicate the stratigraphic locations of specific sedimentary features explained in legend, whilst tic marks to the left of some columns indicate the locations of beds of flat-pebble conglomerate (FPC). Diagrammatic versions of these same sections also appear in Figure 3A of Simonson et al. (in press).**



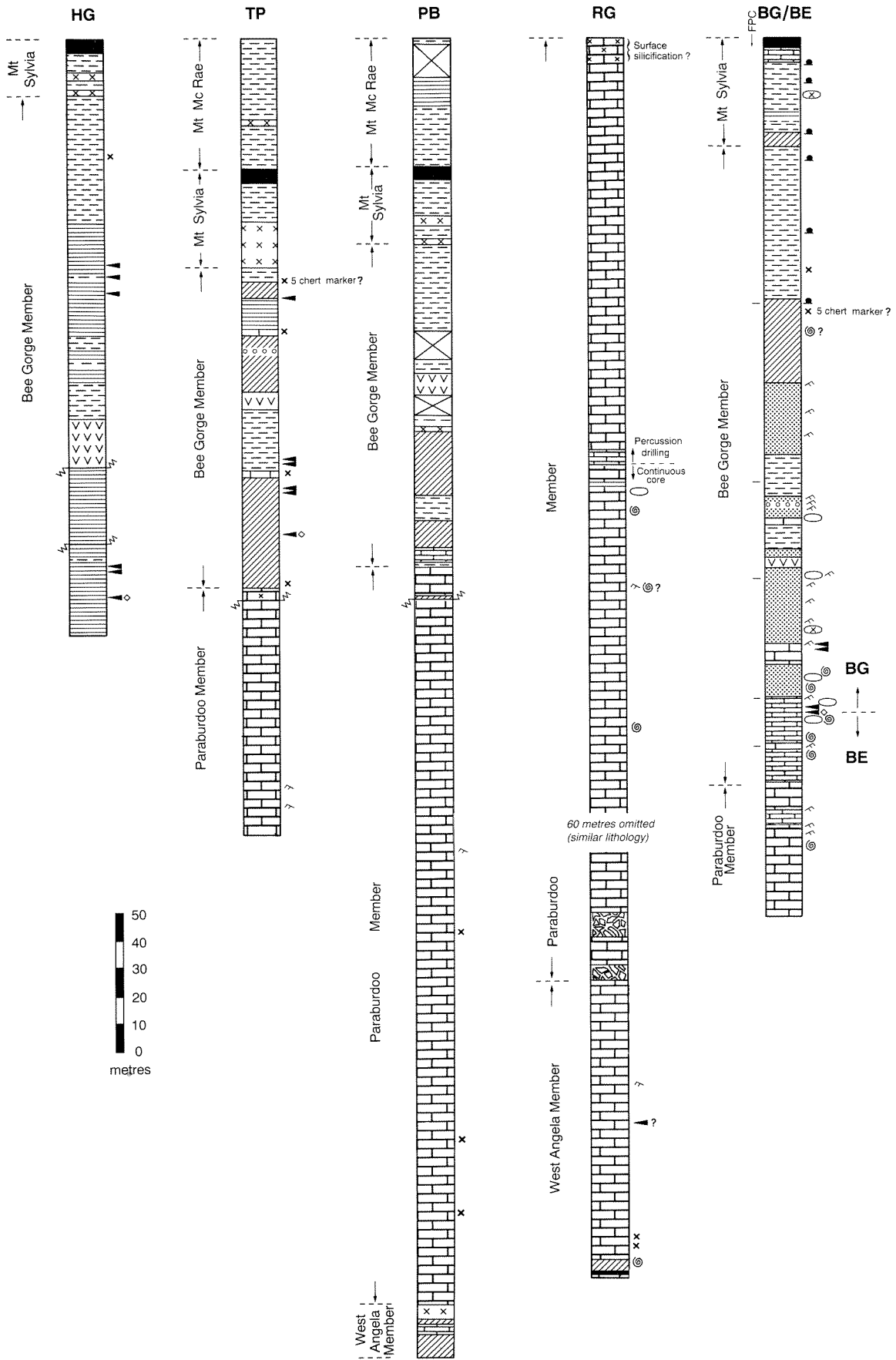
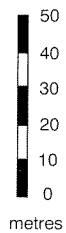
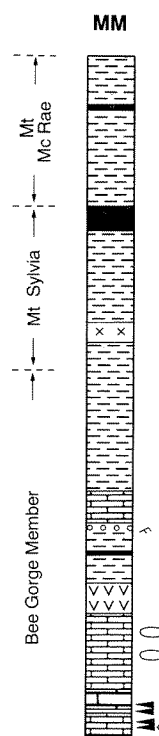
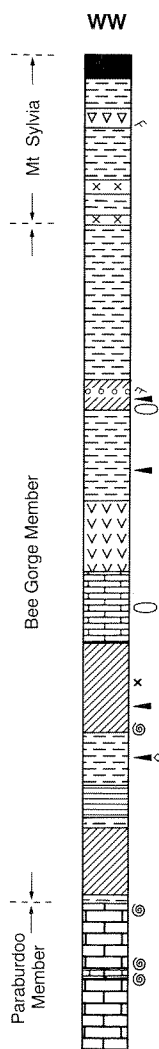
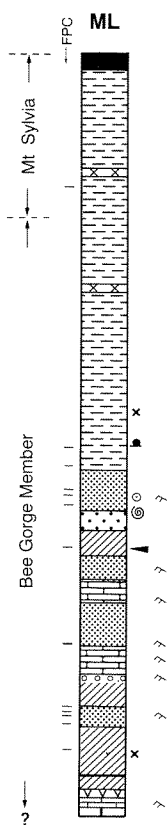
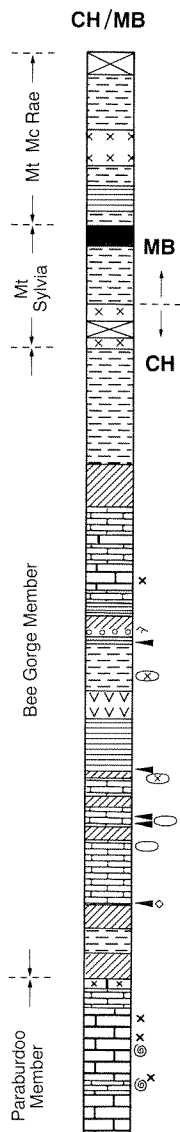
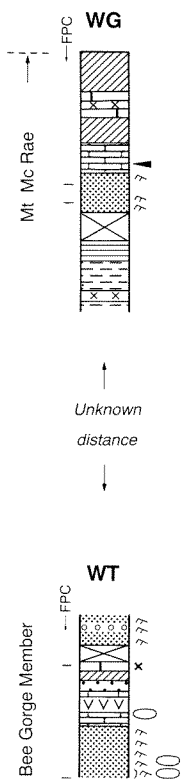


Figure 2. (continued)



argillaceous material. Although they are laterally persistent, these laminations are typically 'lumpy', pinching and swelling on a small scale (Simonson et al., in press, fig. 21). Based on the thin and continuous nature of these laminations, and the absence of any current structures or coarse clastic textures, we believe they originated as carbonate mud.

In addition to thin laminations, small but distinctive soft-sediment folds referred to as roll-up structures are a volumetrically minor but widespread (Fig. 2) component of these dolomite layers. The geometry of these folds (especially the laminations that are rolled up in spirals—Simonson et al., in press, figs 24, 25) indicates some of the thin laminations were stabilized by the presence of cohesive microbial mats (Simonson, 1988b). Corresponding structures occur in the carbonates of the Transvaal Supergroup (Beukes, 1987; Klein et al., 1987) and have been interpreted similarly.

Dolomite layers with well-preserved thin laminations form a continuum with others that contain darker bodies or clots with diffuse margins. Such textures are referred to as pseudo-arenites by Simonson and Hassler (1991) because they appear to be the diagenetically degraded products of the thin carbonaceous laminations. Other thin dolomite layers are massive internally and have a graded appearance due to subtle changes in colour and/or the presence of small, probably intraclastic carbonaceous flakes in their basal parts.

Thin layers of carbonate arenite are also present among the dolomites of the Paraburdoo Member, but are quite rare. These layers show detrital textures consisting of sand-sized peloids or intraclasts and/or structures such as ripple cross-lamination. Most are believed to be turbidites because they are very similar to the arenites of the Bee Gorge Member (see below), but one occurrence of possible hummocky cross-stratification was observed at the TP site (Simonson and Hassler, 1991).

Rare layers rich in ferroan carbonate also occur in the Paraburdoo Member, most notably in the basal part stratigraphically close to the more ferruginous West Angela Member (Blockley et al., 1993). In surface exposures, ferroan carbonates can be readily differentiated from dolomite layers because they develop a thick weathering rind with a distinct golden, orange, or yellow colour. In contrast, a paper-thin, buff-coloured weathering rind develops on the dolomites. Limestones weather a neutral grey, but no limestones were positively identified in the Paraburdoo Member. In fresh drillcore, the carbonate varieties are not as easily differentiated because they all appear uniformly grey.

Like the Paraburdoo Member, the carbonates in the Bee Gorge Member are dominated by thinly laminated layers of dolomite lutite. Unlike the Paraburdoo Member, however, carbonates are much less voluminous than argillite. In addition, appreciable thicknesses of limestone and ferroan carbonate are present in the Bee Gorge Member, and a significant minority of carbonate layers are arenites or flat-pebble conglomerates rather than lutites. The carbonate arenites display features typical of turbidites such as great lateral persistence, normal grading, and

partial (particularly  $t_b-t_c$ ) Bouma sequences. Changes in grain size and palaeocurrent measurements on the climbing ripple cross-laminations that are commonly present in these turbidites indicate they were dispersed south and west across the Hamersley Basin (Simonson et al., in press). Limestones and coarse clastic carbonates are thickest and most abundant in the north-central part of the Hamersley Basin. Ferroan carbonates are most abundant in the stratigraphically higher parts of the Bee Gorge Member.

Carbonates are least abundant in the Mount Sylvia Formation and Mount McRae Shale. Those which are present tend to be rich in ferroan carbonate and lacking in evidence of a coarse clastic origin. The Mount McRae Shale, however, contains one carbonate package (10.6 m thick) rich in limestone arenites at site WG. Like the turbidites of the Bee Gorge Member, these arenites display normal grading and climbing ripple cross-lamination with south- and west-directed palaeocurrents. Layers of flat-pebble conglomerate are also locally present in the Mount Sylvia Formation.

## Argillite

In fresh samples from drillcore, almost all of the argillites in all of the units studied are dark grey to black, and those with little carbonate are highly fissile. Many bedding surfaces appear graphitic, attesting to a high content of carbonaceous matter. In contrast, samples from surface exposures typically have a brownish or reddish colour due to oxidation of carbonaceous material and iron-bearing minerals. Some argillites, particularly in the Mount Sylvia Formation and Mount McRae Shale, are highly bleached and altered to a powdery consistency in surface exposures. Many surface samples of argillites also differ from core samples in having veinlets and more irregular masses of calcite. Breccia textures, inclusions of exotic mineral grains, and other features indicate this calcite represents calcrete formed by relatively recent surface-weathering processes.

The most prominent X-ray peaks in Paraburdoo Member argillites are those of dolomite and quartz, with progressively smaller peaks for chlorite, muscovite (or a similar 10 angstrom clay mineral), and potassium feldspar. The same silicate minerals were also detected in HCl-insoluble residues from associated carbonate layers, although their relative abundances vary somewhat. In contrast, the quartz and chlorite peaks were higher than the carbonate peaks in argillites of the Bee Gorge Member, and calcite and an iron-bearing ankeritic phase were detected in some rocks instead of, or in addition to, dolomite. Mineralogically, Mount Sylvia Formation argillites are very similar to those of the Bee Gorge Member, but those of the Mount McRae Shale differ in that muscovite, rather than chlorite, is the dominant sheet silicate. Kaolinite was detected only in samples of the bleached, powdery argillite, where it is generally the dominant sheet silicate. In contrast, disseminated sulfides are widespread in many samples from drillcore but rare in surface samples.

Stratigraphically, the abundance of carbonate and argillite varies antipathetically. The carbonate-poor Bee Gorge Member contains sequences of virtually uninterrupted argillite tens of metres thick, whereas no package of argillite thicker than about a metre was observed in the carbonate-rich Paraburdoo Member. The ratio of argillite to carbonate is even higher in the Mount Sylvia Formation and Mount McRae Shale, although these units tend to be more altered and less well exposed than the Bee Gorge Member.

Primary and secondary features are present in many of the argillites, although they are not as diverse or informative as those of the carbonates. By far the most abundant primary features in the argillites are very thin laminations that reflect subtle differences in the composition and grain size of the constituent minerals. In general, these laminations are monotonously even and nondescript, but some are rhythmic in nature.

Although rare, two types of exceptionally thick argillite beds occur in the Bee Gorge Member and overlying units. One type comprises massive layers up to 30 cm thick that lack fissility. Some of these layers contain liquefaction structures and possible intraformational pebbles, suggesting they originated via soft-sediment disruption. The other type of thick argillite beds comprises layers up to several centimetres thick that are greener on weathered surfaces and less fissile than normal argillite. These layers resemble the fine volcanoclastic strata of the Main Tuff Interval (described below) and may represent times when fine-grained volcanoclastic material was being added to the normal hemipelagic muds as they were deposited.

Concretions and nodules are the commonest types of secondary features in the argillites of the Paraburdoo and Bee Gorge Members. Carbonate concretions are widespread (Fig. 2), range up to 75 cm long by 15 cm thick, and consist of calcite, dolomite, or ferroan phases. Internally, they can be massive or concentrically layered, but most are thinly laminated. Many display lumpy lamination, and some contain roll-up and related soft-sediment deformation structures (described above). Chert nodules, which occur in argillite but are rare, are described in the next section. Finally, spheroidal nodules of coarsely crystalline pyrite pseudomorphed by hematite were observed in weathered argillites of the Mount McRae Shale in a few localities. These nodules, known as 'Devil's golf balls', are several centimetres in diameter.

## Chert and iron-formation

Nodules (discontinuous masses) and beds (continuous layers) of chert are both present in all of the units we studied. They generally form two discrete populations, although the distinction becomes blurred in the case of a few continuous chert bands with widely spaced gaps. Chert is relatively rare in the Paraburdoo Member and consists almost exclusively of carbonate-hosted nodules. The Bee Gorge Member and overlying units contain a greater abundance of both bedded and nodular chert. Thus, as with argillite and carbonate, the ratio of chert to carbonate increases upsection in the units we studied.

Most nodular chert occurs in carbonate host beds. Chert nodules are usually black (presumably from carbonaceous inclusions) and vary in shape from spheroids and flattened ovoids to more complicated forms with rounded protuberances. The nodules are rarely thicker than 10 cm and tend to be highly elongated parallel to bedding. Carbonate layers rich in chert nodules range up to 2 m in thickness and form excellent local marker beds. Chert nodules hosted by argillite are rare and tend to be more widely spaced and regular (ellipsoidal) in shape than those in carbonate.

Internally, chert nodules in both carbonates and argillites show a variety of fabrics created by subtle variations in the sizes of quartz crystals and/or the abundance of fine impurities. Some nodules are massive whilst others show thin laminations, many of which are continuous with those in the adjacent carbonate. Cross-strata and flat pebbles are likewise pseudomorphed in chert nodules hosted by beds of clastic carbonate. Lastly, some nodules display faint concentric structures and/or gradational margins. All of these characteristics indicate the chert nodules formed via replacement.

Individual layers of bedded chert range from about 2 to 20 cm in thickness. Many occur in bundles of closely spaced layers separated by argillaceous partings that have aggregate thicknesses of 25 to 150 cm. Such bundles typically form excellent marker horizons by way of subtle but consistent differences in the thickness, colour, and degree of podding (described below) of the constituent chert layers. We were able to correlate some of the most distinctive bundles for long distances. For example, one bundle near the top of the Bee Gorge Member informally designated the 'five chert marker' (Fig. 2), is present in both the BC and MP sections, which are 100 km apart. It also appears to be present in the BG and TP sections another 80 to 100 km farther to the east and south respectively (Figs 1 and 2).

Most bedded cherts display thin laminations and lack visible clastic textures, indicating they originated as fine (mud-sized) sediment. In contrast to the chert nodules, we interpret these chert beds as largely primary siliceous lutites for two reasons: nowhere did we observe any chert beds passing laterally into sediment of a different composition, and the chert beds contain some features we did not observe in rocks of any other composition. The best example of the latter is small, irregular pockets of microbreccia like those described from cherty iron-formation by Trendall and Blockley (1970, fig. 45). These microbreccias differ from the flat-pebble conglomerates of the carbonates in three ways: they have a matrix of fine-grained chert rather than sand, their upper and lower contacts both transgress bedding, and the platy 'clasts' are all derived from local layers (usually a single one). Consequently, we concur with Trendall and Blockley (1970) that they formed in situ through soft-sediment disruption. In addition, the thin laminations in the bedded cherts are thicker than those of the argillites, and although they pinch and swell in places, they do so on longer wavelengths than the lumpy lamination of the carbonate lutites.

Some chert beds display thickened portions similar to the chert nodules described above and with the same characteristics as the chert pods of Trendall and Blockley (1970). In contrast to the bulk of the silica in the bedded cherts, which we believe is primary, we interpret these pods as secondary concretions enriched in silica during diagenesis by analogy with concretions of other compositions in other types of host strata (Simonson, 1987b, p. 509).

Thin, laterally discontinuous chert layers with coarser clastic textures also occur at two distinct stratigraphic levels in the Bee Gorge Member at several sites (Fig. 2; see Simonson and Goode, 1989, fig. 3 for more detail). These layers have higher contents of iron-bearing minerals than most of the cherts, giving them greenish and reddish colours. The clastic chert beds at the lower stratigraphic level are coarse arenites to fine, flat-pebble conglomerates. They consist of tabular intraclasts up to 14 mm long, and some are normally graded. The clastic chert beds at the higher stratigraphic level are finer arenites with more equidimensional grains, including some chert oolites. We interpret these clastic chert layers as distal storm deposits, and they are very similar to cherty beds in granular iron-formations such as those of the Nabberu Basin in Western Australia, or the North American iron ranges (Simonson and Goode, 1989).

Iron-bearing minerals are also disseminated in some of the chert lutites, particularly those in the Mount Sylvia Formation and Mount McRae Shale, and layers of true BIF (especially jaspilite) are present locally in the Bee Gorge Member and overlying units (Fig. 2). The thickest and most prominent of the BIFs is informally known as Bruno's Band, which is located at the top of the Mount Sylvia Formation (Trendall and Blockley, 1970, p. 86). This marker bed ranges from 3.6 to 6.7 m in thickness and is present throughout the Hamersley Basin (Fig. 2). The Mount Sylvia Formation also contains two thinner layers of ferruginous chert that are almost as pervasive as Bruno's Band (Fig. 2). These two layers are commonly referred to as BIFs but do not contain enough iron to qualify for that name. These three ferruginous marker beds form a triplet whose proportional spacing is remarkably consistent throughout the Hamersley Basin. BIFs and ferruginous chert lutites both display thin laminations and podding comparable with those of BIFs elsewhere in the Hamersley Group (Trendall and Blockley, 1970; Ewers and Morris, 1981; McConchie, 1984).

## Volcaniclastics

By far the most significant accumulation of volcaniclastic sediments in the units we studied is the Main Tuff Interval (MTI) of the Bee Gorge Member. The MTI is a 4.2 to 16.4 metre-thick sequence of pyroclastic turbidites that has a preserved volume of 200 km<sup>3</sup>. In outcrop, the MTI stands out from the surrounding argillite and chert as a conspicuous ledge which weathers to a distinctive grey-green to olive colour with an orange-red surface stain. Coarser grained portions of this unit, which are often replaced by carbonate, weather to a yellow-brown colour. In general, finer grained and thinner

sections are better preserved than coarse-grained, thick-bedded sections. In core, the MTI ranges from light to dark grey in colour and portions replaced by carbonate may show a crystalline texture.

The MTI is composed of altered pyroclastic material, detrital crystals, and intrabasinal rip-up clasts. Pyroclastic material includes coarse sand- to silt-sized, blocky to oblong vitric grains and coarse sand-sized accretionary and armoured lapilli; all of these have been pervasively altered to a mixture of chlorite, clay minerals, and carbonate. Fine to very fine sand-sized feldspar and quartz crystals are a minor but persistent component of the MTI. Intrabasinal rip-up clasts consist largely of argillite, with minor amounts of chert and carbonate (including concretions), and range from sand to megaclast size. Of these clast types, only accretionary lapilli and sand-sized or larger rip-up clasts are visible to the naked eye.

Three types of turbidite depositional sequences have been recognized in the MTI, based on patterns of sedimentary structures, grain-size trends, and the presence of erosional surfaces. In each measured section, the MTI consists of 14 to 28 of these depositional sequences. The sequence types are as follows:

1. *Thick graded-bed sequences* (45–545 cm thick) consisting of one, or very rarely two, decimetre- to metre-scale beds capped by one to eight centimetre-scale beds. Each sequence base is commonly an irregular erosional surface, and the thick beds in several sequences contain argillite boulders and megaclasts (Hassler, 1990b). Pyroclasts in the thick basal bed are normally graded, as are any intraclasts that are present. Granule-sized intraclasts also occur at the same level as fine sand-sized pyroclasts, indicating density grading. The overlying thin beds are finer grained than the basal thick bed, and the uppermost thin bed is the finest of all. Most thin beds are normally graded, but rare layers with ripple cross-lamination are also present. In heavily weathered sections, only the top of the thick bed and the lowest of the overlying thin beds are exposed.
2. *Thin normally graded-bed sequences* (4–28 cm thick) consisting of one to three 2–10 cm-thick normally graded beds, overlain by one to fourteen thinner normally graded beds, each less than 2 cm thick. Grain size decreases upwards through individual sequences, and some sequences also show double grading as described by Fiske and Matsuda (1964), but bedding thicknesses show no regular patterns. Planar laminations and rare ripple cross-laminations are present within the upper thin graded beds in places. Some sequences are capped by a single layer 5–11 cm thick that is very fine grained.
3. *Complex Bouma sequences* (5–29 cm thick), which include the components of classical Bouma sequences (Bouma, 1962) but commonly show repetitions of  $t_b$ ,  $t_b$ , and  $t_c$  intervals within a single depositional sequence. Sequences with multiple  $t_b$  and  $t_c$  intervals are most common; sequences showing the full range of  $t_a$ – $t_c$  intervals are rare.

We interpret sequence types 1 and 2 (thick graded-bed and thin normally graded-bed sequences respectively) as deposits of highly concentrated turbidity currents dominated by suspension sedimentation, as modeled by Lowe (1988). This is based on the abundance of normal and density grading, the rarity of ripple cross-lamination and planar lamination, and the presence of erosional surfaces and intrabasinal rip-up clasts in these sequences. In contrast, the combination of graded bedding and traction structures in sequence type 3 (complex Bouma sequences) suggests they represent deposition from high- and low-density turbidity currents, as described by Middleton and Hampton (1976) and Lowe (1982).

The MTI records an exceptionally large-volume pyroclastic sedimentation event during deposition of the Wittenoom Formation. A lack of non-volcanogenic interbeds indicates that the MTI accumulated rapidly on the floor of the Hamersley Basin. Palaeocurrent data indicate that the unit was derived from a source volcano located to the north, and that it had a complex depositional history (Hassler, 1991a, in press).

Beds in many MTI sections are cut by distinctive veins that typically occur in networks which traverse bedding packages up to 2.4 m thick. The veins consist of coarsely crystalline carbonate that weathers yellow-brown and contain slivers of the MTI host rock, some of which are displaced downward. Individual veins can be up to 5 mm wide and are elongated perpendicular to bedding. They are generally arcuate to sinuous in cross section and can form polygonal patterns in plan, resembling those formed by desiccation cracks. In addition to the MTI, similar vein networks were observed in a carbonate package high in the Bee Gorge Member at the CH site.

In addition to the highly concentrated volcanics of the MTI, the Bee Gorge Member contains a number of thin, isolated tuff beds. These solitary tuff beds are similar in appearance to the MTI in both cores and surface exposures, e.g. they are greener and less fissile than the ambient argillite. Individual tuff beds rarely exceed 10 cm in thickness and are still recognizable where less than a centimetre thick. Much of the detritus in these thin tuff beds is very fine grained and difficult to resolve microscopically, but where individual grains can be distinguished, they are very well sorted and range up to medium sand size. Many thin tuffs display excellent normal grading, but traction structures such as ripple cross-lamination are rarely present.

The most distinctive and widespread of the thin tuffs is the Crystal-rich Tuff. This bed is normally graded and well sorted throughout, and the clasts reach a maximum size of 0.2 mm at the base of the bed. The clasts are mainly finely crystalline aggregates (some with obvious microlitic textures) and crystalline grains. The latter consist of potassium feldspar (?after plagioclase) and lesser monocrystalline quartz, both of which display many partially to completely euhedral outlines. Such crystals are more abundant in this bed than in any of the other thin tuffs and are generally visible in hand sample; hence the name Crystal-rich Tuff. A few of the aggregate clasts appear to be vesicular, but none have the pronged shapes of felsic shards.

The Crystal-rich Tuff layer persists laterally for hundreds of kilometres and is present throughout most of the Hamersley Basin. It is close to 10 cm thick at all sites with two exceptions: it expands to 19 cm at the GV site in the southeast, and shrinks to 5 cm at the WY site in the southwest. Based on the lack of traction structures, and excellent sorting and grading, we interpret this and other thin tuff layers as direct eruptive fallout deposits. The character of the clasts indicates the volcanic eruptions responsible were probably hydroclastic rather than pyroclastic, i.e. phreatoplinitic rather than plinian (Cas and Wright, 1987, p. 158–162).

In the southeastern part of the Hamersley Basin, the Mount McRae Shale contains a layer of coarser clastic material. We only observed this layer in the WW section (Fig. 2), where it is about 5.3 m thick, and in drillcore from the Mount Whaleback mine area, where it is informally known as the 'volcanic siltstone'. Samples from this layer consist of quartz, chlorite, dolomite, and possibly lesser amounts of potassium feldspar. Petrographically, they show about equal amounts of chert grains, carbonate, and sheet silicates with lesser quartz sand and silt. The carbonates and the sheet silicates both appear to be replacing original detrital grains, whereas the quartz, chert, and small numbers of feldspar grains appear to be original detritus. This layer generally appears massive and structureless, although locally it has rare ripple cross-lamination and soft-sediment deformation structures. Whether these rocks represent a separate episode of volcanism or a highly anomalous influx of siliciclastic sand is unclear because of the limited number of observations, as well as the obscuring effect of the strong tectonic foliation typical of many strata in this part of the Hamersley Basin (Tyler and Thorne, 1990).

Ewers and Morris (1981) presented persuasive geochemical arguments that the S or 'shale' macrobands of the Dales Gorge Member of the overlying Brockman Iron Formation are volcanogenic in origin. In the Bee Gorge Member, the mineralogical compositions of the thin tuff beds and ambient argillite are consistently different. Potassium feldspar and muscovite (or a similar 10 angstrom clay mineral) are abundant in the tuffs but not in the argillite, whereas chlorite is abundant in the argillite but generally undetectable in the tuffs. These differences suggests the argillites of the Bee Gorge Member (and those of the Paraburdoo Member and Mount Sylvia Formation, which are similar) are siliciclastic rather than volcanoclastic in origin. The absence of the only iron-bearing silicate mineral which is abundant in the argillites also explains why the weathered tuffs are less red.

In contrast, the argillites of the Mount McRae Shale contain more muscovite than chlorite, i.e. they are closer to the tuffs mineralogically than to the underlying argillites. This may indicate an upsection increase in the influx of fine volcanoclastic detritus into the Hamersley Basin, in keeping with Ewers and Morris' (1981) interpretation of the S bands in the overlying Brockman Iron Formation.

### **Silicate-melt spherules**

A single turbidite just above the Main Tuff Interval of the Bee Gorge Member is known as the Spherule Marker

Bed (Fig. 2) because it contains an abundance of sand-sized spherules that do not occur at any other level in the Wittenoom Formation, the Mount Sylvia Formation, or the Mount McRae Shale. These spherules resemble silicified oolites in outcrop, but they consist almost entirely of potassium feldspar replaced in part by carbonate minerals. The vast majority of the spherules are coarse to very coarse sand size and have spheroidal to ovoid shapes, although a few are more irregular, e.g. peanut shaped. Internally, most of the spherules display acicular to lath-shaped crystals that radiate inwards from the margins, indicating they are quenched and devitrified droplets of former silicate melt.

The turbidite which hosts the spherules is 12–130 cm thick and generally displays partial ( $t_b$ – $t_c$ ) Bouma sequences. The spherules are usually restricted to discontinuous lenses 3–65 mm thick at the base of the bed. Some of these lenses are cross-stratified and many contain imbricated slabs of carbonate lutite up to 62 cm long and/or finer flat pebbles of highly ferruginous sediment. However, at site BB the spherules are restricted to thin lenses along a single horizon in the argillite underneath the base of the turbidite, indicating they were dispersed independently.

Based on these lines of evidence, we interpret these spherules as melt droplets that were originally part of a strewn field generated by a major bolide impact (Simonson, 1992a). Identical spherules and larger, more irregular silicate bodies with similar textures also occur in a 22.7 m-thick dolomite debris flow deposit (the dolomixtite) near the base of the Carawine Dolomite. Based on evidence presented in Simonson (1992a) and Simonson et al. (in press), we interpret the dolomixtite layer as a more proximal equivalent of the Spherule Marker Bed. In addition, similar spherules occur in a single layer in the S4 band of the Dales Gorge Member of the Brockman Iron Formation (LaBerge, 1966, figs 5, 6, and 7; Trendall and Blockley, 1970, fig. 44B) and may be the product of a subsequent impact.

## Acknowledgements

Our study of the Wittenoom Dolomite would not have been possible without the assistance of many organizations and individuals. Financial support was provided by National Geographic Society grants 3285–86 and 3598–87, and Oberlin College. Logistical support and access to core material were provided by the Geological Survey of Western Australia, Hamersley Iron Pty Limited, CRA Exploration Pty Limited, and Mount Newman Mining Co. Pty Limited through the kind offices of Alec Trendall and Richard Davy, Richard Harmsworth, Adrienne Meakins, and Peter Bellairs respectively. Robert Demicco, Anna Buising, and Daniel Daniel assisted us in the field; Gretchen Hampt, BP America research assistant David Jarvis, and Hughes research assistant Karen Carney assisted us in the laboratory, and BP research assistant Jim Leenhouts helped with both. Discussions with these and many other people, particularly Ian Williams and Richard Morris, were very helpful. In Oberlin, Hugh Bates, Jim Keith, and Peter Munk made the thin sections, and

Veronica Kuszniir prepared the manuscript. John Blockley and Ian Nowak coordinated the technical production of the manuscript at the Geological Survey of Western Australia. We are deeply indebted to all of the people, but most of all to Alec Trendall. He initially brought the need for work on the Wittenoom Dolomite to the attention of the senior author, then supported the project in many ways.

## References

- BARNETT, J. C., 1981, Mesozoic and Cainozoic sediments in the western Fortescue plain: Western Australia Geological Survey, Annual Report 1980, p. 35–42.
- BEUKES, N. J., 1987, Facies relations, depositional environments and diagenesis in a major early Proterozoic stromatolitic carbonate platform to basinal sequence, Campbellrand Subgroup, Transvaal Supergroup, southern Africa: *Sedimentary Geology*, v. 54, p. 1–46.
- BLOCKLEY, J. G., TEHNAS, I. J., MANDYCZEWSKY, A., and MORRIS, R. C., 1993, Proposed stratigraphic subdivisions of the Marra Mamba Iron Formation and the lower Wittenoom Dolomite, Hamersley Group, Western Australia: Western Australia Geological Survey, Report 34, Professional Papers, p. 47–63.
- BOUMA, A. H., 1962, Sedimentology of some flysch deposits. A graphic approach to facies interpretation: Amsterdam, Elsevier.
- CAS, R. A. F., and WRIGHT, J. V., 1987, Volcanic successions: modern and ancient: London, Allen and Unwin.
- FISKE, R. S., and MATSUDA, T., 1964, Submarine equivalents of ash-flows in the Tokiwa Formation, Japan: *American Journal of Science*, v. 262, p. 76–101.
- EWERS, W. E., and MORRIS, R. C., 1981, Studies of the Dales Gorge Member of the Brockman Iron Formation, Western Australia: *Economic Geology*, v. 76, p. 1929–1953.
- GOODE, A. D. T., 1981, The Proterozoic geology of Western Australia, in *The Precambrian Geology of the Southern Hemisphere edited by D. R. HUNTER*: Amsterdam, Elsevier, p. 105–203.
- HASSLER, S. W., 1990a, The Main Tuff Interval of the Wittenoom Dolomite: Evidence for the paleogeography and tectonic setting of the Hamersley Basin, Western Australia: *Third International Archaean Symposium, Proceedings*, p. 185–187.
- HASSLER, S. W., 1990b, Boulder and megaclast transport by fine-grained volcanoclastic turbidity currents, late Archean Hamersley Group, Western Australia: *Geological Society of America, Abstracts with Programs*, v. 22, p. A92.
- HASSLER, S. W., 1991a, Depositional processes, paleogeography and tectonic setting of the Main Tuff Interval of the Wittenoom Dolomite, late Archean Hamersley Group, Western Australia: University of California at Santa Barbara, Ph.D. thesis (unpublished).
- HASSLER, S. W., 1991b, Turbidite sequences and depositional history of the Main Tuff Interval, Wittenoom Dolomite, ca. 2.6 Ga Hamersley Group, Western Australia: *Geological Society of America, Abstracts with Programs*, v. 23, p. A462.
- HASSLER, S. W., 1992, The Main Tuff Interval of the Wittenoom Formation: widespread distal pyroclastic turbidite deposition in the ~2.6 Ga Hamersley Basin, Western Australia: *SEPM Theme Meeting, Fort Collins, Colorado, Abstracts*, p. 31.
- HASSLER, S. W., in press, Depositional history of the Main Tuff Interval of the Wittenoom Formation, late Archean–early Proterozoic Hamersley Group, Western Australia: *Precambrian Research (theme issue on Pilbara Craton)*.
- HASSLER, S. W., and SIMONSON, B. M., 1991, Paleogeography of the early Precambrian Hamersley Basin, Western Australia, and the origin of large banded iron formations: *Geological Association of Canada, Program with Abstracts*, v. 16, p. A52.

- KLEIN, C., BEUKES, N. J., and SCHOPF, J. W., 1987, Filamentous microfossils in the early Proterozoic Transvaal Supergroup: their morphology, significance and paleoenvironmental setting: *Precambrian Research*, v. 36, p. 81–94.
- La BERGE, G. L., 1966, Altered pyroclastic rocks in iron-formation in the Hamersley Range, Western Australia: *Economic Geology*, v. 61, p. 147–161.
- LOWE, D. L., 1982, Sediment gravity flows, II: Depositional models with special reference to the deposits of high-density turbidity currents: *Journal of Sedimentary Petrology*, v. 52, p. 279–297.
- LOWE, D. L., 1988, Suspended-load fallout as an independent variable in the analysis of current structures: *Sedimentology*, v. 35, p. 765–776.
- MacLEOD, W. N., 1966, The geology and iron deposits of the Hamersley Range area, Western Australia: Western Australia Geological Survey, Bulletin 117.
- McCONCHIE, D., 1984, A depositional environment for the Hamersley Group: palaeogeography and geochemistry, in *Archaean and Proterozoic basins of the Pilbara, Western Australia: evolution and mineralization potential* edited by J. R. MUHLING, D. I. GROVES, and T. S. BLAKE: University of Western Australia, Geology Department and University Extension, Publication no. 9, p. 144–190.
- MIDDLETON, G. V., and HAMPTON, M. A., 1976, Subaqueous sediment transport and deposition by sediment gravity flow, in *Marine sediment transport and environmental management* edited by D. J. STANLEY, and D. J. P. SWIFT: New York, John Wiley and Sons Inc., p. 197–218.
- MYERS, J. S., and HOCKING, R. M., (compilers), 1988, Geological map of Western Australia, 1:2 500 000: Western Australia, Geological Survey.
- SIMONSON, B. M., 1987a, 2.5 Ga carbonate turbidites in the banded iron formation-rich Hamersley Group of Western Australia: *Geological Society of America, Abstracts with Programs*, v. 19, p. 846.
- SIMONSON, B. M., 1987b, Early silica cementation and subsequent diagenesis in arenites from four early Proterozoic iron formations of North America: *Journal of Sedimentary Petrology*, v. 57, p. 494–511.
- SIMONSON, B. M., 1988a, Using iron-poor units to constrain the origin of banded iron-formations in the 2.5 Ga Hamersley Basin of Western Australia: *Geological Society of America, Abstracts with Programs*, v. 20, p. 389.
- SIMONSON, B. M., 1988b, Roll-up structures: evidence of microbial mats in 2.5 Ga basinal carbonates of Western Australia: *SEPM Annual Midyear Meeting, Abstracts*, v. 5, p. 50.
- SIMONSON, B. M., 1989, Devitrified silicate glass spheroids of probable impact origin in 2.5 Ga Hamersley Basin, Western Australia: *Geological Society of America, Abstracts with Programs*, v. 21, p. A371.
- SIMONSON, B. M., 1990, Wittenoom Dolomite, in *Third International Archaean Symposium Excursion Guidebook* edited by S. E. HO, J. E. GLOVER, J. S. MYERS, and J. R. MUHLING: University of Western Australia, Geology Department and University Extension, Publication no. 21, p. 50.
- SIMONSON, B. M., 1991, Geological evidence for an early Precambrian microtektite strewn field in the Hamersley Basin of Western Australia: *Geological Association of Canada, Program with Abstracts*, v. 16, p. A115.
- SIMONSON, B. M., 1992a, Geological evidence for a strewn field of impact spherules in the early Precambrian Hamersley Basin of Western Australia, *Geological Society of America, Bulletin*, v. 104, p. 829–839.
- SIMONSON, B. M., 1992b, Geological evidence for a 2.6 Ga strewn field of impact spherules in the Hamersley Basin of Western Australia: *Large Meteorite Impacts and Planetary Evolution Conference, Sudbury, Ontario, Lunar Planetary Institute Contribution*, no. 790, p. 68–69.
- SIMONSON, B. M., and GOODE, A. D. T., 1988, First discovery of ferruginous chert arenites in the early Precambrian of Western Australia: *Geological Society of America, Abstracts with Programs*, v. 20, p. A206.
- SIMONSON, B. M., and GOODE, A. D. T., 1989, First discovery of ferruginous chert arenites in the early Precambrian of Western Australia, *Geology*, v. 17, p. 269–272.
- SIMONSON, B. M., and HASSLER, S. W., 1991, Sedimentology of the Wittenoom Dolomite and overlying formations of the early Precambrian Hamersley Group: Western Australia Geological Survey, Precambrian Report 1991/1 [available only on microfiche].
- SIMONSON, B. M. SCHUBEL, K. A., and HASSLER, S. W., 1991, Carbonate sedimentation in the 2.6 Ga Hamersley Basin of Western Australia: *Geological Association of Canada, Program with Abstracts*, v. 16, p. A115.
- SIMONSON, B. M. SCHUBEL, K. A., and HASSLER, S. W., in press, Carbonate sedimentology of the early Precambrian Hamersley Group of Western Australia: *Precambrian Research* (theme issue on Pilbara Craton).
- TRENDALL, A. F., 1983, The Hamersley Basin, in *Iron-formations: facts and problems* edited by A. F. TRENDALL, and R. C. MORRIS: Amsterdam, Elsevier, p. 69–129.
- TRENDALL, A. F., and BLOCKLEY, J. G., 1970, The iron formations of the Precambrian Hamersley Group, Western Australia: Western Australia Geological Survey, Bulletin 119.
- TYLER, I. M., and THORNE, A. M., 1990, The northern margin of the Capricorn Orogen, Western Australia—an example of an Early Proterozoic collision zone: *Journal of Structural Geology*, v. 12, p. 685–701.



# Further isotopic evidence for the existence of two distinct terranes in the southern Pinjarra Orogen, Western Australia

by

I. R. Fletcher and W. G. Libby

## Abstract

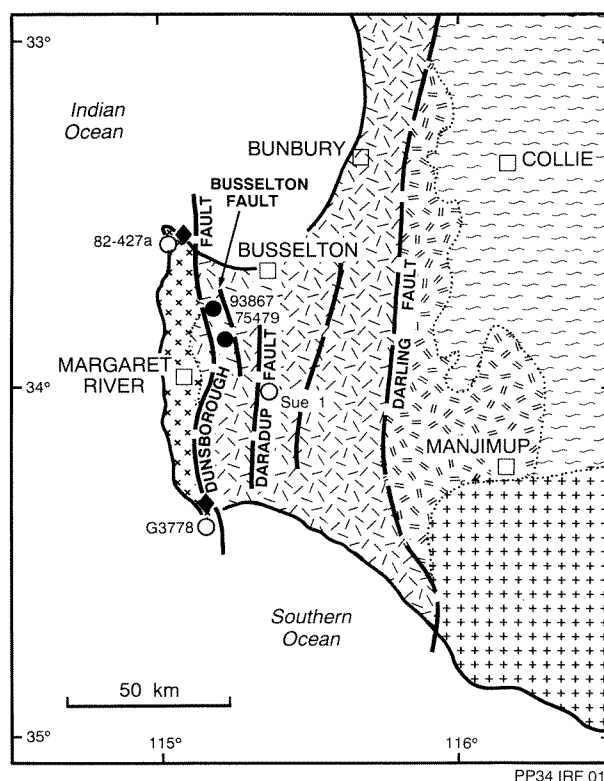
Two samples from the crystalline basement of the Vasse Shelf in the southern part of the Perth Basin have Sm–Nd model ages ( $T_{DM}$ ) of 2011 Ma and 2018 Ma ( $T_{CHUR} \sim 1715$  Ma). These dates are similar to those determined for crystalline rocks elsewhere in the Pinjarra Orogen, including the Bunbury Trough, but are older than those of the Leeuwin Complex. The contact between the Leeuwin Complex and older portions of the Pinjarra Orogen apparently follows the Dunsborough Fault tectonic zone.

**KEYWORDS:** Geochronology, Leeuwin Complex, Perth Basin, Pinjarra Orogen, Sm–Nd, Vasse Shelf.

Several recent papers have considered the evolution of the southwestern corner of Western Australia (Fig. 1), mostly in the context of broad-scale accounts of Proterozoic evolution of the Australian continent (Page et al., 1984; Fletcher et al., 1983, 1985; McCulloch, 1987). There is general agreement that stabilization of the Yilgarn Craton was complete by about 2500 Ma and that the Pinjarra Orogen developed in two distinct stages: the crystalline basement of the Perth Basin forming and stabilizing between about 2200 Ma and 1100 Ma, and the Leeuwin Complex forming less than 1100 Ma ago. However, the validity of this three-stage sequence has been open to question because the geochronological database for the Pinjarra Orogen is quite limited.

New zircon U–Pb ages between about 450 Ma and 600 Ma for samples from two widely spaced localities in the Leeuwin Complex (Fig. 1) were quoted by Wilde and Murphy (1989), who have recently studied and mapped the complex in considerable detail. These ages are consistent with the available Sm–Nd model ages of about 1100 Ma ( $T_{DM}$ ; see Table 1) and with the  $655 \pm 25$  Ma Rb–Sr date given by Compston and Arriens (1968). Thus the broad geochronological framework of the complex is better established, though details of its evolution remain to be determined.

Sm–Nd data have now been obtained (Table 1) for two additional drillcore samples from the basement of the southern portion of the Perth Basin, enabling this crustal unit to be characterized with more confidence than was possible using the one analysis from Fletcher et al. (1985). Both samples are from the Vasse Shelf, between the Dunsborough and Busselton Faults (Figs 1, 2). GSWA 93867 is a weakly carbonated garnet–biotite metasyenogranite from 568 m in CRA borehole CRCH–1, and GSWA 75497 is a garnet–biotite monzosyenitic flaser gneiss from 200.5 m in Treton borehole DDH–2. The model ages ( $T_{DM} = 2018$  Ma and 2011 Ma, respectively) agree closely with published data for the Sue 1 drillcore sample (2059 Ma; Table 1), and with data for more northerly parts of the Pinjarra Orogen



PP34 IRF 01

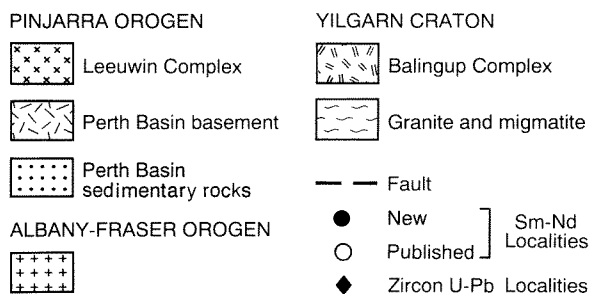


**Figure 1.** Major tectonic subdivisions of crystalline rocks in southwestern Western Australia (after Myers and Hocking, 1988), showing Sm–Nd and zircon U–Pb samples sites in the southern Pinjarra Orogen (Table 1; McCulloch, 1987; Wilde and Murphy, 1988).

**Table 1. Sm–Nd data for felsic samples from the southern portion of the Pinjarra Orogen**

Sample	Sm (ppm)	Nd	$^{147}\text{Sm}/^{144}\text{Nd}$	$^{143}\text{Nd}/^{144}\text{Nd}$ (a)	$T_{\text{CHUR}}$ (b) (Ma)	$T_{\text{MORB}}$ (c) (Ma)	$T_{\text{DM}}$ (d) (Ma)
<b>Perth Basin basement</b>							
93867	16	88	(f) 0.11169 ± 12	0.511667 ± 10	1705	2079	2018
75497	2	12	0.10234 ± 26	0.511548 ± 10	1727	2067	2011
W1672	(Sue #1; Fletcher et al., 1985)				1797	2110	2059
<b>Leeuwin Complex</b>							
G3778 (e)	21	145	0.08596 ± 19	0.512072 ± 21	755	1217	1135
82-427a	(Sugarloaf; data from McCulloch, 1987)				584	1185	1083

(a) Normalized to  $^{146}\text{Nd}/^{144}\text{Nd} = 0.7219$  and corresponding to a measured  $^{145}\text{Nd}/^{144}\text{Nd} = 0.512622$  for BCR-000001 (Fletcher et al., 1991)

(b) Using chondritic parameters [0.1967, 0.51262]

(c) Using an assumed linear evolution of depleted mantle from  $\epsilon_{\text{Nd}}(3.5 \text{ Ga}) = 0$  to  $\epsilon_{\text{Nd}}(0) = +10$  (present-day MORB source).

(d) Using the depleting mantle model of de Paolo (1981).

(e) Listed as 'IF-1' by McCulloch (1987).

(f) All error limits pertain to the final two significant digits

$T_{\text{CHUR}}$  and  $T_{\text{MORB}}$  are listed for ease of comparison with some published data for Western Australia and possibly related terranes (e.g. Sri Lanka; Millisenda et al., 1988).  $T_{\text{DM}}$  is probably a better estimate of 'crustal residence age'.

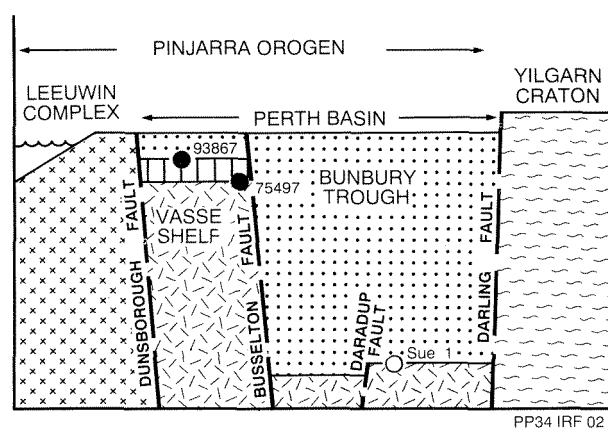


**Figure 2. Schematic structural cross section of the study area, showing relative positions of samples from the Perth Basin basement. The Vasse Shelf dips south (projected surface shown with vertical hatching) and the base of the Bunbury Trough dips north. Vertical exaggeration about 10:1 (Legend as for Fig. 1).**

(Fletcher et al., 1985). The dates are quite distinct from those for the Leeuwin Complex, confirming that the boundary between the Leeuwin Complex and the Perth Basin basement is the Dunsborough Fault tectonic zone rather than the Busselton Fault or the Daradup Fault.

It is clear that in the southwestern extremity of Australia there are extensive terranes of markedly different ages in close juxtaposition (Fig. 3). This may be due, in part, to strike-slip motion along major tectonic zones, particularly the Dunsborough and Darling fault systems (Harris, 1987). However, the great extent of the Pinjarra Orogen and the existence of extensive Proterozoic mobile belts around most of the Yilgarn Craton (McCulloch, 1987) mirror features of the

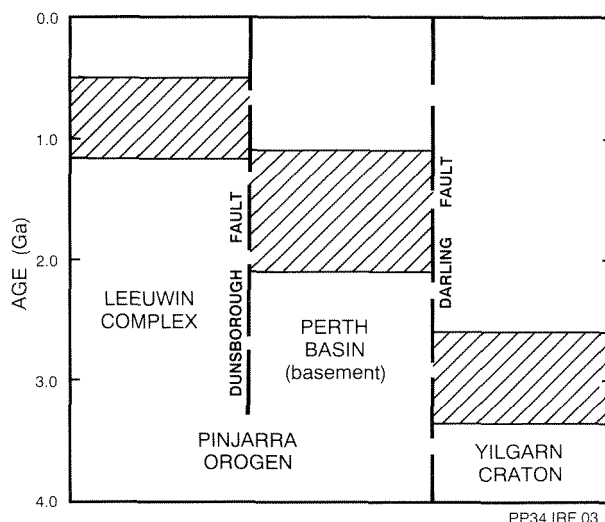


**Figure 3. Evolutionary spans of the southwestern Yilgarn Craton and the Pinjarra Orogen, defined by data from as far north as the Northampton Complex. Older age limits are the earliest identified crust-formation ages ( $T_{\text{DM}}$ ); younger limits are the ages of the youngest known major magmatic or metamorphic events.**

sequential patterns seen in Proterozoic terranes of North America (Bickford, 1988) and argue for lateral growth of continental crust, whether by accretion of younger crustal material or by generation of new crust in continental rifts.

## Acknowledgements

Drillcore samples were made available by CRA Exploration Pty Ltd and Bond Corporation Pty Ltd–Mallina Holdings Ltd. G. Le Blanc Smith provided information for Figure 2, and S. A. Wilde made helpful comments on a draft of this paper.

## References

- BICKFORD, M. E., 1988, The formation of continental crust: Geological Society of America Bulletin, v. 100, p. 1375–1391.
- COMPSTON, W., and ARRIENS, P. A., 1968, The Precambrian geology of Australia: Canadian Journal of Earth Sciences, v. 5, p. 561–583.
- de PAOLO, D. J., 1981, Neodymium isotopes in the Colorado Front Range and crust–mantle evolution in the Proterozoic: Nature, v. 291, p. 193–196.
- FLETCHER, I. R., MYERS, J. S., and AHMAT, A. L., 1991, Isotopic evidence on the age and origin of the Fraser Complex, Western Australia: A sample of Mid-Proterozoic crust: Isotope Geoscience, v. 87, p. 197–216.
- FLETCHER, I. R., WILDE, S. A., LIBBY, W. G., and ROSMAN, K. J. R., 1983, Sm–Nd model ages across the margins of the Archaean Yilgarn Block, Western Australia — II; southwest transect into the Proterozoic Albany–Fraser Province: Geological Society of Australia Journal, v. 30, p. 333–340.
- FLETCHER, I. R., WILDE, S. A., and ROSMAN, K. J. R., 1985, Sm–Nd model ages across the margins of the Archaean Yilgarn Block, Western Australia — III. The western margin: Australian Journal of Earth Sciences, v. 32, p. 73–82.
- HARRIS, L. B., 1987, A tectonic framework for the Western Australian Shield and its significance to gold mineralization, in Recent advances in understanding Precambrian gold deposits *edited by* S. E. HO and D. I. GROVES: University of Western Australia, p. 1–29.
- McCULLOCH, M. T., 1987, Sm–Nd isotopic constraints on the evolution of Precambrian crust in the Australian continent, in Proterozoic lithospheric evolution *edited by* A. KRONER: American Geophysical Union, Geodynamics Series, v. 17, p. 115–130.
- MILISENDA, C. C., LIEW, T. C., HOFMANN, A. W., and KRONER, A., 1988, Isotopic mapping of age provinces in Precambrian high-grade terrains: Sri Lanka: Journal of Geology, v. 96, p. 608–615.
- MYERS, J. S., and HOCKING, R. M. (compilers), 1988, Geological map of Western Australia, 1:2 500 000: Western Australia Geological Survey.
- PAGE, R. W., McCULLOCH, M. T., and BLACK, L. P., 1984, Isotopic record of major Precambrian events in Australia: 27th International Geological Congress, Proceedings, v. 5, p. 25–72.
- WILDE, S. A., and MURPHY, D. M. K., 1988, The Leeuwin Block—evidence on the nature of the Pan-African event in southwestern Australia and its implications for a reconstructed Gondwanaland (abs.): UNESCO/IUGS International Geological Correlation Program, Project 236; Conference on Gondwana Fragments, Nairobi, Kenya, Feb., 1989.



# Cainozoic stratigraphy in the Roe Palaeodrainage of the Kalgoorlie region, Western Australia

by

A. M. Kern and D. P. Commander

## Abstract

Drilling for assessment of groundwater resources in palaeochannels near Kalgoorlie intersected sediments of Middle to Late Eocene age. These sediments consist of a basal sandstone and overlying shale, and could not be correlated directly with the previously erected Rollos Bore Formation, which is poorly known from bores and a shaft near Coolgardie.

New stratigraphic units, the Wollubar Sandstone and the Perkolilli Shale, are defined and described for these early Tertiary sediments occurring in the Roe Palaeodrainage. The sedimentary sequence is distinct from that to the south in the Lefroy Palaeodrainage which contains marine carbonate sediments.

**KEYWORDS:** Cainozoic, stratigraphy, Kalgoorlie, palaeodrainage, drilling

## Introduction

In the course of drilling to assess groundwater resources in the Kalgoorlie region of Western Australia (Commander et al., 1991), a large amount of core material was collected from Tertiary sediments in palaeodrainages. As the Tertiary sediments of the region were not previously well known, new stratigraphic units are defined for the Eocene sedimentary rocks, and brief descriptions are given of Tertiary weathering products and Quaternary units.

The core material, which has been described in detail by Kern et al. (1989), is stored by the Geological Survey of Western Australia, and is available for further study.

## Geological setting

The Kalgoorlie area lies within the Eastern Goldfields Province of the Yilgarn Craton and has been summarized geologically by Griffin (1990). Essentially, it consists of a granite-greenstone terrane of Archaean age with linear, northerly trending belts of supracrustal volcanic and metasedimentary rocks, intruded by granite (Fig. 1).

The present topography is basically a dissected peneplain incised by a Cretaceous to early Tertiary drainage system which discharged eastwards into the Eucla Basin. The remnants of this drainage system have been termed palaeodrainages (Beard, 1972; Bunting et al., 1974; van de Graaff et al., 1977). The Roe Palaeodrainage system (Fig. 1) drained into the Roe Palaeoriver which formerly flowed through the existing Lake Roe area (Smyth and Button, 1989). The Roe Palaeodrainage is bounded to the north and to the south by the Rebecca and Lefroy Palaeodrainages respectively.

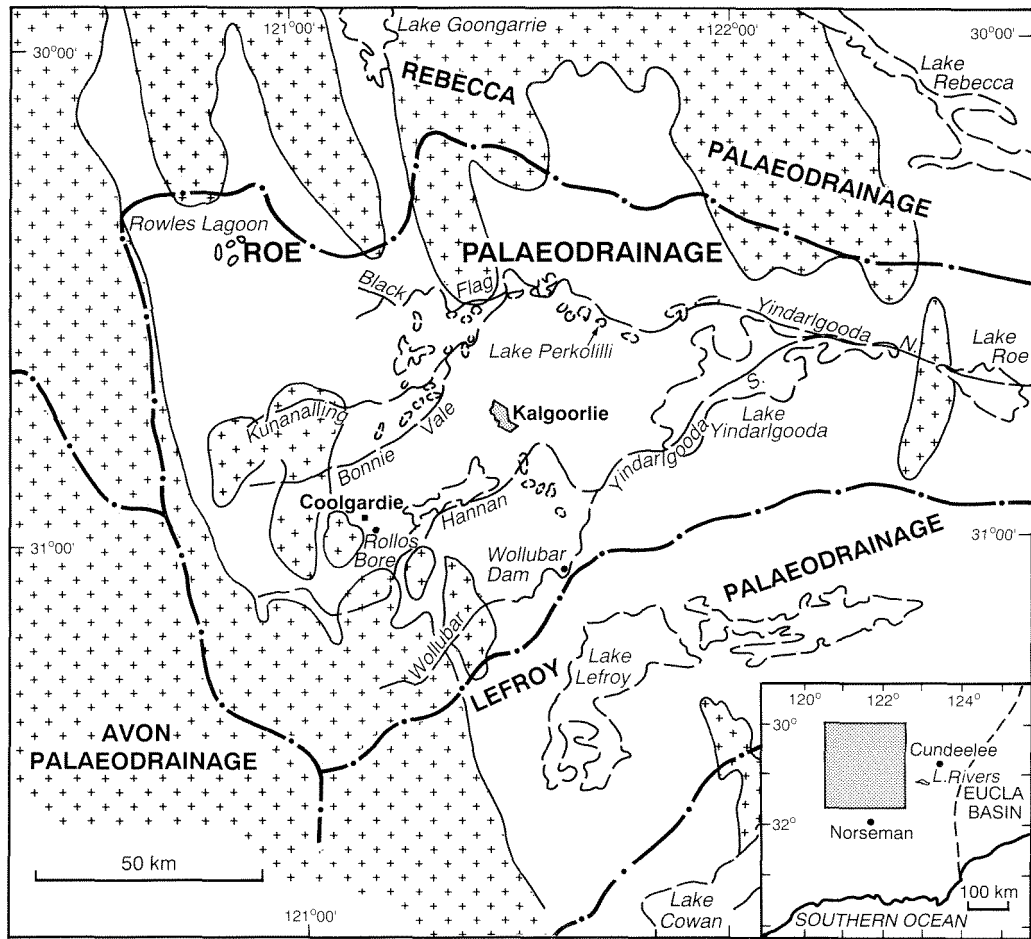
A variety of early Tertiary sedimentary rocks was deposited in the valleys cut by the Roe Palaeoriver and its tributaries. These sediments are now concealed by a surficial cover of Quaternary age, and the broad present-day valleys are occupied by discontinuous salt lakes (playas). Figure 2 shows the probable configuration of the palaeochannel system, and the locations of twenty-two lines drilled during the 1988 groundwater assessment program.

## Previous work

Tertiary sediments from the upper part of the Roe Palaeodrainage, first described by Blatchford (1899) and Maitland (1901), came from an isolated occurrence in Rollos Bore and Shaft, and neighbouring bores, near Coolgardie (Fig. 2). These were later identified as Eocene by Balme and Churchill (1959), and stratigraphic names were formalized by Playford et al. (1975) and by Cockbain and Hocking (1989). Blatchford (1898) also described 'deep leads' at Kanowna, and ascribed a probable late Tertiary age to them.

Clarke (*in* Urquhart, 1956) postulated that the drainage system in the Kalgoorlie region was early Cainozoic, and Urquhart (1956) carried out a refraction seismic survey southeast of Kalgoorlie to locate possible auriferous deep leads. Following extensive drilling for placer gold north and east of Kalgoorlie, Smyth and Button (1989) described the Tertiary sediments in the lower part of the Roe Palaeodrainage east of Kalgoorlie, but did not formalize the stratigraphic nomenclature.

Early Tertiary sediments have also been described from farther south in the Lefroy Palaeodrainage (Griffin, 1989; Jones, 1990) and the Cowan Palaeodrainage (Clarke et al., 1948; Cockbain, 1968a).



PP34 AMK 01

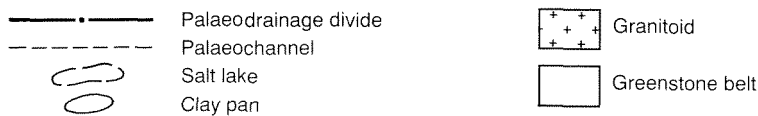


Figure 1. Location map

## Tertiary drainage system

The Early Tertiary rivers within the palaeodrainages cut deep, narrow valleys into the Archaean bedrock. Only the main palaeochannels of the drainage system, now infilled with Middle to Late Eocene sediments, are preserved. In cross section the palaeochannels in the upper parts of the catchments range in width from about 400 to 700 m, and in depth from 25 to 40 m. East of Kalgoorlie, the corresponding widths and depths are about 1000–1500 m and 55–75 m respectively.

The palaeochannels are generally V-shaped and, except in Lines L and M, the flanks are often asymmetric (Fig. 3). In Lines K, N and Q the cross sections are noticeably wide and flat bottomed. It is likely that these lines were drilled oblique to the palaeochannel. Cross sections may also cut across meanders as indicated by the apparent double valley-bottom intersections in Lines K and N.

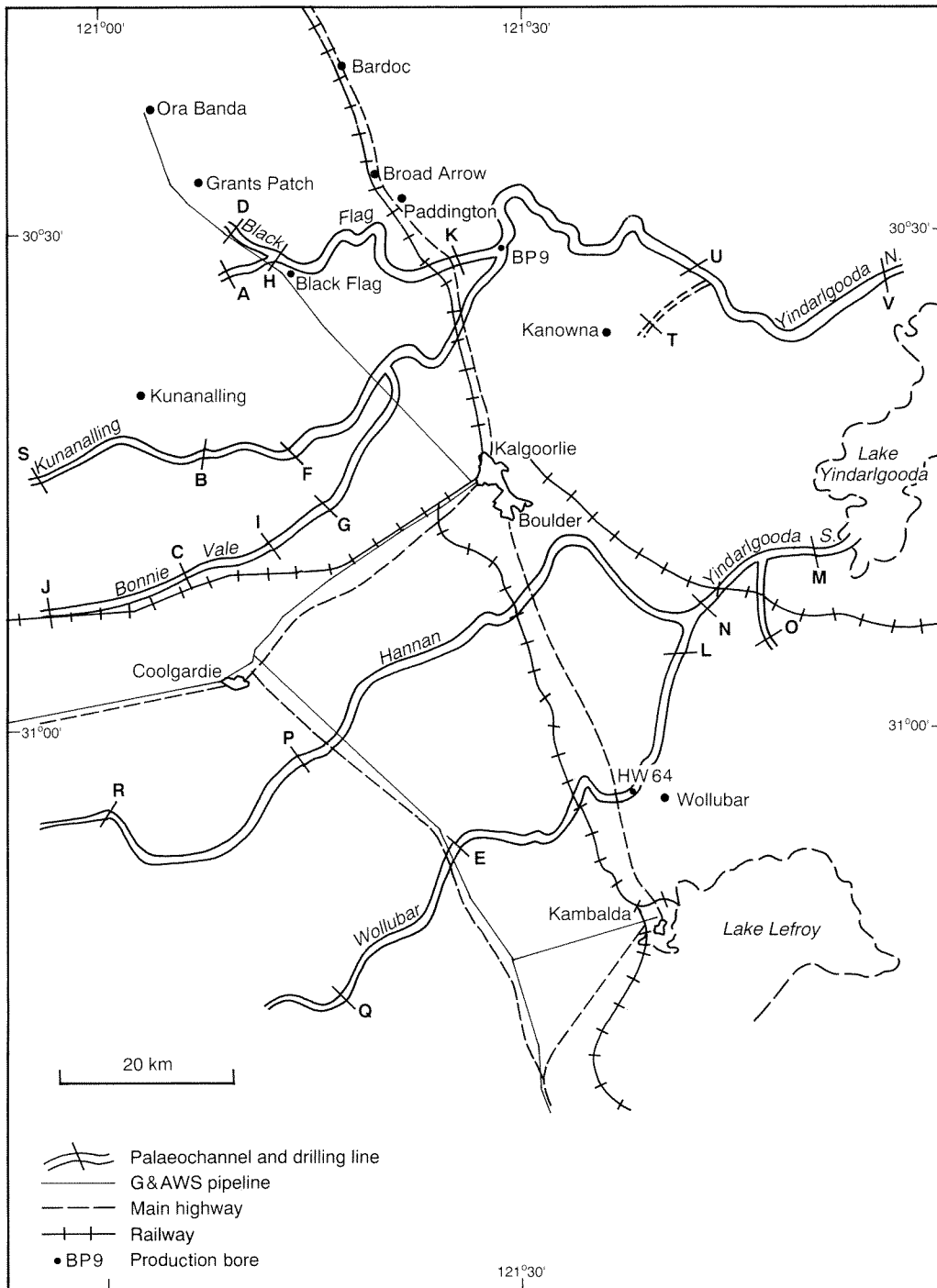
Some cross sections show a deeply incised valley floor on the steeper side of a much wider valley, such as in Lines D, P and R (Fig. 3). This may be due in part to variable

resistance to erosion where there is a complex assemblage of bedrock as in the vicinity of Lines P and R.

The thalwegs of the palaeochannels have low gradients. They are steepest (greater than 1 m per km) in the upper parts of the catchments, especially where the drainage lines traverse relatively resistant greenstone belts. The gradient is more gentle east of Kalgoorlie and is only 0.14 m per km between Lines M and N.

## Stratigraphy

The name Rollos Bore Beds was proposed by Playford et al. (1975) — and amended Rollos Bore Formation by Cockbain and Hocking (1989) — for the dark claystone and shale with thin beds of lignite and minor conglomerate found in Rollos Bore and Shaft and nearby bores. The type section extends from 2 m to a depth of 122 m (about 280 m AHD), based on the geological sections of Maitland (1901), and on a sample from ?119 m dated by Balme and Churchill (1959).



PP34 AMK 02

**Figure 2. Location of drilling lines**

This depth is well below the base of the Tertiary sediments elsewhere in the area (Figs 3 and 4) and the discrepancy may be explained by the original misidentification of weathered Archaean bedrock as Tertiary sediments, and a wrongly marked sample depth. The Tertiary sediments probably extend to a maximum depth of 90 m (310 m AHD), and may be even less than 60 m thick in Rollos Bore.

The present study has confirmed that a consistent division of the Tertiary sediments, into a lower sandstone

and an upper shale, extends over a distance of 150 km (Smyth and Button, 1989). However, because of the uncertain affinity and correlation of the strata in Rollos Bore, the name Rollos Bore Formation is not used in this paper, and new formation names are erected.

The Tertiary sediments in the Roe Palaeodrainage are quite distinct from those in the Lefroy Palaeodrainage (Fig. 5). Those east of Lake Rivers consist of Middle Eocene marine sandstone overlain by spongolite of Late Eocene age (Jones, 1990). However, in the Lake Lefroy

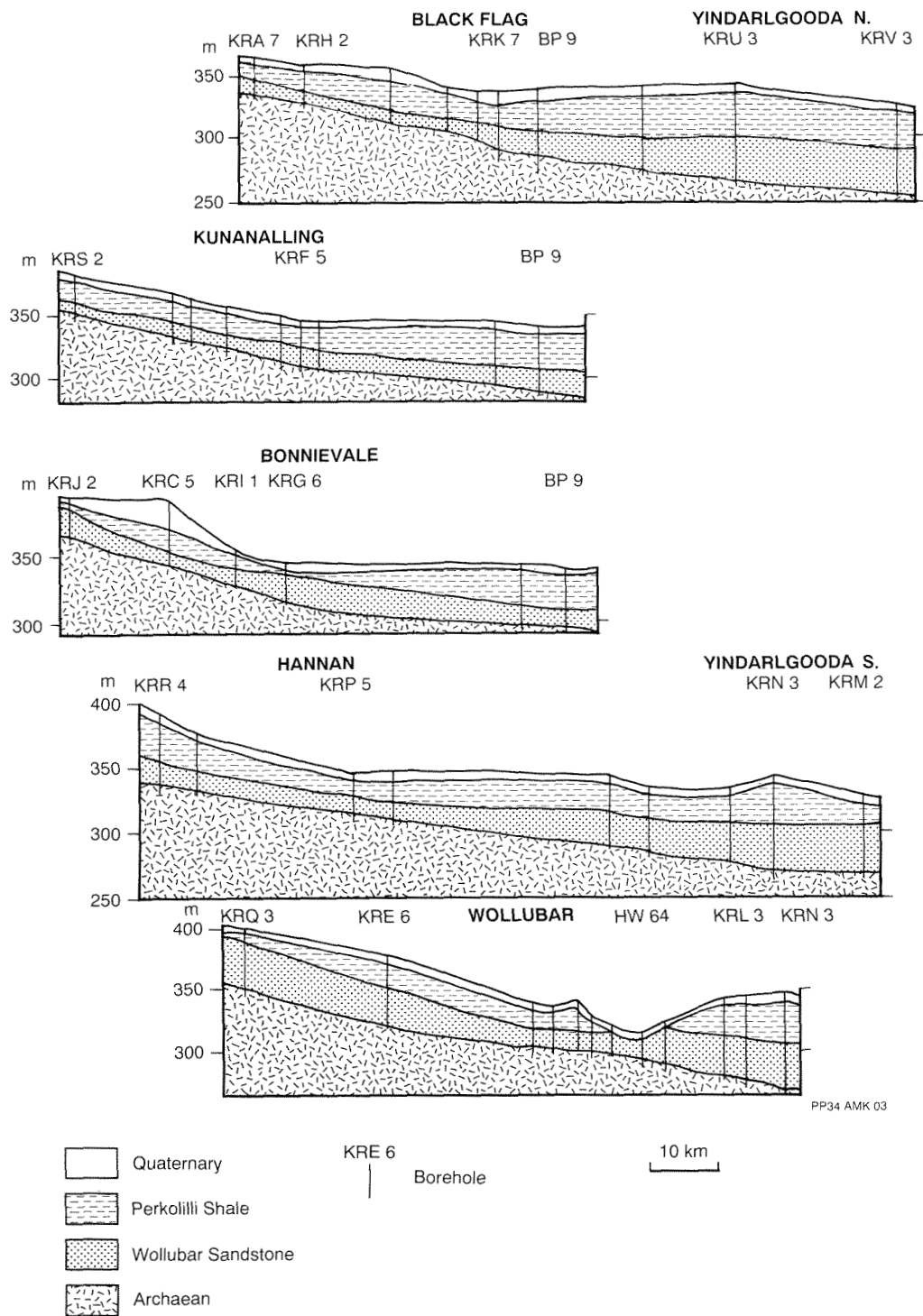


Figure 3. Geological cross sections

area they comprise sandstone, shale, and lignite (Griffin, 1989) overlain by marine carbonate of the Late Eocene Eundynie Group (Cockbain, 1968a).

### Wollubar Sandstone

#### Name

The name Wollubar Sandstone is proposed for a unit of grey to buff sandstone, with minor clay and lignite,

occurring in the Roe Palaeodrainage. The formation is named after Wollubar Dam, about 13 km north of Kambalda (Fig. 2).

#### Type section

The type section lies between 37.7 and 73.5 m in bore KRN-3 (universal grid reference UF 772824, KANOWNA 1:100 000 topographic sheet) situated approximately 30 km southeast of Kalgoorlie (Kern et al., 1989).

## **Lithology**

The Wollubar Sandstone consists of mottled-grey, buff, yellow and brown quartz sandstone with minor conglomerate, clay, silt, carbonaceous siltstone and lignite. The quartz grains are frosted, very coarse to fine, subangular to subrounded and moderately to poorly sorted. Well-sorted quartz is uncommon. The quartz grains are generally more angular in the upper parts of the catchment. Traces of ferromagnesian minerals may be present as accessory minerals, and pyrite occurs at the base of the sand in bore KRN-3. The sand is rarely lithified, although the quartz grains are occasionally bound with siliceous and ferruginous cement. Cross-bedding is developed at some localities. Granitoid rocks are believed to be the primary source of the Wollubar Sandstone.

The base of the Wollubar Sandstone is frequently conglomeratic with subangular pebbles of quartz, and more rarely of Archaean igneous rocks, up to 100 mm in diameter. Beds of clay and sandy clay are commonly found on the sides of the palaeochannels where they interfinger with the sand. Intermittent sandy clay occurs at the top of the sand sequence and grades into the overlying Perkolilli Shale. Thin beds of carbonaceous silt and lignite appear sporadically in bores in the east of the area and, like the clay beds, are present mainly on the sides of the channels.

## **Stratigraphic relationships**

The Wollubar Sandstone rests unconformably on Archaean rocks throughout the Kalgoorlie region, and is typically conformably overlain by the Perkolilli Shale. Occasionally, where this shale is absent, the Wollubar Sandstone is unconformably overlain by late Cainozoic alluvial and colluvial sediments that are difficult to distinguish from the early Tertiary formations. The contact with the Perkolilli Shale is generally sharp, but may be gradational in places.

## **Distribution and thickness**

The Wollubar Sandstone is found only in the palaeochannels and is not seen in outcrop (Fig. 4). It also occurs in lateral tributaries in Lines O and T, where it extends to a higher elevation than in the main palaeochannels.

The formation is 35.8 m thick at the type section and reaches a maximum known thickness of 37.9 m in bore KRM-2 (Kern et al., 1989).

## **Age and correlation**

The lignite and carbonaceous silt in the Wollubar Sandstone contain palynomorphs of the Middle *Nothofagidites asperus* Zone of late Middle to early Late Eocene age (Backhouse, 1989). Similar assemblages have been described from the Werillup Formation in the Bremer Basin (Hos, 1975; Stover and Partridge, 1982). The Wollubar Sandstone probably correlates with the unnamed basal unit of the Eundynie Group (Griffin, 1989) and the Hampton Sandstone in the western part of the Eucla

Basin (Lowry, 1970) and eastern part of the Lefroy Palaeodrainage (Jones, 1990).

## **Environment of deposition**

The Wollubar Sandstone is believed to be essentially a continental fluvial deposit with minor lacustrine and paludal components.

## **Perkolilli Shale**

### **Name**

The name Perkolilli Shale is proposed for the grey clay (mottled reddish brown and yellow where weathered) with minor beds of sandy clay occurring in the Roe Palaeodrainage. The formation is named after Lake Perkolilli situated approximately 30 km northeast of Kalgoorlie (Fig. 2).

### **Type section**

The type section lies between 5.4 and 39.0 m in bore KRU-3 (universal grid reference UG 757203, KANOWNA 1:100 000 topographic sheet), situated 3 km north of Lake Perkolilli along Carmelia Road (Kern et al., 1989). The formation rests conformably on the Wollubar Sandstone and is overlain unconformably by younger, Quaternary deposits.

### **Lithology**

The Perkolilli Shale consists of grey and mottled, dark-red, brown and yellow clay with minor sandy clay. Although the clay is generally plastic, it becomes friable near the surface where it is weathered. It consists mostly of kaolinite (up to 70%) with minor illite and smectite. In places the Perkolilli Shale has been silicified and has a porcelanized texture.

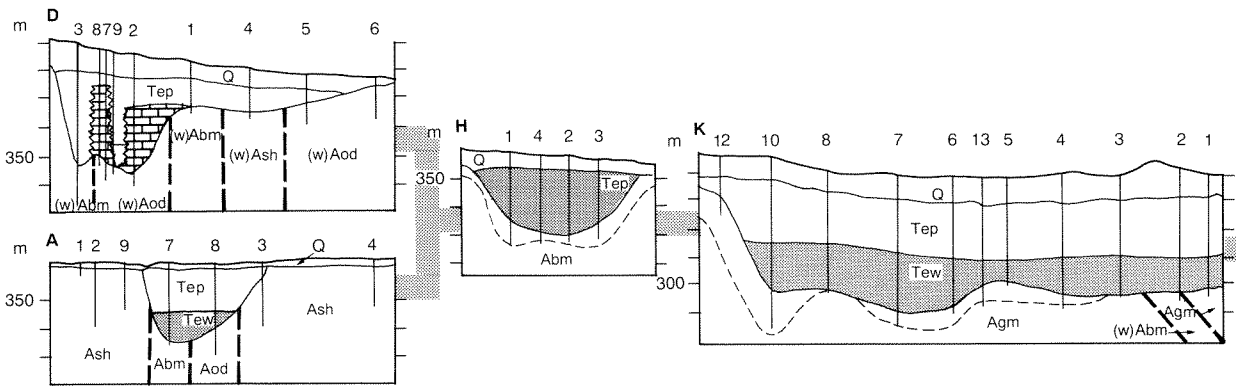
In the upper parts of the Roe Palaeodrainage, on Lines E, J, Q and S (Fig. 4), sandy clay is common at the top of the unit and is difficult to distinguish from Quaternary alluvium (Kern et al., 1989).

Pisolites, consisting of well-rounded ferruginous concretions up to 5 mm diameter, are scattered within the clay. They are more abundant near the base of the formation and are believed to have formed in situ.

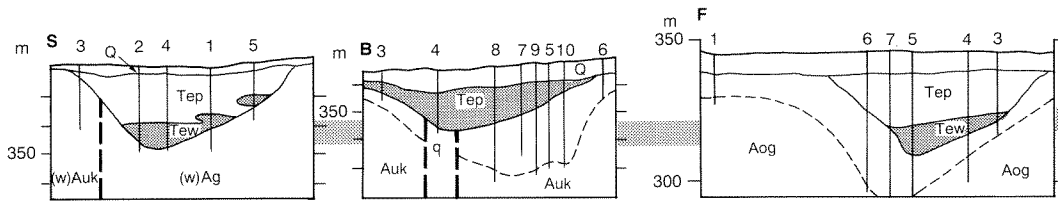
### **Stratigraphic relationships**

The Perkolilli Shale rests conformably on the Wollubar Sandstone. The contact is usually sharp, indicating a rapid change of facies, although in some bores this interface is transitional with alternating beds of sand and clay.

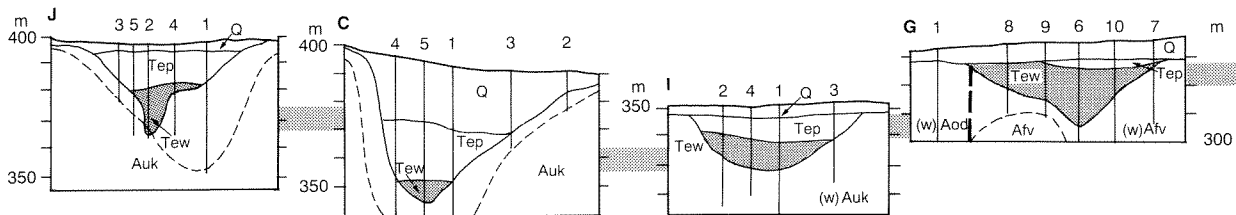
The Perkolilli Shale is in turn unconformably overlain by Quaternary deposits and the top of the formation is frequently weathered. The contact between the Perkolilli Shale and the Quaternary deposits is generally subhorizontal and occurs some 4–6 m below the modern land surface. It is often difficult to distinguish the



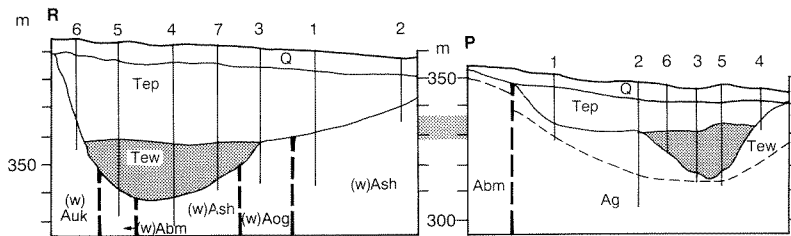
**BLACK FLAG PALAEOCHANNEL**



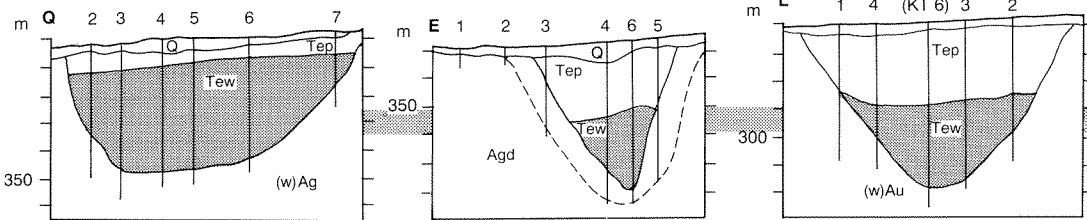
**KUNANALLING PALAEOCHANNEL**



**BONNIE VALE PALAEOCHANNEL**



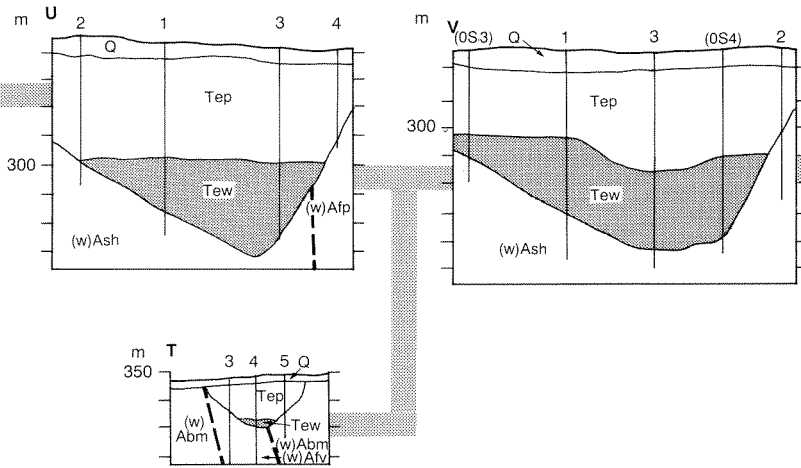
**HANNAN PALAEOCHANNEL**



**WOLLUBAR PALAEOCHANNEL**

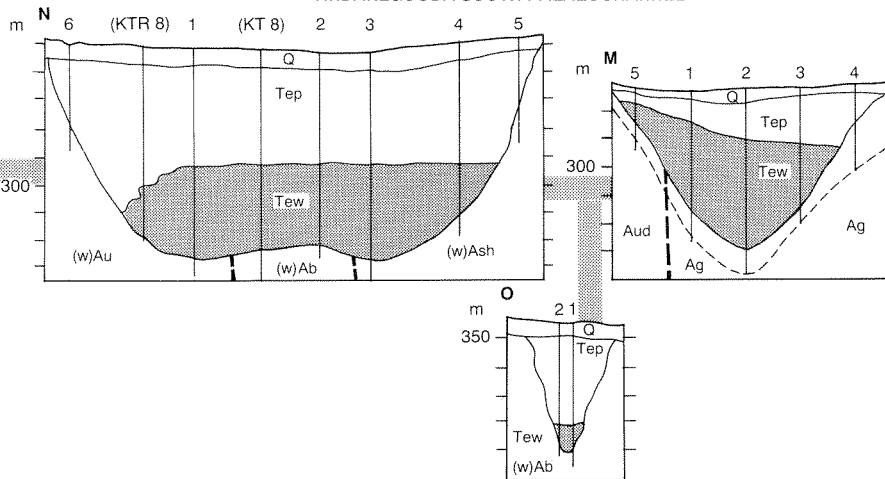
**Figure 4. Longitudinal profiles of palaeochannels**

YINDARLGOODA NORTH PALAEOCHANNEL

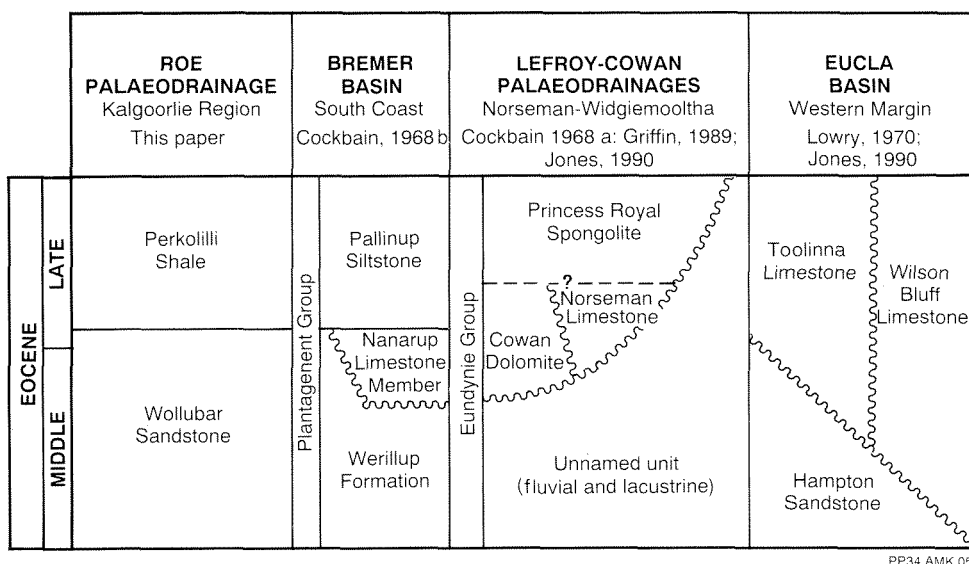


- |   |  |  |
|---|--|--|
| <ul style="list-style-type: none"> <li>┆ Bore hole</li> <li>— Fault</li> <li>Q Quaternary</li> <li>Tepc Calcrete</li> <li>Tep Perkolilli Shale</li> <li>Tew Wollubar Sandstone</li> </ul> | <ul style="list-style-type: none"> <li>Au Ultramafic schist</li> <li>Auk Metakomatite</li> <li>Aud Metadunite</li> <li>Ab Metabasalt</li> <li>Abm High-magnesium metabasalt</li> <li>Aod Metadolerite</li> <li>Aog Metagabbro</li> <li>Afv Felsic metavolcanics</li> <li>APP Metadacite porphyry</li> <li>As Metasedimentary rocks</li> <li>Ash Metamorphosed shale</li> </ul> | <ul style="list-style-type: none"> <li>Granitoid</li> <li>Agm Monzogranitic</li> <li>Agd Granodiorite</li> <li>Agp Pegmatite</li> <li>q Quartz vein</li> <li>(w) Weathered bedrock</li> <li>--- Contact between weathered and fresh bedrock</li> </ul> |
|---|--|--|

YINDARLGOODA SOUTH PALAEOCHANNEL



PP34 AMK 04



PP34 AMK 05

Figure 5. Stratigraphic correlation

contact between the Perkolilli Shale and the clayey Quaternary sediments which may comprise reworked underlying material. The relationship is also obscured by ferruginization, although the Quaternary sediments typically contain more quartz.

#### Distribution and thickness

As with the Wollubar Sandstone, the Perkolilli Shale occurs only in palaeochannels and is not observed as outcrop (Fig. 4). The formation is 33.6 m thick at the type section and reaches a maximum thickness of 39.0 m in bore KRV-3 (Kern et al., 1989).

#### Age and correlation

No palynomorphs were recovered from the formation as the clay is largely oxidized. However, the Perkolilli Shale is assumed to be early Late Eocene in age as it conformably overlies the Wollubar Sandstone.

Lithologically, the Perkolilli Shale correlates with the Pallinup Siltstone of the Plantagenet Group and the lacustrine facies of the lower unnamed unit of the Eundynie Group (Griffin, 1989). The Perkolilli Shale probably correlates with the Princess Royal Spongolite in the Lefroy Palaeodrainage (Jones, 1990), and the Toolinna Limestone and upper part of the Wilson Bluff Limestone of the Eucla Group (Lowry, 1970).

#### Environment of deposition

The Perkolilli Shale is considered to be a freshwater lacustrine deposit, laid down in a drainage system which was drowned as a result of a relatively distant rise in sea level. Unlike the Lefroy Palaeodrainage to the south (Jones, 1990), the closest evidence of Eocene marine deposition in the Roe Palaeodrainage is near Cundeelee, 180 km east of Kalgoorlie (Bunting and van de Graaff, 1977).

### Tertiary weathering

The early Tertiary sediments have been modified by weathering in situ, particularly by processes involving silicification, ferruginization and calcification.

#### Silicification

The localized silicification of the Perkolilli Shale generally occurs just above the contact with the underlying Wollubar Sandstone. Replacement of clay by cryptocrystalline quartz and opal, giving a porcelanized texture, is particularly well developed in Line C; in Line B, silicification occurs above a quartz vein (Kern et al., 1989).

Van de Graaff (1983) observed that silicification generally precedes laterite formation as indicated by common, partial lateritization of silcrete. The age of the silicification in the Tertiary sediments is uncertain.

#### Laterite

A widespread lateritic profile occurs throughout the Eastern Goldfields, and is developed on the Eocene sediments outcropping in the Lefroy Palaeodrainage. In the Roe Palaeodrainage only localized lateritization of the Perkolilli Shale was observed. The upper part of the Perkolilli Shale is typically ferruginized, ranging from a slight ferruginous mottling to a massive and hard limonite-cemented clay. Scattered pisolites also occur in otherwise unferruginized clay. The ferruginized zone is mostly above the modern watertable, but in places extends well below it. Nodular ferruginization occurs throughout the formation in bore KRD-3 (Kern et al., 1989).

#### Calcrete

Massive carbonate development up to 25 m thick, interpreted as a groundwater calcrete, was intersected in

bores along Line D (Kern et al., 1989). The calcrete ranges from friable and powdery to indurated vuggy calcrete, with crystal-lined vugs. In the cores there are very sharp subvertical contacts between calcrete and unaltered Perkolilli Shale, indicating an origin consistent with replacement of clay minerals. It is notable that bores only 150 m apart on Line D show a lateral transition from a completely ferruginized section (KRD-3) to calcrete (KRD-7/8) and, further, to unaltered sediment (KRD-9) within a few hundred metres.

Chemical analyses by the Chemistry Centre (W.A.) show that the composition of the calcrete is calcium–magnesium carbonate (dolomite) with about 29% calcium oxide and 20% magnesium oxide (Table 1). In the three samples analysed the silica content decreased from 6% at 32 m in bore KRD-8 to less than 0.1% at 20 m indicating a progressive removal of silica towards the surface.

The calcrete in Line D appears to be overlain by unaltered colluvial material. Mann and Horwitz (1979) suggest that calcrete formation could have occurred by chemical deposition and replacement over a lengthy period of time, and may still be taking place. Groundwater calcrete was not intersected elsewhere in the drilling program, and is not known to outcrop in the Roe Palaeodrainage. Mann and Horwitz (1979) give the southern boundary of groundwater calcrete as 30°S; the occurrence at Line D is therefore the southernmost documented. Glassford (1987) assigns similar calcrete to the Yeelirrie Member of the Menzies Formation.

## Quaternary

A veneer of unconsolidated sediments of presumed Quaternary age occurs throughout the region. The sediments comprise colluvium, alluvium and playa lake deposits and are described in detail in Kriewaldt (1969). Glassford (1987) describes a similar suite of Tertiary and Quaternary sediments from Yeelirrie 400 km to the north, and has assigned formation names to them.

Most of the detrital deposits consist of colluvium in fans and on broad flood-washed plains. They consist of conglomerate, gravel, sand, and clay derived from the laterite profile and the underlying Archaean bedrock. The thickness of colluvial material is 24 m on Line C at the foot of Mount Burges (Kern et al., 1989), but elsewhere it is less than 10 m.

Alluvial deposits occur along the gently sloping and poorly defined drainage lines and are generally 3–6 m thick. The alluvium consists of sand, silt, and clay in the valley flats, with gravel near bedrock outcrops. The sand is generally poorly sorted and the quartz grains are more angular than in the Tertiary sediments, suggesting a nearby source. The sand is often extremely fine and silty.

Extensive playa lake systems, the largest of which is Lake Yindarlgooda, occur in the palaeodrainage. They contain saline and gypsiferous clay and silt, possibly up to 10 m thick. The margins of the playa lakes, particularly the southern and eastern sides, contain stabilized dune

**Table 1. Chemical analysis of calcrete from bore KRD-8**

Depth (m)	GSWA no.	CCWA no.	CaO%	MgO%	SiO <sub>2</sub> %
20.0	85978	399	31.0	21.0	<0.1
26.4	85979	400	28.5	20.3	3.78
32.8	85980	401	28.2	19.4	6.45

deposits of unconsolidated sand and gypsum. Gypsiferous sand, equivalent to the Miranda Member of the Darlot Formation (Glassford, 1987), was intersected in bores in Line K (Kern et al., 1989).

Where the base of the Quaternary deposits consists of reworked Eocene sediments it is often difficult to establish the contact between the Tertiary and Quaternary units, especially if they are clayey and ferruginized.

Limonite pebbles are common in the Quaternary deposits in the eastern part of the drainage and appear to be derived from older deposits. However, limonite nodules may also have formed in situ in the phreatic zone. Epigenic limestone nodules (kankar) are also common in the area (Kriewaldt, 1969).

## Geological history

The Roe Palaeodrainage and other similar systems were probably in existence in the Early Cretaceous, supplying terrigenous material to the Eucla Basin (Lowry, 1970; Jones, 1990). There was then a hiatus in deposition between the end of the Late Cretaceous and the Middle Eocene, when downwarping of the Eucla Basin recommenced and the complete separation of Australia and Antarctica occurred (McGowran, 1989; Middleton, 1990). The ensuing marine transgressions, and rise in the base level of drainages, resulted in the aggradation of the clastics of the Wollubar Sandstone in the late Middle Eocene and early Late Eocene. This was followed by the development of lacustrine conditions, and the deposition of the Perkolilli Shale in the early Late Eocene. This was coeval with the deposition of the Toolinna and Wilson Bluff Limestones in the Eucla Basin.

The maximum penetration of marine influences occurred during the early Late Eocene marine transgression when sea level approached the present elevation of 320 m AHD in the Kambalda area, south of Kalgoorlie. The sea also presumably drowned the lower part of the Roe Palaeodrainage, but the only evidence of marine sedimentation is 180 km east of Kalgoorlie where spongolite correlating with the Eundynie Group outcrops at an elevation of 300 m AHD on the northern side of Ponton Creek, 3 km south of Cundeelee Mission (Bunting and van de Graaff, 1977).

A period of low erosion rates characterized by soil formation, deep weathering, and lateritization followed the Late Eocene sedimentation. The main period of lateritization in the Kalgoorlie region is likely to have been completed by the Middle Miocene, as the Middle Miocene Colville Sandstone in the northern part of the Eucla Basin shows no sign of lateritization (Lowry, 1970). The

significant concentration of kaolinite in the Perkolilli Shale, possibly resulting from chemical weathering of aluminosilicate minerals, suggests that deep-weathering processes may have already started by the Late Eocene.

Post-Miocene uplift and tilting to the southeast in the Kalgoorlie region is demonstrated by the steady southeastward drop in elevation of the playa lakes which now occupy the palaeodrainages (Bunting et al., 1974). Van de Graaff et al. (1977) estimated a regional tilt to the south of about 1.5 minutes by correlating lake levels in the Eastern Goldfields. Because of the southward tilt, headward erosion from the south has cut back through the catchment divide between the Lefroy and Roe Palaeorivers in the Wollubar area, and diverted both surface drainage and groundwater flow (Commander et al., 1990) from the Wollubar and Hannan Palaeochannels into Lake Lefroy.

Deep weathering of the bedrock adjacent to the palaeochannels occurred after they were filled with Eocene sediments. The presence of saline groundwater could have accelerated the weathering process as the thickness of the weathered zone increases downstream where the salinity is highest.

Since the Miocene, the climate appears to have been largely arid to semi-arid with the river systems becoming inactive, although Early Pliocene sediments have been identified from the upper part of the Cowan Palaeodrainage (Bint, 1981). The salt-lake sediments and associated gypsiferous dunes are believed to have been deposited over cyclic arid and pluvial phases during the Pleistocene.

## Conclusion

The Late Eocene sedimentary rocks in the Roe Palaeodrainage represent a widespread and uniform sequence consisting of a basal fluvial sandstone overlain by a lacustrine shale. They are correlatives of the Plantagenet Group of the Bremer Basin and represent continental facies of formations in the Eucla Basin. The Tertiary sediments originally described from Rollos Bore are atypical, and this nomenclature is now superseded. The definition of the stratigraphy gives a framework for the further study of the auriferous Tertiary sedimentary rocks, and for the assessment and management of the region's groundwater resources.

## References

- BACKHOUSE, J., 1989, Palynology of samples from the Kalgoorlie regional groundwater assessment boreholes KRM-1, KRN-1 and KRN-3: Western Australia Geological Survey, Palaeontology Report 1989/1 (unpublished).
- BALME, B. E., and CHURCHILL, D. M., 1959, Tertiary sediments at Coolgardie, Western Australia: Royal Society of Western Australia, Journal, v. 42, p. 37–43.
- BEARD, J. S., 1972, The vegetation of the Kalgoorlie area, Western Australia: 1:250 000 map series, Vegmap Publications, Sydney.
- BINT, A. N., 1981, An Early Pliocene pollen assemblage from Lake Tay, south-western Australia, and its phytogeographic implications: Australian Journal of Botany, v. 29, p. 277–91.
- BLATCHFORD, T., 1898, So-called deep leads at Kanowna: Western Australia Geological Survey, Annual Report 1897, p. 51–52.
- BLATCHFORD, T., 1899, The geology of the Coolgardie Goldfield: Western Australia Geological Survey, Bulletin 3.
- BUNTING, J. A., and van de GRAAFF, W. J. E., 1977, Cundeelee, W.A.: Western Australia Geological Survey, 1:250 000 Geological Series Explanatory Notes.
- BUNTING, J. A., van de GRAAFF, W. J. E., and JACKSON, M. J., 1974, Palaeodrainages and Cainozoic palaeogeography of the Eastern Goldfields, Gibson Desert and Great Victoria Desert: Western Australia Geological Survey, Annual Report 1973, p. 45–50.
- CLARKE, E. de C., TEICHERT, C., and McWHAE, J. R. H., 1948, Tertiary deposits near Norseman, Western Australia: Royal Society of Western Australia, Journal, v. 32, p. 85–103.
- COCKBAIN, A. E., 1968a, Eocene foraminifera from the Norseman Limestone of Lake Cowan, Western Australia: Western Australia Geological Survey, Annual Report 1967, p. 59–60.
- COCKBAIN, A. E., 1968b, The stratigraphy of the Plantagenet Group, Western Australia: Western Australia Geological Survey, Annual Report 1967, p. 61–63.
- COCKBAIN, A. E., and HOCKING, R. M., 1989, Revised stratigraphic nomenclature in Western Australian Phanerozoic basins: Western Australia Geological Survey, Record 1989/15.
- COMMANDER, D. P., KERN, A. M., and SMITH, R. A., 1991, Hydrogeology of the Tertiary palaeochannels in the Kalgoorlie Region: Western Australia Geological Survey, Record 1991/10.
- GLASSFORD, D. K., 1987, Cainozoic stratigraphy of the Yeelirrie area, northeastern Yilgarn Block, Western Australia: Royal Society of Western Australia, Journal, v. 70, p. 1–24.
- GRIFFIN, T. J., 1989, Widgiemooltha, W.A. (second edition): Western Australia Geological Survey, 1:250 000 Geological Series Explanatory Notes.
- GRIFFIN, T. J., 1990, Eastern Goldfields Province, in Geology and mineral resources of Western Australia: Western Australia Geological Survey, Memoir 3, p. 77–119.
- HOS, D., 1975, Preliminary investigation of the palynology of the Upper Eocene Werillup Formation, Western Australia: Royal Society of Western Australia, Journal, v. 58, p. 1–14.
- JONES, B. G., 1990, Cretaceous and Tertiary sedimentation on the western margin of the Eucla Basin: Australian Journal of Earth Sciences, v. 37, p. 317–329.
- KERN, A. M., SMITH, R. A., and COMMANDER, D. P., 1989, Kalgoorlie regional groundwater assessment bore completion reports. Western Australia Geological Survey, Hydrogeology Report 1989/17 (unpublished).
- KRIEWALDT, M. J. B., 1969, Quaternary geology, Kalgoorlie, Western Australia: University of Western Australia, Ph.D. thesis (unpublished).
- LOWRY, D. C., 1970, The geology of the Western Australian part of the Eucla Basin: Western Australia Geological Survey, Bulletin 122.
- McGOWRAN, B., 1989, The late Eocene transgression in southern Australia: Alcheringa, v. 13, p. 45–68.
- MAITLAND, A. G., 1901, Coolgardie deep leads: Western Australia Geological Survey, Annual Report 1900, p. 22.
- MANN, A. W., and HORWITZ, R. C., 1979, Groundwater calcrete deposits in Australia: some observations from Western Australia: Geological Society of Australia, Journal, v. 26, p. 293–303.
- MIDDLETON, M. F., 1990, Tectonic history of the southern continental margin of Western Australia: Western Australia Geological Survey, Record 1990/8.

- PLAYFORD, P. E., COPE, R. N., COCKBAIN, A. E., LOW, G. H., and LOWRY, D. C., 1975, Phanerozoic, *in* Geology of Western Australia: Western Australia Geological Survey, Memoir 2, p. 223–432.
- SMYTH, E. L., and BUTTON, A., 1989, Gold exploration in the Tertiary palaeodrainage systems of Western Australia: Gold Forum on Technology and Practices — World Gold '89, Reno, Nevada, Nov. 1989.
- STOVER, L. E., and PARTRIDGE, A. D., 1982, Eocene spore-pollen from the Werillup Formation, Western Australia: *Palynology*, v. 6, p. 69–95.
- URQUHART, D. F., 1956, The investigation of deep leads by the seismic refraction method: Australia BMR Bulletin 35.
- van de GRAAFF, W. J. E., 1983, Silcrete in Western Australia: geomorphological settings, textures, structures, and their genetic implications, *in* Residual deposits — surface related weathering processes and materials *edited by* R. C. L. WILSON: Oxford, Blackwell Scientific Publications (for the Geological Society of London), p. 159–166.
- van de GRAAFF, W. J. E., CROWE, R. W. A., BUNTING, J. A., and JACKSON, M. J., 1977, Relict early Cainozoic drainages in arid Western Australia: *Zeitschrift für Geomorphologie N.F.*, v. 21, p. 379–400.



# Municipal waste disposal in Perth and its impact on groundwater quality

by

K-J. B. Hirschberg

## Abstract

There are 99 known abandoned or operating municipal landfill sites in Perth. In order to assess their impact on the groundwater, the Geological Survey of Western Australia investigated groundwater quality near 50 of these sites. Several hundred field tests for ammonia expressed as nitrogen ( $\text{NH}_4\text{-N}$ ) were carried out on private garden reticulation bores and monitoring bores near the selected landfill sites, and about 40 water samples were taken for detailed analysis. Elevated  $\text{NH}_4\text{-N}$  values were found near many of the sites. Concentrations of heavy metals were, however, very low or below detection level. Results from pesticide analyses by the Chemistry Centre (W.A.) for the Health Department in 1991 indicate that the concentration of these substances in monitoring bores is several orders of magnitude lower than the maximum permissible levels. From a human health risk perspective, it appears that Perth's landfill sites have generally performed well, although many of the sites are in hydrogeologically unfavourable locations. The major ammonia plumes delineated coincide with former liquid-waste disposal areas. It is concluded that there is apparently minimal threat to human health from groundwater contamination by landfill leachate. However, the potential impact on the environment through increased nutrient input cannot be disregarded. Continued groundwater-quality monitoring is recommended

**KEYWORDS:** Groundwater, contamination, waste disposal, Perth Basin.

## Introduction

The volume of domestic waste created in Perth has increased considerably over the past few decades. This has resulted from rapid population expansion, increase in garden waste due to restrictions on burning, and changes in product packaging combined with less recycling in a more affluent society. The traditional waste-disposal method has been by landfill, and local government authorities have had the responsibility for collection and disposal of municipal waste. As a result a large number of landfill sites are distributed over the metropolitan region.

Many of the now-abandoned waste-disposal sites were merely dumps; new sites have been planned, and are managed in a more environmentally acceptable way. Nevertheless, the potentially adverse impact of municipal waste disposal on human health and the environment in general through groundwater contamination has become the subject of mounting public concern.

More than 50% of Perth's total water supply is met from shallow groundwater resources. The main public water-supply borefields draw from the Gngangara Mound in the north, and the Jandakot Mound in the south. The maintenance of groundwater quality in these areas is achieved by strict controls over development, and by prohibiting certain activities (such as waste disposal). There are also more than 80 000 private and municipal bores in the metropolitan region. The water from most of these is used for reticulation of private gardens and

public open space, and for industrial purposes. Only very few are used for private domestic consumption.

Following a request by the State Government Senior Officers Committee on Waste Management in 1990, the Geological Survey of Western Australia (GSWA) undertook to assess the risk to human health from groundwater contamination associated with landfills, by investigating a number of operating and abandoned landfill sites in the Perth Metropolitan Region.

## History of landfill site selection

Prior to about 1970, the selection of landfill sites was largely governed by the availability of cheap land within the respective local authority boundaries. Transport distances had to be short to keep costs down, and because the collection and transport of rubbish was initially by horse and cart. Wetlands, consisting of lakes, swamps, and river foreshores, were deemed useless land and were considered to present a health hazard by providing breeding grounds for mosquitoes. Consequently, many of Perth's old landfill sites are found in, or near, such wetlands (Fig. 1) and the dumping was called 'land improvement'. Co-disposal of solid waste with liquid waste, such as night soil, was also common practice. Other targets for waste disposal were abandoned limestone quarries and sand and clay pits. No consideration was given to any potential impact on the environment, including groundwater. Waste disposal into wetlands was

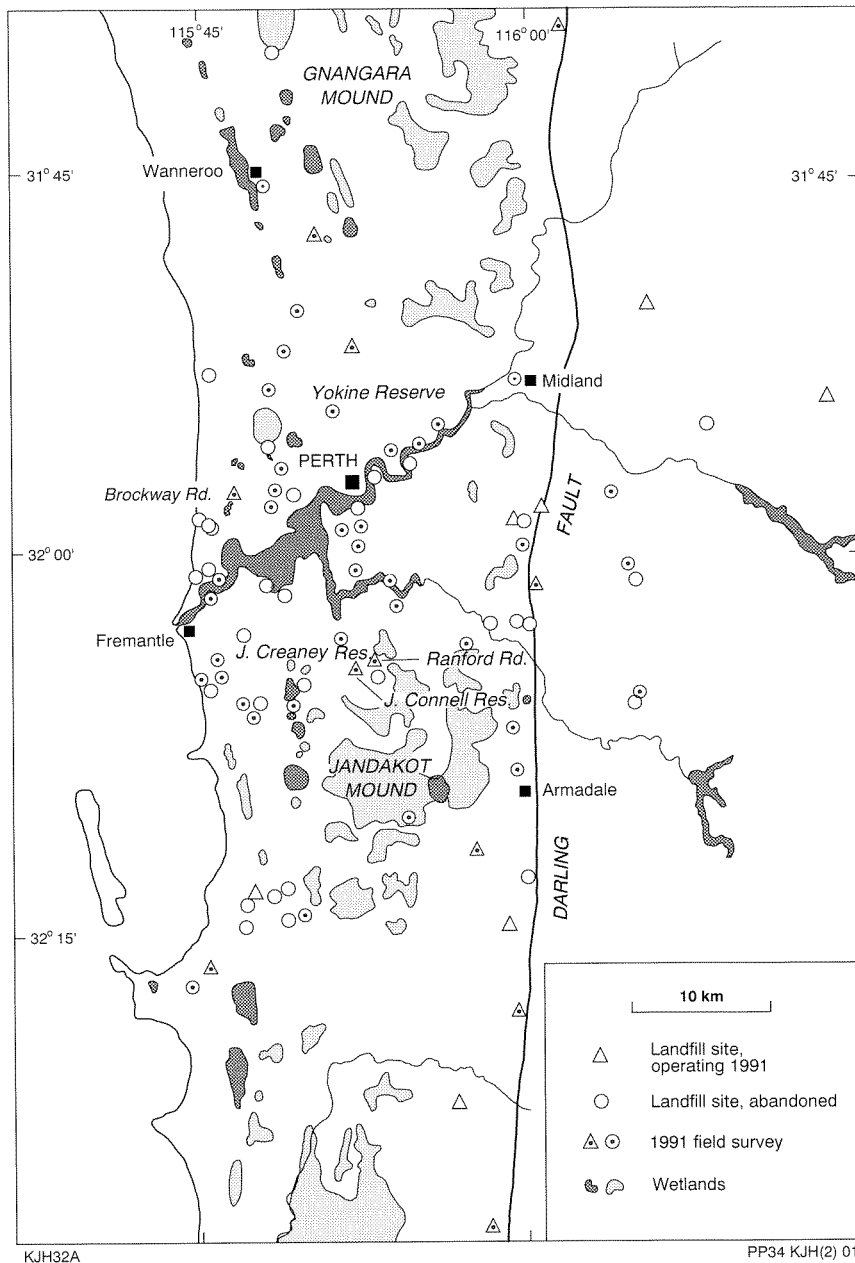


**Figure 1. Location plan, landfill sites and wetlands**

still practised in the early 1980s at Lake Pinjar and Hertha Road.

The change of waste disposal and management from poorly controlled dumping to sanitary landfill, incorporating compaction and regular cover of the waste, was completed by about 1962. Site selection and site management have also improved considerably since about 1970. The growing awareness of the potentially deleterious effects of waste disposal on the environment resulted in the exclusion of certain types of waste and, eventually, in the installation of groundwater monitoring bores at all operating sites.

Rapidly increasing amounts of waste required the establishment of more and more disposal sites by local authorities. This dispersal of waste over numerous sites, however, was considered undesirable by the Health Department of Western Australia, which instigated the formation of waste-disposal zones and, eventually, of regional councils consisting of several local government authorities. The aim was to create a small number of large, well-managed landfill sites, preferably centrally located within the regional council boundaries. The criteria for acceptance of existing sites, formulated by the Health Department and to be issued in a revised form in the near future, will result in some site closures. Concurrently,

the establishment of regional landfill facilities within the area of each regional council will be accelerated.

## Type of waste

The early tips received any waste, both domestic and industrial, created within their intake area. The material is presumed to have consisted of putrescent domestic waste, tree loppings, lawn clippings, paints and thinners, acids and alkalis, car bodies, tyres and batteries, and in later years pesticides and their containers. Over the last few decades, the amount of plastic waste has increased dramatically, as has the number of car bodies and tyres. The disposal of toxic waste such as pesticides and some industrial wastes is no longer permitted; thus leachate from a modern landfill site is potentially less harmful than that from an old disposal site. Some intractable materials, however, are still being disposed of at the present landfill sites. Among these are small amounts of PCBs contained in old fluorescent light fittings, and large numbers of batteries containing lead, cadmium, mercury, and other toxic heavy metals.

## Hydrogeology

Most of the Perth Metropolitan Region lies on the Swan Coastal Plain, which is underlain by a sequence of mainly permeable sediments. From west to east, they consist of the Safety Bay Sand; the Tamala Limestone and its leached sandy facies; the Bassendean Sand; and the Guildford Formation (Fig. 2). These formations are mainly sands or sandy limestone, and only the Guildford Formation consists mostly of clay. Collectively, these sediments are known as the 'superficial formations' (Allen, 1975). They range from 20 to 40 m in thickness and contain unconfined groundwater, with a watertable generally at shallow depth.

The sandy nature of the sediments, in conjunction with the shallow watertable, makes the unconfined aquifer particularly vulnerable to contamination.

## Procedures of investigation

### Site selection

Ninety-nine landfill sites had previously been identified in the metropolitan area (Hirschberg, 1988). In order to reduce this number to a more manageable group for investigation, the following sites were excluded:

1. those which were closed more than about 30 years ago;
2. some operating sites, because they were already the subject of detailed studies (e.g. Yirrigan and Red Hill sites);
3. most of the small landfill sites near the outer margin of the metropolitan region (e.g. Yancheper, Wooroloo, and Wundowie sites).

A representative cross section of 50 sites was selected on the basis of regional distribution, hydrogeological setting, and size of landfill. These are listed in Table 1.

## Methods of study

After a study of bore records held by the GSWA, a detailed bore census was carried out around each site. Water samples from all private reticulation and monitoring bores within a radius of about 500 m were tested in the field for ammonia expressed as nitrogen ( $\text{NH}_4\text{-N}$ ). This parameter is commonly used as a pollution indicator at landfill sites, with values of  $\text{NH}_4\text{-N}$  above 0.5 mg/L generally considered to indicate human influence. The ammonia is generated during the anaerobic decomposition of organic matter such as putrescent household waste, lawn clippings, and tree prunings. It is also a major breakdown product of septic waste.

The field test is based on an ion-specific test solution (Aquamerck) which, after appropriate reaction time with the sample, is analysed colorimetrically. The readings obtained with the field test kits were not considered to be quantitatively accurate. However, they were found to be generally in good agreement with the chemical analyses.

Whenever positive field readings were obtained, the area of the census was widened until zero values were obtained. Where possible, concentrations of  $\text{NH}_4\text{-N}$  were contoured; however, at many sites there were insufficient bores and data points to achieve this.

Samples for chemical analysis were taken from a number of bores, generally where field  $\text{NH}_4\text{-N}$  readings had been 10 mg/L or higher. Analyses for pesticides and other potentially harmful organic compounds were not carried out; however, the results of previous analyses for these substances were reviewed and taken into consideration.

## Results of investigation

### Field $\text{NH}_4\text{-N}$ readings

Table 1 lists the numbers, in each of the selected sensitivity brackets, of both field tests and samples taken for analysis by the Chemistry Centre of W.A. (CCWA).

The bore census failed to locate any bores near nine of the 50 sites; at a further eleven sites, only one or two bores were found, and limited field testing and sampling was carried out. Most of the 276 field tests, however, were undertaken on private or monitoring bores close to the remaining 30 sites.

Thirty-four samples from 16 sites were submitted for chemical analysis, the results of which are presented in Table 2. Full analyses (including heavy metals) were carried out on 17 of the samples, while analyses of fewer parameters were made on the remainder.

Only five sites had a sufficient number of data points in the various sensitivity ranges to allow contouring of

**Table 1. Details of field investigations**

Local authority	Landfill site	Lithology (a) (Formation)		Number of field NH <sub>4</sub> -N tests						No. of CCWA analysis
				Total	<0.5	0.5–3	3–5	5–10	>10	
				mg/L						
Armadale	Hopkinson Rd, Armadale	Cl	(GF)	2	1	-	1	-	-	4
	Springdale Rd, Karragullen	Cl	(Gr)	3	2	1	-	-	-	-
	Third Avenue, Kelmscott	Cl	(GF)	7	4	2	-	-	1	-
	Nicholson Rd, Jandakot	Sd	(DS)	(b)	-	-	-	-	-	-
Bassendean	Ashfield Res., Ashfield	Cl–Sd	(BS)	7	4	2	-	1	-	1
Bayswater	Slade Street, Bayswater	Cl	(Al)	2	2	-	-	-	-	-
Canning	Centenary Ave, Wilson	Sd	(BS)	12	8	4	-	-	-	-
	Adenia Res., Willetton	Sd	(BS)	8	4	4	-	-	-	-
	Ranford Rd, Willetton	Sd	(BS)	27	7	11	1	1	7	2
Cockburn	Howson Way, Bibra Lake	L/s	(TL)	1	1	-	-	-	-	-
	Dixon Res., Hamilton Hill	L/s	(TL)	2	2	-	-	-	-	-
	Dubove Pk, Spearwood	L/s	(TL)	2	2	-	-	-	-	-
	Bibra Lake, Bibra Lake	L/s	(TL)	2	2	-	-	-	-	-
East Fremantle	Preston Point, East Fremantle	L/s	(TL)	6	6	-	-	-	-	-
Fremantle	Daly St, South Fremantle	L/s	(TL)	5	2	-	-	-	-	-
	Mather Rd, Beaconsfield	L/s	(TL)	2	2	-	-	-	-	-
Gosnells	Walter Padbury Pk, Thornlie	Cl	(GF)	9	6	1	1	1	-	1
	Bickley Rd, Orange Grove	Cl	(GF)	4	4	-	-	-	-	-
	Carole/Church Rds, Maddington	Cl	(GF)	1	1	-	-	-	-	-
	Kelvin Road, Orange Grove	Cl	(LF)	11	9	2	-	-	-	2
Kalamunda	Hartfield Pk, Forrestfield	Cl	(GF)	3	3	-	-	-	-	-
	Lawnbrook Road, Bickley	Cl	(GF)	(b)	-	-	-	-	-	-
	Ledger Rd, Gooseberry Hill	Cl	(Gr)	(b)	-	-	-	-	-	-
	Kent Rd, Maida Vale	Cl	(GF)	(b)	-	-	-	-	-	-
Kwinana	Durrant Ave, Kwinana	L/s	(TL)	1	-	1	-	-	-	-
Melville	John Connell Res., Leeming	Sd	(BS)	30	6	5	2	2	15	2
	John Creaney Res., Bull Creek	Sd	(BS)	19	9	3	2	2	3	2
Mosman Park	Fairbairn St, Mosman Park	L/s	(TL)	2	2	-	-	-	-	-
Nedlands	Brockway Rd, Mt Claremont	L/s	(TL)	29	6	3	11	2	7	7
Rockingham	Ennis Ave, Rockingham	L/s	(TL)	4	-	1	-	1	2	2
	Old Golf Course, Rockingham	L/s	(TL)	6	6	-	-	-	-	1
Serpentine–Jarrahdale	Elliot Rd, Keysbrook	Cl	(GF)	3	1	2	-	-	-	-
	Karnup Rd, Serpentine	Cl	(GF)	(b)	-	-	-	-	-	-
	Cardup Siding Rd, Cardup	Cl	(GF)	(b)	-	-	-	-	-	-
South Perth	Morris Mundy Oval, Kensington	Sd	(BS)	2	2	-	-	-	-	-
	Ernest Johnson Oval, South Perth	L/s	(TL)	4	4	-	-	-	-	-
	Manning Rd, Manning	Sd	(BS)	13	5	3	3	2	-	3
	Thelma St, Como	Sd	(BS)	4	2	-	1	-	1	2
Stirling	Gibney Res., Maylands	Cl	(BS–GF)	3	3	-	-	-	-	-
	Delawney St, Balcatta	L/s	(TL)	5	2	3	-	-	-	-
	Hertha Rd, Osborne Park	L/s	(TL)	5	3	-	-	-	2	1
	Yokine Res., Coolbinia	L/s	(TL)	11	2	4	-	-	-	-
Subiaco	Shenton Pk Lake, Shenton Park	L/s	(TL)	(b)	-	-	-	-	-	-
	Mabel Talbot Pk, Jolimont	L/s	(TL)	(b)	-	-	-	-	-	-
	Rosalie Park, Subiaco	L/s	(TL)	(b)	-	-	-	-	-	-
Swan	Blackadder Creek, Midland	Cl	(GF)	4	4	-	-	-	-	-
	Morrison Rd, Bullsbrook	Cl	(Col)	5	1	4	-	-	-	1

Table 1. (continued)

Local authority	Landfill site	Lithology (a) (Formation)	Number of field NH <sub>4</sub> -N tests					No. of CCWA analysis	
			Total	<0.5	0.5-3	3-5	5-10		>10
Wanneroo	Badgerup Rd, Wangara	L/s (TL)	3	1	2	-	-	-	-
	Hudson Res., Girrawheen	L/s (TL)	3	3	-	-	-	-	-
	Ariti Ave, Wanneroo	L/s (TL)	4	3	1	-	-	-	-
<b>Total:</b>			<b>276</b>	<b>137</b>	<b>60</b>	<b>23</b>	<b>12</b>	<b>44</b>	<b>34</b>

Note: (a) L/s = limestone/resid. sand  
Sd = sand  
Cl = clay

(TL) = Tamala Limestone  
(GF) = Guildford Formation  
(Al) = alluvium

(BS) = Bassendean Sand  
(Gr) = weathered granite  
(Col) = colluvium

concentrations. The Ranford Road (Fig. 3) and John Connell Reserve (Fig. 4) sites are large operating landfills, while the Brockway Road site (Fig. 5) at Mount Claremont, a large regional landfill, was closed in early 1992. John Creaney Reserve (Fig. 6) and Yokine Reserve (Fig. 7) sites closed in the 1970s.

All five sites have extensive plumes of NH<sub>4</sub>-N extending downgradient in the direction of the regional groundwater flow. The plume length generally ranges from 500 to 1500 m, and the width from 400 to 700 m; the Brockway Road plume is the largest found during the investigation, with a length of about 2000 m, and a width of about 1000 m.

### Chemical analyses

All groundwaters sampled are sodium-chloride waters, usually with a near-neutral pH, a highly variable hardness depending on the hydrogeological environment, and a salinity (Table 2) ranging from 200 to 1000 mg/L total dissolved solids (TDS).

Ammonia-N analyses (Table 3) confirmed that the field tests yield semi-quantitative results useful for an initial screening of an area. The major cause of variability appears to have been due to a differing test-strip interpretation by individual field staff.

The chemical analyses confirmed the existence of the extensive plumes of NH<sub>4</sub>-N, with maxima in the plume centres up to 100 mg/L and averages of between 20 and 40 mg/L. These concentrations greatly exceed the level of 0.5 mg/L, commonly used as a contamination indicator. However, the risk to human health from the ingestion of ammonia is generally considered to be small. Nitrate levels are well below the maximum permissible level of 10 mg/L nitrate-N, apart from one sample from the Kelvin Road tip. The chemical analyses suggest that denitrification may not play a major role at depth in the aquifer, and that the reducing conditions allow the ammonia to persist in high concentrations up to several hundred metres from the source.

The analyses of heavy metals were expected to yield levels of at least noticeable concentrations. However, nearly all of those analysed (Cd, Pb, Cu, Cr, Ni, and Zn) produced values below the respective maximum permissible levels, and 57% of all heavy metal analyses were below detection level. The exceptions were one value for cadmium (Manning Road) of 0.035 mg/L, which exceeded the maximum limit of 0.01 mg/L; and one value for zinc (Ashfield Reserve) of 32 mg/L, more than twice the current desirable level of 15 mg/L. The latter high level was probably due to industrial activities some distance upgradient. Manganese concentrations were also high in several samples; however, as with high iron values, these are quite common in Perth groundwater and are considered more a nuisance than a health or environmental risk.

### Pesticides

Owing to the specialized sampling required and the high cost of analysis, the samples were not analysed for residual pesticides or other artificial organic compounds. In an earlier study of the Hertha Road landfill site (Bestow, 1977), water samples were analysed for HCB, DDT, dieldrin, and organophosphorus pesticides. It was found that the concentrations for these pesticides were all several orders of magnitude lower than the maximum permissible levels.

In 1991, the Health Department sampled all landfill monitoring bores for organochlorine and organophosphorus pesticides, total aliphatic and aromatic hydrocarbons, polyaromatic hydrocarbons, and PCBs and atrazine. The analyses were carried out by the CCWA. Several samples showed values above detection level for aromatic and polyaromatic hydrocarbons and organochlorines, and one sample had a higher than desirable PCB concentration. All these samples were from bores within the landfill sites. Pesticide levels and other organic constituents are consequently expected to be very much lower at short distances from the landfill. The CCWA concluded in its comments on the chemical analyses that 'widespread pollution of groundwater is not indicated', although continued monitoring was advisable.

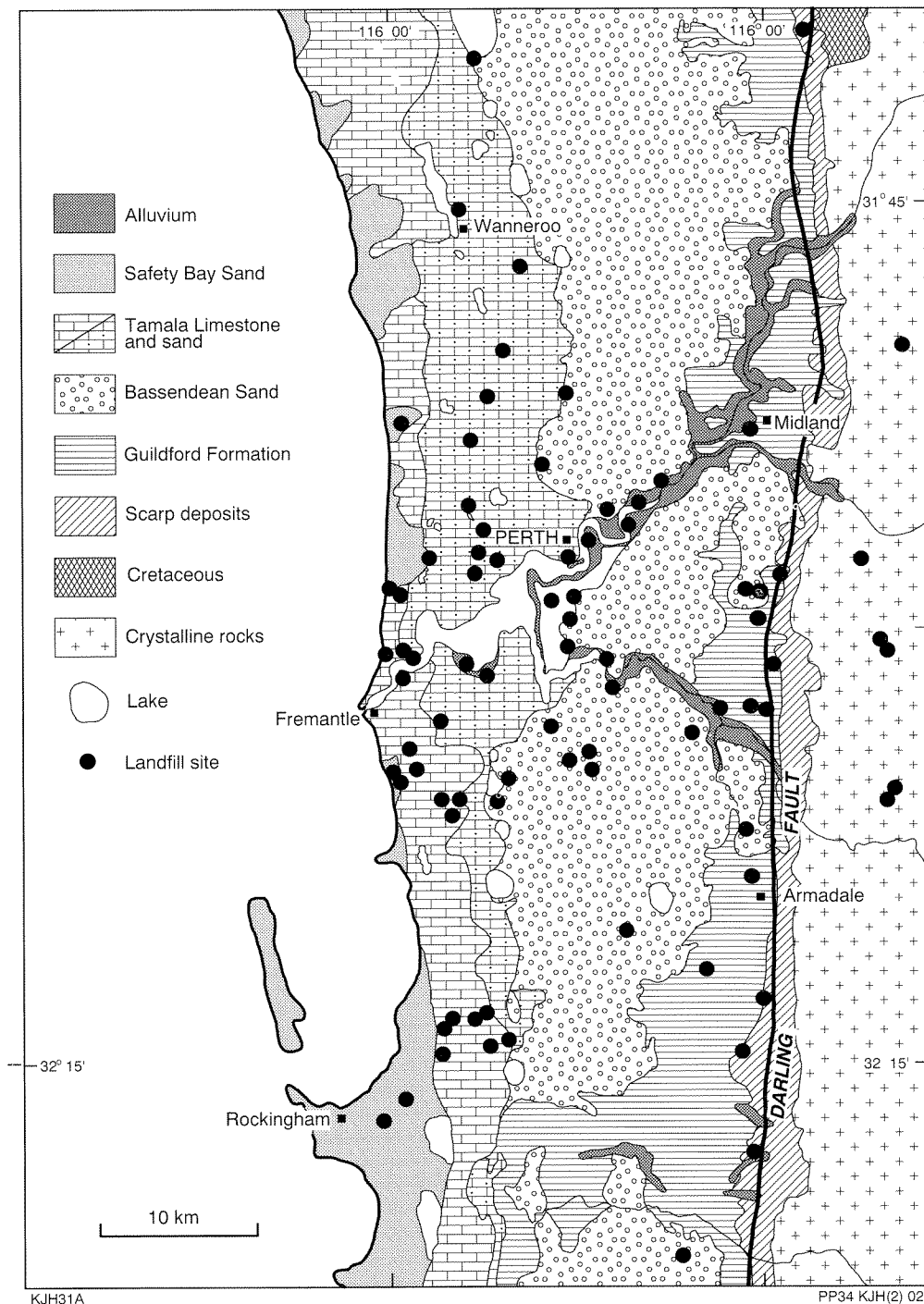


Figure 2. Generalized geology

## Other potential sources of ammonia

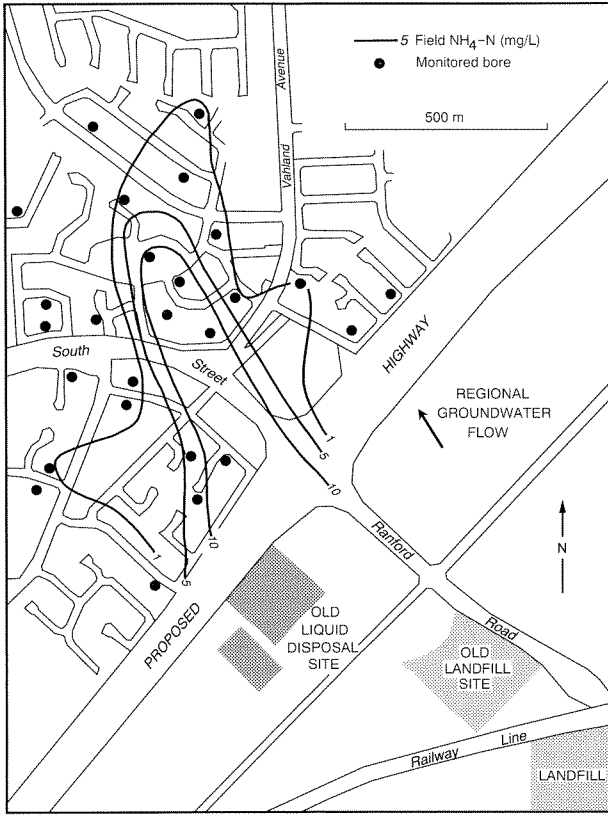
### Septic systems

Large parts of Perth are not deep-sewered (Fig. 8), and the potential  $\text{NH}_4\text{-N}$  input from septic tanks can be considerable (Whelan et al., 1981; Appleyard and Bawden, 1986; Appleyard, 1992). However, this input is generally diffuse and concentrations cannot therefore easily be contoured. The input of nutrients from septic systems is at present not quantifiable, and may not be significant

when compared with concentrations in pollution plumes from landfill sites.

### Fertilizer application

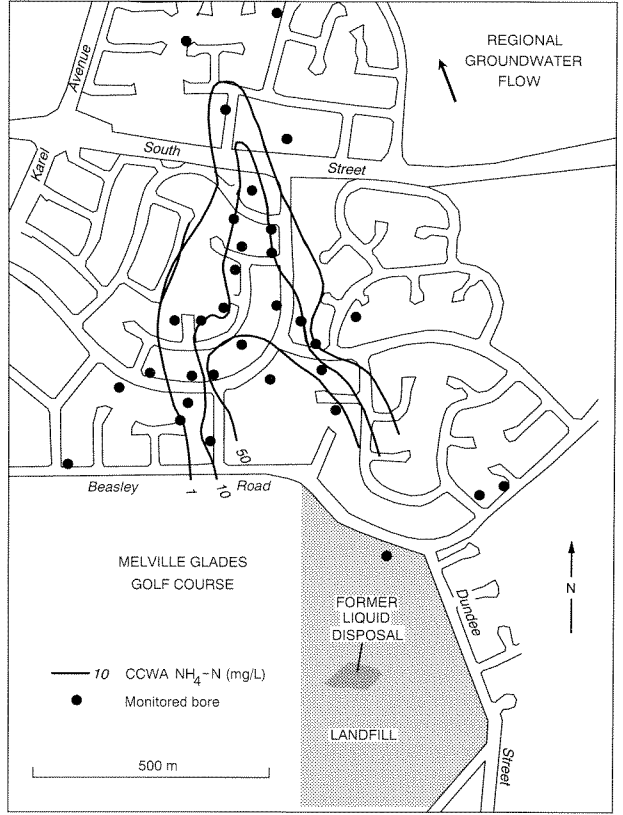
Large amounts of fertilizers are applied annually to Perth's gardens, parks, ovals, and golf courses. Most of this fertilizer is in the form of superphosphate, which contains about 50% ammonium sulfate. Many of the abandoned landfill sites have been converted to sportsgrounds, with consequent high fertilizer use.



KJH27A

PP34 KJH(2) 03

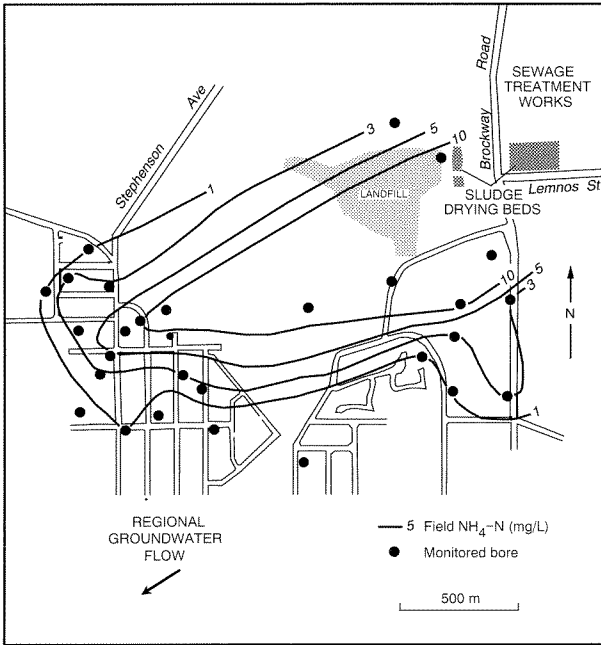
Figure 3. Ranford Road disposal site



KJH26A

PP34 KJH(2) 04

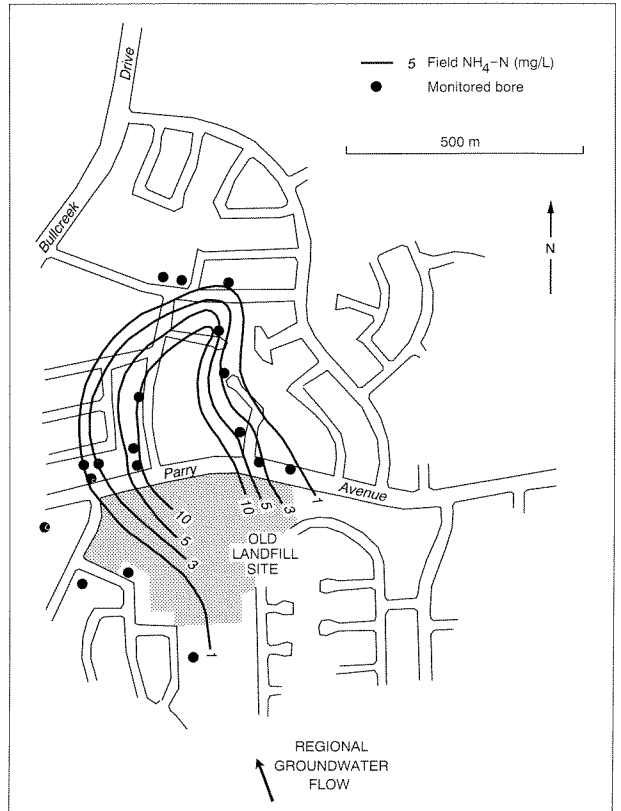
Figure 4. John Connell Reserve disposal site



KJH29A

PP34 KJH(2) 05

Figure 5. Brockway Road disposal site



KJH28A

PP34 KJH(2) 06

Figure 6. John Creaney Reserve disposal site

**Table 2. Results of chemical analyses**

<i>Local authority GSWA no.</i>	<i>Site Sample locality</i>	<i>pH</i>	<i>Colour (TCU)</i>	<i>Conductivity (mS/m at 25°C)</i>	<i>Total dissolved solids (calc. at 180°C)</i>	<i>Total hardness (as CaCO<sub>3</sub>)</i>	<i>Total alkalinity (as CaCO<sub>3</sub>)</i>	<i>Ca</i>	<i>Mg</i>	<i>Na</i>	<i>K</i>	<i>HCO<sub>3</sub></i>	<i>Cl</i>	<i>SO<sub>4</sub></i>	<i>NO<sub>3</sub></i>	<i>SiO<sub>2</sub></i>	<i>Cd</i>	<i>Pb</i>	<i>Mn</i>	<i>Cu</i>	<i>Cr</i>	<i>NO<sub>3</sub>-N</i>	<i>NH<sub>4</sub>-N</i>	<i>Ni</i>	<i>Zn</i>
<b>Armadale</b>	<b>Hopkinson Rd</b>																								
111229(a)	MPB red 10 m	5.4	-	603	-	-	-	-	-	-	5	-	-	-	-	-	-	-	-	-	-	0.05	0.88	-	-
111230(a)	MPB yellow 15 m	5.9	-	173	-	-	-	-	-	-	5	-	-	-	-	-	-	-	-	-	<0.02	0.06	-	-	-
111231(a)	MPB green 21 m	5.9	-	190	-	-	-	-	-	-	5	-	-	-	-	-	-	-	-	-	<0.02	0.23	-	-	-
111232(a)	MPB blue 26 m	5.9	-	194	-	-	-	-	-	-	5	-	-	-	-	-	-	-	-	-	<0.02	0.59	-	-	-
<b>Bassendean</b>	<b>Ashfield Res.</b>																								
103064	45 Haig Street	4.0	120	185	1380	580	<2	112	73	178	15	<2	167	817	<1	16	0.004	0.02	2.3	0.02	0.02	<0.02	2.7	0.08	3
<b>Canning</b>	<b>Ranford Rd</b>																								
103059	37 Trident Tee	5.6	55	39.4	200	26	16	4	4	48	5	20	65	55	<1	7	<0.001	0.01	-	0.04	<0.02	0.02	9.3	-	<0.0
103060	27 Merrifield Circ.	6.8	120	65.9	380	220	79	74	11	33	8	96	54	159	<1	1	<0.001	0.02	-	0.05	<0.02	0.03	8.5	-	<0.0
<b>Fremantle</b>	<b>Daly St</b>																								
111217	33 Douro Street	7.2	-	140	770	-	-	-	-	-	<1	-	-	-	-	-	<0.001	<0.01	-	0.05	0.05	0.20	13	-	<0.0
<b>Gosnells</b>	<b>Walter Padbury Pk</b>																								
103067	30 Rushbrook Way	7.9	-	131	-	-	266	57	30	182	12	-	-	-	-	-	<0.001	0.02	0.24	0.05	<0.02	0.09	9.3	<0.05	0.0
<b>Gosnells</b>	<b>Kelvin Rd</b>																								
103065	Lot 331 Kelvin Rd	7.9	20	59.9	310	110	95	8	22	80	2	116	117	19	<1	7	<0.001	<0.01	0.16	<0.02	<0.02	0.04	0.06	<0.05	0.0
103066	Lot 249 Victoria Rd	6.7	-	46.2	-	69	-	3	15	61	2	-	-	-	-	-	<0.001	<0.01	<0.02	0.02	<0.02	11	0.07	<0.05	0.0
<b>Melville</b>	<b>John Connell Res.</b>																								
103061	41 Gracechurch Cr	7.1	180	205	920	281	689	65	29	128	70	840	201	9	<1	1	<0.001	0.02	-	0.04	0.02	<0.02	97	-	<0.0
103062	73 Gracechurch Cr.	5.9	60	66.9	350	101	39	11	18	84	8	47	142	41	16	6	<0.001	0.02	-	0.05	<0.02	3.5	5.1	-	0.0
<b>Melville</b>	<b>John Creaney Res.</b>																								
111218	91 Perry Ave	6.7	-	78.2	430	-	-	-	-	-	34	-	-	-	-	-	<0.001	<0.01	-	<0.02	<0.02	0.02	15	-	0.0
111221	1 Litic Way	6.5	-	84.5	460	-	-	-	-	-	21	-	-	-	-	-	<0.001	<0.01	-	<0.02	<0.02	<0.02	22	-	<0.0
<b>Nedlands</b>	<b>Brockway Rd</b>																								
111222	100 Rochedale Rd	7.6	15	156	880	451	457	138	26	159	17	557	231	12	<1	22	-	-	-	-	-	0.04	3.6	-	-
111223	John XXIII College	7.7	15	156	720	320	361	92	22	116	27	440	154	51	29	11	<0.001	<0.01	-	0.02	0.02	0.26	27	-	<0.0
111224	Tip gatehouse	7.6	20	159	650	251	361	71	18	91	25	440	151	46	11	18	0.001	0.02	-	0.41	<0.02	0.07	34	-	-
111225	7 Whitney Cres.	7.5	10	115	660	352	344	113	17	101	12	420	161	26	<1	15	-	-	-	-	-	0.02	2.4	-	-

Table 2. (continued)

Local authority GWSA no.	Site Sample locality	pH	Colour (TCU)	Conductivity (mS/m at 25°C)	Total dissolved solids (calc. at 180°C)	Total hardness (as CaCO <sub>3</sub> )	Total alkalinity (as CaCO <sub>3</sub> )	Ca	Mg	Na	K	HCO <sub>3</sub>	Cl	SO <sub>4</sub>	NO <sub>3</sub>	SiO <sub>2</sub>	Cd	Pb	Mn	Cu	Cr	NO <sub>3</sub> -N	NH <sub>4</sub> -N	Ni	Zn	
<b>Nedlands (cont.)</b>																										
111226	Adderley St	7.8	5	93.9	520	246	221	74	15	89	12	270	130	52	<1	15	<0.001	<0.01	-	0.02	<0.02	0.09	4.9	-	0.0	
111227	Hamilton Lane	7.8	10	175	880	358	362	99	27	173	28	442	243	54	18	16	<0.001	0.01	-	0.02	<0.02	4.0	34	-	0.0	
111228	101 Rochedale Rd	7.8	5	140	760	354	330	109	20	144	15	403	220	29	2	18	<0.001	0.01	-	0.02	<0.02	0.42	2.2	-	0.0	
<b>Rockingham Ennis Ave</b>																										
103068(a)	MPB red 10 m	7.6	-	194	-	-	-	-	-	-	49	-	-	-	-	-	0.004	<0.01	<0.02	<0.02	<0.02	0.05	29	<0.05	<0.0	
103069(a)	MPB blue 27 m	8.4	-	87.9	-	-	-	-	-	-	16	-	-	-	-	-	0.004	<0.01	<0.02	0.03	<0.02	0.26	9.6	<0.05	0.0	
<b>Rockingham Old Golf Course</b>																										
103070	Wallaroo Rugby Club	8.1	-	62.4	-	-	-	-	-	-	2	-	-	-	-	-	0.001	<0.01	<0.02	<0.02	<0.02	1.6	0.76	<0.05	0.0	
<b>South Perth Manning Rd</b>																										
111236(a)	MPB black 5 m	8.3	-	99.8	-	-	-	-	-	-	61	-	-	-	-	-	0.035	0.02	0.04	0.06	<0.02	<0.02	3.1	<0.05	0.2	
111237(a)	MPB green 16.5 m	6.0	-	28.3	-	-	-	-	-	-	2	-	-	-	-	-	0.003	0.01	<0.02	0.04	<0.02	0.11	0.13	<0.05	0.0	
111240	Trinity Playing Fld	6.6	-	65.2	-	-	-	-	-	-	34	-	-	-	-	-	<0.001	<0.01	0.02	<0.02	<0.02	<0.02	4.7	<0.05	0.1	
<b>South Perth Thelma St</b>																										
111238(a)	MPB black 6.3 m	7.7	-	270	-	-	-	-	-	-	14	-	-	-	-	-	0.001	<0.01	0.41	<0.02	<0.02	0.02	69	<0.05	0.0	
111239(a)	MPB blue 35.9 m	4.8	-	20.6	-	-	-	-	-	-	0	-	-	-	-	-	0.004	<0.01	<0.02	<0.02	<0.02	0.35	0.28	<0.05	0.0	
<b>Stirling Hertha Rd</b>																										
111233	Lot 7 Hertha Rd	7.6	30	152	810	458	200	134	30	100	32	244	160	195	10	24	<0.001	<0.01	0.10	<0.02	0.02	<0.02	22	<0.05	0.0	
<b>Stirling Yokine Res.</b>																										
111234	Sir D. Brand Sch.	5.2	80	77.4	300	63	10	7	11	72	18	12	129	44	1	10	<0.001	<0.01	<0.02	0.02	<0.02	<0.02	22	<0.05	0.0	
111235	Coolbinia Prim. Sch.	7.5	15	71.8	380	138	60	19	22	77	8	73	132	81	<1	8	<0.001	<0.01	0.02	0.02	<0.02	0.03	4.7	<0.05	<0.0	
<b>Swan Morrison Rd Bullsbrook</b>																										
103063	Darling Ra. Saddl.	6.2	5	102	590	111	50	15	18	152	15	61	260	30	<1	72	<0.001	<0.01	-	0.02	<0.02	<0.02	0.18	-	0.0	

Note: All values in mg/L except for pH, colour, and conductivity  
(a) denotes multi-port monitoring bore

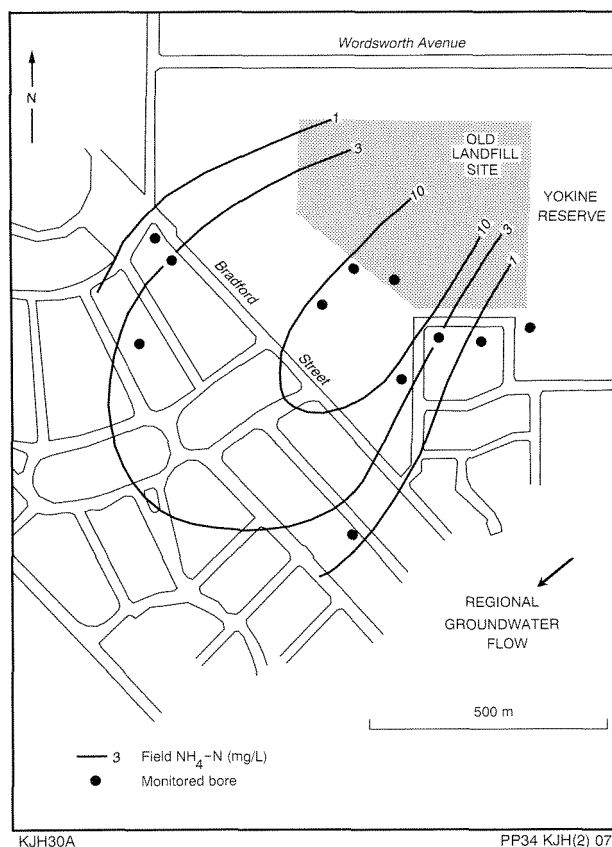


Figure 7. Yokine Reserve disposal site

Superimposed on the plumes resulting from municipal landfill, this is certain to have some impact on  $\text{NH}_4\text{-N}$  concentrations in groundwater.

### Liquid domestic -waste disposal

Bulk liquid (including septic) wastes have a greater potential than solid waste to pollute groundwater. They are applied as a 'shock load' in liquid form (Hirschberg, 1984), whereas leachate from solid waste has to be generated first by interaction between waste and water. The three most extensive and concentrated  $\text{NH}_4\text{-N}$  plumes are all associated with sites where large amounts of septic wastes have been disposed (Figs 3, 4 and 5), and probably result more from the liquid waste than the landfill.

### Role of hydrogeological setting

The hydrogeological setting, in particular the lithology of sediments beneath a site and depth to watertable, was expected to have a major influence on the size and severity of any contamination plume. Of the 50 landfill sites investigated, 22 are underlain by Tamala Limestone (including its predominantly sandy facies); nine are in Bassendean Sand; and 19 are in a predominantly clayey environment, including three sites in clay derived from the weathering of granite (Table 1).

Table 3. Comparison of ammonia—N determinations

Landfill site	Bore location	$\text{NH}_4\text{-N}$	$\text{NH}_4\text{-N}$
		(mg/L) CCWA	(mg/L) Field
Hopkinson Road	MPB blue	0.59	3.0
Ashfield Reserve	45 Haig Street	2.7	5–10
Ranford Road	37 Trident Terrace	9.3	>10
	27 Merrifield Circle	8.5	>10
Daly Street	33 Douro Street	13	10
Walter Padbury Park	30 Rushbrook Way	9.3	5–10
Kelvin Road	Lot 331 Kelvin Road	0.06	1–3
	Lot 249 Victoria Road	0.07	0
John Connell Reserve	41 Gracechurch Crescent	97	>10
	73 Gracechurch Crescent	5.1	10
John Creaney Reserve	91 Perry Avenue	15	10
	1 Litic Way	22	10
Brockway Road	100 Rochdale Road	3.6	5–10
	John XXIII College	27	>10
	Tip gatehouse	34	>10
	7 Whitney Crescent	2.4	10
	Adderley Street	4.9	>10
	Hamilton Lane	34	>10
	101 Rochdale Road	2.2	5
Ennis Avenue	MPB red	29	>10
	MPB blue	9.6	>10
Old Golf Course	Walloo Rugby Club	0.76	0–0.5
Manning Road	MPB black	3.1	5–10
Thelma Street	MPB black	69	10
Hertha Road	Lot 7 Hertha Road	22	10
Yokine Reserve	near Sir D. Brand School	22	10
	Coolbinia Primary School	4.7	10
Morrison Road	Darling Range Saddlery	0.18	1–3

As expected, the predominant factor in plume development appears to be the permeability of the strata. The low infiltration of rainwater and leachate in a clay environment, combined with much higher adsorptive capacities of clays than those of sands, appears to restrict the development of leachate plumes in clay. Only two of the  $\text{NH}_4\text{-N}$  field tests which gave readings above 5 mg/L, were from sites predominantly in clay.

The main contamination plumes have developed in the Bassendean Sand and the Tamala Limestone, both of which have high permeabilities and generally low adsorptivities.

Depth to watertable appears to play a lesser role than lithology in the development of contamination plumes. The watertable was found to be generally shallower in clay than in sand or limestone; however, no extensive plumes were found in clay, and the  $\text{NH}_4\text{-N}$  concentrations were also generally very much lower than those in sand or limestone.

### Limitations and merits of method

The investigation was designed to determine the degree of risk to human health from groundwater contamination by leachate from landfills, by attempting to define the extent of contamination plumes. The approach was to

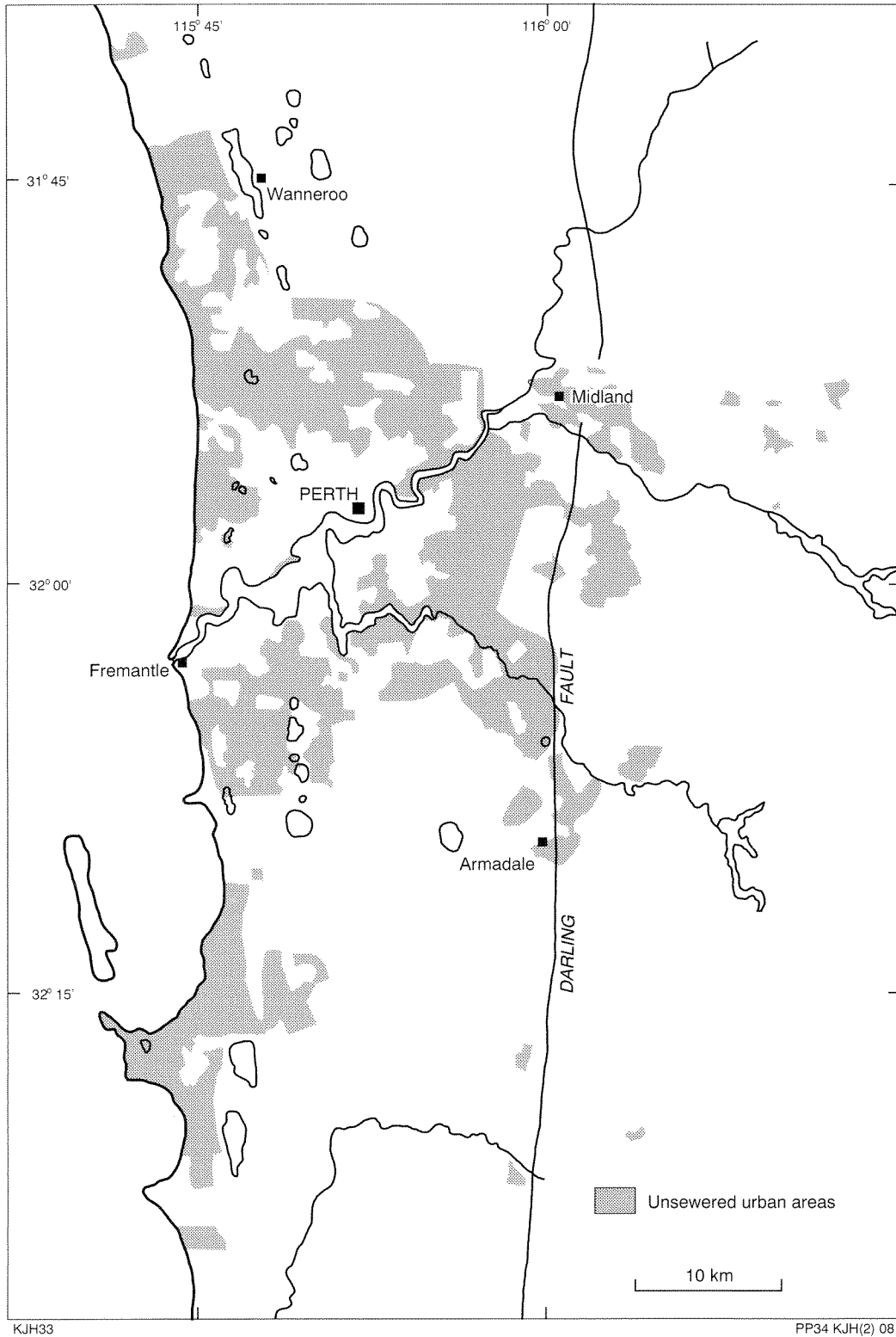


**Figure 8. Unsewered urban areas, Perth**

analyse water from bores in the vicinity of a number of sites. This approach has inherent limitations. For example, these bores may not all be in hydrogeologically suitable positions, and they may also be completed in different horizons of the respective aquifer. Any attempt at contouring of particular contaminant concentrations can, therefore, only be an approximation of the true extent and

shape of a contamination plume, and also cannot reflect a three-dimensional picture. For the determination of the latter, multiple monitoring points at different locations and to different depths are required.

Apart from some limited studies (Bestow, 1977; Barber et al., 1991) no detailed study of the size and shape of

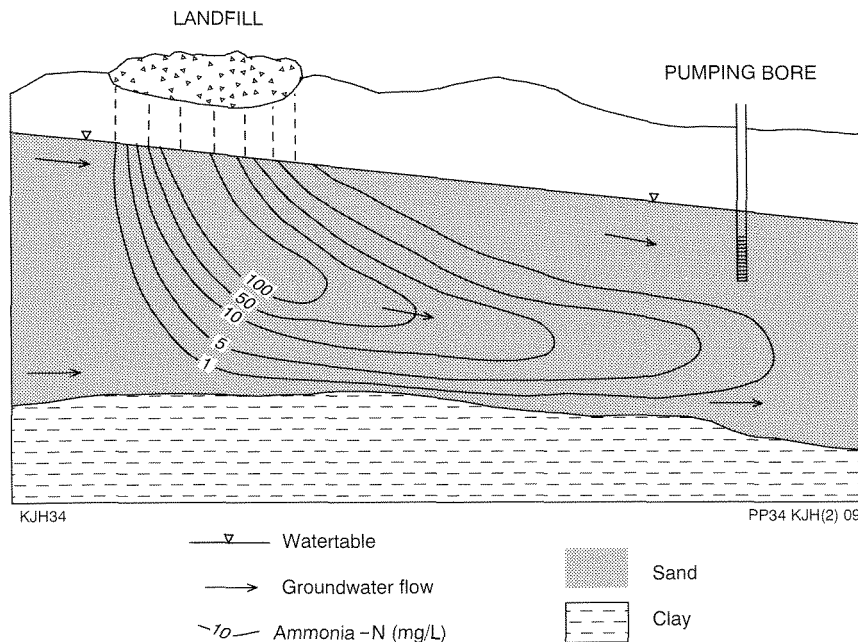


Figure 9. Schematic cross section through a contamination plume

groundwater contamination plumes associated with landfill sites has been undertaken in Perth. Overseas studies have found that pollution plumes emanating from landfill sites typically have a boot-shaped configuration due to gravity differences between leachate and groundwater, and subsequent movement with the general groundwater flow (Fig. 9). Consequently, a shallow bore near the toe of a plume may not intercept any of the contamination which lies beneath it.

During its travel with the groundwater, the strength of the contamination plume is reduced, to varying degrees, by each of the processes of dilution, dispersion, diffusion, adsorption, biodegradation, and chemical reactions.

Despite the above limitations, the results of the investigation showed the merits of this approach. The field-screening of private and monitoring bores for  $\text{NH}_4\text{-N}$  proved to be a fast and reliable indicator to determine the presence of groundwater contamination, as confirmed by chemical analyses. The field measurements were readily and cheaply obtainable and, as long as over-interpretation is avoided, a qualitative assessment of the groundwater quality near landfill sites can be achieved.

## Conclusions

Provided inherent limitations are not ignored, field testing for  $\text{NH}_4\text{-N}$  in water from bores in the vicinity of landfill sites has proved to be useful for the determination of the extent of leachate pollution plumes.

Groundwater contamination was found near 21 of 50 investigated sites. However, the contamination appears to consist almost exclusively of elevated levels of ammonia, and increased salinity. Ammonia appears to persist over long distances and periods of time. Analyses for the major

ions were generally in the range of normally expected background values, and heavy metals were orders of magnitude below maximum permissible levels. Other studies have shown that pesticides and hydrocarbon compounds were usually well below permissible residual limits, or below detection level. Several large plumes of  $\text{NH}_4\text{-N}$  in groundwater were delineated, and it appears that most of these may be at least partly due to co-disposal of domestic liquid waste.

The development of groundwater contamination plumes appears highly dependent on the permeability and nature of the strata below a site, and to a lesser extent on the depth to the watertable. The development of leachate plumes in predominantly clayey sediments appears largely restricted by the low permeabilities of clays, combined with generally high adsorptive capacities. The main leachate plumes were found to emanate from landfill sites located on Bassendean Sand and Tamala Limestone, both with high permeabilities and generally low adsorptive capacities.

From a human health risk perspective, Perth's landfills have performed quite well; especially when considering that many of the sites are in hydrogeologically unfavourable positions. The potential impact on human health due to leachate production from landfill sites is considered to be very low, as only a small number of irrigation bores in the vicinity of the sites appears to be affected. Furthermore, very few, if any, of these bores are used as a source of drinking water. The Water Authority's borefields are under no threat of contamination from landfill sites, as the latter are all hydraulically downgradient from the borefields.

The potential threat of nutrient input from waste disposal into wetlands needs to be considered in the management of the wetlands.

To ensure continued protection of the groundwater resources and the environment, a high standard of landfill site selection, construction, and management (including groundwater monitoring) is required. Wherever possible, sites should be selected in areas of clay, preferably with a watertable at several metres depth, although this situation is rarely achievable on the Swan Coastal Plain. The requirements for lining and leachate interception should be addressed on a case-by-case basis, with due consideration of all hydrogeological aspects.

## References

- ALLEN, A. D., 1975, Outline of the hydrogeology of the superficial formations of the Swan Coastal Plain: Western Australia Geological Survey, Annual Report 1975, p. 31–42.
- APPLEYARD, S. J., and BAWDEN, J., 1986, The effects of urbanisation on nutrient levels in the unconfined aquifer underlying Perth, Western Australia: Australian Water Resources Council Conference on Groundwater Systems Under Stress, Brisbane, Proceedings, p. 587–594.
- APPLEYARD, S. J., 1992, Estimated nutrient loads discharged into the Swan–Canning Estuary from groundwater: Western Australia Geological Survey, Hydrogeology Report 1992/20 (unpublished).
- BARBER, C., DAVIES, G. B., BUSELLI, G., and HEIGHT, M. I., 1991, Monitoring and predicting the development of leachate plumes in groundwater: CSIRO Division of Water Resources, Water Resources Series no. 5.
- BESTOW, T. T., 1977, The movement and changes in concentration of contaminants below a sanitary landfill, Perth, Western Australia, *in* Effects of Urbanization and Industrialization on the Hydrological Regime and on Water Quality: Proceedings of Amsterdam Symposium, 1977, UNESCO Publication no. 123, p. 370–379.
- HEALTH DEPARTMENT OF WESTERN AUSTRALIA, 1992, Criteria for sanitary landfills in the metropolitan area: Health Department of Western Australia, Discussion Paper (unpublished).
- HIRSCHBERG, K-J., 1984, Liquid waste disposal in Perth — a hydrogeological assessment: Western Australia Geological Survey, Report 19, Professional Papers for 1984.
- HIRSCHBERG, K-J., 1988, Inventory of proven and inferred groundwater contamination sites, to accompany Perth North and Perth South Sheets 1:100 000: Western Australia Geological Survey, Record 1988/4.
- WHELAN, B. R., BARROW, N. J., and CARBON, B. A., 1981, Movement of phosphate and nitrogen from septic tank effluent in sandy soils near Perth, Western Australia: Groundwater Pollution Conference, Perth, 1979, Proceedings.



# Palynology and correlation of Permian sediments in the Perth, Collie, and Officer Basins, Western Australia

by

John Backhouse

## Abstract

In southern Western Australia extensive Permian deposits are present in the Perth Basin, in small fault-controlled basins such as the Collie Basin, and in the Officer Basin east of the Yilgarn Craton. Palynomorphs are the only fossils consistently present through these widely separated sequences and are the basis for biostratigraphic correlations outlined here.

The Permian sequence in the recently investigated Collie Basin ranges from Stage 2 into the *Protohaploxylinus rugatus* zone (equivalent to lower Stage 5b/c). In the southern Perth Basin, the Stockton Formation and the Sue Coal Measures extend from Stage 2 almost to the beginning of the Triassic. The first appearances of *Camptotriletes warchianus* and *Microbaculispora* sp. A, are used for correlation above the *P. rugatus* datum (lower Stage 5) in the Sue Coal Measures. The overlying Sabina Sandstone contains assemblages dated as probable latest Permian and Early Triassic. These data are used to correlate shallow boreholes on the Vasse Shelf. In the northern Perth Basin a sequence of glaciogene, marine and coal measure deposits ranges from Stage 2 to the lower part of the *Praecolpatites sinuosus* zone and is unconformably overlain by correlatives of the highest part of the Sue Coal Measures. All assemblages from the Officer Basin fall within Stage 2 or the *Pseudoreticulatispora confluens* Zone.

Periglacial sediments of Stage 2 and *P. confluens* Zone age contain similar palynomorph assemblages over a wide area of southern Western Australia, but regional differences become apparent in the Late Permian.

Sediments of Stage 2 age vary in thickness locally. The *P. confluens* Zone is represented by some 300 m of sediments in the northern Perth Basin and by less than 30 m of section in the southern Perth and Collie basins.

**KEYWORDS:** Permian, palynology, Australia, Perth Basin, Collie Basin, Officer Basin

## Introduction

In the Perth Basin Permian sediments are assumed to underlie at depth all the younger sediments. They are seen in outcrop only in the Irwin River area in the north of the basin, and are intersected in boreholes between the coast and the Irwin River outcrops, and in the southern Perth Basin, mainly south of Busselton.

Permian sediments are known on the Yilgarn Craton in the Collie Basin and from the structurally similar but smaller Wilga and Boyup Basins in the south (Fig. 1).

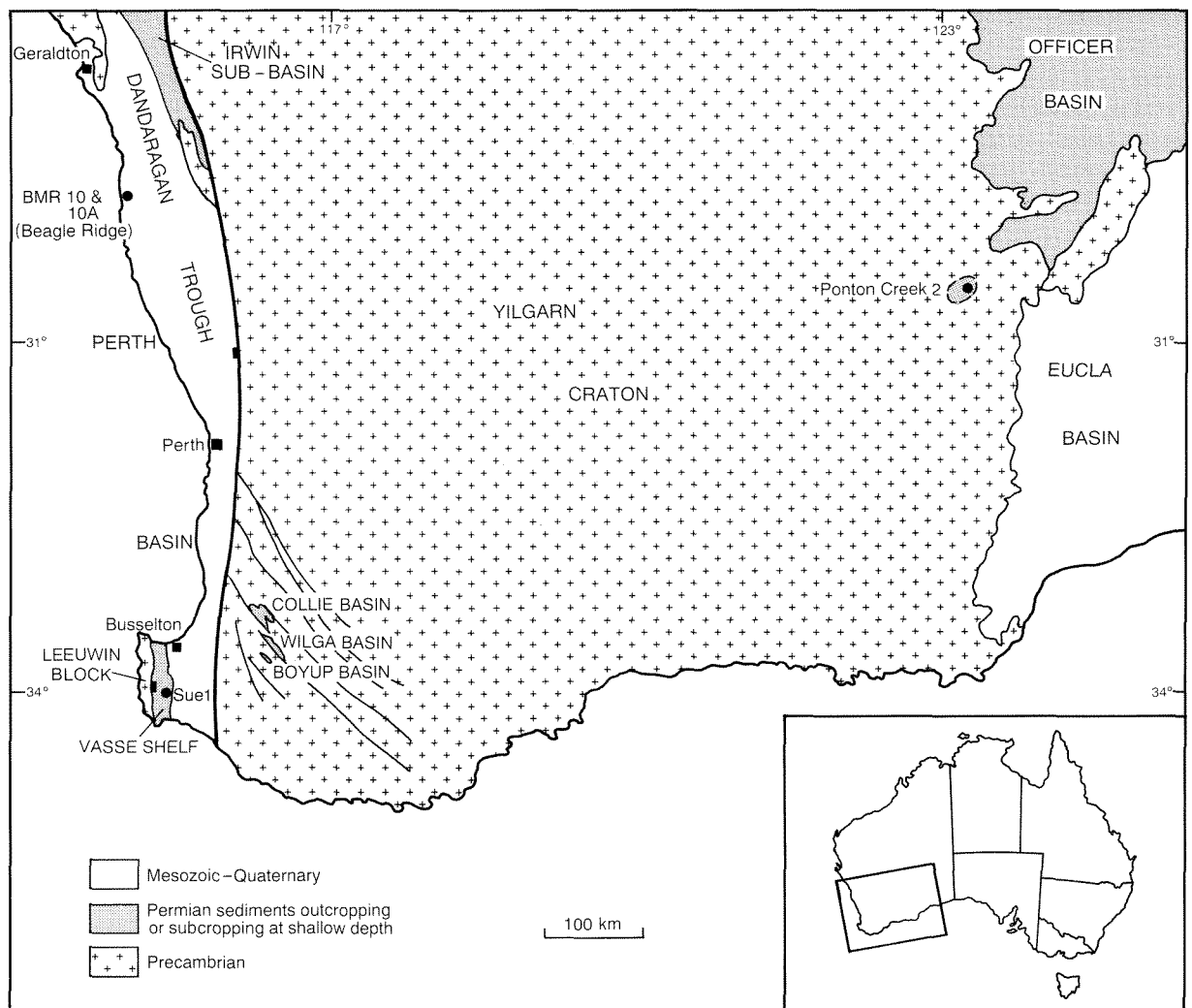
On the eastern margin of the Yilgarn Craton, 700 km east of the Perth Basin, Early Permian sediments of the Officer Basin onlap Archaean igneous and metamorphic rocks, and are overlain by thin Cretaceous and Eocene deposits.

Permian palynomorphs and their stratigraphic distribution in the Collie Basin are the subjects of a recent study (Backhouse, 1991), which presented a detailed palynostratigraphic scheme for the basin. The present

study builds on the results of that investigation by reviewing palynomorph assemblages from other Permian basins in southwestern Australia, in the context of the palynostratigraphy developed in the Collie Basin.

## The Collie Basin

Permian sediments in the Collie Basin have been described in detail by Lord (1952), Low (1958), Playford et al. (1975), and more recently by Kristensen and Wilson (1986) and Wilson (1990). The basin contains up to 330 m of Stockton Formation, which includes diamictite in the lower part and periglacial, pale-grey claystone and buff-coloured, well-sorted sandstone in the upper part. At the top of the Stockton Formation in one borehole is a dark shale band a few centimetres thick conformably overlain by poorly sorted sandstone of the Collie Coal Measures (Backhouse, 1991). The Collie Coal Measures is a cyclic sequence of sandstone, siltstone, claystone and coal (Kristensen and Wilson, 1986), with a maximum thickness of about 800 m. Named seams for each Collie Basin sub-



GSWA 25928

Figure 1. Location map of southwestern Australia

basin and previously recognized members are shown in Kristensen and Wilson (1986) and Wilson (1990). Earlier authors correlated the Collieburn Member with the Premier Member (=Chicken Creek Member in Kristensen and Wilson, 1986), and the Cardiff Member with the Muja Member. Palynological work has shown these correlations to be only partly correct (Backhouse, 1991). The Collie Basin stratigraphy is being revised (Le Blanc Smith, 1993).

### Palynostratigraphy of the Collie Basin

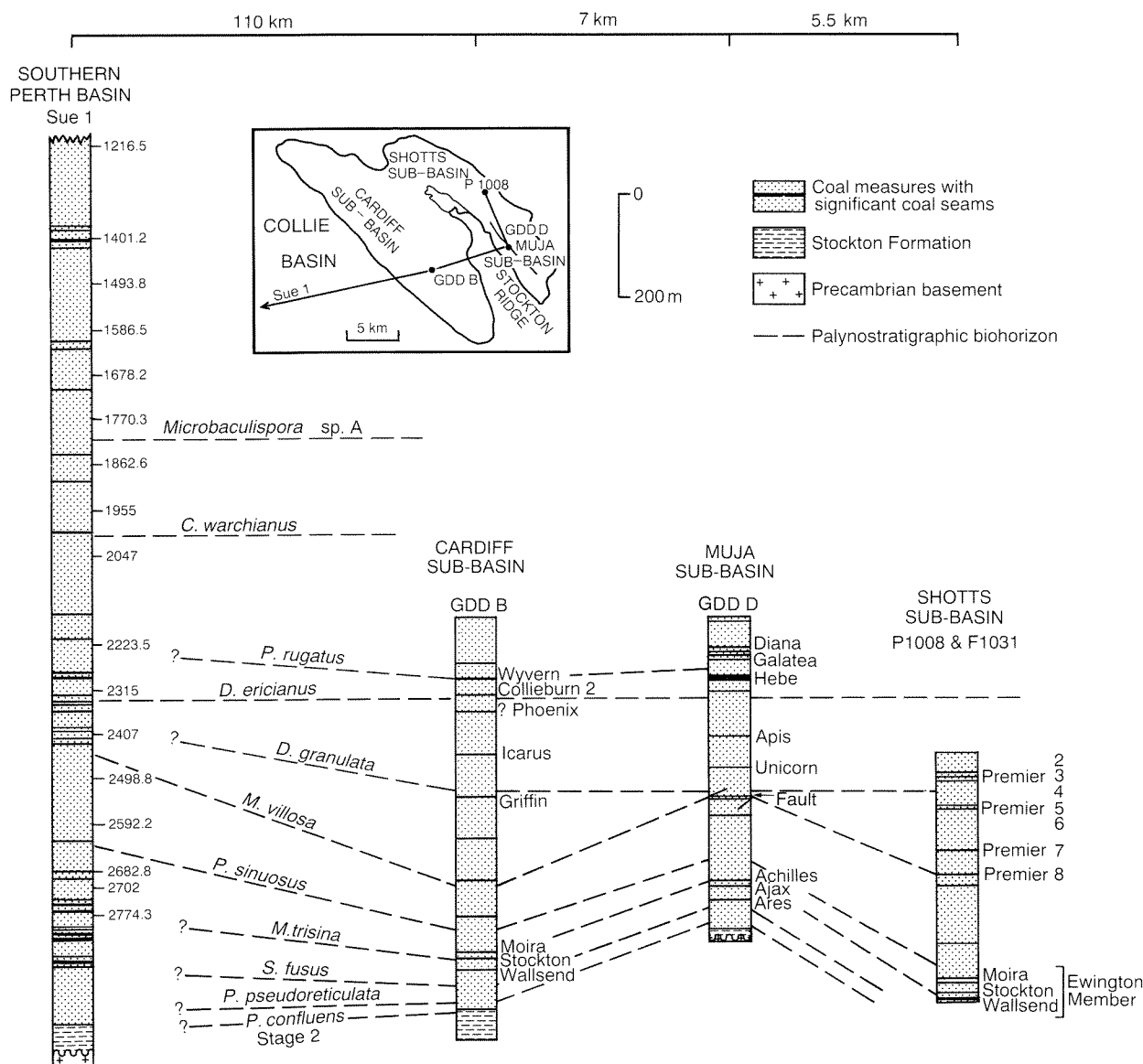
A summary of the palynostratigraphic results from the Collie Basin is presented in Backhouse (1990), and the detailed systematics are covered in Backhouse (1991). The ten palynostratigraphic units used are, in descending order:

*Protohaploxylinus rugatus* zone  
*Didecitriletes ericianus* zone  
*Dulhuntyispora granulata* zone

*Microbaculispora villosa* zone  
*Praecolpatites sinuosus* zone  
*Microbaculispora trisina* zone  
*Striatopodocarpites fusus* zone  
*Pseudoreticulatispora pseudoreticulata* zone  
*Pseudoreticulatispora confluens* Opper-zone (Foster and Waterhouse, 1988)  
 Stage 2 (see Kemp et al., 1977)

As used by Backhouse (1990, 1991) and in this report, Stage 2 is equivalent to Upper Stage 2 as defined in Norvick (1971) and Kemp et al. (1977). It also corresponds to the redefined Stage 2 of Powis (1984), although unlike Powis *Microbaculispora micronodosa* and *Horriditriletes tereteangulatus* are not recognized as characteristic components of Stage 2 (see Backhouse, 1991).

The presence of *Pseudoreticulatispora confluens* is a prerequisite for recognition of the *P. confluens* Zone (Foster and Waterhouse, 1988). Foster and Waterhouse (1988) intended this zone to include assemblages



GSWA 25929

Figure 2. Correlation of borehole intervals in the southern Perth and Collie Basins. For location of Sue 1 see Figure 3

previously assigned to Stage 2 and possibly to Stage 1 as defined by Kemp et al. (1977), but in the Collie Basin *P. confluens* is restricted to a narrow interval below the *P. pseudoreticulata* zone. Assemblages below this level are referred to Stage 2 (Backhouse, 1991).

Above the *P. confluens* Zone each zone is defined by the first appearance of the eponymous species. Some of the zones, such as the *D. ericianus* and *P. pseudoreticulata* zones, are readily identified because the index species shows a high sample frequency near the base of its range. Other zones, notably the *M. trisina* and *P. rugatus* zones, are difficult to recognize with confidence (Backhouse, 1991).

Using these zones it has been possible to correlate the sequences in the Cardiff, Shotts and Muja Sub-basins of

the Collie Basin (Fig. 2). The Ewington Member (Fig. 2) starts in the upper part of the *S. fusus* zone and extends into the *M. trisina* zone, with the *P. sinuosus* zone starting 20–40 m above the highest Ewington Member seam. The *M. villosa* zone starts at approximately the level of the Premier 8 seam in borehole P 1008 in the Shotts Sub-basin (Fig. 2), and some 160 m below the Griffin Seam in Government Deep Drillhole (GDD) B in the Cardiff Sub-basin. In GDD D in the Muja Sub-basin the stratigraphic distance between the start of the *P. sinuosus* zone and the start of the *D. ericianus* zone is 322 m, 128 m less than the equivalent stratigraphic distance in GDD B. This is taken as the thickness of the section faulted out by the Muja Fault in GDD D.

*Dulhuntyispora granulata* first appears in GDD B between the Icarus and the Griffin Seams (Fig. 2). In

P 1008 this biohorizon lies between Premier Seams 4 and 5, and in GDD D it lies between a fault zone and the Unicorn Seam. It is suggested that the Icarus Seam correlates with Premier Seams 3 and 4, and the Griffin Seam correlates with Premier Seams 5 and 6, although other minor seams may be involved.

In the Cardiff Sub-Basin the *D. ericianus* zone consistently starts within, or just below, Colliburn 2 Seam and 40–70 m below the thick and economically important Wyvern Seam. In borehole GDD D, in the Muja Sub-Basin, this biohorizon lies 18 to 39 m below the exceptionally thick Hebe Seam. On this evidence it is suggested that the Wyvern and Hebe Seams are probable lateral equivalents. This is supported by the first appearance of *Protohaploxylinus rugatus* immediately above the Wyvern Seam in GDD B and near the base of the Galatea Seam, 30 m above the Hebe Seam in GDD D. *P. rugatus* was not recorded from any borehole or mine section below the Hebe or Wyvern Seams.

## Wilga and Boyup Basins

No material has been examined for this study from the Wilga and Boyup Basins. The Stockton Formation is present in both basins and the thin coal measure sequences are considered to be equivalent to the Ewington Member of the Collie Basin. This is supported by the small amount of unpublished palynological data on the two basins.

## Southern Perth Basin

Permian sediments have been intersected in deep petroleum exploration boreholes in the southern Perth Basin (Fig. 3). In Sue 1 and Alexandra Bridge 1, west of the Busseton Fault, they are present at relatively shallow depth below heavily oxidized sediments of unknown age. Permian strata were intersected at shallow depth on the northern Vasse Shelf in Quindalup 2 and 3 (Fig. 3). Subsequent coal exploration on the Vasse Shelf has provided a large quantity of core material from the Lower Permian. In Blackwood 1 and Canebreak 1 the Permian is present below oxidized sediments of assumed Cretaceous to Triassic age at depths of 2449 m and 1709 m respectively. Farther north the Permian is present at depths greater than 3700 m in Whicher Range 1–3, Wonnerup 1 and Sabina River 1 (Fig. 3).

### Vasse Shelf

#### Sue 1

Sue 1 penetrated over 1800 m of Permian overlying Precambrian granitic basement. It is the longest and best sampled Permian subsurface sequence in the southern Perth Basin and is used by Backhouse (1990) and in this report as a reference section for palynostratigraphic correlation.

The Permian sequence in this borehole is the type section for the Sue Coal Measures (Playford and Low,

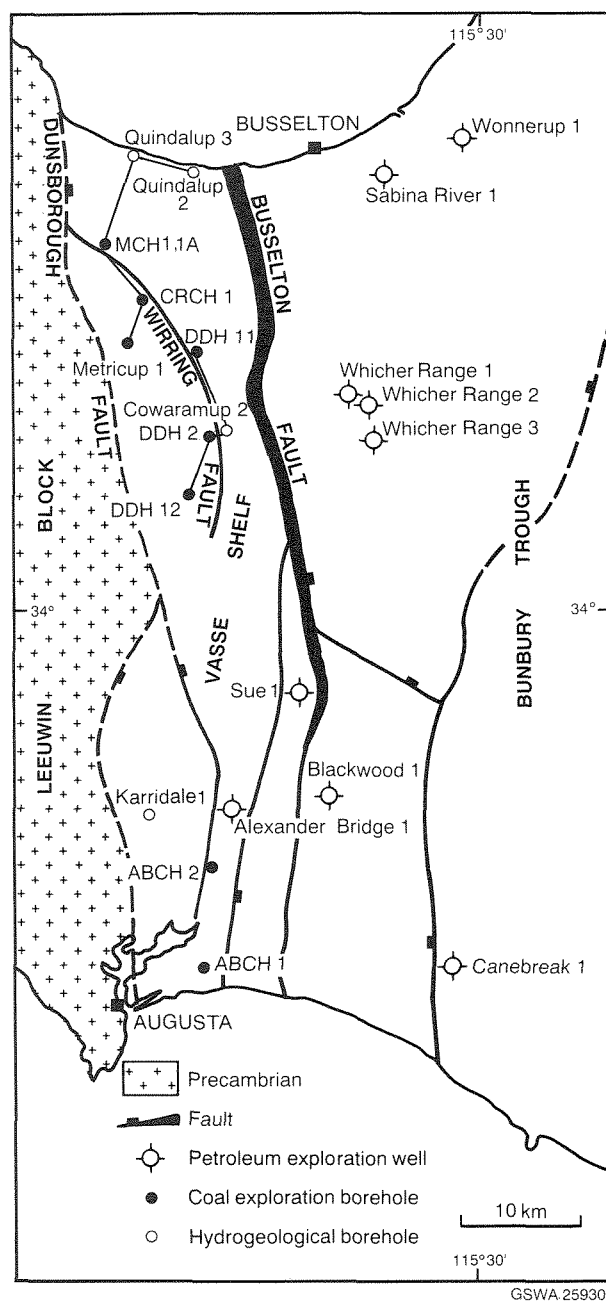


Figure 3. Location map of boreholes in the southern Perth Basin

1972). A glaciene unit is recognized at the base of the sequence (Backhouse, 1990). On the basis of limited lithologic and palynological data it seems probable that the lowest 54 m of Permian sediments in Sue 1 belongs in this unit. Pending a comprehensive review of Permian stratigraphic nomenclature it is proposed to refer this glaciene unit to the Stockton Formation of the Collie Basin, which it closely resembles. The type section of the Sue Coal Measures is emended to 1216–3003 m in Sue 1.

Figure 4 is a distribution chart for selected palynomorph species in Sue 1. No reliable samples are available from the section below 2774.6 m, but from the well-completion report (Williams and Nicholls, 1966) it seems likely that the section below 3003 m belongs in the



levels. Several other species appear in Sue 1 at higher stratigraphic levels than might be anticipated from their known ranges in the Collie Basin.

The 2315.0 m sample contains forms of *D. ericianus* with short spines, morphologically transitional to *M. villosa*. The same morphotype is present in the Collie Basin at the base of the *D. ericianus* range. The 2315.0 m level is therefore taken to be near the base of the *D. ericianus* zone in Sue 1 (Fig. 2).

A correlation of Sue 1 with borehole GDD B in the Collie Basin (Fig. 2) displays the similarity in overall thickness of coal measures between the Collie and Perth Basins up to the *D. ericianus* zone. Above this level several forms are present in Sue 1 that are not recorded from the Collie Coal Measures. At 1955–1957.4 m a diverse assemblage contains *Camptotriletes warchianus* and *Densipollenites indicus*. At a slightly higher level (1770.3–1771.2 m) a distinctive species of *Microbaculispora* first appears — *Microbaculispora* sp. A (Fig. 5), a morphotype which displays widely spaced, large, low grana over the entire exinal surface. The first occurrences of *C. warchianus* and *Microbaculispora* sp. A are potentially useful biohorizons and are shown in Figures 2 and 12. Several other unusual forms of *Microbaculispora* are present above this level, together with some undescribed spore species. Other species present above 1678.4–1680.1 m that are not known from the Collie Basin include: *Verrucosiporites* sp. cf. *V. trisectatus*, *Dulhuntyispora parvithola*, *Shizopollis* sp. cf. *S. woodhousei*, *Triadispora* sp. cf. *T. epigona* and *Chordasporites?* sp. A.

The highest sample in Sue 1 (1216.5 m) contains *Polypodiisporites* sp. A (= *Tuberculatosporites modicus* in Segroves, 1970) and *Granulatisporites quadruplex*, species present in the Wagina Sandstone of the northern Perth Basin.

Segroves (1970, fig. 4) shows *G. quadruplex* ranging through the Early Permian High Cliff Sandstone and Irwin River Coal Measures, whereas his illustrated specimens are from a sample he indicates to be from the Wagina

Sandstone. Re-examination of this sample has confirmed the Wagina Sandstone provenance.

#### Other borehole intervals on the Vasse Shelf

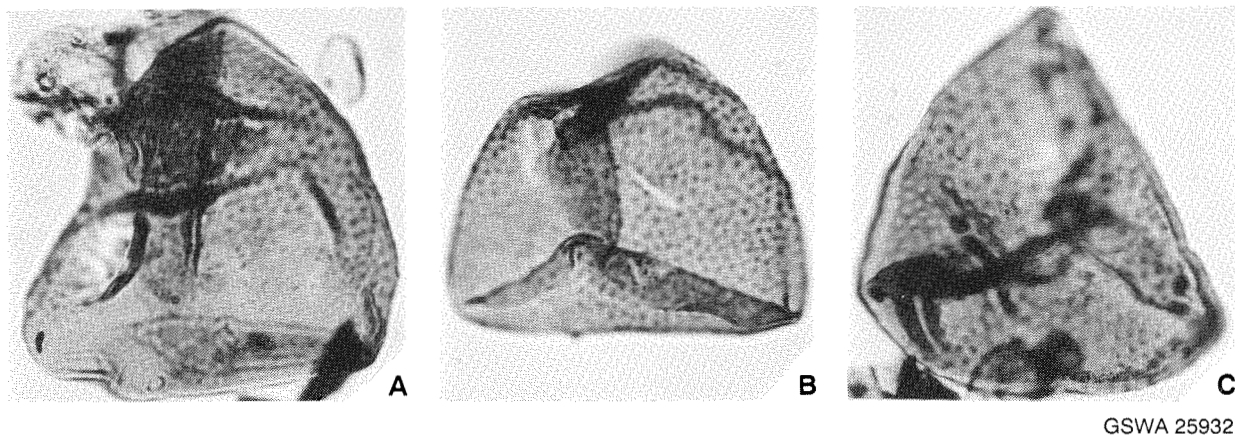
Assemblages similar to those in the upper part of the Sue Coal Measures in Sue 1 are present in the Permian interval in Alexandra Bridge 1 from a core at 612.6–615.7 m and a sidewall core at 410.9 m.

In addition to petroleum exploration wells, a large number of shallower boreholes have penetrated Permian sediments on the Vasse Shelf (Fig. 3). Most of the boreholes are located in the northern part of the Vasse Shelf, to the west of the Wirring Fault, and penetrate the Early Permian. Others located to the east of the Wirring Fault and in the south penetrate younger Permian sediments (Fig. 3).

The boreholes CRCH 1, Metricup 1, DDH 2 and probably Quindalup 2 reached the Stockton Formation (Fig. 6), which in this area is 100–250 m below the lowest coal seams. In Metricup 1 the lowest sample (575.1 m) contains a Stage 2 assemblage without *Pseudoreticulatispora confluens*, although *P. confluens* is present at 514.3 and 492.2 m. In CRCH 1 *P. confluens* is present in the two lowest samples (567.0 and 561.7 m) in a thin interval of Stockton Formation overlying granitic basement. A weathered zone occupies the top of the Stockton Formation in DDH 2. Stage 2 assemblages below the weathered zone do not contain *P. confluens*. The restriction of *P. confluens* to the uppermost Stockton Formation and the lowermost few metres of coal measures is consistent with the range of this species in the Collie Basin.

DDH 12 is the only borehole studied in detail from west of the Wirring Fault that did not reach the Stockton Formation.

To the north and west of the Wirring Fault Quindalup 3, MCH 1 and 1A, DDH 11 and Cowaramup 2A penetrate younger Permian sediments that contain *Camptotriletes warchianus* (Fig. 6). A crude correlation



GSWA 25932

Figure 5. *Microbaculispora* sp. A, all figures x750. A,B, Sue 1, 1403.8 m; C, Sue 1, 1770.3 m



can be made between the 620 m sample in Cowaramup 2A and the 1770.3 m sample in Sue 1 based on the first appearance of *Microbaculispora* sp. A, and between the 350 m sample in Cowaramup 2A and the 1586.5 m sample in Sue 1 based on the first appearance of *Verrucosisporites* sp. cf. *V. triseccatus*. Using these tentative correlations, and assuming a uniform stratigraphic thickness down to the top of the Stockton Formation, the throw on the Warring Fault between DDH 2 and Cowaramup 2A is estimated at 1650–1750 m (Fig. 6).

ABCH 1 and 2 on the southern Vasse Shelf penetrated Late Permian sediments that yielded *Didecitriletes ericianus*, *Camptotriletes warchianus*, *Polypodiisporites* sp. A, *Densipollenites indicus*, and *Triadispora* sp. cf. *T. epigona*. Apart from the absence of *Microbaculispora* sp. A the assemblages from these two boreholes are similar to those from Sue 1 above 1955 m.

The borehole series CRCH, MCH, and ABCH were drilled by CRA Exploration Pty Ltd, the DDH series by Mallina Holdings Ltd and Bond Corporation Pty Ltd joint venture, and Metricup 1 by BHP Co. Ltd. The Quindalup, Cowaramup, and Karridale hydrogeological boreholes were drilled by the Geological Survey of Western Australia.

## Bunbury Trough

In the southern Bunbury Trough, Blackwood 1 and Canebreak 1 palynomorph assemblages from the Permian intervals correspond to the *D. ericianus* zone, or above.

Five wells have been drilled into the Permian in the northern Bunbury Trough (Fig. 3). They all intersected the Sue Coal Measures at depths greater than 3800 m. A few samples of equivocal Late Permian age were obtained from the immediately overlying Sabina Sandstone.

Samples from the top of the Sue Coal Measures in Wonnerup 1 yield typical Permian morphotypes, but samples from 4058.7 m and 4078.2 m (Fig. 7), in the lower part of the Sabina Sandstone, contain *Limatulasporites fossulatus*, *Lundbladispota* sp., *Densoisporites playfordii*, *Guttulapollenites hannonicus*, *Ephedripites* sp. and *Weylandites lucifer*. Other miospores are referable to the genera *Falcisporites*, *Horriditriletes*, *Punctatosporites*, *Lundbladispota* and *Protohaploxypinus*. These assemblages (designated *G. hannonicus* in Figure 7) contain few species in common with assemblages from the Sue Coal Measures, nor do they contain *Triplexisporites playfordii* or *Playfordiaspora velata*. *P. velata* is present in a cuttings sample at 4075.2 m, which suggests its presence within or just above the 4058.7–4078.2 m interval. The next sidewall core sample uphole at 3842.3 m contains *Densoisporites playfordii*, *Kraeuselisporites cuspidus*, *K. saeptatus* and *Lundbladispota wilmottii*. These species are present in the Early Triassic Kockatea Shale of the northern Perth Basin. This interval probably falls within the Triassic *Lunatisporites pellucidus* or *Protohaploxypinus samoilovichii* Zones of Helby et al. (1987)(Fig. 7).

Samples from core 1 (3898.3 and 3899.9 m) in Whicher Range 2 contain the following unequivocally Permian species:

*Horriditriletes* sp. cf. *Acanthotriletes superbus*  
*Dictyotriletes aules*  
*Indospora clara*  
*Plicatipollenites* sp.  
*Protohaploxypinus amplus*  
*Striatopodocarpites fusus*  
*Leschikisporites* sp.  
*Weylandites lucifer*

*Triplexisporites playfordii*, *Playfordiaspora velata* and a number of unidentified spores, which include species of *Polypodiisporites*, are also present. These assemblages are designated *P. velata* in Figure 7, and probably correlate with the *Weylandites* Zone of Kemp et al. (1977) and the *Playfordiaspora velata (crenulata)* Zone of Foster (1982), although the precise relationship to the eastern Australian zones is necessarily speculative. A similar assemblage is present at 3860 m in Whicher Range 3 (Ingram, 1982).

Samples from core 20 (3737.5, 3739.3 m) in Whicher Range 1 yielded rich and diverse assemblages with *P. velata*, *T. playfordii*, *Densoisporites playfordii*, *Kraeuselisporites cuspidus*, *K. saeptatus*, *Limatulasporites fossulatus*, *Taeniaesporites obex* and rare *Aratrisporites* sp. This assemblage is considered to be Early Triassic in age and similar in age to the assemblage in Wonnerup 1 at 3842.3 m.

The suggested stratigraphic relationship of samples from the Sabina Sandstone is shown in Figure 7. A more closely spaced series of samples through the Sabina Sandstone is required to fully resolve the palynostratigraphy at this level in the southern Perth Basin.

## Northern Perth Basin

In the northern Perth Basin Permian sediments outcrop in the Irwin Sub-basin, located between the Urella and Darling Faults (Fig. 8), and underlie Mesozoic strata in the Dandaragan Trough to the west of the Urella Fault. Segroves (1967, 1969, 1970) studied palynofloras from all the Permian units and assembled these data in a palynostratigraphic scheme for the Permian of the Perth Basin (Segroves, 1972). The following samples originally studied by Segroves were reprocessed: Campbell's Water Bore (Holmwood Shale), UWA 4 (Woolaga Creek) Borehole (Wagina Sandstone), Eradu Coal Bore (Wagina Sandstone), seven samples from BMR 10 and 10A (Carynginia Formation to Fossil Cliff Member of Holmwood Shale), six samples from the 47 1/4 Mile Bore (Wagina Sandstone and Carynginia Formation), four samples from Wicherina X49 (Wagina Sandstone) and five samples from Wicherina 1 (Wagina Sandstone to Holmwood Shale). Additional material was examined from Wicherina 1, Abbarwardoo 1 and Yardarino 2. The top part of the Holmwood Shale was sampled in Per 7, IRRC 1 and IRRC 2, and the Carynginia Formation and Irwin River Coal Measures were sampled in IRCH 1 (Fig. 8).

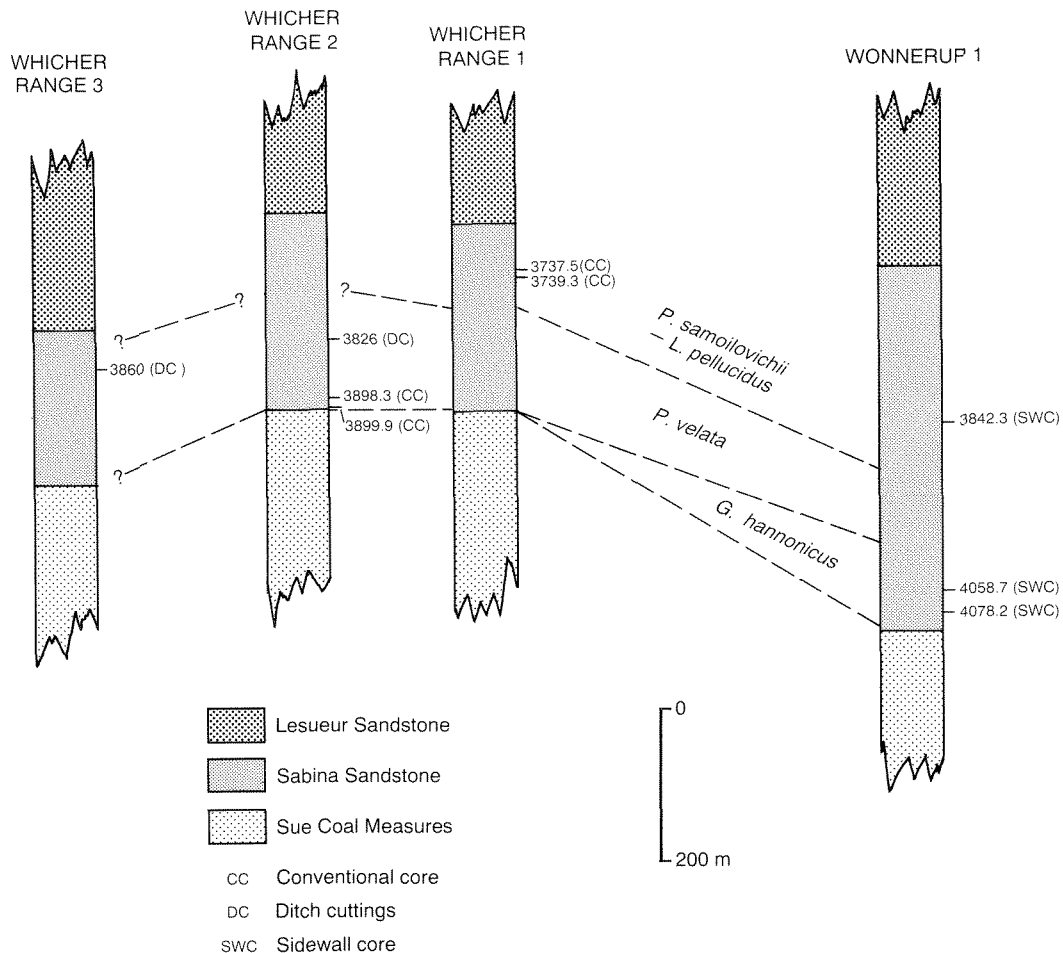


Figure 7. Correlation of the uppermost Permian and the basal Triassic in Whicher Range 1-3 and Wonnerup 1

The boreholes Per 7, IRRC 1 and 2, and IRCH 1 were drilled by CRA Exploration Pty Ltd.

### Nangetty Formation and Holmwood Shale

The basal Permian unit, the glaciogene Nangetty Formation, attains a thickness of 1500 m near the Urella Fault (Playford et al., 1976). The Holmwood Shale conformably overlies the Nangetty Formation and attains a maximum thickness of 450 m in the Irwin Sub-basin. It contains several lenses of fossiliferous limestone and three of them, the Fossil Cliff, Woolaga and Beckett Members, are named units recognized in outcrop.

The distribution of palynomorphs in the Nangetty Formation and Holmwood Shale is shown in Figure 9. The three samples from the Nangetty Formation yielded few palynomorphs and more species may be present in this unit than are recorded here (see Segroves, 1969, 1970).

The Holmwood Shale can be divided into a thick lower part that contains *Jayantisporites pseudozonatus*, and a rather thin upper part from which this species is absent, but in which

*Pseudoreticulatispora pseudoreticulata* is present (Figs 9, 13); *P. pseudoreticulata* is absent from samples in the lower section of the unit. The upper section of the lower part of the Holmwood Shale (Abbarwardoo 1, 497 and 607 m) is placed in the *P. confluens* Zone. The 972 and 1103 m samples from Whicherina 1 contain specimens transitional between *Microbaculispora grandegrnulata* and *Pseudoreticulatispora confluens*, but do not contain true *P. confluens* morphotypes. On this evidence the lowest part of the Holmwood Shale is considered to lie within Stage 2 (Figs 9, 13).

The fossiliferous members can not be reliably identified in boreholes, and the relationship of the samples listed in Figure 9 to the outcropping members is not known. The palynoflora from the Fossil Cliff Member described in Foster et al. (1985) belongs in the *P. pseudoreticulata* zone and therefore corresponds to the upper Holmwood Shale as delineated in this paper.

The available samples do not clarify the age of the Holmwood Shale/Nangetty Formation boundary. It is assumed, in the absence of any contrary evidence, that the Nangetty Formation falls entirely within Stage 2.

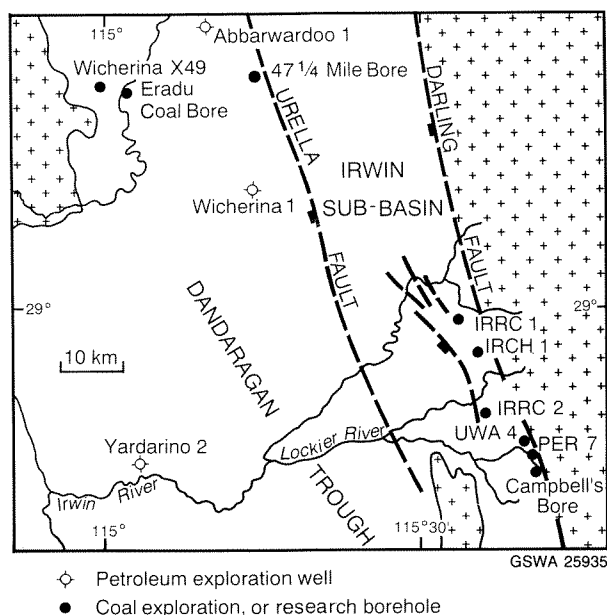


**Figure 8.** Location map for boreholes in the northern Perth Basin

## Irwin River Coal Measures and Carynginia Formation

The Holmwood Shale is conformably overlain by the High Cliff Sandstone, and above this unit lie the Irwin River Coal Measures and the Carynginia Formation. Segroves (1969, 1970) did not differentiate the palynoflora of the High Cliff Sandstone from the Irwin River Coal Measures, and no samples from it were examined as part of this study. The High Cliff Sandstone probably correlates with part of the sandstone section between the Stockton Formation and the lowest coal seams in the Collie and southern Perth Basins.

The Irwin River Coal Measures in IRCH 1 (Fig. 10) contain *Microbaculispora trisina* (small specimens), *Gondisporites ewingtonensis*, *G. wilsonii*, *Laevigatosporites colliensis*, *Striatopodocarpites fusus*, *Weylandites magmus* and *Mehlisphaeridium fibratum*. These species indicate a correlation with the *S. fusus* and *M. trisina* zones of the Collie Basin. This is supported by the abundance of *Horriditriletes tereteangulatus* and the absence of *Praeacolatites sinuosus*.

*Praeacolatites sinuosus* is recorded from the lowest Carynginia Formation sample in borehole IRCH 1 (Fig. 10), but unequivocal examples of *P. sinuosus* are absent from all other samples from this unit. Segroves (1970, 1972) shows this species ranging down to the High Cliff Sandstone, but this range is not supported by the present data. Other significant species to appear in the Carynginia Formation are *Weylandites lucifer*, *Columnisporites* sp. cf. *C. peppersii* and *Maculatasporites* sp. A. *Gondisporites ewingtonensis* ranges into the upper part of the unit. *Altitriletes densus*, *Dictyotriletes aules* and *Microbaculispora villosa* are absent. These data indicate a correlation with the lower part of the *P. sinuosus* zone.

Spinose acritarchs, mainly *Micrhystridium* and *Veryhachium*, are frequent in the upper part of the Carynginia Formation, but rare in the lower part, an indication that more open marine conditions prevailed in the later phase of deposition.

Samples from IRCH 1 at 28.3 and 41.3 m were examined for microfossils by Dr V. Palmieri (1989, pers. comm.) who suggests a cold, marginal marine environment of deposition for the Carynginia Formation, based on foraminifers.

## Wagina Sandstone

The species identified from the Wagina Sandstone are listed in Figure 11. The presence of *Dulhuntyispora parvithola*, *Camptotriletes warchianus*, *Microreticulatisporites bitriangulatus*, *Verrucosisporites* sp. cf. *V. trisecatus* and *Triadispora* sp. cf. *T. epigona* suggests a correlation with the upper part of the Sue Coal Measures, although *Microbaculispora* sp. A is absent. Several species not recorded in the Sue Coal Measures are present in the Wagina Sandstone and *Polypodiisporites* sp. A, which is extremely rare in the southern Perth Basin, is an abundant component of many assemblages.

The Wagina Sandstone clearly post-dates the youngest Permian sediments of the Collie Basin. On palynological grounds it correlates broadly with the 1216.5–1955 m interval in Sue 1, but it may be synchronous with only part of this interval.

## Age of the sequence

The ages of the upper part of the Holmwood Shale, the High Cliff Sandstone and the Carynginia Formation, based on macrofossil evidence, are discussed in detail by Archbold (1982) and Archbold et al. (in press). The ages suggested by these authors for units in the Perth Basin from the Asselian to the Early Baigendzhinian are shown in Figure 12. Ages shown above this level are largely speculative.

## Officer Basin

In the Officer Basin Late Palaeozoic sediments are represented by the Paterson Formation, a flat-lying sequence of diamictite, sandstone, siltstone and claystone. Palynomorphs from the Paterson Formation were described by Kemp (1976), who assigned them all to Stage 2. In Ponton Creek 2 on the Yilgarn Craton, just beyond the southwestern margin of the Officer Basin (Fig. 1), approximately 48 m of late Eocene sediments overlie 509 m of Paterson Formation, which includes 272 m of diamictite and laminated claystone at the base overlain by 237 m of silty, blue-grey claystone with a thin sandstone bed near the top. Samples from the diamictite below 285 m yielded sparse Stage 2 assemblages in which *Punctatisporites gretensis* and radially monosaccate pollen are the most consistent components. More diverse Stage 2 assemblages are present in the overlying claystone

YARDARINO 2		WICHERINA 1			ABBARWARDOO 1			(CRA) IRRC 1			(CRA) IRRC 2		PER 7	Borehole/Well
3027	3026	1375	1103	972	607	497	226	137	120	109	137	122	174	DEPTH IN METRES
														SPECIES
														<i>Cycadopites cymbatus</i>
														<i>Microbaculispora tentula</i>
														<i>Plicatipollenites</i> spp.
														<i>Alisporites</i> spp.
														<i>Punctatisporites gretensis</i>
														<i>Verrucosporites andersonii</i>
														<i>Potonieisporites balmei</i>
														<i>Protohaploxypinus limpidus</i>
														<i>Quadrifurcites horridus</i>
														<i>Brevitriletes parvatus</i>
														<i>Leiotriletes virkii</i>
														<i>Microbaculispora grandegrinata</i>
														<i>Limitisporites rectus</i>
														<i>Horriditriletes ramosus</i>
														<i>Retusotriletes diversiformis</i>
														<i>Pteruchipollenites gracilis</i>
														<i>Horriditriletes tereteangulatus</i>
														<i>Jayantisporites pseudozonatus</i>
														<i>Marsupipollenites striatus</i>
														<i>Protohaploxypinus amplus</i>
														<i>Densosporites rotundidentatus</i>
														<i>Brevitriletes cornutus</i>
														<i>Convrrucosporites naumoviae</i>
														<i>Sahnites</i> sp.
														<i>Pseudoreticulatispora confluens</i>
														<i>Gondisporites wilsonii</i>
														<i>Indotriradites splendens</i>
														<i>Striatoabieites multistriatus</i>
														<i>Tetraporina tetragona</i>
														<i>Brazilea plurigenus</i>
														<i>Dibolisporites disfacies</i>
														<i>Rattiganispora? minor</i>
						cf.								<i>Maculatisporites amplus</i>
														<i>Potonieisporites novicus</i>
														<i>Spongocystia eraduica</i>
														<i>Leiotriletes directus</i>
														<i>Brevitriletes levis</i>
														<i>Densoisporites solidus</i>
						cf.	cf.							<i>Jayantisporites variabilis</i>
														<i>Cymatiosphaera gondwanensis</i>
														<i>Mehlisphaeridium regulare</i>
														<i>Verrucosporites</i> sp. cf. <i>quasigobbettii</i>
														<i>Maculatisporites minimus</i>
														<i>Microbaculispora micronodosa</i>
														<i>Pseudoreticulatispora pseudoreticulata</i>
														<i>Scheuringipollenites maximus</i>
														<i>Vittatina scutata</i>
														<i>Procoronaspora spinosa</i>
														<i>Striatopodocarpites cancellatus</i>
														<i>Diatomozonosporites townrowii</i>
														<i>Gondisporites</i> sp.
														<i>Cymatiosphaera</i> sp. A
														<i>Brazilea scissa</i>
														<i>Rattiganispora apiculata</i>
														<i>Tiwariasporites simplex</i>
Nangetty Fm		middle-lower			upper								LITHOSTRATIGRAPHIC UNITS	
		HOLMWOOD SHALE												
Stage 2			<i>P. confluens</i>		<i>P. pseudoreticulata</i>								PALYNOSTRATIGRAPHIC UNITS	

GSWA 25936

Figure 9. Palynomorph distribution in the Nangetty Formation and Holmwood Shale

IRWIN RIVER COAL MEASURES				CARYNGINIA FORMATION					STRATIGRAPHIC UNIT	
152.5	123.0	103.5	91.4	87.0	66.0	49.5	34.3	28.3	25.3	DEPTH IN METRES
										SPECIES
										<i>Brevitriletes cornutus</i>
										<i>B. levis</i>
										<i>Brazilea scissa</i>
										<i>Florinites eremus</i>
										<i>Gondisporite</i> sp. cf. <i>G. raniganjensis</i>
										<i>Horriditriletes ramosus</i>
										<i>H. tereteangulatus</i>
										<i>Indotriradites splendens / I. niger</i>
										<i>Jayantisporites</i> sp. A of Backhouse, 1991
										<i>J. variabilis</i>
										<i>Laevigatosporite colliensis</i>
										<i>Leiotriletes directus</i>
										<i>Marsupipollenites striatus</i>
										<i>M. triradiatus</i>
										<i>Microbaculispora micronodosa</i>
										<i>M. tentula</i>
										<i>Potonieisporites</i> sp.
										<i>Protohaploxypinus amplus</i>
										<i>P. limpidus</i>
										<i>Quadrisporites horridus</i>
										<i>Scheuringipollenites maximus</i>
										<i>S. ovatus</i>
										<i>Striatopodocarpites cancellatus</i>
										<i>S. fusus</i>
										<i>Alisporites</i> spp.
										<i>Gondisporites ewingtonensis</i>
										<i>G. wilsonii</i>
										<i>Interradisporea robusta</i>
										<i>Mehlisphaeridium fibratum</i>
										<i>M. regulare</i>
										<i>Pteruchipollenites gracilis</i>
										<i>Tiwariisporites simplex</i>
										<i>Verrucosisporites andersonii</i>
										<i>Weylandites magmus</i>
										<i>Retusotriletes diversiformis</i>
										<i>Microbaculispora trisina</i> (small)
										<i>Peltacystia venosa</i>
										<i>Plicatipollenites</i> sp.
										<i>Sahnites</i> spp. (see Backhouse 1991 )
										<i>Micrhystridium</i> sp.
										<i>Baculatisporites bhardwaji</i>
										<i>Praecolpatites sinuosus</i>
										<i>Brazilea plurigenus</i>
										<i>Pseudoreticulatispora pseudoreticulata</i>
										<i>Vittatina fasciolata</i>
										<i>Weylandites lucifer</i>
										<i>Leschikisporis cestus</i>
										<i>Grandispora</i> sp. A of Segroves, 1970
										<i>Secarisporites lacunatus</i>
										<i>Limitisporites rectus</i>
										<i>Peltacystia monile</i>
										<i>Procoronaspora spinosa</i>
<i>M. trisina</i>				<i>P. sinuosus</i>					<b>PALYNOSTRATIGRAPHIC UNIT</b>	

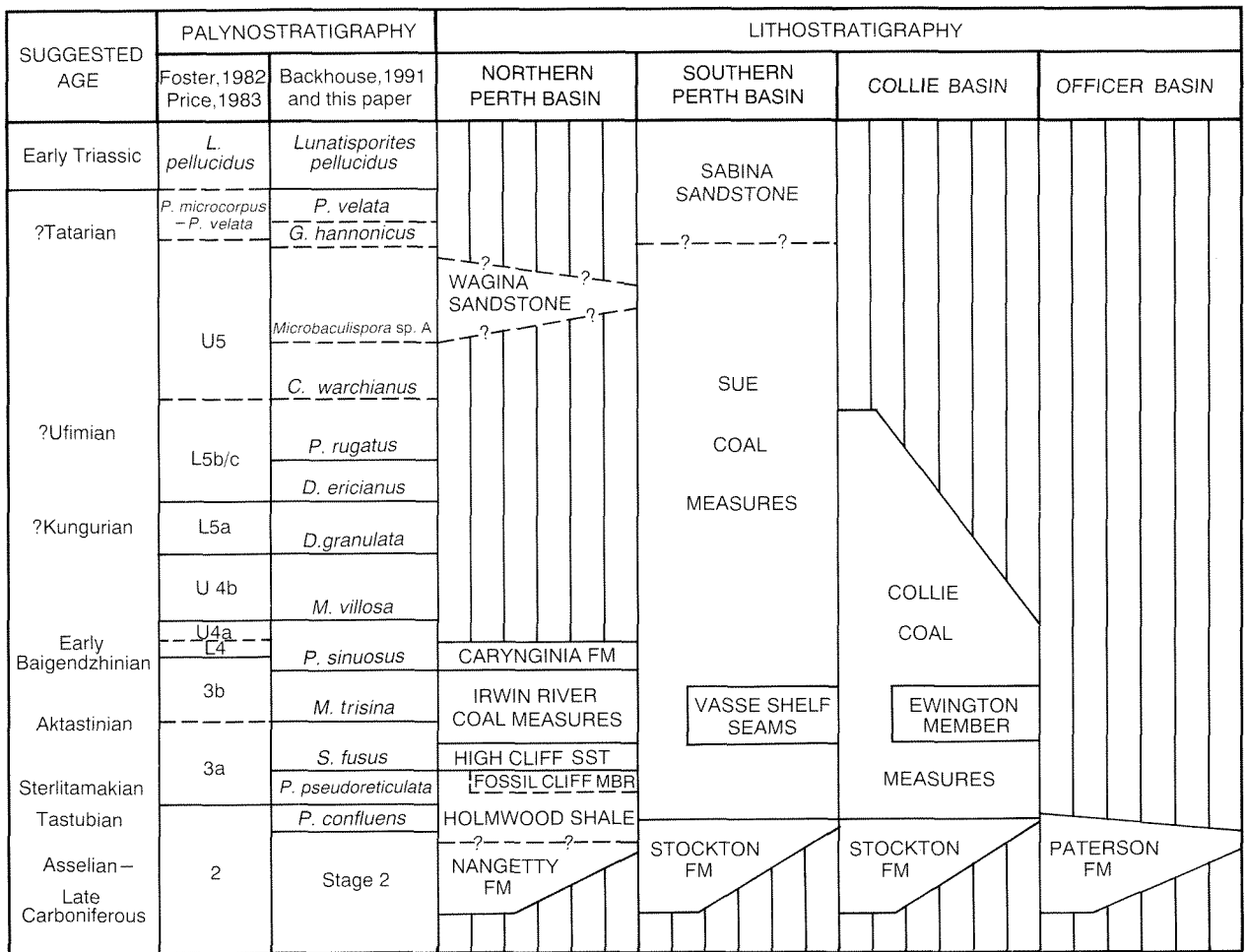
GSWA 25937

Figure 10. Palynomorph distribution in the Irwin River Coal Measures and Carynginia Formation in (CRA) IRCH 1

UWA 4		Wicherina 1		47 1/4 Mile Bore		Wicherina X49		Borehole/Well	
27.7 m	512.7 m	347.5 m	111.9 m	110.0 m	106.4 m	58.2 m	DEPTH	SPECIES	
					cf.				<i>Altitriletes densus</i>
									<i>Baculatisporites</i> sp.
									<i>Baltisphaeridium</i> sp.
									<i>Bipartitisporis tumulosus</i>
									<i>Brazilea plurigenus</i>
									<i>B. scissa</i>
									<i>Brevitriletes cornutus</i>
									<i>Campotriletes warchianus</i>
									<i>Circulisporites parvus</i>
									<i>Cyclogranisporites</i> sp. A of Backhouse, 1991
									<i>Densipollenites indicus</i>
									<i>Dictyotriletes aules</i>
									<i>Didecitriletes ericianus</i>
									<i>Dulhuntyispora dulhuntyi</i>
									<i>D. inornata</i>
									<i>D. parvithola</i>
									<i>Fiorinites eremus</i>
									<i>Gondisporites</i> sp.
									<i>Horriditriletes filiformis</i>
									<i>H. tereteangulatus</i>
									<i>Indospora clara</i>
									<i>Indotriradites enormis</i>
									<i>Indotriradites splendens/l. niger</i>
									<i>Laevigatosporites colliensis</i>
									<i>Leiotriletes directus</i>
									<i>Limitisporites rectus</i>
									<i>Maculatasporites amplus</i>
									<i>Marsupipollenites striatus</i>
									<i>M. triradiatus</i>
									<i>Mehlisphaeridium fibratum</i>
									<i>M. regulare</i>
									<i>Microbaculispora micronodosa</i>
									<i>M. trisina</i> (large )
									<i>Microreticulatisporites bitriangularis</i>
									<i>Peltacystia calvitium</i>
									<i>P. galeoides</i>
									<i>P. monile</i>
									<i>P. venosa</i>
									<i>Plicatipollenites</i> spp.
									<i>Polypodiisporites</i> sp. A
									<i>Praecolpatites sinuosus</i>
									<i>Protohaploxylinus amplus</i>
									<i>P. limpidus</i>
					cf.				<i>P. microcorpus</i>
									<i>P. rugatus</i>
									<i>Punctatisporites gretensis</i>
									<i>Retusotriletes diversiformis</i>
									<i>Scheuringipollenites maximus</i>
									<i>S. ovatus</i>
									<i>Schizosporis dejerseyi</i>
									<i>Striatoabieites multistriatus</i>
									<i>Striatopodocarpites cancellatus</i>
									<i>S. fusus</i>
									<i>Tiwariasporites simplex</i>
									<i>Triadispora</i> sp. cf. <i>T. epigona</i>
									<i>Verrucosisporites</i> sp. cf. <i>V. trisecatus</i>
									<i>Weylandites lucifer</i>

GSWA 25938

Figure 11. Palynomorph distribution in samples from the Wagina Sandstone



GSWA 25939

Figure 12. Correlation of palynostratigraphic and lithostratigraphic units in the Perth, Collie and Officer Basins

sequence. A single sample from the top of the claystone (87–90 m) contained *Pseudoreticulatispora confluens* and *Indotriradites splendens*. The palynostratigraphic sequence is therefore similar to the Collie and southern Perth basins, with a thick Stage 2 followed by a thin *P. confluens* Zone.

Permian sediments younger than the *P. confluens* Zone are not known from the Officer Basin.

## Summary

A correlation of the Permian sequences from the Perth, Collie and Officer basins, based on palynological data, is shown in Figure 12. The lowest parts of each sequence are correlated, using true stratigraphic thicknesses, in Figure 13.

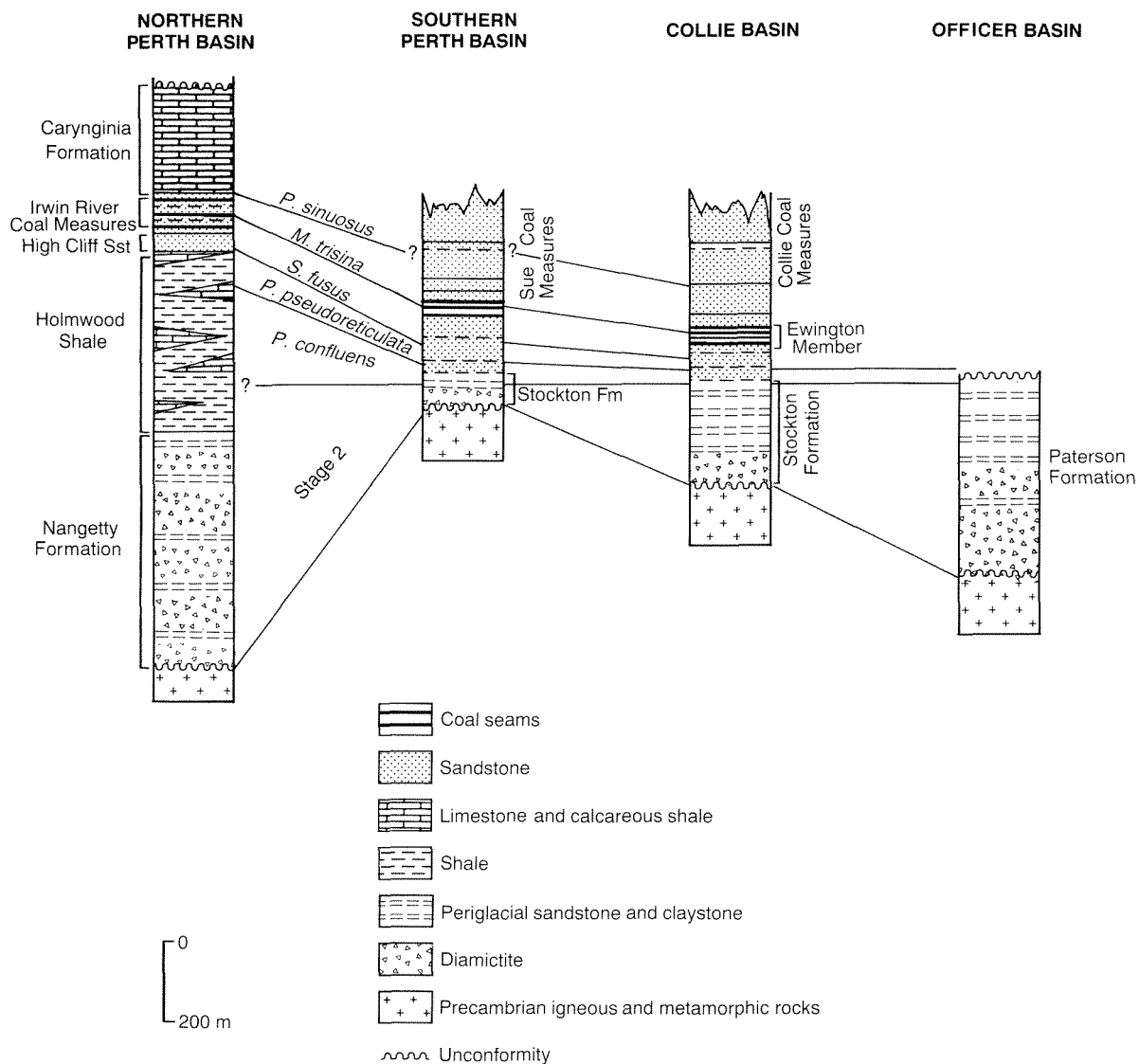
The thickest glaciogene periglacial sequence is represented by the Nangetty Formation and Holmwood Shale in the northern Perth Basin. On lithological and palynological grounds the Paterson and Stockton formations correlate with the Nangetty Formation and all three units belong largely in Stage 2. Where the Stockton Formation overlies a basement high it is thin and may fall entirely within the *P. confluens* Zone; where it is thick only

the uppermost part, transitional to the overlying coal measures, contains *P. confluens*.

In the Collie and southern Perth basins the *P. confluens* Zone occupies the uppermost claystone bands of the Stockton Formation and the basal few metres of the Collie and Sue Coal Measures. It is succeeded by the *P. pseudoreticulata* zone, which occurs in fluvial sandstone and shale. The *S. fusus* zone starts within the sandstone and shale sequence about half way between the top of the Stockton Formation and the lowest coal seams.

In the northern Perth Basin the lowest part of the Holmwood Shale is Stage 2 and the rest of the Holmwood Shale falls within the *P. confluens* and *P. pseudoreticulata* zones. The succeeding High Cliff Sandstone probably belongs to the *S. fusus* zone, and the Irwin River Coal Measures fall within the *S. fusus* and *M. trisina* zones. The Irwin River Coal Measures are therefore the same age as the Ewington Member of the Collie Coal Measures and the lowest Sue Coal Measures, as represented by seams on the Vasse Shelf.

This early period of coal formation extended over most of the area now occupied by the Perth Basin, and over the southwestern Yilgarn Craton. The eastern limit of the coal measures is not known, but they may have originally



GSWA 25940

Figure 13. Correlation of earliest Permian units in the Perth, Collie and Officer Basins, showing true stratigraphic thicknesses

covered most of the southern Yilgarn Craton (Backhouse, 1990). Coal measures of the same age are present in the Arckaringa, Pederika and Cooper Basins of South Australia (Thornton, 1979).

The marine period represented by the Carynginia Formation was restricted to the northern Perth Basin. In the south, coal measure deposition continued into the Late Permian.

The palynological biostratigraphy of the latest Permian and earliest Triassic in the southern Perth Basin is not fully resolved. Significant sedimentological changes between the Sue Coal Measures and the Sabina Sandstone evidently led to rapid changes in the palynoflora. The palynological evidence suggests a hiatus between the Sue Coal Measures and the Sabina Sandstone.

The Wagina Sandstone of the northern Perth Basin is equivalent in age to the upper part of the Sue Coal Measures. No sediments of latest Permian age, equivalent to those of the Sabina Sandstone, are present in the northern Perth Basin.

## Acknowledgements

Basil Balme and Gina Rockette of the University of Western Australia made available slides, residues and rock material from the University of Western Australia collection. This assistance is gratefully acknowledged. Staff of CRA Exploration Pty Ltd, Mallina Holdings Ltd, and West Australian Petroleum Pty Ltd kindly made available material from boreholes in the Perth Basin, and Western Collieries Ltd and The Griffin Coal Mining Company Ltd allowed access to borehole and mine material from the Collie Basin.

## Alphabetical list of miospore and acritarch species mentioned in this paper

### Miospores

- Altitriletes densus* Venkatachala and Kar 1968  
*Baculatisporites bharadwaji* Hart 1963  
*Bascanisporites undosus* Balme and Hennelly 1956  
*Brevitriletes cornutus* (Balme and Hennelly) Backhouse 1991  
*Brevitriletes levis* (Balme and Hennelly) Bharadwaj and Srivastava 1969  
*Brevitriletes parmatus* (Balme and Hennelly) Backhouse 1991  
*Camptotriletes warchianus* Balme 1970  
*Columnisporites heyleyri* Doubinger *emend.* Alpern and Doubinger 1973  
*Columnisporites* sp. cf. *C. peppersii* Alpern and Doubinger 1973  
*Convruccosporites naumoviae* (Hart) Backhouse 1991  
*Cycadopites cymbatus* (Balme and Hennelly) Segroves 1970  
*Cyclogranisporites* sp. A (Backhouse, 1991)  
*Densipollenites indicus* Bharadwaj 1962  
*Densoisporites playfordii* (Balme) Dettmann 1963  
*Densoisporites solidus* Segroves 1970  
*Densosporites rotundidentatus* Segroves 1970  
*Diatomozonotriletes townrowii* Segroves 1970  
*Dibolisporites disfacies* Jones and Truswell (in press)  
*Dictyotriletes aules* Rigby in Rigby and Hekel 1977  
*Didecitriletes ericianus* (Balme and Hennelly) Venkatachala and Kar 1965  
*Dulhuntyispora dulhuntyi* Potonié *emend.* Price 1983  
*Dulhuntyispora granulata* Price 1983  
*Dulhuntyispora inornata* Segroves *emend.* Price 1983  
*Dulhuntyispora parvithola* (Balme and Hennelly) Potonié 1960  
*Ephedripites* sp.  
*Florinites eremus* Balme and Hennelly 1955  
*Gondisporites ewingtonensis* Backhouse 1988  
*Gondisporites raniganjensis* Bharadwaj 1962  
*Gondisporites wilsonii* Backhouse 1988  
*Grandispora* sp. A (Segroves, 1970)  
*Granulatisporites quadruplex* Segroves 1970  
*Guttulapollenites hannonicus* Goubin 1965  
*Horriditriletes filiformis* (Balme and Hennelly) Backhouse 1991  
*Horriditriletes ramosus* (Balme and Hennelly) Bharadwaj and Salujha 1964  
*Horriditriletes* sp. cf. *Acanthotriletes superbus* Foster 1979  
*Horriditriletes tereteangulatus* (Balme and Hennelly) Backhouse 1991  
*Indospora clara* Bharadwaj 1962  
*Indotriradites enormis* (Segroves) Foster 1979  
*Indotriradites niger* (Segroves) Backhouse 1991  
*Indotriradites splendens* (Balme and Hennelly) Foster 1979  
*Interradispora robusta* (Foster) Foster 1979  
*Jayantisporites pseudozonatus* Lele and Makada 1972  
*Jayantisporites* sp. A (Backhouse, 1991)  
*Jayantisporites variabilis* (Anderson) Backhouse 1991  
*Kraeuselisporites cuspidus* Balme 1963  
*Kraeuselisporites saeptatus* Balme 1963  
*Laevigatosporites colliensis* (Balme and Hennelly) Venkatachala and Kar 1968  
*Leiotriletes directus* Balme and Hennelly 1956  
*Leiotriletes virkii* Tiwari 1965  
*Leschikisporis cestus* Segroves 1970  
*Limatulasporites fossulatus* (Balme) Helby and Foster 1979  
*Limitisporites rectus* Leschik 1956  
*Lundbladispora* sp. A (Foster, 1979, 1982)  
*Lundbladispora wilmottii* Balme 1963  
*Marsupipollenites striatus* (Balme and Hennelly) Foster 1979  
*Marsupipollenites triradiatus* Balme and Hennelly 1956  
*Microbaculispora grandegrnulata* Anderson 1977  
*Microbaculispora micronodosa* (Balme and Hennelly) Anderson 1977  
*Microbaculispora* sp. A (this paper)  
*Microbaculispora tentula* Tiwari 1965  
*Microbaculispora trisina* (Balme and Hennelly) Anderson 1977  
*Microbaculispora villosa* (Balme and Hennelly) Bharadwaj 1962  
*Microreticulatisporites bitriangulatus* Balme and Hennelly 1956  
*Phaselisporites cicatricosus* (Balme and Hennelly) Price 1983  
*Playfordiaspora velata* (Leschik) Stevens 1981  
*Polypodiisporites* sp. A (= *Tuberculatosporites modicus* Balme and Hennelly in Segroves, 1970)  
*Potonieisporites balmei* (Hart) Segroves 1969  
*Potonieisporites novicus* Bharadwaj 1954  
*Praecolpatites sinuosus* (Balme and Hennelly) Bharadwaj and Srivastava 1969  
*Procoronaspora spinosa* (Anderson) Backhouse 1991  
*Protohaploxypinus amplus* (Balme and Hennelly) Hart 1964  
*Protohaploxypinus limpidus* (Balme and Hennelly) Balme and Playford 1967  
*Protohaploxypinus microcorpus* (Schaarschmidt) Clarke 1965  
*Protohaploxypinus rugatus* Segroves 1969  
*Pseudoreticulatispora confluens* (Archangelsky and Gamarro) Backhouse 1991  
*Pseudoreticulatispora pseudoreticulata* (Balme and Hennelly) Bharadwaj and Srivastava 1969  
*Pteruchipollenites gracilis* (Segroves) Foster 1979  
*Punctatisporites gretensis* Balme and Hennelly 1956  
*Rattiganispora apiculata* Playford and Helby 1968  
*Rattiganispora? minor* (Anderson) Backhouse 1991  
*Retusotriletes diversiformis* (Balme and Hennelly) Balme and Playford 1967  
*Sahnites* spp. (Backhouse, 1991)  
*Scheuringipollenites maximus* (Hart) Tiwari 1973  
*Scheuringipollenites ovatus* (Balme and Hennelly) Foster 1975  
*Schizopollis* sp. cf. *S. disaccoides* Venkatachala and Kar 1964  
*Secarisporites lacunatus* (Tiwari) Backhouse 1991  
*Shizopollis* sp. cf. *S. woodhousei* Venkatachala and Kar 1964

*Striatoabieites multistriatus* (Balme and Hennelly) Hart 1964  
*Striatopodocarpites cancellatus* (Balme and Hennelly) Hart 1963  
*Striatopodocarpites fusus* (Balme and Hennelly) Potonié 1956  
*Taeniaesporites obex* Balme 1963  
*Tiwariasporites simplex* (Tiwari) Maheshwari and Kar 1967  
*Triadispora* sp. cf. *T. epigona* Klaus 1964  
*Triplexisporites playfordii* (de Jersey and Hamilton) Foster 1979  
*Verrucosiporites andersonii* (Anderson) Backhouse 1988  
*Verrucosiporites* sp. cf. *V. gobbettii* Jones and Truswell (in press)  
*Verrucosiporites* sp. cf. *V. trisecatus* Balme and Hennelly 1956  
*Vittatina fasciolata* (Balme and Hennelly) Bharadwaj 1962  
*Vittatina scutata* (Balme and Hennelly) Bharadwaj 1962  
*Weylandites lucifer* (Bharadwaj and Salujha) Foster 1975  
*Weylandites magmus* (Bose and Kar) Backhouse 1991

#### **Acritarchs**

*Brazilea plurigenus* (Balme and Hennelly) Foster 1979  
*Brazilea scissa* (Balme and Hennelly) Foster 1975  
*Chordasporites?* sp. A (Foster, 1979).  
*Cymatiosphaera gondwanensis* (Tiwari) Backhouse 1991  
*Cymatiosphaera* sp. A (Backhouse, 1991)  
*Maculatasporites amplus* Segroves 1967  
*Maculatasporites minimus* Segroves 1967  
*Maculatasporites* sp. A (Backhouse, 1991)  
*Mehlisphaeridium fibratum* Segroves 1967  
*Mehlisphaeridium regulare* Anderson 1977  
*Peltacystia calvitium* Balme and Segroves 1966  
*Peltacystia galeoides* Segroves 1967  
*Peltacystia monile* Balme and Segroves 1966  
*Peltacystia venosa* Balme and Segroves 1966  
*Quadrifidites horridus* Hennelly ex Potonié and Lele 1961  
*Schizosporis dejerseyi* Segroves 1967  
*Spongocystia eraduica* Segroves 1967  
*Tetraporina tetragona* (Pant and Mehtra) Anderson 1977

## **References**

ARCHBOLD, N.W., 1982, Correlation of the Early Permian faunas of Gondwana: implications for the Gondwanan Carboniferous-Permian boundary: *Journal of the Geological Society of Australia*, v. 29, p. 267-276.  
ARCHBOLD, N.W., DICKINS, J.M., and THOMAS, G.A., (in press), Correlations and age of the Western Australian Permian marine faunas, in *The Permian fossils of Western Australia edited by S. K. Skwarko*: Western Australia Geological Survey, Bulletin 136.  
BACKHOUSE, J., 1990, Permian palynostratigraphic correlations in southwestern Australia and their geological implications: Review of Palaeobotany and Palynology, v. 65, p. 229-237.

BACKHOUSE, J., 1991, Permian palynostratigraphy of the Collie Basin, Western Australia: Review of Palaeobotany and Palynology, v. 67, p. 237-314.  
FOSTER, C.B., 1982, Spore-pollen assemblages of the Bowen Basin, Queensland (Australia): their relationship to the Permian/Triassic boundary: Review of Palaeobotany and Palynology, v. 36, p. 165-183.  
FOSTER, C.B., PALMIERI, V., and FLEMING, P.J.G., 1985, Plant microfossils, Foraminiferida and Ostracoda, from the Fossil Cliff Formation (Early Permian, Sakmarian), Perth Basin, Western Australia, in *Stratigraphy, palaeontology, malacology* (papers in honour of Dr. Nell Ludbrook) edited by J.M. LINDSAY: South Australian Department of Mines and Energy, Special Publication 5, p. 61-106.  
FOSTER, C.B., and WATERHOUSE, J.B., 1988, The *Granulatisporites confluens* Opper-zone and Early Permian marine faunas from the Grant Formation on the Barbwire Terrace, Canning Basin, Western Australia: *Australian Journal of Earth Sciences*, v. 35, p. 135-157.  
HELBY, R., MORGAN, R., and PARTRIDGE, A.D., 1987, A palynological zonation of the Australian Mesozoic: *Association of Australasian Palaeontologists, Memoir 4*, p. 1-94.  
INGRAM, B.S., 1982, Palynology Report for Whicher Range 3: Whicher Range No. 3 Well Completion Report, v. 2, app. 1 (unpublished).  
KEMP, E.M., 1976, Palynological observations in the Officer Basin, Western Australia: *Australia BMR, Bulletin 160*, p. 23-39.  
KEMP, E.M., BALME, B.E., HELBY, R.J., KYLE, R.A., PLAYFORD, G., and PRICE, P.L., 1977, Carboniferous and Permian palynostratigraphy in Australia and Antarctica: a review: *BMR Journal of Australian Geology and Geophysics*, v. 2, p. 177-208.  
KRISTENSEN, S.E., and WILSON, A.C., 1986, A review of coal and lignite resources of Western Australia: Thirteenth Congress of the Council of Mining and Metallurgical Institutions, Singapore, Proceedings, v. 2, Geology and Exploration, p. 87-97.  
LE BLANC SMITH, G., 1993, Geology and Permian coal resources of the Collie Basin, Western Australia: Western Australia Geological Survey, Report 38.  
LORD, J.H., 1952, Collie Mineral Field: Western Australia Geological Survey, Bulletin 105, pt. 1, p. 1-247.  
LOW, G.H., 1958, Collie Mineral Field: Western Australia Geological Survey, Bulletin 105, pt. 2, p. 1-135.  
NORVICK, M., 1971, Some palynological observations on Amerada Thunderbolt No. 1 well, Galilee Basin, Queensland: *Australia BMR, Record 1971/53* (unpublished).  
PLAYFORD, P.E., COCKBAIN, A.E., and LOW, G.H., 1976, Geology of the Perth Basin, Western Australia: Western Australia Geological Survey, Bulletin 124, p. 1-311.  
PLAYFORD, P.E., COPE, R.N., COCKBAIN, A.E., LOW, G.H., and LOWRY, D.C., 1975, Phanerozoic, in *Geology of Western Australia: Western Australia Geological Survey, Memoir 2*, p. 223-433.  
PLAYFORD, P.E., and LOW, G.H., 1972, Definitions of some new and revised rock units in the Perth Basin: Western Australia Geological Survey, Annual Report for 1971, p. 44-46.  
POWIS, G.D., 1984, Palynostratigraphy of the Late Carboniferous Sequence, Canning Basin, W.A. in *The Canning Basin, W.A., edited by P.G. PURCELL*: Geological Society of Australia/PESA Symposium, Perth 1984, Proceedings, p. 429-438.  
SEGROVES, K.L., 1967, Cutinized microfossils of probably non-vascular origin from the Permian of Western Australia: *Micropaleontology*, v. 13, p. 289-305.  
SEGROVES, K.L., 1969, Saccate plant microfossils from the Permian of Western Australia: *Grana Palynologica*, v. 9, p. 174-227.

- SEGROVES, K.L., 1970, Permian spores and pollen grains from the Perth Basin, Western Australia: *Grana*, v. 10, p. 43–73.
- SEGROVES, K.L., 1972, The sequence of palynological assemblages in the Permian of the Perth Basin, Western Australia: Second Gondwana Symposium, South Africa 1970, Proceedings, p. 511–529.
- THORNTON, R.C.N., 1979, Regional stratigraphic analysis of the Gidgealpa Group, southern Cooper Basin, South Australia: South Australia Geological Survey, Bulletin 49, p. 1–140.
- WILLIAMS, C.T., and NICHOLLS, J., 1966, Sue No. 1 well completion report: West Australian Petroleum Pty. Limited (unpublished).
- WILSON, A.C., 1990, Collie Basin, *in* Geology and mineral resources of Western Australia: Western Australia Geological Survey, Memoir 3, p. 525–531.

# Hydrogeology of the Collie Basin, Western Australia

by  
J. S. Moncrieff

## Abstract

The Collie Basin, in the southwest of Western Australia, contains important fresh groundwater resources. An exploratory drilling program has provided new information on the hydrogeology of the area. The basin comprises two grabens, the Premier and Cardiff Sub-basins, which are separated by a basement high. The geology of the basin is reviewed, with particular emphasis on the contribution of the drilling in the areas of stratigraphy and structure.

The hydrogeology of the Collie Basin is complex and reflects the complicated geological environment. The basin contains a regional groundwater flow system in the Collie Coal Measures. Groundwater flow is generally from the margin of the Cardiff Sub-basin, and from a groundwater mound in the northern Premier Sub-basin, towards the Collie River where discharge occurs. The groundwater is unconfined in the upper part and confined at depth. There are about  $7300 \times 10^6 \text{ m}^3$  of groundwater in storage for most of which the salinity is lower than 750 mg/L (total dissolved solids). Annual recharge is estimated to be  $31 \times 10^6 \text{ m}^3$ , of which about  $26 \times 10^6 \text{ m}^3$  is rainfall recharge (13% of average annual rainfall) and some  $5 \times 10^6 \text{ m}^3$  is from streams. Groundwater abstraction at mines and from production borefields exceeds estimated annual recharge by about 25%. This has led to mining of the groundwater resources. Consequently, the watertable has been depressed over about  $100 \text{ km}^2$  of the basin with groundwater heads at depth having been modified over an even greater area, and possibly to the boundary of the basin.

**KEYWORDS:** Collie Basin, hydrogeology, geology, groundwater, groundwater resources

## Introduction

The Collie Basin, which lies about 160 km south-southeast of Perth in the southwest of Western Australia (Fig. 1), contains the State's only producing coal mines. These provide fuel for the generation of about 70% of the electricity which is consumed in the southwest of the State. There are seven operating mines in the basin; the Muja and Chicken Creek opencut mines operated by The Griffin Coal Mining Company, and Western Collieries' WO3 and WO5 opencut mines and WD2, WD6, and WD7 underground mines (Fig. 2).

The basin contains substantial resources of fresh groundwater in an area where the groundwater is typically brackish to saline and in small supply. These resources are important for both coal mining and power generation: control of groundwater inflows to both opencut and underground mines is essential to ensure safe and efficient operation, and groundwater from the basin is used for cooling at the nearby Muja Power Station. Despite the importance of groundwater, investigations to date have focused on the various mine groundwater-control schemes and power station water supplies. There has been no systematic investigation to provide a regional understanding of the basin hydrogeology.

In 1986 the Geological Survey of Western Australia (GSWA) proposed a drilling and testing program aimed at improving the knowledge of the hydrogeology of the basin to allow better assessment and management of the groundwater resources (Moncrieff, 1986). The need for

this work was emphasized in a major report on landuse planning in the basin (Collie Land Use Working Group, 1987) and in a draft water resources management strategy for the basin (Water Authority of Western Australia, 1988). It was intended that the investigation program be conducted in two phases. The current study was designed to define the configuration of the watertable, identify groundwater recharge and discharge areas and the directions of shallow groundwater flow, and to provide a network of bores for monitoring watertable fluctuations. It is recognized that the deeper aquifers have been highly disturbed due to groundwater abstraction and, in subsequent work, the hydrogeology of the deeper parts of the basin will be investigated. Phase 1 of the investigation program was undertaken during 1989 and the scope, data analysis and conclusions form the subject of this paper.

## Location and topography

The Collie Basin, which lies some 50 km east of Bunbury (Fig. 1), is about 27 km long, up to 13 km wide, and has an area of approximately  $225 \text{ km}^2$ . The town of Collie is situated on the northern margin of the basin.

The basin lies within a northwesterly trending valley in the Darling Plateau. The land surface slopes towards the northwest from about 250 m Australian Height Datum (AHD) at the southern extremity of the basin to about 160 m AHD at the northern end near the upstream part of the Wellington Reservoir. Hills on the Darling Plateau

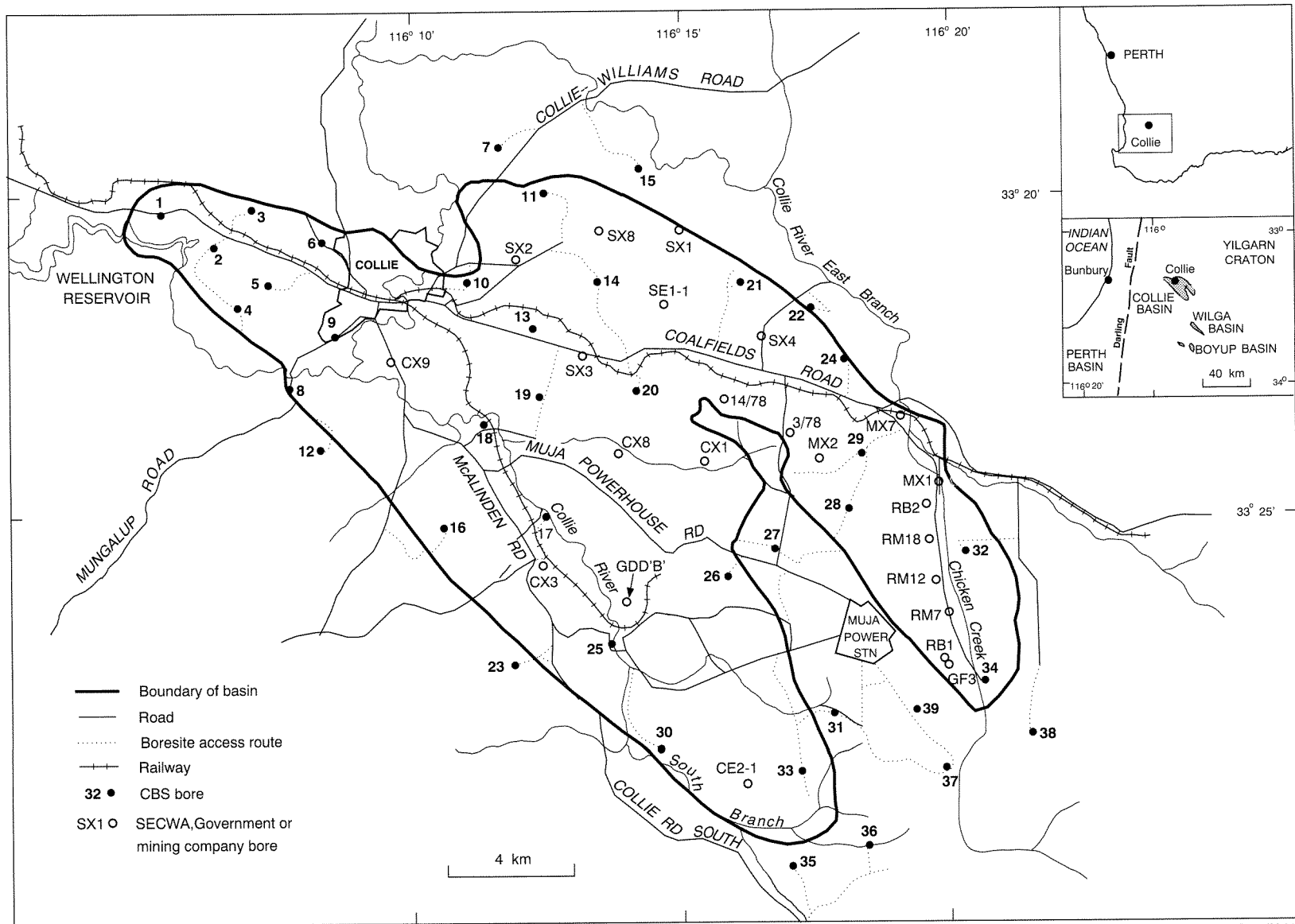


Figure 1. Location

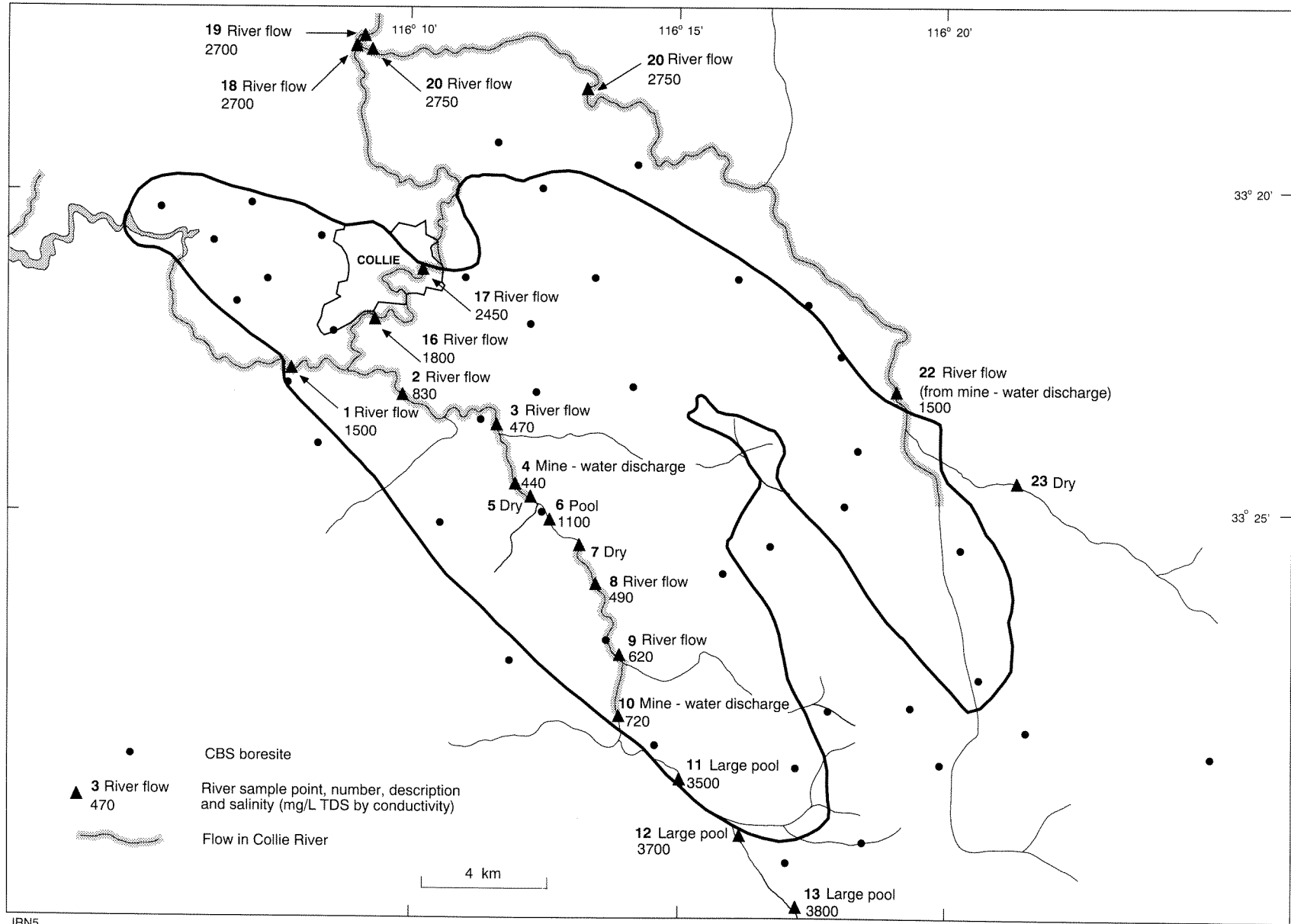


Figure 2. River sampling, April 1990

to either side and north of the basin reach an elevation of about 350 m AHD. In places there is a decrease of elevation across the basin margin into the basin.

## Drainage

The area is drained by two major tributaries of the Collie River; the Collie River East Branch and the Collie River South Branch (hereafter referred to as the East Branch and the South Branch), which flow northwest towards the Wellington Reservoir. The stream valleys inside the basin are broad and shallow whereas outside they are generally steep sided and controlled by structure in the Yilgarn Craton. Wetlands occur in the source areas of many of the tributaries which rise inside the basin.

Water pumped from operating mines is discharged at several places to the South Branch and also to Chicken Creek, a tributary of the East Branch. Power station blowdown water is also discharged to the Collie River system via Chicken Creek.

Flow in the East Branch ceases east of the Collie Basin during summer, but is maintained downstream from near the eastern margin of the basin (Fig. 3) by water discharged from the Chicken Creek mine. Flow in the South Branch also ceases south of the basin during summer. However, it is maintained inside the basin by discharge of mine water at several locations in an 8 km-long section near the WO5 opencut mine, between some 500 m south of sampling point 7 and sampling point 10 (Fig. 3). Flow in the South Branch is permanent downstream of where mine water is discharged to the river between sampling points 4 and 5. Permanent pools, which are maintained by groundwater discharge, remain in the river bed when there is no flow. River flow recommences in these sections after the first major winter rain, but may cease again if the rainfall does not persist.

River water in flowing sections of the South Branch had a salinity of about 450–830 milligrams per litre total dissolved solids (mg/L TDS) during April 1990, but the water from some of the pools had a higher salinity, from 1100–6700 mg/L (Fig. 3). The salinity of the water in the East Branch at that time ranged from 1500–3000 mg/L, and downstream of the confluence of the two branches it was about 1500–1800 mg/L.

## Climate

The Collie area has a Mediterranean climate with hot, dry summers and cool, wet winters. Annual rainfall averages around 1100 mm in the extreme northwest and decreases to 742 mm at the Muja Power Station in the southeast. About 75% of the rain falls in the five months from May to September, and the average annual potential evaporation at Collie is 1650 mm.

## Previous work

The first detailed geological investigation of the area was undertaken by Lord (1952). Accounts of the general

geology are also given by Low (1958), Lowry (1976), Wilde (1981), Wilde and Walker (1982), Park (1982), Kristensen and Wilson (1986), and Wilson (1990). Recent work by the Geological Survey on various aspects of the geology is described by Backhouse and Wilson (1989), Wilson (1989), and Davy and Wilson (1989). An extensive review of the geology of the basin is currently being undertaken (Le Blanc Smith, 1993).

Numerous unpublished hydrogeological reports have been prepared by consultants for the State Energy Commission of Western Australia (SECWA) and mining companies including, since 1986, biennial reviews of the groundwater-level monitoring that is undertaken in the basin for SECWA. Descriptions of the hydrogeology and groundwater resources of the basin have been prepared by Hirschberg (1976), Moncrieff (1985) and Allen (1991). Groundwater-control schemes at some of the mines are described by Vogwill and Brunner (1985), Humphries and Hebblewhite (1988), Hammond and Boyd (1988), and Dundon et al. (1988).

## Investigation program

Forty-seven bores were constructed from June to September 1989 at 39 sites on a 3 km grid which follows the long axis of the basin (Fig. 1). Bores were sited to augment the existing SECWA monitoring bore network and to avoid opencut mines. Eleven sites lie outside the accepted limit of the Collie Coal Measures and three sites are alongside wetlands (CBS14, CBS21 and CBS27). The bores are identified by the prefix 'CBS' (Collie Basin Shallow) followed by the site number. At sites where multiple bores were drilled an alphabetical suffix (commencing with 'A') is added to the bore identifier.

A watertable-monitoring bore, with a 5–12 m slotted interval beginning at a nominal depth of 5 m below the watertable, was drilled at each site. At six sites (CBS2, CBS9, CBS14, CBS17, CBS21 and CBS25), an additional bore was constructed to allow monitoring of an interval about 50 m below the surface. The slotted interval in these bores is 3.5–8 m long. At site CBS14 a third monitoring bore, of intermediate depth, was also constructed. CBS18 was drilled alongside an existing monitoring bore (PWD5/80) that is open at 26–32 m depth (about 25 m below the watertable). An additional bore was drilled to 347 m at site CBS5 to investigate the stratigraphy in the area and to provide groundwater information from a deep interval in the northwestern part of the basin.

The watertable-monitoring bores, other than CBS5B and the intermediate bore at site CBS14, were drilled by a contractor using the reverse circulation (RC) air-core method. The other bores were drilled by the Department of Mines Drilling Branch using the wireline-core method, except at site CBS5 where the mud-rotary method was used.

Lithological samples were taken over 1 m intervals during the RC drilling, and 3 m intervals during the mud-rotary drilling. These samples and core from the other bores are stored in the GSWA core library. Palynological

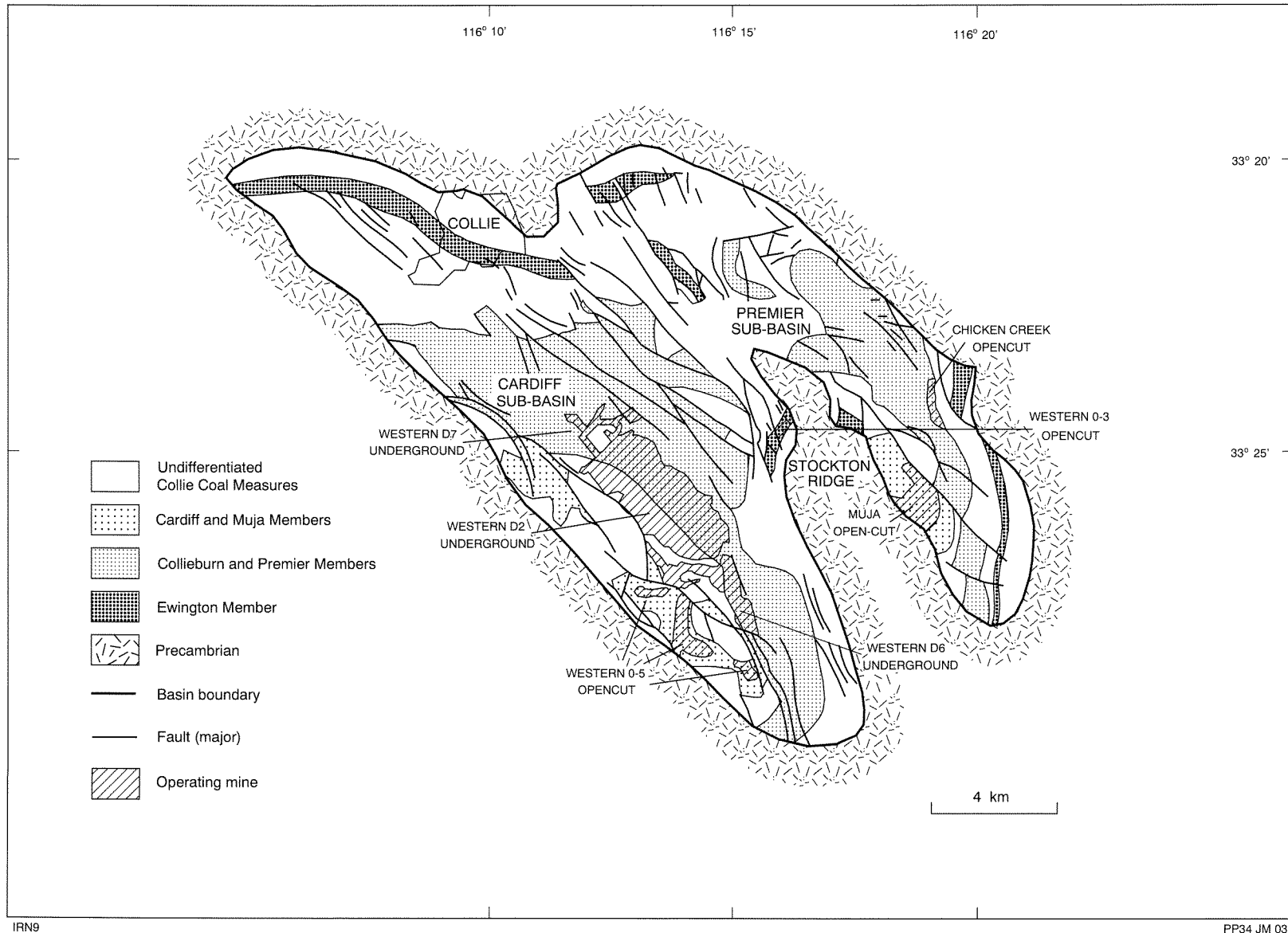


Figure 3. Pre-Cretaceous geology showing subcrop of faults, coal members and operating mines (modified after Wilson, 1990; Le Blanc Smith, 1990)

Table 1. Summary of bore data

Bore	AMG Zone 50		Construction		Total depth (m bns)	Elevation		Slotted interval (m bns)	Potentiometric head (m AHD) (c)	Salinity TDS (mg/L)	Airlift yield (m <sup>3</sup> /day)	Status of bore
	Easting	Northing	Commenced	Completed		Concrete pad (m AHD)	Top of casing (m AHD)					
CBS1	414 930	6 310 710	28.06.89	28.06.89	21	187.127	187.714	14.5 – 20.5	180.619	1 350	2	obs.
CBS2A	416 480	6 309 750	29.06.89	29.06.89	12	176.802	177.570	5 – 11	173.247	40	6.2	obs.
CBS2B	416 480	6 309 750	22.08.89	22.08.89	45	176.581	177.452	39 – 45	171.577	110	6.2	obs.
CBS3	417 670	6 310 850	30.06.89	30.06.89	23	194.614	195.407	16 – 22.5	188.482	500	(e) -	obs.
CBS4	417 150	6 308 010	05.08.89	08.07.89	57	222.603	223.415	42 – 54	179.245	240	(e) -	obs.
CBS5A	418 080	6 308 680	13.09.89	21.09.89	347	229.902	230.528	305 – 311	190.213	220	19.2	obs.
CBS5B	418 080	6 308 680	21.09.89	25.09.89	67	229.880	230.785	(b) 245 – 52.7	178.907	(d) 380	(e) -	obs.
CBS6	419 540	6 310 050	01.07.89	01.07.89	21	205.689	206.198	8 – 17	199.358	740	2.3	obs.
CBS7	424 870	6 312 560	01.07.89	01.07.89	13	215.840	216.618	7 – 13	214.718	1 160	14.4	obs.
CBS8	418 680	6 305 600	04.07.89	04.07.89	11	186.665	187.310	4 – 10	183.980	300	2.9	obs.
CBS9A	419 950	6 307 160	04.07.89	04.07.89	15	187.435	188.168	7 – 13	182.958	130	3.9	obs.
CBS9B	419 950	6 307 160	15.08.89	16.08.89	57	187.159	188.058	48 – 54	180.663	560	5.1	obs.
CBS10	423 920	6 308 910	04.07.89	04.07.89	15	201.448	202.138	9 – 15	200.158	7 150	(e) -	obs.
BS11	426 180	6 311 300	09.08.89	10.08.89	24	225.107	225.943	10 – 16	214.453	1 990	(e) -	obs.
CBS12	419 730	6 304 040	30.07.89	01.09.89	19	222.066	223.002	11 – 19	210.269	690	1.6	obs.
CBS13	425 810	6 307 510	11.07.89	11.07.89	15	213.337	214.271	6 – 15	204.321	1 950	(e) -	obs.
CBS14A	427 662	6 308 724 (a)	11.07.89	12.07.89	9	212.744	213.670	1 – 7	211.832	80	5.8	obs.
CBS14B	427 661	6 308 726 (a)	12.07.89	13.07.89	21	212.907	213.704	14 – 20	211.294	70	6.6	obs.
CBS14C	427 656	6 308 729 (a)	17.08.89	21.08.89	54	213.147	214.036	32 – 35.5	210.098	170	6.2	obs.
CBS15	428 820	6 312 150	10.08.89	10.08.89	9	206.217	206.937	0 – 6	204.439	580	3.2	obs.
CBS16	423 160	6 301 640	18.07.89	18.07.89	21	212.305	213.267	12 – 21	199.479	280	2.9	obs.
CBS17A	426 230	6 302 060	10.07.89	10.07.89	12	183.124	183.871	3 – 10.5	175.993	600	0.6	obs.
CBS17B	426 230	6 302 060	29.08.89	30.08.89	48	183.163	184.118	39 – 45	164.343	1 100	3.3	obs.
CBS18	424 410	6 304 560	14.07.89	14.07.89	9	182.674	183.527	3 – 9	181.167	70	14.4	obs.
CBS19	425 960	6 305 300	17.07.89	17.07.89	36	217.654	218.569	24.5 – 33.5	190.664	290	5.4	obs.
CBS20	428 920	6 305 720	13.07.89	14.07.89	25	damaged	213.511	18 – 24	195.491	680	3.3	obs.
CBS21A	431 625	6 308 500	11.07.89	11.07.89	9	211.102	211.975	0 – 5	210.468	70	8.6	obs.
CBS21B	431 690	6 308 520	23.08.89	24.08.89	42	-	-	-	-	-	-	abd
CBS21C	431 690	6 308 520	24.08.89	25.08.89	51	-	-	-	-	-	-	abd
CBS21D	431 690	6 308 520	28.08.89	28.08.89	49	211.810	212.754	43 – 49	202.476	210	7.8	obs.
CBS22	433 800	6 307 850	08.08.89	09.08.89	15	-	-	-	-	-	-	abd
CBS23	425 280	6 297 680	18.07.89	19.07.89	15	223.729	224.481	6 – 15	220.716	390	(e) -	obs.
CBS24	434 940	6 306 460	07.08.89	08.08.89	42	233.625	234.509	28 – 35	205.319	450	1.7	obs.
CBS25A	428 120	6 298 260	09.07.89	09.07.89	9	186.360	187.331	1 – 7	183.241	1 110	10.8	obs.
CBS25B	428 120	6 298 260	31.08.89	31.08.89	48	186.607	187.501	39 – 45	81.073	210	7.2	obs.
CBS26	431 300	6 300 190	30.07.89	01.08.89	63	238.448	239.332	50 – 62	191.147	390	6.2	obs.
CBS27	432 660	6 300 940	10.07.89	10.07.89	10	216.830	217.565	0 – 6	215.835	490	1.7	obs.
CBS28	434 910	6 302 180	02.08.89	04.08.89	66	255.093	256.084	60 – 66	189.604	1 310	(e) -	obs.
BS29	435 300	6 303 690	04.08.89	05.08.89	45	240.303	241.206	33 – 45	206.298	370	2.3	obs.
CBS30	429 480	6 295 340	28.07.89	28.07.89	30	211.693	212.580	21 – 29	190.245	1 000	3.2	obs.
CBS31	434 580	6 296 110	21.07.89	21.07.89	12	230.222	231.177	5 – 11	224.469	2 280	6.6	obs.
CBS32	438 450	6 300 960	06.08.89	06.08.89	9	219.723	220.573	1 – 9	214.723	110	2.2	obs.

Table 1. (continued)

Bore	AMG Zone 50		Construction		Total depth (m bns)	Elevation		Slotted interval (m bns)	Potentiometric head (m AHD) (c)	Salinity TDS (mg/L)	Airlift yield (m <sup>3</sup> /day)	Status of bore
	Easting	Northing	Commenced	Completed		Concrete pad (m AHD)	Top of casing (m AHD)					
CBS33	433 570	6 294 580	25.07.89	06.08.89	63	235.654	236.540	51 – 63	183.245	730	1.0	obs.
CBS34	438 880	6 297 080	06.08.89	06.08.89	9	223.269	224.069	1 – 8	221.549	70	7.2	obs.
CBS35	433 000	6 291 640	18.07.89	18.07.89	12	197.629	198.594	2 – 10	195.086	70	4.8	obs.
CBS36	435 350	6 292 360	18.07.89	18.07.89	9	216.534	217.416	2 – 8	216.108	7 320	3.3	obs.
CBS37	437 820	6 294 570	20.07.89	20.07.89	13	230.279	230.982	2 – 8	227.452	9 350	8.6	obs.
CBS38	440 100	6 295 340	05.08.89	05.08.89	12	232.480	233.316	1.7 – 10.7	232.221	6 320	2.9	obs.
CBS39	436 860	6 296 370	26.07.89	27.07.89	23	242.519	243.451	11 – 23	232.341	2 460	0.6	obs.
Aggregate depth					1 662							

NOTE:

- (a) Surveyed co-ordinates by Griffin Coal Mining Co. Ltd
- (b) Bore not constructed to design specifications
- (c) December 1989

- (d) Bailed sample
- (e) Little or no airlift flow obtained

- bns below natural surface
- abd abandoned
- obs observation

examinations were undertaken on 18 samples from 11 of the bores (Backhouse, 1990).

The bores were levelled to the Australian Height Datum either by the Surveys and Mapping Division of the Department of Mines, or by the Griffin Coal Mining Company. Geophysical logging of six bores, CBS4, CBS5, CBS14, CBS16, CBS21 and CBS29, was undertaken by the mining companies on whose tenements the bores are located.

The bores were developed by airlifting and water samples were submitted to the Chemistry Centre (W.A.) for chemical analysis.

Waterlevels in all bores were recorded at monthly intervals (Moncrieff, 1990) and, between December 1989 and February 1991, waterlevels in six bores (CBS14A, CBS14B, CBS17A, CBS17B, CBS21A and CBS21D) were continuously monitored. Additional watertable information from existing bores was supplied by SECWA and the mining companies.

A summary of the bore data is given in Table 1 and more detailed information is available in Moncrieff (1991a,b).

## Geology

### Setting

The Collie Basin is a small Permian sedimentary basin on the southwestern Yilgarn Craton and contains remnants of a once-extensive Permian cover over the Precambrian rocks of the region (Wilson, 1990). Two similar but smaller basins, the Wilga and the Boyup Basins, lie about 15 km and 30 km respectively south of the Collie Basin (Fig. 1). Sedimentary rocks analogous to those in the Collie Basin occur in the southern Perth Basin.

The Collie Basin is bilobate in plan and elongate parallel to the dominant northwesterly structural trend of the surrounding Yilgarn Craton (Fig. 2). The lobes are separated by a fault-controlled basement high, the Stockton Ridge and its subsurface extension, which divides the basin into the Cardiff and Premier Sub-basins (Wilson, 1990). The Premier Sub-basin includes the Muja and Shotts Sub-basins recognized by Lord (1952). There are about 1000 m of Permian sedimentary rocks in the Collie Basin (Le Blanc Smith, 1993).

The margin of the Collie Basin and the Permian strata inside the basin are concealed by a veneer of Cretaceous and Cainozoic sedimentary rocks. The basin boundary is mainly faulted; elsewhere it is an unconformity and has been inferred from geological mapping, gravity surveys and limited bore data. The drilling intersected both Permian and Cretaceous strata outside the basin margin shown by Gozzard and Jordan (1986, 1987) and Wilson (1990) but, because these strata were either thin (<20 m) or not fully penetrated, the previously accepted basin boundary is used in this report.

## Stratigraphy

The stratigraphic succession in the area is given in Table 2. The descriptions which follow of the units intersected by the drilling are intentionally brief as detailed lithological descriptions may be found in Wilson (1990). The rock units in the Collie Basin are lithologically similar and consequently boundaries in boreholes are often difficult to recognize.

### Yilgarn Craton

Granitic rocks of the Yilgarn Craton are exposed outside the basin, and close to the basin margin in several places (Fig. 4). The drilling outside the basin intersected granitic, gneissic, schistose, or doleritic rocks, or overlying weathered profile at 11 sites. Within the basin, only drillhole CBS11 intersected basement. Previous drilling has shown that the basement immediately underlying the sedimentary rocks in the basin is smooth and striated in places (Low, 1958), but a 0.6 m-thick weathered section was penetrated above fresh basement in CBS11 (Moncrieff, 1991a).

### Stockton Formation

The Stockton Formation which consists of claystone, sandstone, mudstone, and tillite was intersected at three sites (CBS11, CBS35 and CBS36), and possibly at two others (CBS7 and CBS39) where weathering has made identification difficult. Bores CBS35 and CBS36 are located south of the previously proven extent of the formation in the Cardiff Sub-basin. The formation was fully penetrated in CBS7, CBS11 and CBS39 attaining a maximum thickness of 11 m in the latter bore. Elsewhere its maximum known thickness is 330 m in the Cardiff Sub-basin and 60 m in the Premier Sub-basin (Wilson, 1990). The thickness of the formation varies greatly due to its deposition on an undulating basement. The formation unconformably overlies Precambrian crystalline rocks and is conformably overlain by the Collie Coal Measures.

An Early Permian age (Asselian to Sakmarian) is assigned to the Stockton Formation, and sedimentary structures and microflora indicate subaqueous deposition during periglacial or cold-temperate climatic conditions (Wilson, 1990). Samples from the formation from CBS11 are assigned to the *Pseudoreticulatispora confluens* Zone or Stage 2 (Backhouse, 1991).

### Collie Coal Measures

The Collie Coal Measures were intersected at 26 sites although the base was penetrated only at CBS11. The maximum thickness drilled is about 344 m in CBS5A: the position of the unconformity which defines the base of the overlying Nakina Formation is uncertain in this bore. A weathered section from about 30 m to 235 m (GF 3, Fig. 1) thick, depending on the depth and thickness of major coal and shale beds, occurs at the top of the formation. The Collie Coal Measures have a stratigraphic thickness of about 1050 m, of which the top 975 m is coal bearing (Le Blanc Smith, 1993); however, because of



**Table 2. Stratigraphic units in the Collie Basin (modified after Park, 1983)**

		COLLIE BASIN	
		CARDIFF	PREMIER
		SUB-BASIN	SUB-BASIN
CRETACEOUS		Nakina Formation	
PERMIAN	UPPER	Cardiff Member	Muja Member
		Collieburn Member	Premier Member
	LOWER	Ewington Member	
	Stockton Formation		
PRECAMBRIAN		Yilgarn Craton	

faulting, the maximum drilled thickness is only about 740 m (GDD 'B', Fig. 1). The formation is unconformably overlain by the Nakina Formation.

A light-coloured, variable-grained, at times pebbly sandstone, which contains varying amounts of clay, constitutes about 60% of the Collie Coal Measures. The sandstone in the weathered section at the top of the formation is usually poorly lithified but with depth it becomes more indurated. Cavities, of uncertain origin, have been intersected by many bores. In the southern Premier Sub-basin cavities occur near coal seams and faults, and may be up to 4.5 m deep and extend for hundreds of metres (Vogwill and Brunner, 1985).

Pale siltstone and black shale were intersected in millimetre- to centimetre-scale interbedded sections up to 1.5 m thick. Core from these sections has a distinctive layered appearance. Typically the proportion of shale increases upward and the rock may grade into shale or carbonaceous shale.

The coal-bearing parts of the Collie Coal Measures consist of cyclic, upward-fining sequences of sandstone, siltstone, shale and coal, each resting on an erosional base (Wilson, 1990). Cycles are sometimes incomplete and parts of each may be repeated before the next cycle commences. In the CBS bores, cycles range from 3 m to 13 m in thickness and exhibit structures (bedding, laminations, cross-stratification, etc.) similar to those described by Wilson (1989). The major coal-bearing strata in each sub-basin are grouped into three members (Table 2) whose subcrop distribution is shown in Figure 2.

Individual coal seams are generally less than 4 m thick but range from centimetre scale to 13 m. Seam washouts and seam partings occur in places. The coal seams of the lowermost Ewington Member can be broadly correlated over the entire basin whereas the overlying sequence is more variable and correlations have proved difficult (Park, 1982; Kristensen and Wilson, 1986; Davy and Wilson, 1989). Unnamed sequences up to 300 m thick separate the members. These consist mainly of silty and clayey sandstone and sandy mudstone, but include some coal seams (Backhouse, 1991).

The Collie Coal Measures were deposited during the Permian (Sakmarian, probably to Kazanian) in a fluvial (braided stream) environment (Wilson, 1990). Samples from the bores ranged from the *Pseudoreticulatispora confluens* to the *Protohaploxylinus rugatus* zones (Backhouse, 1991).

### *Nakina Formation*

The Nakina Formation was intersected in 28 bores and attains a probable maximum thickness of 23 m in CBS28. Although the maximum known thickness of the formation is about 30 m, considerable variation results from its deposition on the undulating and eroded surface of the Collie Coal Measures, and from post-depositional erosion. The contact with the Collie Coal Measures is indistinct in many of the bores. Alluvial, eolian, and swamp deposits unconformably overlie the formation and a laterite capping is present in topographically high areas. A palaeochannel infilled with sand and gravel extending from the Stockton Ridge to the Muja opencut mine area has been intersected in boreholes (Brunner, I., 1989, pers. comm.).

The formation consists of sandstone and mudstone with lesser amounts of claystone and conglomerate, all of which are usually poorly lithified. Thin bedding and cross-bedding are well developed in exposures at the Muja opencut. The sandstone which ranges from clean to clayey and silty, is predominantly light coloured, coarse grained and poorly sorted. Where the proportions of clay and silt increase it grades into mudstone. A thin basal pebble conglomerate was intersected in a few bores and a basal ferruginized section also occurs in places.

The Nakina Formation is believed to be a fluvial deposit (Wilson, 1990) and consists of detritus eroded from the Yilgarn Craton or reworked from the Collie Coal Measures. Backhouse and Wilson (1989) have assigned an Early Cretaceous age to the basal part of the formation based on its palynological similarity to the Leederville Formation of the southern Perth Basin. No suitable samples for palynological examination were obtained during the drilling program.

### *Laterite and sand*

Laterite is developed both on the sedimentary rocks of the Collie Basin and on the crystalline rocks of the Yilgarn Craton. Both massive and pisolitic laterite were intersected during the drilling. In the basin, massive laterite is restricted mainly to topographically high areas, where pisolitic laterite also occurs. Elsewhere pisolitic

laterite is found associated with sand and fine gravel, and may be colluvial in origin. The laterite developed over sedimentary rocks is generally sandy and is overlain in most places by a thin cover of pale- to medium-grey, medium- to coarse-grained residual or eolian sand.

#### ***Alluvium, colluvium, and swamp deposits***

Broad areas of sandy alluvium and colluvium occur along most of the stream valleys inside the basin. These deposits are mainly less than 2 m thick and in this paper are collectively termed surficial sand. Alluvium conceals the Collie Coal Measures where the Collie River has incised the formation.

Swamp deposits up to about 1.5 m thick consisting of silty, clayey, slightly peaty ferruginized sandstone overlain by surficial sand, were intersected at sites CBS14 and CBS21.

### **Structure**

The Cardiff and the Premier Sub-basins are grabens that are deepest near their western margins. The overall structure of the Permian strata within the Cardiff Sub-basin consists of a doubly plunging, asymmetric syncline with a northwesterly axial trace along the deepest part (Wilson, 1990). This structure is overprinted with numerous faults and low-amplitude cross folds with axial traces that trend broadly northeast (Le Blanc Smith, 1989). These faults and folds complicate many of the larger structural features of the Premier Sub-basin. The Permian strata dip at low angles, but near the basin margins dips are steeper, and consequently sedimentary rocks from deeper in the succession are unconformably overlain by the flat-lying Nakina Formation.

The faults trend mainly northwest and most have normal displacements, with downthrows towards the deepest parts of the sub-basins (Fig. 2). Throws are generally less than 50 m, but range up to 200 m (Wilson, 1990); they may vary considerably along strike, or even reverse in direction (apparent scissors movement). These variations are associated with strike-slip movement along faults which penetrate the folded strata (Le Blanc Smith, 1989). Vertical displacement on the boundary faults may be as much as 1 km and may have been accompanied by considerable lateral movement.

### **Hydrogeology**

The main aquifers in the Collie Basin are sandstone in the Collie Coal Measures, surficial sand deposits, and sand and sandstone in the Nakina Formation. In most of the bores the watertable is in the Collie Coal Measures; generally, the shallower units are saturated only in parts of the northern and southern Premier Sub-basin, and locally near drainage lines.

The basin is surrounded by crystalline rocks with an overlying lateritic weathering profile. These rocks are of low permeability and contain mainly brackish or saline groundwater.

### **Groundwater flow system**

In the Collie Basin the Collie Coal Measures are in hydraulic continuity with the Nakina Formation and surficial sand and form an inhomogeneous, anisotropic, multi-layered aquifer system that has a maximum saturated thickness of about 1050 m. The thickness of permeable sandstone in the aquifer system, averaged over the basin, is estimated to be about 325 m. The basin contains a regional groundwater flow system which is unconfined near the surface and confined at depth. Individual sandstone aquifers in the Collie Coal Measures are separated by confining beds of shale and coal; however, hydraulic connection across them may occur (Hammond and Boyd, 1988). Porosity is mainly intergranular but fracture porosity also occurs at depth (Vogwill and Brunner, 1985).

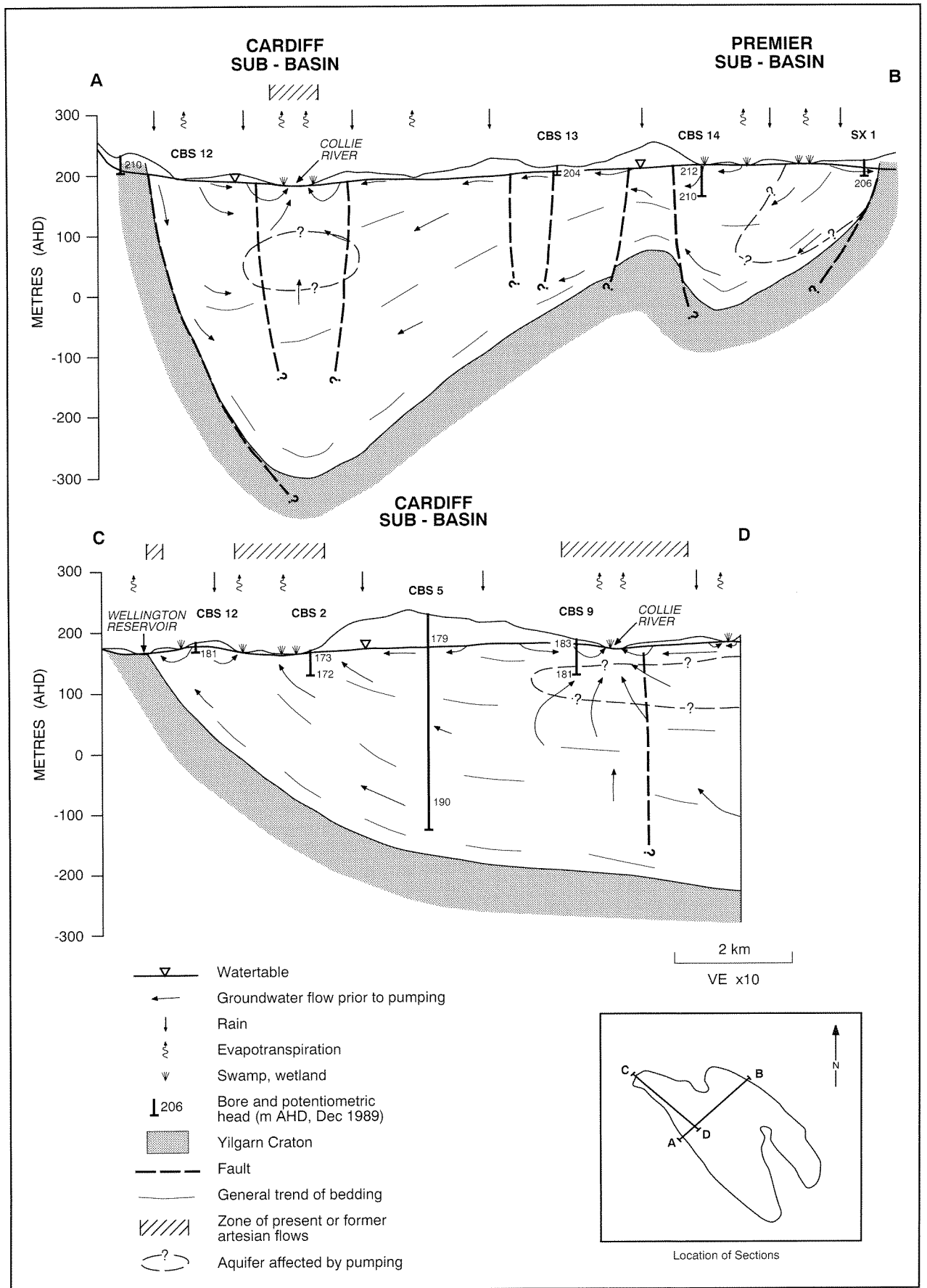
The flow system is bounded at the top by the watertable and at the base by impermeable claystone of the Stockton Formation, or by basement rocks (where the Stockton Formation is absent). Laterally, there is hydraulic connection across the basin margin in both the Nakina Formation and the surficial sand; however, the saturated thickness is believed to be small and, for the purpose of this paper, the flow-system boundary is assumed to coincide with the basin margin. Superimposed on the regional flow system within the basin are inferred local groundwater flow systems near surface water features, and also structurally controlled intermediate groundwater flow systems (Fig. 5).

Groundwater flow in the basin is complex due to the vertical stacking of aquifers and lateral stratal discontinuities caused by faulting, washouts, attenuation of beds, and mine workings. Faults may be either permeable or impermeable depending on the lithologies that are in contact across them (Vogwill and Brunner, 1985). Furthermore, faults may exert some structural control on groundwater flow at depth. Uncased exploration bores, bores in which the casing has failed, and poorly constructed bores may also facilitate groundwater movement across confining beds. The interpretation of groundwater flow is further complicated by the effects of large-scale groundwater withdrawals.

Regional groundwater flow at depth is poorly understood. Most existing deep groundwater-observation bores have been constructed to monitor the effects of pumping at operating mines or to provide baseline groundwater information in areas where mines are proposed. These bores are open only at stratigraphic levels which are of interest for groundwater control at the mines, but data from them have locally provided a good understanding of the hydrogeology. The remaining deep groundwater-observation bores in the basin are open mainly over several intervals and at different stratigraphic levels, and data from them are unsuitable for determining the regional groundwater flow system.

#### ***Watertable configuration***

The configuration of the watertable (Fig. 4) is broadly a subdued replica of the topography. The highest groundwater levels (about 230 m AHD) coincide with the



IRN10

PP34 JM 05

Figure 5. Diagrammatic sections showing conceptual groundwater flow in the northern Collie Basin

topographic divide between the South and East Branches where a groundwater mound extends along the Stockton Ridge and into the northern Premier Sub-basin. The sedimentary rocks are unsaturated in CBS22 on the eastern side of the mound near the margin of the basin where fresh basement was intersected at 10.5 m depth. The zone above fresh basement is also unsaturated on parts of the Stockton Ridge. The highest watertable elevations along the southwestern margin of the basin parallel the topographic divide between the South Branch and the Preston River to the west.

The watertable slopes down towards the South and East Branches, towards Chicken Creek, and locally towards smaller drainage lines inside the basin. The hydraulic gradient is steepest around the edges of the southern Cardiff Sub-basin, locally around some streams in the northern Cardiff and Premier Sub-basins, and adjacent to opencut mines. Permanent wetlands occur where the watertable is at the surface. Temporary perched watertables have been observed in the Nakina Formation after heavy rain (Brunner, I., 1990, pers. comm.).

### Potentiometric-head distribution

Potentiometric heads in the deeper CBS bores (that are open about 50 m below the watertable), in PWD5/80 which is alongside CBS18, and in selected deep SECWA bores are shown in Figure 6. The highest heads occur in the Premier Sub-basin (211 m AHD in ME1) and the lowest in the central Cardiff Sub-basin (164 m AHD in CBS17B).

Between September 1989 and February 1991, a downward head gradient was observed between the watertable and the deeper intervals in the flow system at most sites where heads from multiple-depth intervals are recorded (Fig. 6). The steepest gradient occurred at CBS17, where the maximum head difference was 16.69 m over 35 m depth (July 1990, Table 3), and is a consequence of pumping for groundwater control at the underlying WD2 mine (at a depth of about 150–200 m). A downward head potential of 8.65–9.81 m over 43 m depth occurred at CBS21 on the northeastern margin of the Premier Sub-basin. The hydraulic head at depth here may be depressed due to abstraction of groundwater from the Shotts Borefield for water supply to the Muja Power Station (Fig. 6).

The largest upward head gradient, of 10.80–11.84 m over 245 m depth, was observed at CBS5 in the northern Cardiff Sub-basin (Table 3). The deep observation interval at this site (CBS5A) is 257 m below the watertable. Upward head gradients were also observed during December 1989 at CE1 and CE2 in the southern Cardiff Sub-basin, where groundwater heads are affected by pumping. At 3 sites (CBS18, SE1 and MX6) there was no difference between the heads recorded from the shallow and the deep intervals.

### Recharge

Recharge to the watertable is mainly by direct infiltration of rainfall. Groundwater recharge also occurs

from the South Branch in the southern Cardiff Sub-basin, where the river stage is higher than the watertable during most of the year and, seasonally, by seepage from streams which rise outside the basin and flow onto permeable Collie Basin sediments. Discharge from mine dewatering also provides groundwater recharge.

Rainfall recharge is concentrated during the period of highest rainfall, between May and September. The amount of recharge varies annually and spatially as indicated by different hydrograph responses (Moncrieff, 1991b). Annual variations are caused mainly by differences in the amount and intensity of rainfall. Areal variations result primarily from differences in permeability at the surface. Surficial sand, which occurs over large areas of the basin, favours infiltration of rainfall and groundwater recharge, particularly where the watertable is in the sand or where the sand is underlain by permeable sandstone. Groundwater recharge is enhanced by a decrease in evapotranspiration from areas where the watertable has been lowered by groundwater abstraction.

Total groundwater recharge to the basin is estimated to be  $31 \times 10^6 \text{ m}^3/\text{year}$  and the net average rainfall recharge about  $26 \times 10^6 \text{ m}^3/\text{year}$  (13% of average rainfall) based on the following water balance for the basin.

$$\text{Surface water: } \mathbf{If} + \mathbf{GD} + \mathbf{RO} + \mathbf{Re} = \mathbf{Of}$$

$$(10^6 \text{ m}^3/\text{year}) \quad 122 + 4 + 15 + 14 = 155$$

$$\text{Groundwater: } \mathbf{RR} (= \mathbf{GR} + \mathbf{IR}) + \mathbf{XR} = \mathbf{GD} + \mathbf{Ab} + \mathbf{s}$$

$$(10^6 \text{ m}^3/\text{year}) \quad 26 (= 25 + 1) + 5 = 4 + 39 + (-12)$$

- where: **If** = surface water inflow,  
**GD** = groundwater discharge to streams (baseflow),  
**RO** = rainfall runoff (from inside the basin),  
**Re** = the amount of water that is discharged to streams after abstraction at borefields or mines,  
**Of** = surface water outflow,  
**RR** = rainfall recharge,  
**GR** = groundwater recharge from rainfall,  
**IR** = induced recharge due to decreased evapotranspiration from about 100 km<sup>2</sup> of the basin where the watertable is depressed due to groundwater abstraction (Fig. 4),  
**XR** = extra-basin recharge from streams which flow into the basin,  
**Ab** = the volume of groundwater being pumped from borefields and mine groundwater-control operations,  
**s** = change in groundwater storage.

Surface water flow and runoff have been calculated from data in Loh and Stokes (1981).

Recharge can also be estimated from chlorinity data. The average chlorinity of rainfall in the Collie area estimated from data collected at other rainfall stations in the region (Hingston, F., 1990, pers. comm.) is about 7 mg/L. The chlorinity of water samples collected from

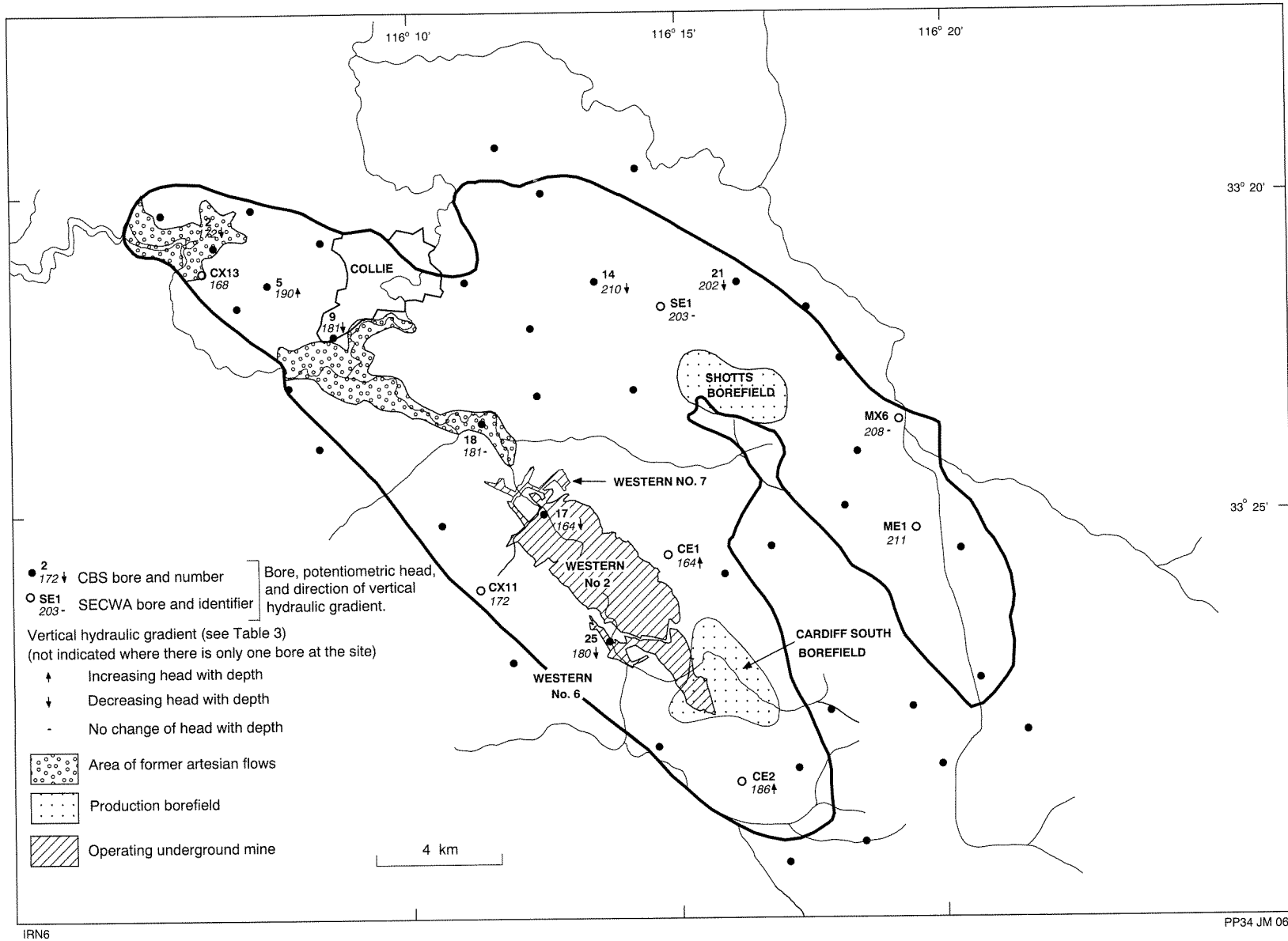


Figure 6. Potentiometric-head distribution, December 1989

bores in sandy areas of the basin, where the watertable is shallow, ranged from 13 mg/L in CBS2A to 35 mg/L in CBS14A. These values indicate local recharge rates of 20–50% of rainfall but, because of variations in the depth to the watertable, and the variable nature of the sediments above and below the watertable, the average recharge over the basin is likely to be less than this.

The watertable in the bores in both 1989 and 1990 was usually highest during September–October, after the period of most rainfall, and lowest during April–May, at the end of summer. However, there was considerable variation, particularly of the lowest waterlevels, around these times. Also, in many bores, the timing and magnitude of waterlevel changes have been modified due to drawdowns caused by groundwater abstraction from the basin (Fig. 4).

A comparison of waterlevels recorded in May and October 1990 shows a rise of the watertable at most sites (Fig. 7). Inside the basin, in the areas largely unaffected by pumping, the patterns of watertable rise varied. In the northern Premier Sub-basin rises were uniformly 0.5–1.0 m whereas they were more inconsistent in the northern Cardiff Sub-basin (0.1–2.3 m). Part of this inconsistency is due to the large variations in the depth to the watertable in the northern Cardiff Sub-basin compared with those in the northern Premier Sub-basin. The level of the watertable in bores on the eastern side of the Cardiff Sub-basin (CBS19, CBS26 and CBS33) and in the central Premier Sub-basin (CBS24 and CBS29) decreased due to drawdowns caused by pumping from the basin.

The largest watertable rises between May and October 1990 occurred outside the basin on the Stockton Ridge in CBS27 (3.2 m) and CBS39 (8.3 m). CBS27 is sited alongside a wetland where groundwater recharge is concentrated by seasonal flow in an adjacent stream. The watertable in the bore rises sharply with the onset of streamflow, usually in April–May, and falls gradually after streamflow ceases around September. In CBS39, about 7 m of the watertable rise occurred during July 1990 and a watertable fall of similar magnitude occurred during January 1991. The reasons for these sudden watertable changes, which are followed by periods of comparatively small fluctuations, are uncertain.

### **Groundwater flow**

Regional groundwater flow is strata controlled in the Collie Coal Measures. Shale or coal units retard both vertical groundwater movement and, where they intersect the watertable, lateral groundwater movement. Unconfined groundwater flow occurs in the surficial sand or in the Nakina Formation where the watertable is above the Collie Coal Measures. Flow in the Nakina Formation may be locally concentrated in palaeochannels.

Regional groundwater flow, based on the apparent hydraulic gradient of the watertable, is mainly northeast and southwest towards the South and East Branches, Chicken Creek and, particularly in the northern Premier Sub-basin, to tributaries of the East Branch which flow from the basin (Fig. 4). Groundwater flow is diverted towards the Muja and WO5 opencut mines in the southern parts of the sub-basins.

There is potential for vertical movement of groundwater under the prevailing vertical hydraulic gradients in the basin (Table 3). Downward flow from the watertable to deeper parts of the flow system occurs where there is a downward head potential but the amount is uneven areally and depends on the nature of the rock units in the Collie Coal Measures. Increased vertical hydraulic gradients established as a result of groundwater abstraction at depth also promote downward groundwater flow from the watertable. Downward flow is probably concentrated in the northern Premier Sub-basin and along the basin margin where the elevation of the watertable is sufficient to initiate downward flow (Fig. 5). Steeper dipping strata near the margin enables flow to move deeper into the basin.

The areas where there is upward groundwater flow are indeterminate. There is potential for groundwater movement from the base of the flow system under the upward hydraulic gradient that exists in the northern Cardiff Sub-basin (CBS5). There may also be upward flow along the eastern side of the sub-surface extension of the Stockton Ridge in the northern Premier Sub-basin (Fig. 5).

The direction of regional groundwater flow in the deeper parts of the flow system is uncertain but is thought to be towards the South Branch. Flow is also diverted towards areas of groundwater abstraction but the areal extent of diverted flow is not known. There is probably groundwater flow across the sub-surface extension of the Stockton Ridge from the Premier to the Cardiff Sub-basin (Fig. 5).

### **Discharge**

Groundwater discharge occurs by evapotranspiration, baseflow to the Collie River and its tributaries, and pumping (see *Abstraction*).

Evapotranspiration has been estimated to account for about 90% of the rain (90% of  $171 \times 10^6 \text{ m}^3$ ) that falls onto the Collie Basin (Collie Land Use Working Group, 1987). Part of this is evaporated from wetlands or transpired by vegetation which draws water directly from the watertable. The effects of evapotranspiration have been observed in both CBS14A and CBS21A, which are alongside wetlands, and where the watertable appears to fluctuate diurnally. The hydrograph of CBS14A for February 1990 (Fig. 8) shows that the watertable is usually lowest in the late afternoon, after the hottest part of the day, and highest soon after dawn. The average waterlevel change within this period (0.026 m) is at the limit of the accuracy of the recording instrument. Nevertheless, the fluctuations are believed to be real because the waterlevel in the deeper bore at the site does not exhibit similar fluctuations.

Baseflow occurs in the northern Cardiff Sub-basin where the watertable is not affected by pumping and the Collie River is a gaining stream (Fig. 5). Groundwater discharge to tributaries of the Collie River is shown by re-entrants in the watertable contours on Figure 4. The tributaries which rise in the northern Premier Sub-basin

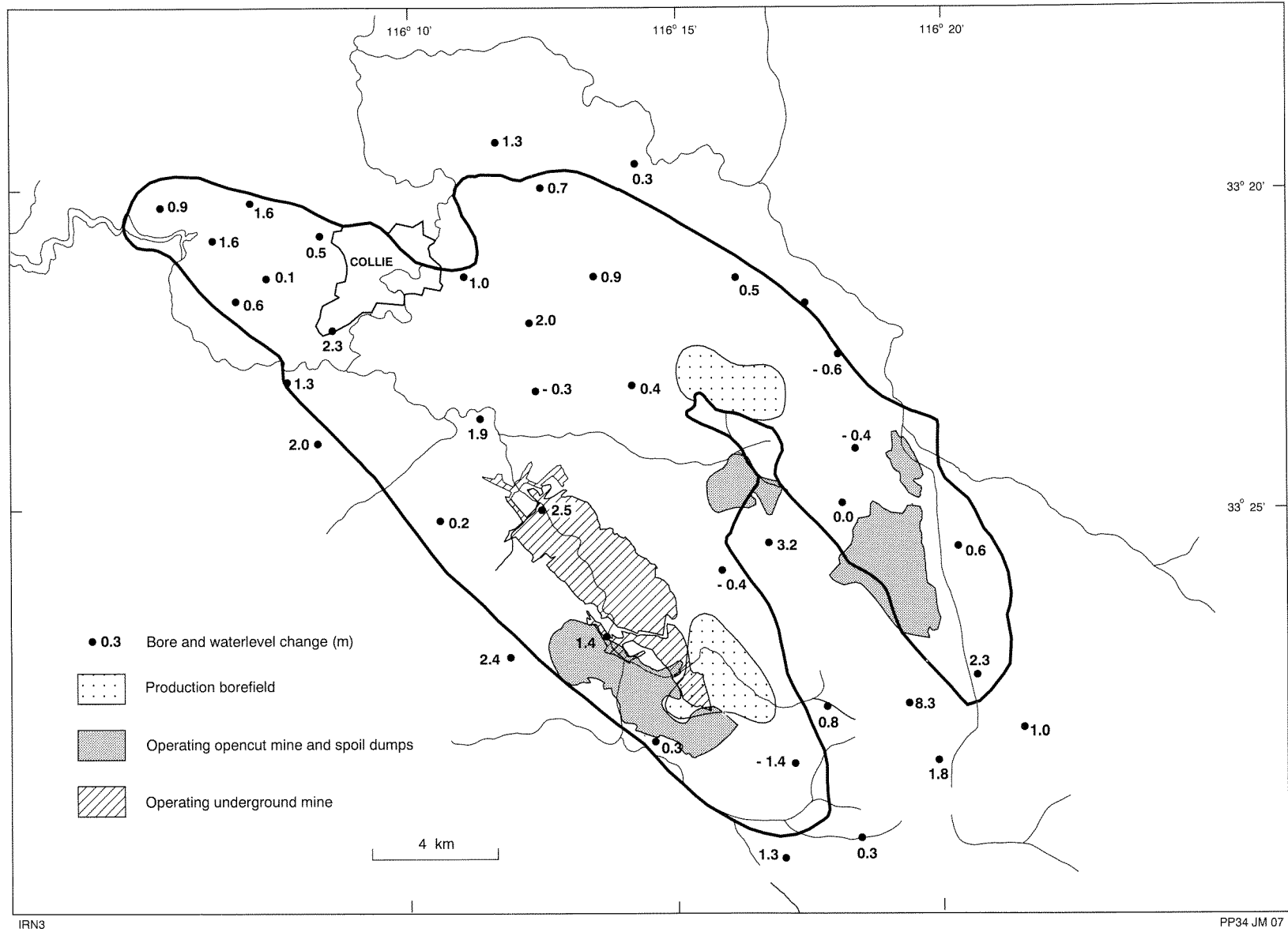


Figure 7. Waterlevel change, May to October 1990

**Table 3. Groundwater head difference with depth**

Bores CBS	Vertical separation of intervals (m)	Head difference (m)				Direction (a)
		Max.	Date	Min.	Date	
2A 2B	34	1.83	14.08.90	1.40	04.09.89	down
5B 5A	245	11.84	20.11.90	10.80	11.09.90	up
9A 9B	41	2.48	11.09.90	1.16	13.06.90	down
14A 14B	13	1.78	19.06.90	0.57	12.12.89	down
14B 14C	17	1.68	22.11.90	1.28	19.06.90	down
14A 14C	30	3.06	19.07.90	1.90	07.02.91	down
17A 17B	35	16.69	19.07.90	4.64	05.09.89	down
18 PWD5/80	23	1.08	17.07.90	0.05	05.02.91	down
21A 21D	43	9.81	15.06.90	8.65	11.10.90	down
25A 25B	36	4.34	17.07.90	2.12	07.03.90	down

(a) up—increasing head with depth; down—decreasing head with depth

near CBS11, CBS14 and CBS21 flow into the East Branch outside the basin.

Artesian flows, implying upward groundwater head gradients and the potential for upward groundwater movement, were once common from bores drilled in topographically low areas in the northern Cardiff Sub-basin near the Collie River (Fig. 7). Flows were recorded from as shallow as 21 m below the surface (Lord, 1952). Groundwater abstraction has lowered potentiometric heads in some stratigraphic intervals in the flow system. There is now a downward hydraulic gradient between the watertable and 50 m depth in the Collie Coal Measures in this area (CBS9 Table 3) although, to the northwest, there is an upward hydraulic gradient between the base of the Collie Coal Measures and the watertable (CBS5 Table 3).

### Abstraction

According to SECWA and Water Authority of Western Australia data, about  $39 \times 10^6$  m<sup>3</sup>/year of groundwater is withdrawn from production borefields and operating mines in the Collie Basin. The greater part of this is abstracted from the Collie Coal Measures, although dewatering of the Nakina Formation is also undertaken for opencut mining. The water-balance calculations indicate that some of the groundwater comes from storage. After treatment to raise the pH and remove dissolved gases and iron, most of the water is used for cooling at the Muja Power Station. The remainder is discharged either to the South Branch, from where it may be returned to the groundwater flow system by leakage from the river bed, or to Chicken Creek, which

flows out of the basin. The groundwater that is discharged directly to Chicken Creek is also first treated to raise the pH and remove iron. Some groundwater is pumped from the basin for use in sawmilling and there is minor groundwater abstraction by private users for domestic purposes and stock watering.

Groundwater withdrawals have affected the watertable over an estimated 100 km<sup>2</sup> of the basin (Fig. 4). The areas influenced are difficult to define accurately because the effects are generally small and are often difficult to distinguish from seasonal watertable fluctuations. The effect on the watertable is also influenced by the location of the abstraction and geological structure.

Depressions in the watertable are centred mainly around groundwater abstraction areas and result either from pumping in the upper part of the flow system or from downward leakage through confining beds to deeper parts of the flow system where groundwater heads are affected by abstraction. Hydrographs from site CBS17 (Fig. 9), above the WD2 underground mine, show there was a drawdown of 11.8 m in CBS17B (slotted interval about 33 m below the watertable) and 2.8 m in CBS17A (open interval at the watertable) between November 1989 and May 1990. Much of the drawdown of the watertable is probably due to vertical leakage of groundwater to deeper intervals in the Collie Coal Measures, although some results from seasonal fluctuation. The watertable recovers when flow recommences in the adjacent South Branch. This usually occurs in autumn and is due to groundwater recharge by leakage from the river. The watertable variation in CBS17A reflects the change of about 3 m in river level during 1990.

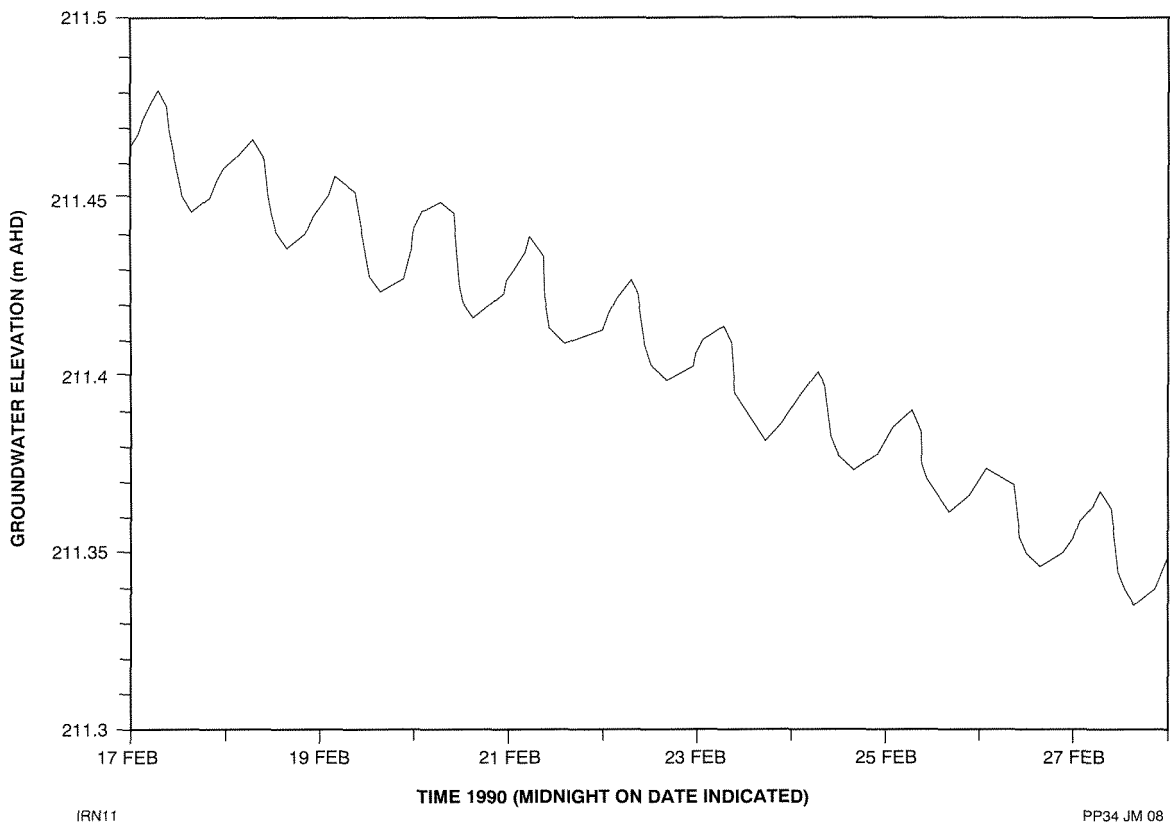


Figure 8. Hydrograph CBS14A

The watertable may also be depressed in more distant areas where sandstone aquifers which are being depressurized at depth are either present at the watertable, or in direct contact with the overlying Nakina Formation below the watertable. In the southern Cardiff Sub-basin the effects of pumping at the Cardiff South Borefield and the WO5 opencut mine extend to near the southern margin of the basin (CBS33) and, in the Premier Sub-basin, the effects of pumping at Shotts Borefield extend well north of the borefield itself (Fig. 4). The elevation of the watertable in CBS33 has declined steadily since recordings began in September 1989 and, by the beginning of May 1991, it had fallen by 6.4 m to 58.8 m below the natural surface (Moncrieff, 1991b).

Depressions in the watertable surround the WO5, Muja/Chicken Creek and, to a lesser extent, the WO3 opencut mines. In these areas groundwater is drawn directly from the upper part of the flow system as well as from deeper intervals. The Nakina Formation is completely dewatered in the mine areas and the pumping has caused partial dewatering and the formation of perched watertables in some aquifers in the Collie Coal Measures (Vogwill and Brunner, 1985). Dewatering at the Muja opencut has allowed mining to progress to a depth of about 200 m below the original watertable.

Groundwater abstraction has greatly altered the hydraulic-head distribution at depth in the basin. The areal extent of drawdowns associated with the pumping is not

known; however, it probably extends to the basin boundaries. Waterlevels have been lowered substantially around the mines and borefields. Drawdowns of as much as 110 m from pre-mining levels at the Muja opencut (Vogwill and Brunner, 1985) and 77 m at the WD7 underground mine (Hammond and Boyd, 1988) have been reported. There is limited monitoring of groundwater levels from producing intervals around the Cardiff South and Shotts borefields (Fig. 7) but drawdowns of 50–60 m occur in the production bores themselves.

Flow of the South Branch in the southern Cardiff Sub-basin is probably indirectly affected by the groundwater abstraction. Increased leakage of river water to the groundwater is likely to be occurring in response to the depressed groundwater levels. The duration of river flow after winter rainfall has almost certainly decreased and some of the pools that remain, which according to local residents were once permanent, are now dry for long periods.

#### Storage

If the average thickness of sandstone above the Stockton Formation is taken to be 325 m and a specific yield of 0.1 is applied, then about  $7300 \times 10^6 \text{ m}^3$  of commandable groundwater is stored in the Collie Basin. This is comparable with storage estimates of  $6750 \times 10^6 \text{ m}^3$  by the Collie Land Use Working Group (1987) and  $7000 \times 10^6 \text{ m}^3$  by Allen (1991).

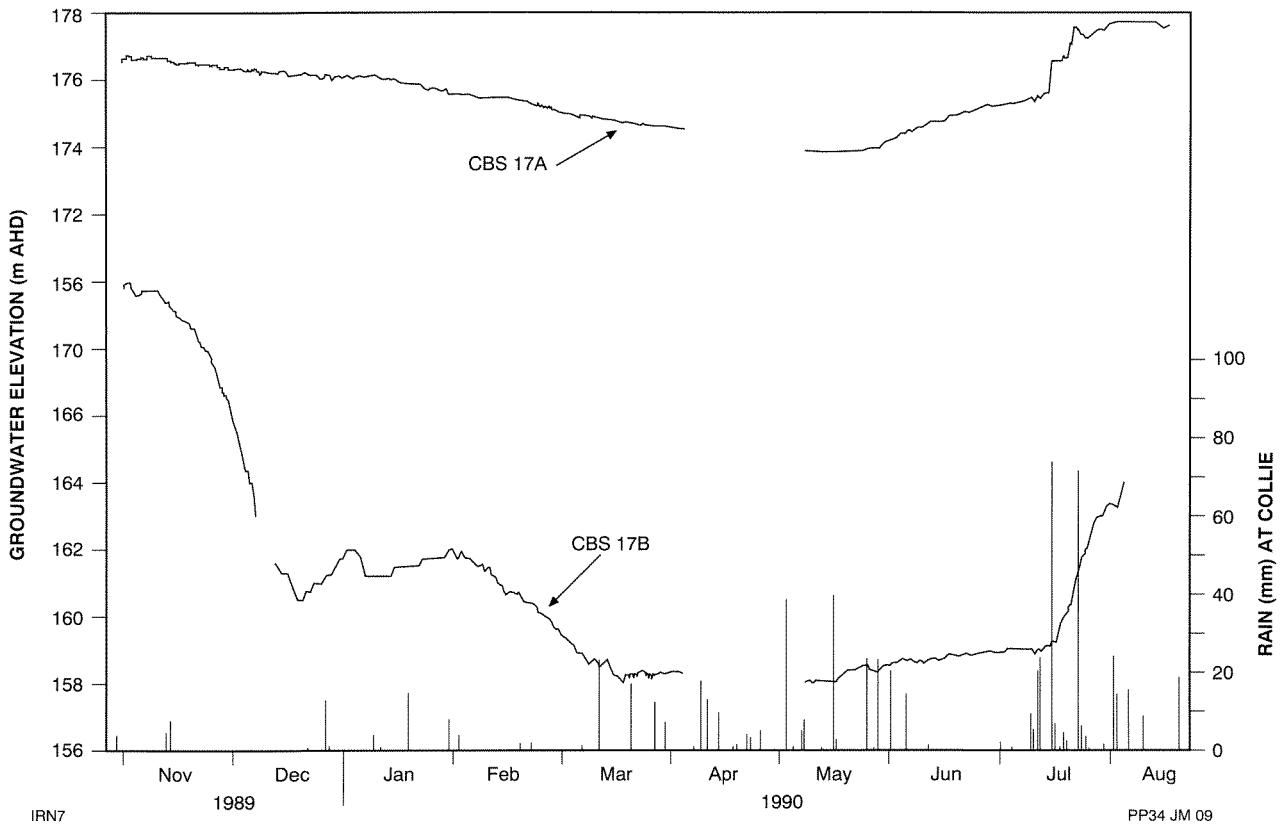


Figure 9. Hydrographs CBS17A and CBS17B

## Groundwater quality

### Salinity

The salinity of the groundwater at the watertable is highly variable (Fig. 10) and reflects local variations in lithology, topography, landuse and depth to the watertable. Consequently it is not possible to contour the data reliably. The salinity at the watertable in sandstones of the Collie Coal Measures and Nakina Formation is typically less than 750 mg/L TDS (Fig. 10). Very low-salinity groundwater (<100 mg/L) occurs where the watertable is in the upper few metres of the surficial sands (CBS2A, CBS14A, CBS18, CBS21A, and CBS34). High TDS concentrations (>1000 mg/L) occur where the watertable is in clayey sedimentary rocks. In CBS10, which is open against claystone, the salinity was 7150 mg/L.

The salinity of groundwater from the deeper intervals at seven sites where more than one bore was constructed is generally less than 500 mg/L (Fig. 10). With two exceptions the salinity at these sites increases with depth. Groundwater of comparable salinity is obtained from the Shotts and Cardiff South Borefields; elsewhere in the basin the salinity is generally less than 750 mg/L. Water discharged from the Chicken Creek mine is about 1000 mg/L.

Groundwater salinity outside the basin is highly variable. The lowest salinity groundwater occurs where

the watertable is shallow and in surficial sand (70 mg/L in CBS35). Higher salinity groundwater (2000–10 000 mg/L) occurs in the weathered basement rocks on the southern part of the Stockton Ridge, and south of the Premier Sub-basin.

### Hydrochemistry

Chemical analyses of groundwater samples from the bores are given in Table 4. The groundwater is mainly sodium–chloride type (Fig. 11). The deeper groundwater from CBS5A is markedly different from the shallow groundwater in having a higher proportion of bicarbonate ion. The proportions of chloride and of sodium generally increase with salinity.

The sample from CBS12, which is in weathered granitic rock outside the basin, contained comparatively high proportions of both sulfate and bicarbonate ion, and a high ratio of  $\text{Na}^+(\text{Ca}^{++}+\text{Mg}^{++})$ ; however, samples from other bores in the weathered granitic rock are similar in composition to groundwater within the basin.

Groundwater inside the basin is mainly acidic; pH values from 2.6 (CBS17B) to 7.6 (CBS5A) were recorded (Table 4). The lowest pH values generally occur in bores near existing or abandoned mines (CBS11, CBS17, CBS20, CBS25 and CBS30), in bores with open intervals near shale or coal strata (CBS1, CBS8 and CBS24), and in bores in the northern Cardiff Sub-basin where the

Table 4. Chemical analyses

Bore Interval	Sample Number (a)	pH	Colour (TCU)	EC (mS/m @ 25°C)	TDS	T. Hard.	T. Alk.	Ca	Mg	Na	K	HCO <sub>3</sub>	Cl	SO <sub>4</sub>	NO <sub>3</sub>	SiO <sub>2</sub>	B	F	H+
CBS1	93401	3.8	<5	277	1 350	161	<2	2	38	418	8	<2	815	50	1	20	0.05	<0.1	0.5
CBS2A	93402	5.7	30	7.6	40	16	3	3	2	9	<1	4	13	12	<1	2	0.02	0.1	-
CBS2B	93403 (c)	6.0	5	18.5	110	15	7	1	3	25	3	8	45	7	<1	18	0.02	<0.1	-
CBS3	93404 (b)	6.1	<5	105	500	125	7	4	28	143	4	9	290	16	<1	14	0.03	<0.1	-
CBS4	93405 (b)	5.6	<5	48.6	240	31	4	1	7	75	1	5	137	7	<1	7	0.03	<0.1	-
CBS5A	93406 (c)	7.6	35	36.6	220	80	120	27	3	35	16	146	34	15	<1	19	0.03	0.2	-
CBS6	93407	4.5	<5	152	740	98	2	3	22	240	1	2	422	32	<1	21	0.04	<0.1	-
CBS7	93408	7.7	<5	217	1 160	231	121	20	44	342	1	148	563	49	<1	65	0.04	0.4	-
CBS8	93409	4.0	<5	58.5	300	27	<2	1	6	93	1	<2	147	30	<1	24	0.02	<0.1	-
CBS9A	93410	5.8	<5	25.7	130	25	3	<1	6	37	<1	4	70	6	3	8	0.02	<0.1	-
CBS9B	93411 (c)	6.0	5	109	560	129	11	9	26	150	10	14	310	17	<1	27	0.02	<0.1	-
CBS10	93412 (b)	3.0	<5	1 330	7 150	1 500	<2	96	307	2 170	27	<2	4 230	249	<1	68	0.04	0.5	1.7
CBS11	93413 (b)	2.9	<5	409	1 990	385	<2	21	81	591	17	<2	1 170	76	<1	33	0.06	0.8	0.9
CBS12	93414 (c)	6.9	160	137	690	36	112	3	7	317	2	137	104	161	<1	30	0.05	0.4	-
CBS13	93415 (b)	3.3	5	387	1 950	542	<2	26	116	533	9	<2	1 170	77	<1	21	0.12	0.2	0.4
CBS14A	93416	5.7	65	14.7	80	16	3	<1	4	21	1	4	35	8	<1	4	<0.01	0.1	-
CBS14B	93417	5.7	5	13	70	8	2	<1	2	19	<1	3	34	3	<1	9	<0.01	0.1	-
CBS14C	93418 (c)	5.8	10	35.5	170	30	4	2	6	49	1	5	93	10	<1	10	0.01	0.1	-
CBS15	93419	7.0	<5	113	580	178	34	22	30	143	4	41	301	19	11	25	0.05	0.1	-
CBS16	93420	5.8	5	55	280	54	4	2	12	77	3	5	155	7	<1	16	0.01	<0.1	-
CBS17A	93421	3.6	<5	116	600	185	<2	10	39	129	11	<2	253	112	9	32	0.02	0.1	0.1
CBS17B	93422 (c)	2.6	<5	261	1 100	290	<2	19	59	278	10	<2	587	121	<1	23	0.02	0.1	1.4
CBS18	93423	5.4	15	10.9	70	8	2	<1	2	15	2	2	26	13	<1	10	0.02	0.1	-
CBS19	93424	6.3	35	58.3	290	50	16	2	11	88	1	20	151	19	<1	9	0.03	0.1	-
CBS20	93425	3.7	<5	141	680	100	<2	2	23	214	3	<2	380	37	<1	17	0.03	<0.1	0.1
CBS21A	93426	5.7	120	12.7	70	21	5	<1	5	13	5	6	20	18	3	5	0.03	<0.1	-
CBS21D	93427 (c)	5.8	40	40.4	210	23	12	1	5	71	2	15	105	11	<1	10	0.02	<0.1	-
CBS23	93428 (b)	7.1	15	70.5	390	43	36	4	8	117	2	44	178	19	<1	35	0.03	0.4	-
CBS24	93429	4.5	<5	90.5	450	72	<2	4	15	140	1	<2	253	28	<1	11	0.04	0.1	-
CBS25A	93430	4.0	<5	223	1 110	296	<2	15	63	300	4	<2	635	56	<1	34	0.02	0.1	0.1
CBS25B	93431 (c)	6.4	10	38.8	210	27	16	1	6	55	8	19	100	10	<1	24	0.02	<0.1	-
CBS26	93432	6.0	5	76.9	390	63	7	4	13	119	3	9	210	24	<1	11	0.04	<0.1	-
CBS27	93433	5.0	140	92.6	490	96	4	4	21	136	2	5	248	42	7	30	0.03	0.1	-
CBS28	93434 (b)	6.5	1 300	248	1 310	331	234	27	64	466	8	286	578	13	1	13	1.10	0.1	-
CBS29	93435	5.1	<5	73.7	370	68	2	4	14	108	8	2	209	10	<1	19	0.02	<0.1	-
CBS30	93436	4.5	15	202	1 000	145	<2	2	34	332	1	<2	571	47	<1	14	0.03	0.1	-
CBS31	93437	7.3	10	418	2 280	462	57	35	91	677	5	70	1 290	99	<1	43	0.03	0.1	-
CBS32	93438	6.1	25	21.7	110	16	5	<1	4	31	1	6	57	7	<1	5	0.01	<0.1	-
CBS33	93439 (c)	6.4	60	136	730	179	58	24	29	215	12	71	323	80	<1	13	0.04	0.1	-
CBS34	93440	6.3	30	13.4	70	21	14	2	4	15	2	17	24	9	1	7	0.03	<0.1	-
CBS35	93441	6.1	5	13.2	70	16	9	<1	4	15	2	11	29	7	2	6	0.01	<0.1	-
CBS36	93442	6.4	5	1 300	7 320	1 690	20	48	383	2 170	8	24	4 390	225	<1	83	0.02	0.4	-

Table 4. (continued)

Bore Interval	Sample Number (a)	pH	Colour (TCU)	EC (mS/m @ 25°C)	(mg/L)														
					TDS	T. Hard.	T. Alk.	Ca	Mg	Na	K	HCO <sub>3</sub>	Cl	SO <sub>4</sub>	NO <sub>3</sub>	SiO <sub>2</sub>	B	F	H+
CBS37	93443	6.8	5	1 640	9 350	2 640	32	156	548	2 670	11	39	5 540	364	<1	37	0.02	0.1	-
CBS38	93444	4.5	<5	1 130	6 320	1 530	<2	68	330	1 920	5	<2	3 830	121	<1	48	0.01	0.3	-
CBS39	93445	6.7	5	458	2 460	544	23	35	111	729	6	28	1 440	77	<1	48	0.02	0.6	-

NOTE:

- (a) Airlift samples taken about 1 month after completion of bore following further development
- (b) Airlift samples taken at completion of bore only
- (c) Airlift samples taken at completion of development

- TCU True colour units
- EC Electrical conductivity
- TDS Total dissolved solids (by calculation)

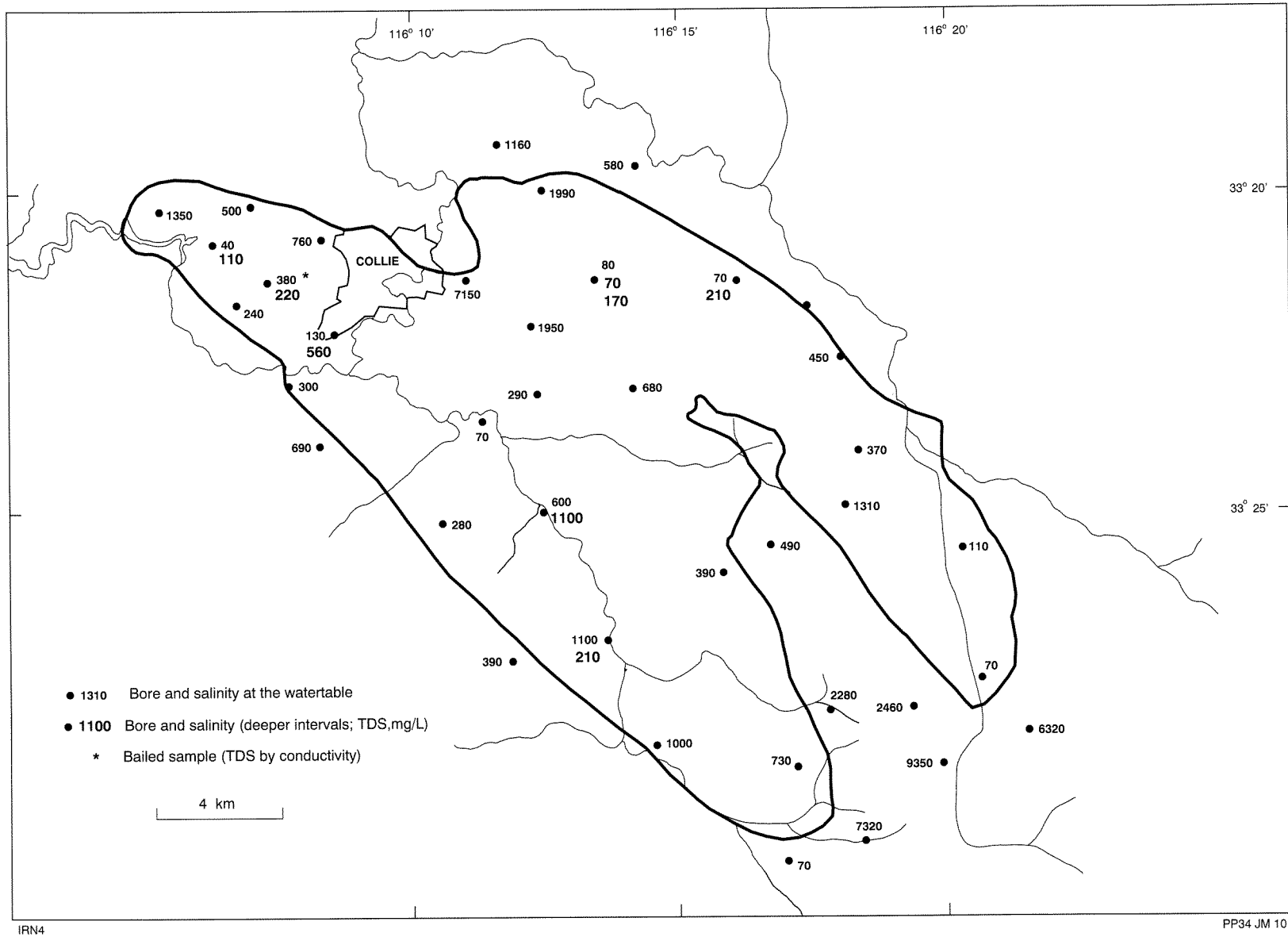


Figure 10. Groundwater salinity

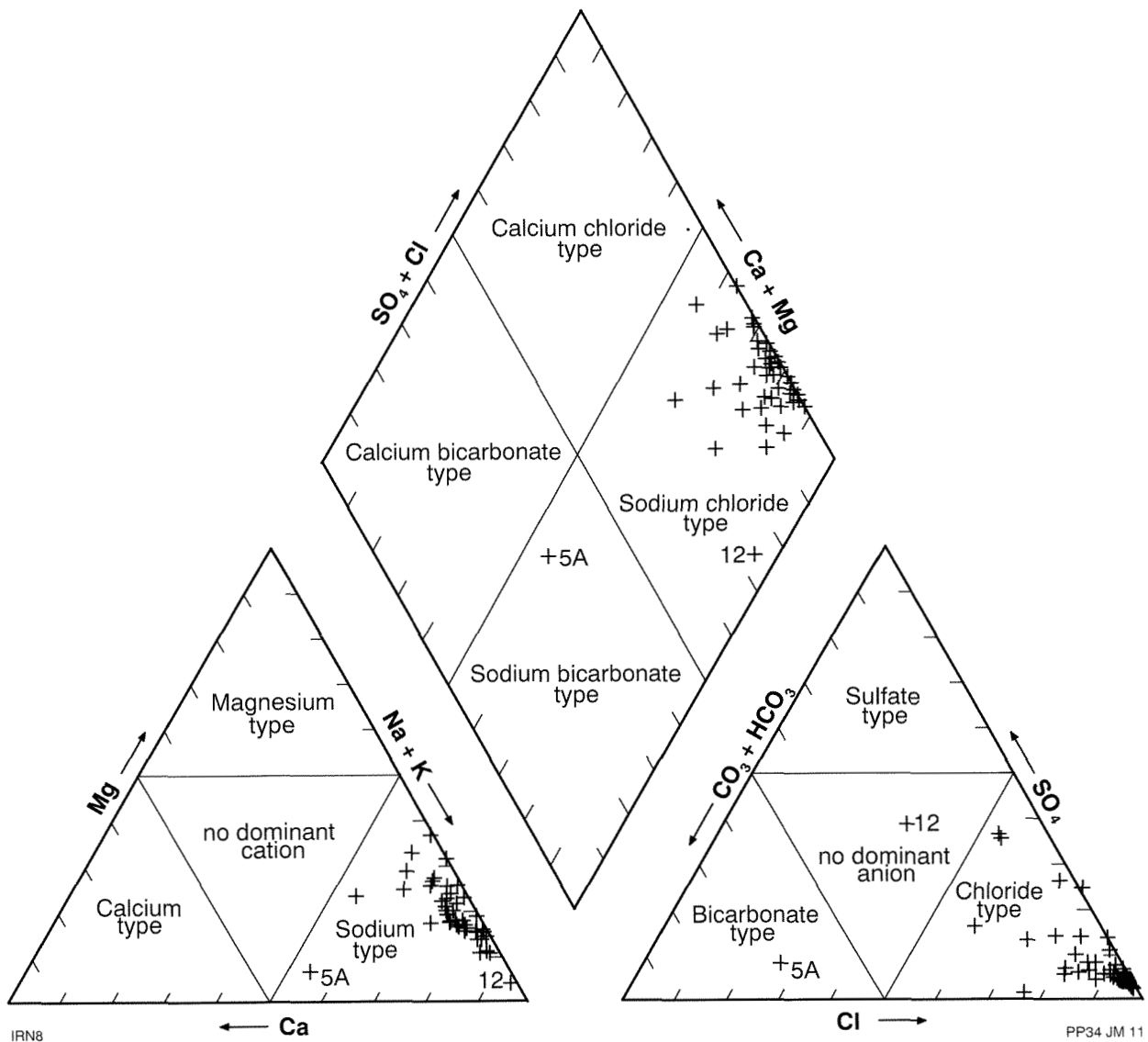


Figure 11. Piper trilinear diagram

watertable rests in clayey strata (CBS6, CBS10 and CBS13). The groundwater outside the basin is typically of neutral pH. CBS27 is sited alongside a swampy drainage line and contains slightly acidic groundwater (pH 5.0) as does CBS38 (pH 4.5), which is drilled in granitic rocks south of the Premier Sub-basin.

High concentrations of iron and sulfate ion (Vogwill and Brunner, 1985), and dissolved hydrogen sulfide and carbon dioxide (Hammond and Boyd, 1988), are common in groundwater from inside the basin. The groundwater is highly corrosive as a result of the acidity, dissolved gases, and chloride content.

Heavy metals were not determined but they occur in low concentrations in the basin and some are concentrated in the residues that are left after burning of the coal (Wilson and Davy, 1989). Groundwater in the basin may contain background concentrations of these elements, particularly near ash dumps.

## Conclusions

Important fresh groundwater resources occur in the Collie Basin. The drilling program has provided new geological and hydrogeological information which, with existing data, has allowed the most detailed account of the hydrogeology to date. The study has shown that the groundwater regime reflects the complex structure and stratigraphy of the basin and that the aquifers have been greatly affected by coal mining and groundwater abstraction.

The regional watertable is now defined with reasonable accuracy and this, together with watertable monitoring, has allowed identification of areas in the basin which are affected by changes in the groundwater regime. The work has also enabled recalculation of the water balance and groundwater resources to be made. It is estimated that the basin contains about  $7300 \times 10^6 \text{ m}^3$  of fresh (<750 mg/L TDS), commandable groundwater in storage, and that total

recharge is  $31 \times 10^6 \text{ m}^3/\text{year}$  comprising rainfall recharge of about  $26 \times 10^6 \text{ m}^3/\text{year}$  (13% of average annual rainfall) and recharge from streams of about  $5 \times 10^6 \text{ m}^3/\text{year}$ .

Groundwater abstraction is estimated to be about  $39 \times 10^6 \text{ m}^3/\text{year}$  and thus exceeds total recharge. As a consequence the watertable in the basin is depressed over an estimated  $100 \text{ km}^2$ . Groundwater heads at depth are similarly affected, but over a larger area extending possibly to the basin boundary. Changes occurring within the groundwater system are also affecting stream flow, and may have other environmental consequences.

Further work, entailing deeper drilling, will be directed towards gaining a better understanding of the hydrogeology at depth in the Collie Basin.

## Acknowledgements

The Griffin Coal Mining Company Limited and Western Collieries Limited kindly allowed access to unpublished hydrogeological data.

## References

- ALLEN, A. D., 1991, Groundwater resources of the Phanerozoic sedimentary basins of Western Australia: International Conference On Groundwater In Large Sedimentary Basins, Proceedings, Perth 1990.
- BACKHOUSE, J., 1990, Palynology of Collie Basin shallow boreholes 4-34: Western Australia Geological Survey, Palaeontology Report 1990/34 (unpublished).
- BACKHOUSE, J., 1991, Permian palynostratigraphy of the Collie Basin, Western Australia: Review of Palaeobotany and Palynology, v. 67, p. 237-314.
- BACKHOUSE, J., and WILSON, A. C., 1989, New records of Permian and Cretaceous sediments from the southwestern part of the Yilgarn Block: Western Australia Geological Survey, Report 25, Professional Papers, p. 1-5.
- COLLIE LAND USE WORKING GROUP, 1987, A report to cabinet on land-use planning in the Collie Basin, May 1987.
- DAVY, R., and WILSON, A. C., 1989, Geochemical study of inorganic components of the Collie Coal Measures: Western Australia Geological Survey, Report 26, Professional Papers, p. 1-30.
- DUNDON, P. J., HUMPHRIES, D., and HEBBLEWHITE, B., 1988, Roof depressurization for total extraction mining trials Collie Basin, Western Australia: The Third International Mine Water Congress, Proceedings, Melbourne, Australia, p. 743-752.
- GOZZARD, J. R., and JORDAN, J. E., 1986, Collie Sheet 2131-III: Western Australia Geological Survey, 1:50 000 Environmental Geology Map Series.
- GOZZARD, J. R., and JORDAN, J. E., 1987, Muja Sheet 2131-II: Western Australia Geological Survey, 1:50 000 Environmental Geology Map Series.
- HAMMOND, G., and BOYD, G., 1988, Dewatering at Western No. 7 Colliery: The Third International Mine Water Congress, Proceedings, Melbourne, Australia, p. 733-741.
- HIRSCHBERG, K-J. B., 1976, Collie Basin groundwater resources: Western Australia Geological Survey, Hydrogeology Report 1457 (unpublished).
- HUMPHRIES, D., and HEBBLEWHITE, B. K., 1988, Introduction of total mining extraction in conjunction with strata dewatering at Collie, Western Australia: Australian Journal of Coal Mining Technology and Research, v. 19, p. 45-56.
- KRISTENSEN, S. E., and WILSON, A. C., 1986, A review of the coal and lignite resources of Western Australia, in Geology and Exploration edited by D. A. BERKMAN: Council of Mining and Metallurgical Institutions, Congress, 13th, Singapore, 1986, Publications, v. 2, p. 87-97.
- LE BLANC SMITH, G., 1989, Structural evidence from the Collie Coalfield, in Proceedings of the Perth Basin Offshore Symposium, Perth, Western Australia, 1989: Western Australia Department of Mines (unpublished).
- LE BLANC SMITH, G., 1990, Coal, in Geology and Mineral Resources of Western Australia: Western Australia Geological Survey, Memoir 3, p. 625-631.
- LE BLANC SMITH, G., 1993, The geology and coal resources of the Collie Basin: Western Australia Geological Survey, Report 38.
- LOH, I. C., and STOKES, R. A., 1981, Predicting stream salinity changes in South-Western Australia: Agricultural Water Management, v. 4, p. 227-254.
- LORD, J. H., 1952, Collie Mineral Field: Western Australia Geological Survey, Bulletin 105, part 1.
- LOW, G. H., 1958, Collie Mineral Field: Western Australia Geological Survey, Bulletin 105, part 2.
- LOWRY, D., 1976, Tectonic history of the Collie Basin, Western Australia: Geological Society of Australia Journal, v. 23, p. 95-104.
- MONCRIEFF, J. S., 1985, The geology and hydrogeology of the Collie Basin: Western Australia Geological Survey, Hydrogeology Report 2673 (unpublished).
- MONCRIEFF, J. S., 1986, Collie Basin proposed hydrogeological investigations, phase 1: Western Australia Geological Survey, Hydrogeology Report 2718 (unpublished).
- MONCRIEFF, J. S., 1990, Collie Basin Shallow Project groundwater level monitoring: Western Australia Geological Survey, Hydrogeology Report 1990/45 (unpublished).
- MONCRIEFF, J. S., 1991a, Collie Basin Shallow Project bore completion reports: Western Australia Geological Survey, Hydrogeology Report 1991/8 (unpublished).
- MONCRIEFF, J. S., 1991b, Hydrogeology of the upper part of the Collie Basin: Western Australia Geological Survey, Hydrogeology Report 1991/24 (unpublished).
- PARK, W. J., 1982, The geology of the Muja Sub-basin, a model for the Collie Basin, in Coal Resources: origin, exploration and utilization in Australia edited by C. W. MALLETT: Geological Society of Australia, Symposium Proceedings, p. 319-340.
- VOGWILL, R. I. J., and BRUNNER, I. G., 1985, Dewatering and depressurization at the Muja Open Cut, Collie Basin, Western Australia, in Hydrogeology in the Service of Man, Memoirs of the 18th Congress of the International Association of Hydrogeologists, Cambridge, 1985, Part 4, p. 207-223.
- WATER AUTHORITY OF WESTERN AUSTRALIA, 1988, Collie coal basin water resources management strategy: Water Authority of Western Australia, Report WG60 (unpublished).
- WILDE, S. A., 1981, The Collie Basin, in Mineral Fields of the Southwest, Western Australia compiled by T. E. JOHNSTON: Geological Society of Australia, Fifth Australian Geological Convention, Excursion Guide A 4, p. 33-45.
- WILDE, S. A., and WALKER, I. W., 1982, Collie, Western Australia: Western Australia Geological Survey 1:250 000 Geological Series Explanatory Notes, 39p.

WILSON, A. C., 1989, Palaeocurrent directions in the Collie Coal Measures — the implications for sedimentation and basin models: Western Australia Geological Survey, Report 25, Professional Papers, p. 85–91.

WILSON, A. C., 1990, Collie Basin, in Geology and Mineral Resources of Western Australia: Western Australia Geological Survey, Memoir 3, p. 525–531.